

Look-Up Table for Two-Phase Frictional Pressure Drop Multiplier

BY

Ihab Hisham Alsurakji

A Thesis Presented to the
DEANSHIP OF GRADUATE STUDIES

KING FAHD UNIVERSITY OF PETROLEUM & MINERALS

DHAHRAN, SAUDI ARABIA

In Partial Fulfillment of the
Requirements for the Degree of

MASTER OF SCIENCE

In

Mechanical Engineering

May, 2012



**In the name of Allah, the Most Gracious and the
Most Merciful**

KING FAHD UNIVERSITY OF PETROLEUM AND MINERALS
DHAHRAN 31261, SAUDI ARABIA

DEANSHIP OF GRADUATE STUDIES

This thesis, written by IHAB ALSURAKJI under the direction of his thesis advisor and approved by his thesis committee, has been presented to and accepted by the Dean of Graduate Studies, in partial fulfillment of the requirements for the degree of MASTER OF SCIENCE in MECHANICAL ENGINEERING.

Thesis Committee



Dr. Meamer El Nakla (Advisor)



Dr. Abdel Salam Al-Sarkhi (Member)



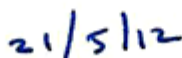
Dr. Mohamed A. Habib (Member)



Dr. Amro M. Al-Qutub
(Department Chairman)



Dr. Salam A. Zummo
(Dean of Graduate Studies)



Date



Dedicated

to

*My Beloved Parents, Brothers and My
Fiancee*

ACKNOWLEDGMENTS

All praise and thanks are due to Almighty Allah, Most Gracious and Most Merciful, for his immense beneficence and blessings. He bestowed upon me health, knowledge and patience to complete this work. May peace and blessings be upon prophet Muhammad (PBUH), his family and his companions.

Thereafter, acknowledgement is due to KFUPM for the support extended towards my research through its remarkable facilities and for granting me the opportunity to pursue graduate studies.

I acknowledge, with deep gratitude and appreciation, the inspiration, encouragement, valuable time and continuous guidance given to me by my thesis advisor, Dr. Meamer El Nakla. I am highly grateful to my Committeemember Dr. Dr. Abdel Salam Al-Sarkhi for his valuable guidance, suggestions and motivation. I am also grateful to my Committee member, Dr. Mohamed A. Habib for his constructive guidance and support.

I am deeply indebted and grateful to KACST for their help and support during research.

You who I carry your name with pride, who I miss from an early age, who my heart trembles when I remember you, who you leave me for God's mercy, I gift you this thesis ...*my father*

To my angel in my life, to the meaning of love and the meaning of compassion, dedication and to the source of patience, optimism and hope...*my mother*.

To my brothers and my sister, who I see certain optimism and happiness in their smile. To the flame of intelligence and thinking.

To my fiancée who shared me every moment throughout my studying.

Special thanks are due to my senior colleagues at the university, for their help, prayers and who provided wonderful company and good memories that will last a life time.

TABLE OF CONTENTS

ACKNOWLEDGMENTS	V
TABLE OF CONTENTS.....	VI
LIST OF TABLES	VIII
LIST OF FIGURES	IX
THESIS ABSTRACT (ENGLISH)	XIII
THESIS ABSTRACT (ARABIC)	XIV
NOMENCLATURE	XV
INTRODUCTION	1
CHAPTER 2	5
LITERATURE REVIEW	5
2.1.FRICTIONAL PRESSURE DROP FOR SINGLE-PHASE FLOW	6
2.2.FRICTIONAL PRESSURE DROP FOR TWO-PHASE FLOW	10
2.2.1.Basic Equations of Two-Phase Flow	11
2.2.1.1.Conservation of Mass	11
2.2.1.2.Conservation of Momentum	12
2.2.1.3.Conservation of Energy	12
2.3.TWO-PHASE FRICTIONAL PRESSURE DROP MODELS AND CORRELATIONS	13
2.4.EXPERIMENTAL WORK DONE ON TWO-PHASE FRICTIONAL PRESSURE DROP	27
2.5.PREVIOUS WORK DONE ON LOOK-UP-TABLE	38
CHAPTER 3	39
PROBLEM STATEMENT AND OBJECTIVE OF STUDY	39
3.1.OBJECTIVES OF THE STUDY	39
3.2.PARAMETERS	40
3.3.METHODOLOGY	40
CHAPTER 4	42
COMPARISON BETWEEN CORRELATIONS AND EXPERIMENTAL DATA ..	42

4.1. EFFECT OF FLOW PARAMETERS ON TWO-PHASE FRICTIONAL PRESSURE DROP	42
4.2.ASSESSMENT OF TWO-PHASE FRICTIONAL PRESSURE DROP CORRELATIONS	48
CHAPTER 5	68
LOOK-UP-TABLE.....	68
5.1.GENERAL	68
5.2.SELECTING DIMENSION, PARAMETERS AND RANGES OF THE LOOK-UP TABLE ...	68
5.3.CONSTRUCTING SKELETON TABLE	73
5.4.UPDATING THE SKELETON TABLE.....	79
5.5.SMOOTHING THE UPDATED TABLE.....	85
5.6.LOOK-UP-TABLE ASSESSMENT	87
CHAPTER 6	109
LOOK-UP-TABLE PROCEDURE	109
6.1.PROCEDURES OF USING THE LUT.....	109
6.2.EXAMPLES ON HOW TO USE THE LUT	111
CHAPTER 7	116
CONCLUSIONS AND RECOMMENDATIONS	116
REFERENCES	118
APPENDIX A	126
APPENDIX B	135
VITA	147

LIST OF TABLES

TABLE 1 SUMMARY OF TWO-PHASE FRICTIONAL PRESSURE DROP PREDICTION MODELS AND CORRELATIONS	22
TABLE 2 DATA COLLECTED	36
TABLE 3 STATISTICAL COMPARISONS WITH EXPERIMENTAL RESULTS IN TERMS OF PERCENTAGE ERRORS	49
TABLE 4 ERROR MAPPING TABLE	50
TABLE 5 EQUIVALENT SATURATED PRESSURES CORRESPONDING TO WATER AND R134A	71
TABLE 6 NEW SKELETON TABLE	78
TABLE 7 SUMMARY OF EXPERIMENTAL DATA USED IN UPDATING THE SKELETON TABLE	83
TABLE 8 PART OF THE DATA ASSESSMENT OF LUT	88
TABLE 9 STATISTICAL COMPARISON BETWEEN LUT, CORRELATIONS, AND EXPERIMENTAL RESULTS IN TERMS OF PERCENTAGE ERRORS	92
TABLE 10 STATISTICAL COMPARISONS BETWEEN LUTS, AND EXPERIMENTAL RESULTS IN TERMS OF PERCENTAGE ERRORS	102
TABLE 11 SUMMARY OF EXPERIMENTAL DATA USED IN LUT	102
TABLE 12 SUMMARY OF SINGLE-PHASE FLOW EXAMPLE.....	113
TABLE 13 SUMMARY OF TWO-PHASE FLOW EXAMPLE.....	115

LIST OF FIGURES

FIGURE 1 TWO-PHASE FRICTIONAL PRESSURE GRADIENT VERSUS MASS QUALITY FOR WATER-STEAM FLOW IN 13.4 MM AT SYSTEM PRESSURE EQUAL TO 2 MPa AND VARIANT MASS FLUX FOR AUBE [47].....	44
FIGURE 2 TWO-PHASE FRICTIONAL PRESSURE GRADIENT VERSUS MASS QUALITY FOR R-11 FLOW IN 46.6 MM AT SYSTEM PRESSURE EQUAL TO 0.16 MPa AND VARIANT MASS FLUX FOR McMILLAN [36]	45
FIGURE 3 TWO-PHASE FRICTIONAL PRESSURE GRADIENT VERSUS MASS FLUX FOR R-11 FLOW IN 46.6 MM AT SYSTEM PRESSURE EQUAL TO 0.16 MPa AND VARIANT MASS QUALITY FOR McMILLAN [36].....	46
FIGURE 4 TWO-PHASE FRICTIONAL PRESSURE GRADIENT VERSUS MASS QUALITY FOR WATER-STEAM FLOW IN 13.4 MM AT MASS FLUX EQUAL TO $4500 \text{ KG.M}^{-2}.\text{SEC}^{-1}$ AND VARIANT SYSTEM PRESSURE FOR AUBE [47]	47
FIGURE 5-A COMPARISON OF TWO-PHASE FRICTIONAL PRESSURE GRADIENT WITH SIX CORRELATIONS FOR KLAUSNER [45] WITH SIX CORRELATIONS.	55
FIGURE 5-B COMPARISON OF TWO-PHASE FRICTIONAL PRESSURE GRADIENT WITH SIX CORRELATIONS FOR AUBE F. [47] WITH SIX CORRELATIONS.	56
FIGURE 5-C COMPARISON OF TWO-PHASE FRICTIONAL PRESSURE GRADIENT WITH SIX CORRELATIONS FOR McMILLAN H. [36] WITH SIX CORRELATIONS.	57
FIGURE 6-A COMPARISON FOR CALCULATED AND MEASURED TWO-PHASE FRICTIONAL PRESSURE GRADIENT FOR AUBE [47] AND SEVERAL CORRELATIONS AT LOW PRESSURE-HIGH MASS FLUX.	58
FIGURE 6-B COMPARISON FOR CALCULATED AND MEASURED TWO-PHASE FRICTIONAL PRESSURE GRADIENT FOR AUBE [47] AND SEVERAL CORRELATIONS, LOW PRESSURE-HIGH MASS FLUX.	59
FIGURE 6-C COMPARISON FOR CALCULATED AND MEASURED TWO-PHASE FRICTIONAL PRESSURE GRADIENT FOR AUBE [47] AND SEVERAL CORRELATIONS AT MEDIUM PRESSURE-HIGH MASS FLUX.	60

FIGURE 6-D COMPARISON FOR CALCULATED AND MEASURED TWO-PHASE FRICTIONAL PRESSURE GRADIENT FOR AUBE [47] AND SEVERAL CORRELATIONS AT MEDIUM PRESSURE-HIGH MASS FLUX.	61
FIGURE 7 COMPARISON FOR CALCULATED AND MEASURED TWO-PHASE FRICTIONAL PRESSURE GRADIENT FOR McMILLAN [36] AND SEVERAL CORRELATIONS AT LOW PRESSURE-LOW MASS FLUX.	62
FIGURE 8 COMPARISON FOR CALCULATED AND MEASURED TWO-PHASE FRICTIONAL PRESSURE GRADIENT FOR KLAUSNER [45] AND SEVERAL CORRELATIONS AT LOW PRESSURE-LOW MASS FLUX.	63
FIGURE 9 COMPARISON FOR CALCULATED AND MEASURED TWO-PHASE FRICTIONAL PRESSURE GRADIENT FOR HASHIZUME [40]AND SEVERAL CORRELATIONS AT LOW PRESSURE-LOW MASS FLUX.	64
FIGURE 10 COMPARISON FOR CALCULATED AND MEASURED TWO-PHASE FRICTIONAL PRESSURE GRADIENT FOR BENBELLA [63] AND SEVERAL CORRELATIONS AT LOW PRESSURE-MEDIUM MASS FLUX.	65
FIGURE 11-A COMPARISON FOR CALCULATED AND MEASURED TWO-PHASE FRICTIONAL PRESSURE GRADIENT FOR HASHIZUME [44] AND SEVERAL CORRELATIONS AT HIGH PRESSURE-MEDIUM MASS FLUX.	66
FIGURE 11-B COMPARISON FOR CALCULATED AND MEASURED TWO-PHASE FRICTIONAL PRESSURE GRADIENT FOR HASHIZUME [44] AND SEVERAL CORRELATIONS AT HIGH PRESSURE-LOW MASS FLUX.	67
FIGURE 12 FLOW CHART SHOWN THE CONSTRUCTING SKELETON TABLES FROM BEST CORRELATIONS.....	75
FIGURE 13 FLOW CHART ERROR MAPPING PROGRAM.....	76
FIGURE 14 PRESENTATION OF EXPERIMENTAL DATA POINT SURROUNDED BY TABLE MATRIX POINTS	81
FIGURE 15 FLOW CHART FOR UPDATING THE SKELETON TABLE WITH EXPERIMENTAL DATA.....	84
FIGURE 16 FLOW CHART FOR SMOOTHING THE LOOK-UP-TABLE	87
FIGURE 17 FLOW CHART SHOWN ERROR ASSESSMENTS FOR LOOK-UP-TABLE	89

FIGURE 18 COMPARISON OF TWO-PHASE FRICTIONAL PRESSURE GRADIENT BETWEEN LUT AND EXPERIMENTAL DATA SETS.	91
FIGURE 19 COMPARISON FOR CALCULATED AND MEASURED TWO-PHASE FRICTIONAL PRESSURE GRADIENT FOR AUBE [47] AND LUT AT LOW TO MEDIUM PRESSURE AND AT MASS FLUX EQUAL TO $4500 \text{ KG.M}^{-2}.\text{S}^{-1}$; SOLID SYMBOLS, REPRESENT EXPERIMENTAL DATA; OPEN SYMBOLS, REPRESENT LUT DATA.....	93
FIGURE 20 COMPARISON FOR CALCULATED AND MEASURED TWO-PHASE FRICTIONAL PRESSURE GRADIENT FOR MCMILLAN [36] AND LUT AT LOW PRESSURE EQUAL TO 0.165 MPa AND AT LOW MASS FLUX; SOLID SYMBOLS, REPRESENT EXPERIMENTAL DATA; OPEN SYMBOLS, REPRESENT LUT DATA.....	94
FIGURE 21 COMPARISON FOR CALCULATED AND MEASURED TWO-PHASE FRICTIONAL PRESSURE GRADIENT FOR KLAUSNER [45] AND LUT AT LOW PRESSURE EQUAL TO 0.17 MPa AND AT LOW MASS FLUX; SOLID SYMBOLS, REPRESENT EXPERIMENTAL DATA; OPEN SYMBOLS, REPRESENT LUT DATA.....	95
FIGURE 22 COMPARISON FOR CALCULATED AND MEASURED TWO-PHASE FRICTIONAL PRESSURE GRADIENT FOR HASHIZUME [44] AND LUT AT HIGH PRESSURE EQUAL TO 11.0 MPa AND AT MEDIUM TO LOW MASS FLUX; SOLID SYMBOLS, REPRESENT EXPERIMENTAL DATA; OPEN SYMBOLS, REPRESENT LUT DATA.....	96
FIGURE 23 COMPARISON FOR CALCULATED AND MEASURED TWO-PHASE FRICTIONAL PRESSURE GRADIENT FOR BENBELLA [63] AND LUT AT LOW PRESSURE-MEDIUM MASS FLUX; SOLID SYMBOLS, REPRESENT EXPERIMENTAL DATA; OPEN SYMBOLS, REPRESENT LUT DATA.....	97
FIGURE 24 COMPARISON BETWEEN MEASURED TWO-PHASE FRICTIONAL PRESSURE GRADIENT FOR AUBE [47], LUT AND SIX CORRELATIONS AT MEDIUM PRESSURE EQUAL TO 2.5 MPa AND AT HIGH MASS FLUX EQUAL TO $4500 \text{ KG.M}^{-2}.\text{SEC}^{-1}$	98
FIGURE 25 COMPARISON BETWEEN MEASURED TWO-PHASE FRICTIONAL PRESSURE GRADIENT FOR HASHIZUME [44], LUT AND SIX CORRELATIONS AT MEDIUM PRESSURE EQUAL TO 11.0 MPa AND AT HIGH MASS FLUX EQUAL TO $920 \text{ KG.M}^{-2}.\text{SEC}^{-1}$	99
FIGURE 26 COMPARISON BETWEEN MEASURED TWO-PHASE FRICTIONAL PRESSURE GRADIENT FOR MCMILLAN [36], LUT AND SIX CORRELATIONS AT MEDIUM	

PRESSURE EQUAL TO 0.165 MPa AND AT HIGH MASS FLUX EQUAL TO 216 K.G.M ⁻² .SEC ⁻¹	100
FIGURE 27 COMPARISON BETWEEN EXPERIMENTAL, SMOOTHED-LUT, UPDATED-LUT, AND SKELETON-LUT FOR TWO-PHASE FRICTIONAL PRESSURE DROP GRADIENT FOR AUBE [47] AT DENSITY RATIO (DR) = 84.62, REYNOLDS NUMBER (RE) = 480,000, PRESSURE (P) = 2.0 MPa, AND MASS FLUX (G) = 4500 K.G.M ⁻² .SEC ⁻¹	103
FIGURE 28 COMPARISON BETWEEN EXPERIMENTAL, SMOOTHED-LUT, UPDATED-LUT, AND SKELETON-LUT FOR TWO-PHASE FRICTIONAL PRESSURE DROP GRADIENT FOR KLAUSNER [45] AT DENSITY RATIO (DR) = 145.39, REYNOLDS NUMBER (RE)= 10,000, PRESSURE (P) = 0.17 MPa, AND MASS FLUX (G) = 327 K.G.M ⁻² .SEC ⁻¹	104
FIGURE 29 COMPARISON BETWEEN EXPERIMENTAL, SMOOTHED-LUT, UPDATED-LUT, AND SKELETON-LUT FOR TWO-PHASE FRICTIONAL PRESSURE DROP GRADIENT FOR HASHIZUME [44] AT DENSITY RATIO (DR) = 10.74, AND REYNOLDS NUMBER (RE)= 342,953.9021, PRESSURE (P) = 11.0 MPa, AND MASS FLUX (G) = 920 K.G.M ⁻² .SEC ⁻¹	105
FIGURE 30 COMPARISON BETWEEN EXPERIMENTAL AND LUT FOR TWO-PHASE FRICTIONAL PRESSURE DROP MULTIPLIER; SOLID SYMBOLS, REPRESENT EXPERIMENTAL DATA; OPEN SYMBOLS, REPRESENT LUT DATA	106
FIGURE 31 COMPARISON BETWEEN EXPERIMENTAL AND LUT FOR TWO-PHASE FRICTIONAL PRESSURE DROP MULTIPLIER; SOLID SYMBOLS, REPRESENT EXPERIMENTAL DATA; OPEN SYMBOLS, REPRESENT LUT DATA	107
FIGURE 32 COMPARISON BETWEEN EXPERIMENTAL AND LUT FOR TWO-PHASE FRICTIONAL PRESSURE DROP MULTIPLIER; SOLID SYMBOLS, REPRESENT EXPERIMENTAL DATA; OPEN SYMBOLS, REPRESENT LUT DATA	108

THESIS ABSTRACT (ENGLISH)

NAME: IHAB HISHAM ALSURAKJI

TITLE: LOOK-UP TABLE FOR TWO-PHASE FRICTION
PRESSURE DROP MULTIPLIER

MAJOR FIELD: MECHANICAL ENGINEERING

DATE OF DEGREE: JUMADA AL-AKHIRAH 1433 (H) (MAY 2012 G)

Accurate prediction of two-phase friction pressure drop requires knowledge of the Two-Phase Friction Pressure Drop Multiplier, Φ_{LO}^2 , used for calculating two-phase friction pressure drop. Many Correlations and models are previously made to predict the two-phase friction multiplier, but the problem that there is inconsistency in prediction as the models perform adequate for some regions and non-adequate in others. Therefore, it is needed to construct a single component two-phase look-up-table, to predict the two-phase frictional pressure drop multiplier. A skeleton table for $\Phi_{LO}^2(DR, Re, x)$ was constructed using leading correlations. The table then was updated with available experimental data which are enhanced to reduce the error in correlations predictions. Three dimensional smoothing was applied on the updated table. Detailed error assessment of the table was presented with comparing its predictions against experimental data as well as leading models and correlations. As a result, constructing such a table guarantees covering wide ranges of flow conditions with error 7% lower than the best prediction among existing models and correlations.

MASTER OF SCIENCE DEGREE

KING FAHD UNIVERSITY OF PETROLEUM AND MINERALS

Dhahran, Saudi Arabia

THESIS ABSTRACT (ARABIC)

ملخص الرسالة

الاسم: إيهاب هشام السركجي

عنوان الرسالة: جداول البحث لمعامل الضرب لفقد الضغط الاحتكاكي ثنائي الحالة

التخصص: الهندسة الميكانيكية

تأريخ التخرج: جمادى الآخرة 1433 هـ - (مايو 2201 م)

تم في هذا البحث بناء جداول البحث للتنبؤ بمعامل فقدان الضغط الاحتكاكي للمواد ثنائية الحالة. هذا التنبؤ الدقيق يتطلب معرفة ما يسمى بمعامل فقدان الضغط الاحتكاكي المضاعف، Φ_{LO}^2 . يوجد هناك عدد كبير من التنبؤات لـ Φ_{LO}^2 . ولكن المشكله ان هناك تضارب في التنبؤ بين هذه التنبؤات ، كما انه بعض من هذه التنبؤات في تطبيقات معينة تتنبأ بشكل جيد الى حد ما ولكنها سيئة في تطبيقات اخرى. ولهذا جاءت الحاجة لبناء جدول للتنبؤ بمعامل فقدان الضغط الاحتكاكي للمواد ثنائية الحالة . وكانت أولى المراحل بتشبيد جدول هيكلي لـ $\Phi_{LO}^2(DR, Re, x)$ بالاعتماد على افضل التنبؤات الرائدة في هذا المجال. اما المرحلة الثانية فكانت بتحديث الجدول الهيكلي ببيانات مخبرية تم تجميعها من مراجع مختلفه تم الاشارة اليها في سياق هذه الدراسة ، وهذه البيانات من شأنها ان تحسن وبشكل فعال في تنبؤ الجدول المراد انشائه. وتكمن المرحلة الاخيرة بتطبيق برنامج يعمل على تعميم ثلاثي الابعاد للجدول الذي تم تحديثه في مرحلة سابقة. وتم في نهاية هذه الدراسة تقييم مفصل لأداء جدول البحث بالمقارنة مع بيانات مخبرية وايضاً مع عدد من التنبؤات الرائدة في هذا المجال. ونتيجة لذلك ، فقد كانت نسبة الخطأ في التنبؤ افضل من التنبؤات اللاتي تمت المقارنة معهن بنسبة 7 %.

شهادة ماجستير علوم

جامعة الملك فهد للبترول والمعادن

الظهران ، المملكة العربية السعودية

NOMENCLATURE

B	Chisholm's parameter	(---
Bo	Bond number	(---
C	Chisholm Coefficient	(---
DR	Density Ratio, $\left(\frac{\rho_L}{\rho_G}\right)$	(---
d _i	Internal Diameter	(mm)
e _n	Percentage error	(---
Fr	Froude number	(---
f_{TP}	Two-phase friction factor	(---
f_{Lo}	Liquid phase friction factor	(---
G _T	total Mass flux, (G _L +G _G)	(kg.m ⁻² .s ⁻¹)
La	Laplace constant	(---
\dot{m}_G	Mass flow rate of gas	(kg.s ⁻¹)
\dot{m}_{total}	Total mass flow rate	(kg.s ⁻¹)
n	Exponent	(---
Re	Reynolds Number, $\left(\frac{G_T D}{\mu_L}\right)$	(---
S	Slip ratio	(---
u	Velocity	(ms ⁻¹)
ν_L	Specific volume of liquid	(m ³ .kg ⁻¹)

We_L	Liquid Weber	(---
X	Lockart-Martinelli parameter	(---
x	Quality	(---
Y	Ratio of the frictional pressure gradients	
	used in Chisholm correlation	(---

Gradients and differences

v_{LG}	Difference in specific volumes of saturated liquid and vapor, ($v_G - v_L$)	($m^3.kg^{-1}$)
$\left(\frac{dP}{dL}\right)_{TP}$	Two-phase frictional pressure drop	(---
$\left(\frac{dP}{dL}\right)_{LO}$	Single-phase frictional pressure drop	(Pa)

Greek Symbols

α	Void Fraction	(---
ε_1	Average Error	(---
ε_2	RMS Error	(---
ρ	Density	($kg.m^{-3}$)
ϕ_{Lo}^2	Two-phase frictional multiplier	(---
μ	Viscosity	($N.s.m^{-2}$)
v	Specific volume	(---
σ	Surface Tension	($N.m^{-2}$)
Ω	Two-phase frictional multiplier for chen (2001)	(---

Subscripts

Bf	Bankoff
Cha	Chawla
Ch	Chisholm
Exp.	Experiment
g	Gas phase
gd	Grönnerud
H	Homogenous
i	Internal
L	Liquid phase
LG	Liquid Gas
LO	Liquid Only
Pred.	Predicted
SP	Single phase
TP	Two-Phase
tt	Turbulent turbulent

CHAPTER 1

INTRODUCTION

Many engineering applications like oil transport, electric power generation, designing heat exchangers and refrigeration and air-conditioning applications need accurate prediction of two-phase frictional pressure drop which is an important parameter for the design of pipelines, evaporators...etc. In fact, the fluids inside the pipelines are exposed to a number of disturbances such as; transition from laminar to turbulent due to increase in flow rate, interaction between phases, deformation of the interfaces, sheer stress between phases and the channel wall, and the inclination of the pipelines from horizontal to vertical. These types of disturbances are enhancing to loss more and more from the total pipelines pressure.

Total pressure drop in two-phase flow system is generally due to gravitation, acceleration and friction. This can be expressed as

$$\left(\frac{dp}{dz}\right)_{Total} = \left(\frac{dp}{dz}\right)_{Frictional} + \left(\frac{dp}{dz}\right)_{Acceleration} + \left(\frac{dp}{dz}\right)_{Gravitaional} \quad (1)$$

Actually, gravitational and acceleration pressure drop can be easily tackled where the gravitational pressure drop depends on the void fraction within the pipe, and considers the pipe orientation. For the acceleration pressure drop, it happens for the case of evaporation and condensation, but in this study this term equal to zero because an adiabatic

experimental data have been used. But for frictional pressure drop, it is most important and difficult term to predict and requires tedious analysis due to existence the superficial friction between phases and the shear stress between phase and the channel wall.

Moreover, evaluation the pressure gradient components, frictional, acceleration, and gravitational, requires knowledge of such physical properties as the density and viscosity, and the flow parameters as the mass flux and the friction factor. For single-phase flow it is relatively easier to predict the friction factor than two-phase flow. The relationship between the friction factor and the Reynolds number and relative pipe roughness is well presented by the Moody friction factor, Fanning friction factor, and by many other investigators as will see later.

The complexity of the solution of the pressure gradient equations for two-phase flow arises from the above mentioned parameters. The correlations predict the pressure gradient in two-phase flow usually differ in the way these variables are defined or calculated. In this study, only one component from the total pressure gradient presented in Equation 1 have been considered which is the frictional pressure drop.

Other complexity in the frictional part arises from Two-Phase Friction Multiplier “ Φ_{LO}^2 ”. This term used for calculating two-phase friction pressure drop. Φ_{LO}^2 is a unique function of flow quality, pressure, mass flux and possibly heat flux or wall superheat if the flow channel is heated.

Generally, the two-phase frictional pressure drop is evaluated by

$$\left(\frac{dp}{dz}\right)_{TP} = \Phi_{LO}^2 \left(\frac{dp}{dz}\right)_{LO} \quad (2)$$

where:

$$\left(\frac{dp}{dL}\right)_{LO} : \text{is the single-phase liquid frictional pressure drop}$$

$$\Phi_{LO}^2 : \text{is the two-phase frictional multiplier.}$$

In practice there are two methods used to calculate two-phase frictional pressure drops. The first method utilizes the Homogeneous flow Model where a relation for wall shear stress, τ_w , and relative velocity between the phases is developed empirically. The other method is by using two-fluid or drift flux model where one uses the separated flow model for τ_w and substitutes the empirical relation for relative velocity by the complete solution of each phase momentum equation. Both methods result in obtaining Φ_{LO}^2 .

Numerous correlations predicted frictional pressure drop found in the literature and summarized in the chapter 2. The problem of these correlations is the limitation of usage. These correlations are specific for a certain ranges of application, and if these correlations applied for other application range a huge error may occurs. Regarding to Ould-Didi et al. [1], no models available in the literature are giving adequate prediction for all ranges of two-phase frictional pressure drops.

To overcome the large prediction errors of the correlations, the confusion in using the right correlation, the limited application range of the correlations ... etc, Look-Up Table (LUT) has been constructed from the best available correlations available in the literature. This LUT is a tool used to predict the two-phase frictional pressure drop multiplier as a function of density ratio (DR), Reynolds number (Re), and mass quality (x) for a flow in small to moderate pipe diameter with accuracy superseding existing prediction techniques. In fact, density ratio, Reynolds number, and mass quality are dimensionless numbers and assure the generality for the LUT for any data sets available. In addition to that, these dimensionless groups taken into consideration many physical properties and flow parameters such as; pressure, pipe diameter, kinematic viscosity, mass flux...etc.

In this study, six prediction correlations of two-phase frictional pressure drop have been selected based on [1] and evaluated against experimental data sets which are collected from different resources. Further statistical analyses are presented to nominate the best correlations among of them. After that, a skeleton table has been built based on the best correlations nominated in previous step. This table is updated with available experimental data and smoothed to obtain the final shape of Look-Up-Table.

CHAPTER 2

LITERATURE REVIEW

Two-phase flow is the simultaneous movement of two differing phases, where the phase refers to the state of the matter (i.e. solid, liquid or gas). Two-phase flows can occur as either single-component flow or two-component flow. Single component two-phase flows occur when both the phases are of the same chemical composition. This type of flow typically involves some sort of phase change such as melting or boiling. Two-component two-phase flow involves the simultaneous movement of two different phases with differing chemical compositions. Phase changes are generally not associated with two-component two-phase flow. It is towards the single-phase flow such as steam-water flow in an adiabatic flow channel.

As presented in Chapter 1, two-phase pressure drop is due to three components; frictional, gravitational, and acceleration. The main important component is the frictional. Two-phase frictional pressure drop is associated with the behavior and the interaction of the phases inside the channel wall. Many parameters play an important role on the amount of the frictional pressure drop such as; pressure, density, viscosity, mass flux, pipe diameter, friction factor...etc. other parameter such as; pipe orientation and phase change are not considered because they are related to the gravitational and acceleration pressure drop components. Many researchers tried to create a variable

which guaranteed satisfy prediction and contained all or some of the parameters mentioned above. This variable is known as two-phase pressure multiplier Φ_{LO}^2 . Collier and Thome [2] generated a formula based on homogeneous flow principle as shown in Equation 3.

$$\phi_{LO}^2 = \frac{dP/dL}{dP/dL_{LO}} = \frac{f_{TP}}{f_{LO}} \left(1 + x \frac{v_{LG}}{v_L} \right) \quad (3)$$

where:

f_{TP} : is the two-phase friction factor.

f_{LO} : is the liquid phase friction factor.

x : is the mass quality.

v_{LG} : is the difference in specific volumes of saturated liquid and vapor, $m^3.kg^{-1}$

v_L : is the specific volume of liquid, $m^3.kg^{-1}$

2.1. Frictional Pressure Drop for single-phase flow

As mentioned above many factors are affecting the frictional pressure drop like flow viscosity, flow velocity, roughness of pipe, and the characteristic length of channel...etc. By assuming that the flow is steady and incompressible, then the friction pressure drop for single-phase flow can be calculated using the Darcy-Weisbach equation involving a friction factor, f , hydraulic diameter, D_h , and the mean fluid velocity, U , as follows:

$$\left(\frac{dP}{dL}\right)_{F,SP} = \left(\frac{f}{D_h}\right)\left(\frac{\rho U^2}{2}\right) \quad (4)$$

where:

$\left(\frac{dp}{dL}\right)_{F,SP}$: is the single-phase frictional pressure drop

$D_h = \frac{4A}{P}$: Hydraulic diameter.

F : Friction factor.

ρ : Density (Kg.m^{-3})

The flow inside the channel can be laminar or turbulent. For laminar flow and by using Blasius equation, the friction factor, f , only depends on the Reynolds number.

$$f = \frac{16}{\text{Re}} \quad (5)$$

For turbulent flow, it depends not only on the Reynolds number but also on the relative roughness of the contact surface. Many researchers try to derive correlation for the friction factor for rough pipes. One of them, Nikuradse [3], performed experiments on some artificially rough pipes and derived a friction factor equation for rough pipes as

$$f^{0.5} = 1.14 - \left[2 \times \log\left(\frac{z}{D}\right) \right] \quad (6)$$

where:

$\frac{z}{D}$: is the relative roughness of pipe surface.

For smooth pipes, Blasius provided a friction factor expression written as

$$f = \frac{0.075}{\text{Re}^{0.25}} \quad (7)$$

Equation 7 is valid for Reynolds numbers from 3500 up to about 100000[2]. Another equation based on the data of commercial smooth pipes, Colebrook [4], presented the friction factor as

$$f^{-0.5} = -2 \times \log \left(\frac{z/D}{3.7} + \frac{2.51}{\text{Re} \sqrt{f}} \right) \quad (8)$$

Based on Equation 8, Moody [5] generated a graph that shows the friction factor as a function of Reynolds number and relative roughness. Since it is difficult to get information for the actual pipe roughness, the experimental data do not always fit the value obtained from both the Colebrook equation and the Moody chart.

The pressure gradient due to momentum exchange between wall-fluid for single-phase flows forms the basis of some models used for two-phase flows. Equation 9 represents the momentum balance for the mixture which is directly applicable to the single-phase flow case.

$$\frac{dP}{dL} = -\frac{1}{A_f} \frac{d}{dL} \left(\frac{W^2}{\rho A_f} \right) - \frac{1}{2} \left(\frac{P_w}{A_f} \right) f_w \frac{W|W|}{\rho A_f^2} - \rho g \sin \theta \quad (9)$$

where:

P_w : wetted perimeter (m) .

W : Mass rate of flow (Kg/sec).

A_f : flow area occupied by liquid phase (m^2).

The first and third terms in the right-hand side refers to momentum flux, and gravitational pressure drop, respectively. The momentum exchange between wall-fluid, the second term on the right-hand side of Equation 9, is the frictional pressure gradient for the flow, as shown in Equation 10.

$$\left(\frac{dP}{dL} \right)_{fw} = -\frac{1}{2} \left(\frac{4}{D_h} \right) f_w \frac{W|W|}{\rho A_f^2} \quad (10)$$

where:

$\left(\frac{dP}{dL} \right)_{fw}$: Frictional pressure gradient for the flow

f_w : is wall friction factor.

D_h : Hydraulic Diameter (m).

Many parameters like velocity of the fluid, geometry of the flow channel, and transport properties for the fluid are considered as factors affecting wall friction factor. The wall friction factor for laminar flow can be determined, in many cases, by the solution of the Navier-Stokes equations. For turbulent flows experimental data are needed to determine the friction factor as introduced earlier in this chapter.

For the case of a straight flow channel with parallel walls, it was found that the pressure acts normal to the wall and does not contribute to the forces acting on the

fluid relative to the flow direction. So that, the momentum exchange between wall-fluid is due only to shear forces acting at the wall-fluid interface.

2.2. Frictional Pressure Drop for Two-Phase Flow

The pressure drop for single-phase flow is considered as much lower than that for two-phase due to the presence of an inter-phase shear force between two fluids. Usually, many assumptions are introduced to simplify the complexity of two-phase flow. Many parameters are used by many researchers to describe two-phase in a flow field, the two-phase friction multiplier approach which account for the effects of the presence of a two-or-multi-phase mixture in a flow field is a general accepted engineering model for two-phase flow.

Among the earlier two-phase friction multiplier models and correlations are those by Martinelli and his coworkers [6-7], Thom [8], Dukler [9], Baroczy [10], and Chisholm [11]. More recent correlations include those of Reddy[12] and Friedel [18]. The performance of the earlier correlations has been summarized by Collier and Thome [2] and the performance of the earlier correlations against Friedel correlation has been summarized by Whalley [13]. Comparisons of the predictions of some of these correlations with experimental data will be discussed later.

2.2.1. Basic Equations of Two-Phase Flow

Many types of forces can occur while the fluid flows in the channel. Such forces are pressure force on the channel element, gravitational force, wall shear force between the phase and the channel wall, interfacial shear forces between the phases, and the rate of generation of momentum of each phase due to mass transfer. In fact, these types of forces are affecting the fluid distributions inside the channel. Then, if the flow pattern is unpredictable then, the fluctuation in pressure drop and density is taken into consideration.

A general form for the differential balance equation can be written by introducing the fluid density " ρ_k ", the flux " J_k ", and the body source " ϕ_k " of any quantity " ψ_k " defined for a unit mass as the following:

$$\frac{\partial \rho_k \psi_k}{\partial t} + \nabla \cdot (v_k \rho_k \psi_k) = -\nabla \cdot J_k + \rho_k \phi_k \quad (11)$$

The first term of the above equation is the time rate of change of the quantity per unit volume, whereas the second term is the rate of convection per unit volume. The right-hand side terms represent the surface flux and the volume source.

2.2.1.1. Conservation of Mass

The conservation of mass "continuity equation" states that in any steady state process, the rate at which mass enters a control volume is equal to the rate at which mass leaves the control volume. It can be expressed in a differential form by setting

$\phi_k = 0, \psi_K = 1, J_K = 0$. As an example of such simplifications Equation 11 are assumed no surface and volume sources of mass with respect to a fixed mass volume. Then, we obtain:

$$\frac{\partial \rho_k}{\partial t} + \nabla \cdot (\rho_k v_k) = 0 \quad (12)$$

Where t is time and v is the flow velocity vector field. If density " ρ " is constant, the mass continuity equation simplifies to a volume continuity equation:

$$\nabla \cdot v_k = 0 \quad (13)$$

2.2.1.2. Conservation of Momentum

The conservation of momentum can be obtained from Equation 11 by introducing the surface stress tensor T_k and the body force g_k , thus we set $\psi_k = v_k$, $\phi_k = g_k$, $J_k = -T_k = P_k I - J_K$. Where I is the unit tensor. Here we have split the stress tensor " T_k " into the pressure term and the viscous stress. In view of Equation 11 we have:

$$\frac{\partial \rho_k v_k}{\partial t} + \nabla \cdot (v_k \rho_k v_k) = -\nabla \cdot P_k + \nabla \cdot J_k + \rho_k g_k \quad (14)$$

2.2.1.3. Conservation of Energy

The balance of energy can be written by considering the total energy of the fluid. Thus

by setting $\psi_k = v_k + \frac{v_k^2}{2}$, $\phi_k = g_k \cdot v_k + \frac{q_k}{2}$, $J_k = q_k - T_k \cdot v_k$. Where v_k , q_k , \dot{q}_k represent the internal energy, heat flux and the bodyheating, respectively. It can be seen here that both the flux and the body source consist of the thermal effect and the mechanical effect. By substituting these variables into Equation 11, we have the total energy equation:

$$\frac{\partial \rho_k \left(v_k + \frac{v_k^2}{2} \right)}{\partial t} + \nabla \cdot \left(\rho_k \left(v_k + \frac{v_k^2}{2} \right) v_k \right) = -\nabla \cdot q_k + \nabla \cdot (T_k \cdot v_k) + \rho_k g_k \cdot v_k + \dot{q}_k \quad (15)$$

As a result, these three local equations, express the three basic physical laws of the conservation of mass, momentum, and energy. In order to solve these equations, it is necessary to specify the fluxes and the body sources as well as the fundamental equation of state.

2.3. Two-Phase Frictional Pressure Drop Models and Correlations

Several two-phase flow frictional pressure drop models have been developed. Each model is developed using assumptions of the physics of the flow, which are somehow adequate for a specific flow regime. However, models that accurately predict frictional pressure drop for all flow regimes without discontinuities could not be found in the literature. Many assumptions are introduced to simplify the complexity of two-phase flow and to investigate the two-phase frictional pressure drop. Two models will be considered. The first one is the homogeneous model which combines two phases in

one continuous phase with average properties and flow conditions. This model predicts the bubbly flow much better than the other flow regimes. The second model is the separated flow model which treats the two phases separately based on the assumption of two different phase velocities. It considers the phases moving separately in two streams with a distinct inter-phase boundary separating them. The separate flow model gives satisfactory results when the flow is stratified or annular.

Homogenous two-phase frictional pressure drop models have been developed for circular pipes such as the ones presented by [6-7, 14-18]. Those researchers developed frictional pressure gradient correlation for air-water system based on two-phase momentum energy balance in vertical and horizontal pipe flow. Isbin et. al. [19], Owens [20], and Cicchitti et. al. [21] methods can be regarded as variations of the homogeneous model.

Martinelli and Nelson [6] developed two-phase multiplier to relate the two-phase frictional pressure drop to equivalent flow single-phase frictional pressure drop. They also covered the estimation of the accelerative component and predict the pressure drop during forced circulation boiling and condensation for the adiabatic flow of low pressure air-water mixtures by assuming that the flow regime would always be turbulent for both phases. They established a relationship between Φ_{LO} and Lockhart and Martinelli parameter, X_{tt} , up to critical pressure level, and they were noting that as

the pressure is increased towards the critical point, the densities and viscosities of the phases become similar.

Lockhart and Martinelli Method [7] is one of the first methods developed for the two-phase liquid only multiplier (Φ_{LO}^2). Lockhart and Martinelli were working on a series of studies of isothermal two-phase two-component flow in horizontal tubes. These studies proposed a generalized method for calculating the frictional pressure gradient for isothermal two-component flow in a horizontal two-phase flow at low pressure. Also, they assumed that a definite portion of the flow area is assigned to each phase. And they came up to the following equation;

$$\phi_{Lo}^2 = 1 + \frac{C}{X} + \frac{1}{X^2} \quad (16)$$

where:

C : Chisholm Coefficient

X : Lockhart-Martinelli parameter

Friedel [22] introduced a correlation to improve friction pressure drop predictions for horizontal and vertical two-phase flow. Friedel's correlation is one of the most widely used correlations in predicting two-phase frictional pressure drop. It was obtained by optimizing an equation for Φ_{LO}^2 , by utilizing the Froude number (ratio of inertial to gravitational forces) and Weber number (ratio of inertial to surface tension forces),

based on approximately 25,000 adiabatic pressure drop data covering the following conditions corresponding to water:

Pressure: 20 – 21,200 kPa

Mass flux: 20 – 10,330 kg·m⁻²·s⁻¹

Quality: 0 - 1

Hydraulic diameter: 0.001 - 0.26 m

And his two-phase multiplier is

$$\phi_{LO}^2 = E + \frac{3.24 \times F \times H}{Fr^{0.045} We^{0.035}} \quad (17)$$

where:

E, F, H: defined in Table 1

Fr:Froude number

We: Weber Number

Chisholm[11]proposed an extensive empirical method applicable to a wide range of operating conditions. His two-phase frictional pressure drop multiplier is determined as;

$$\phi_{Ch}^2 = 1 + (Y^2 - 1) \left[Bx^{\left(\frac{2-n}{2}\right)} (1-x)^{\left(\frac{2-n}{2}\right)} + x^{2-n} \right] \quad (18)$$

where:

n: is the exponent from the friction factor expression of Blasius ($n = 0.25$)

B, Y: is the Chisholm's parameters which are defined in Table 1.

Muller-Steinhagen and Heck [23] produced correlation for two-phase flow, water-air, in pipes to predict the frictional pressure drop for two-phase flow in pipes. They compared their correlation results with fourteen correlations using data bank containing 9300 data points of frictional pressure drop for a variety of fluids and flow conditions as indicated in their paper [23]. Their correlation includes single-phase liquid and gas frictional pressure drop and predicts correctly the influence of flow parameters.

Grönnerud [24] developed two-phase frictional pressure drop correlation specifically for refrigerants. His correlation was based on liquid Froude number. His two-phase frictional pressure drop multiplier is determined as;

$$\Phi_{gd} = 1 + \left(\frac{dp}{dz} \right)_{Fr} \left[\frac{(\rho_L / \rho_G)}{(\mu_L / \mu_G)^{0.25}} - 1 \right] \quad (19)$$

where:

$\left(\frac{dp}{dz} \right)_{Fr}$: Frictional pressure gradient depends on the Froude number. More details in

Table 1.

Zhang et al. [25] explored a correlation for two-phase frictional pressure drop and void fraction based on separated flow and drift-flux model and based on data sets collected from the literature. Also they worked on two-phase friction multiplier and void fraction by correlating parameters such as, Chisholm parameters and the distribution parameter.

Beattie[26] derived two-phase friction equations depending basically on mixing length theory. These equations were compared with experimental data, this data taken from different resources, of five flow conditions; bubble flow, wavy gas-liquid interface, flow with very small bubbles, attached wall bubbles, and dry wall. The results from comparison were encouraging.

Chen et al.[27]investigated the effect of surface tension and mass flux on two-phase frictional pressure drop of air-water and R-410a in small horizontal tubes. Chen et al. correlation corrected for these effects using Webber number and Bond number. They condensed R410A at $(3-15)^{\circ}\text{C}$ in several horizontal tubes ranging between 3.17 and 9 mm i.d. for the mass fluxes of $(50-600) \text{ kg.m}^{-2}.\text{sec}^{-1}$, and studied the condensation of air–water at room temperature in several horizontal tubes ranging between 1.02 and 7.02 mm i.d. for the mass fluxes of $(50-3000) \text{ kg.m}^{-2}.\text{sec}^{-1}$.

Cavallini et al.[28]investigated the condensation heat transfer and pressure drop of new HFC refrigerants (R134a, R125, R32, R410A, R236ea) in a horizontal smooth

tube. In addition to that they studied the Condensation of halogenated refrigerants inside smooth tubes. In fact, their model was a modification for the Friedel's correlation to develop an annular flow model during the condensation in an 8 mm i.d. horizontal tube for the mass fluxes of $(100\text{--}750)\text{kg.m}^{-2}.\text{sec}^{-1}$ at saturation temperatures between 30 and 50 °C. As a result of the study, a model for predicting condensing heat transfer coefficient was developed by means of frictional pressure drop.

Mishima and Hibiki[29]proposed two-phase pressure drop correlation by modifying Lockhart and Martinelli equation. Mishima and Hibikiinvestigated two-phase frictional pressure drop for upward flow of air–water in small diameter 1–4 mm i.d. vertical tubes. Their model has limitations accounting for the superficial velocities of vapor and liquid of phases.

Wilson et al. [30]derived two-phase friction equations depending basically on Lockhart and Martinelli parameter (X).Wilson et al. performed an experiment for pressure drop and condensation heat transfer for R134a and R410A in several 1.84–7.79 mm i.d horizontal flattened round smooth, axial, and helical micro-fin-tubes for the mass fluxes between 75 and 400 $\text{kg.m}^{-2}.\text{sec}^{-1}$ at the saturation temperatures of 35 °C.

Tran et al. [31]proposed a pressure drop correlation by modifying Chisholm's correlation [11] to consider surface tension effects. An experimental investigation and correlation development for R134a, R12, and R113 during flow boiling in small

diameter horizontal circular (2.4, 2.46, and 2.92 mm) and rectangular (4.06-1.7 mm) tubes at boiling pressures between 138 and 836 KPa and for mass fluxes between 33 and 832 $\text{kg.m}^{-2}.\text{sec}^{-1}$.

Souza et al.[17]predicted the frictional pressure drop during horizontal two-phase flow of pure and mixed refrigerants. Souza et al. showed the effect of oil in R12 and R134a on the pressure drop in a hydraulic diameter of 10.9 mm horizontal flattened tube for the mass fluxes of (200–600) $\text{kg.m}^{-2}.\text{sec}^{-1}$.

Wang et al. [32] proposed two-phase pressure drop correlation by modifying Lockhart and Martinelli correlation. Wang et al. performed visual observation experiment to study the two-phase flow pattern of R22, R134a, and R407C in a 6.5 mm i.d smooth horizontal tube for mass fluxes of (50–700) $\text{kg.m}^{-2}.\text{sec}^{-1}$ at the condensing temperatures of 2.6–20 $^{\circ}\text{C}$.

Garimella [33-34]developed flow regime based modelfor intermittent and annular, mist, and disperse flow regimes. Garimella investigated the pressure drop and heat transfer in circular micro-channelsof R134a in 0.5–4.91 mm i.d. horizontal tubes at the condensing temperature of 52 $^{\circ}\text{C}$ for mass fluxes between 150 and 750 $\text{kg.m}^{-2}.\text{sec}^{-1}$.

Lee and Lee[35] found a correlations for two-phase multiplier for air–water flow within hydraulic diameter of (0.4-20 mm, 1.2-20 mm, 4-20 mm) rectangular horizontal

channel. Their model has limitations with the Reynolds number and Lockhart and Martinelli [7] parameter.

Table 1 shows a summary of the above mentioned correlations.

Table 1 Summary of Two-Phase frictional pressure Drop prediction Models and Correlations

References	Frictional Pressure Drop Models/Correlations	Remarks															
Homogenous	$\phi_{Lo}^2 = \left[1 + \frac{x(\rho_L - \rho_G)}{\rho_G} \right] \left[1 + \frac{x(\mu_L - \mu_G)}{\mu_G} \right]^{-0.25} \left(\frac{dP}{dL} \right)_{Lo} = \frac{2}{D} f_L \frac{G^2}{\rho_{2\phi}} \frac{1}{\rho_{2\phi}} = \frac{x}{\rho_G} + \frac{1-x}{\rho_L}$ $\mu_{2\phi} = x\mu_G + (1-x)\mu_L \text{ Re} = \frac{GD}{\mu_{2\phi}} \text{ Re} < 2000 \Rightarrow f_L = \frac{16}{\text{Re}} \text{ Re} > 2000 \Rightarrow f_L = C_L (\text{Re})^{-n}$	- C, m, and n are the Blasius constant.															
Lockhart and Martinelli (1949)	$\left(\frac{dP}{dL} \right)_{TP,L} = \phi_{Lo}^2 \left(\frac{dP}{dL} \right)_{Lo} \left(\frac{dP}{dL} \right)_{TP,G} = \phi_{Go}^2 \left(\frac{dP}{dL} \right)_{Go} \left(\frac{dP}{dL} \right)_{Lo} = \frac{2}{D} f_L \frac{(1-x)^2 G^2}{\rho_L}$ $\left(\frac{dP}{dL} \right)_{Go} = \frac{2}{D} f_G \frac{x^2 G^2}{\rho_G} \phi_{Lo}^2 = 1 + \frac{C}{X} + \frac{1}{X^2} \phi_{Go}^2 = 1 + CX + X^2 \quad X = \left(\frac{1-x}{x} \right)^{0.9} \left(\frac{\rho_G}{\rho_L} \right)^{0.5} \left(\frac{\mu_L}{\mu_G} \right)^{0.1}$ $\text{Re}_L = \frac{GD}{\mu_L} \text{ Re}_G = \frac{GD}{\mu_G} \text{ Re}_L > 2000 \Rightarrow f_L = C_L (\text{Re}_L)^{-n}$ $\text{Re}_L < 2000 \Rightarrow f_L = \frac{16}{\text{Re}_L} \text{ Re}_G > 2000 \Rightarrow f_G = C_G (\text{Re}_G)^{-n} \text{ Re}_G < 2000 \Rightarrow f_G = \frac{16}{\text{Re}_G}$	<p>-The value of C depend on the regimes of the liquid and Gas as follow:</p> <table border="1"> <thead> <tr> <th>Liquid</th> <th>Gas</th> <th>C</th> </tr> </thead> <tbody> <tr> <td>Turbulent</td> <td>Turbulent</td> <td>20</td> </tr> <tr> <td>Laminor</td> <td>Turbulent</td> <td>12</td> </tr> <tr> <td>Turbulent</td> <td>Laminor</td> <td>10</td> </tr> <tr> <td>Laminor</td> <td>Laminor</td> <td>5</td> </tr> </tbody> </table> <p>-L-M is applicable for $0 < x \leq 1$ - C, m, and n are the Blasius constant.</p>	Liquid	Gas	C	Turbulent	Turbulent	20	Laminor	Turbulent	12	Turbulent	Laminor	10	Laminor	Laminor	5
Liquid	Gas	C															
Turbulent	Turbulent	20															
Laminor	Turbulent	12															
Turbulent	Laminor	10															
Laminor	Laminor	5															
Friedel (1979)	$\left(\frac{dP}{dL} \right)_{TP,L} = \phi_{Lo}^2 \left(\frac{dP}{dL} \right)_{Lo} \left(\frac{dP}{dL} \right)_{Lo} = \frac{2}{D} f_L \frac{G^2 (1-x)^2}{\rho_L} \quad \phi_{Lo}^2 = E + \frac{3.24 \times F \times H}{Fr^{0.045} We^{0.035}}$ $E = (1-x)^2 + \left(x^2 \frac{\rho_L f_G}{\rho_G f_L} \right) F = x^{0.78} (1-x)^{0.224}, \quad We = \frac{G^2 D}{\sigma \times \rho_{2\phi}} \quad Fr = \frac{G^2}{g D \rho_{2\phi}^2}$ $H = \left(\frac{\rho_L}{\rho_G} \right)^{0.91} \left(\frac{\mu_G}{\mu_L} \right)^{0.19} \left(1 - \frac{\mu_G}{\mu_L} \right)^{0.7} \quad \rho_{2\phi} = \left(\frac{x}{\rho_G} + \frac{1-x}{\rho_L} \right)^{-1}$	<p>-It is applicable for $0 \leq x \leq 1$ - it is recommended when $\frac{\mu_L}{\mu_G} < 1000$ - C, m, and n are the Blasius constant. -Reynolds number and friction factor as presented in Lockhart-Martine lli Correlation.</p>															
Chisholm (1973)	$\left(\frac{dP}{dL} \right)_{TP,L} = \left(\frac{dP}{dL} \right)_{Lo} \phi_{Ch}^2 \left(\frac{dP}{dL} \right)_{TP,G} = \left(\frac{dP}{dL} \right)_{Go} \phi_{Ch}^2 \left(\frac{dP}{dL} \right)_L = \frac{2 f_L G^2}{D \cdot \rho_L} \left(\frac{dP}{dL} \right)_{Go} = \frac{2 f_G G^2}{D \cdot \rho_G}$	<p>-It is applicable for $0 \leq x \leq 1$ - C, m, and n are the Blasius constant. -Reynolds number and friction</p>															

References	Frictional Pressure Drop Models/Correlations	Remarks
	$\phi_{Ch}^2 = 1 + (Y^2 - 1) \left[Bx^{\left(\frac{2-n}{2}\right)} (1-x)^{\left(\frac{2-n}{2}\right)} + x^{2-n} \right]$ $Y = \sqrt{\frac{\left(\frac{dP}{dL}\right)_{GO}}{\left(\frac{dP}{dL}\right)_{LO}}}$ $0 < Y < 9.5 \quad 9.5 < Y < 28 \quad Y > 28$ $B = \frac{55}{G^{0.5}}, G \geq 1900 \quad B = \frac{250}{YG^{0.5}}, G \leq 600 \quad B = \frac{15000}{Y^2 G^{0.5}}$ $B = \frac{2400}{G}, 500 < G < 1900 \quad B = \frac{21}{Y}, G > 600$ $B = 4.8, G < 500$	factor as presented in Lockhart-Martinelli Correlation.
Muller-Steinhagen and Heck (1986)	$\left(\frac{dP}{dL}\right)_{TP} = G(1-x)^{\frac{1}{3}} + Bx^3, \quad B = \left(\frac{dP}{dL}\right)_{GO} = \frac{2f_G G^2}{D \cdot \rho_G}, \quad A = \left(\frac{dP}{dL}\right)_{LO} = \frac{2f_L G^2}{D \cdot \rho_L}$	-It is applicable for $0 \leq x \leq 1$ - C, m, and n are the Blasius constant. -Reynolds number and friction factor as presented in Lockhart-Martinelli Correlation.
Grönnerud (1972)	$\left(\frac{dP}{dL}\right)_{TP,L} = \left(\frac{dP}{dL}\right)_{LO} \phi_{gd}^2 \left(\frac{dP}{dL}\right)_{LO} = \frac{2f_L G^2 (1-x)^2}{D \cdot \rho_L} \phi_{gd} = 1 + \left[\frac{dP}{dL}\right]_{Fr} \left[\frac{\left(\frac{\rho_L}{\rho_G}\right)}{\left(\frac{\mu_L}{\mu_G}\right)^{0.25}} - 1 \right]$ $\left[\frac{dP}{dL}\right]_{Fr} = f_{Fr} \left[x + 4 \left(x^{1.8} - x^{10} f_{Fr}^{0.5} \right) \right] Fr_L = \frac{G^2}{g \cdot d_i \cdot \rho_L^2}, Fr_L < 1 \dots f_{Fr} = Fr_L^{0.3} + 0.0055 \left(\ln \left(\frac{1}{Fr_L} \right) \right)^2$ $Fr_L = \frac{G^2}{g \cdot d_i \cdot \rho_L^2}, Fr_L \geq 1 \dots f_{Fr} = 1$	-It is applicable for $0 \leq x < 1$ -Reynolds number and friction factor as presented in Lockhart-Martinelli Correlation.

References	Frictional Pressure Drop Models/Correlations	Remarks
Banko ff (1960)	$\left(\frac{dP}{dL}\right)_L = \left(\frac{dP}{dL}\right)_{Lo} \phi_{Bf}^{\frac{7}{4}} \left(\frac{dP}{dL}\right)_{Lo} = \frac{f_{Lo} G^2}{2.d_i \rho_L} \alpha = \frac{0.71 + 2.35 \left(\frac{\rho_G}{\rho_L}\right)}{1 + \left(\frac{1-x}{x}\right) \left(\frac{\rho_G}{\rho_L}\right)} \text{Re}_G = \frac{G d_i}{\mu_G} \text{Re}_L = \frac{G d_i}{\mu_L}$ $\phi_{Bf} = \frac{1}{1-x} \left[1 - \alpha \left(1 - \frac{\rho_G}{\rho_L} \right) \right]^{\frac{3}{7}} \left[1 + x \left(\frac{\rho_L}{\rho_G} - 1 \right) \right]$	
Chawla (1967)	$\left(\frac{dP}{dL}\right)_L = \left(\frac{dP}{dL}\right)_G \phi_{Cha} \left(\frac{dP}{dL}\right)_{Go} = \frac{f_{Go} G^2}{2.d_i \rho_G} \phi_{Cha} = x^{1.75} \left[1 + S \left(\frac{1-x}{x} \cdot \frac{\rho_G}{\rho_L} \right) \right]^{2.375}$ $S = \frac{U_G}{U_L} = \frac{1}{9.1 \left[\left(\frac{1-x}{x} \right) (\text{Re}_G \cdot Fr_H)^{-0.167} \left(\frac{\rho_L}{\rho_G} \right)^{-0.9} \left(\frac{\mu_L}{\mu_G} \right)^{-0.5} \right]} Fr_H = \frac{G^2}{g.d_i \rho_{TP}^2}$	
Chen (2001)	$\left(\frac{dP}{dL}\right)_L = \left(\frac{dP}{dL}\right)_{friedel} \Omega \Omega = \begin{cases} \frac{0.0333 \text{Re}_{Lo}^{0.45}}{\text{Re}_g^{0.09} (1 + 0.4 \exp(-Bo))}, Bo < 2.5 \\ \frac{We^{0.2}}{(2.5 + 0.6Bo)}, Bo \geq 2.5 \end{cases} We \frac{G^2 d}{\sigma \cdot \rho_{TP}}$ $Bo = g(\rho_L - \rho_G) \left(\frac{\left(\frac{d}{2}\right)^2}{\sigma} \right)$	
Cavallini (2002)	$\left(\frac{dP}{dL}\right)_L = \left(\frac{dP}{dL}\right)_{Lo} \phi_{LO}^2 \phi_{LO}^2 = E + \frac{1.262 F.H}{We^{0.1458}} E = (1-x)^2 + \left(x^2 \frac{\rho_L f_G}{\rho_G f_L} \right) F = x^{0.6978} We = \frac{G^2 d_i}{\sigma \cdot \rho_{AVE}}$ $H = \left(\frac{\rho_L}{\rho_G} \right)^{0.3278} \left(\frac{\mu_G}{\mu_L} \right)^{-1.181} \left(1 - \frac{\mu_G}{\mu_L} \right)^{3.477}$	

References	Frictional Pressure Drop Models/Correlations	Remarks
Mishima and Hibiki (1997)	$\left(\frac{dP}{dL}\right)_L = \left(\frac{dP}{dL}\right)_{LO} \phi_{LO}^2 \phi_L^2 = 1 + \frac{C}{X} + \frac{1}{X^2} \quad C = 21(1 - e^{-0.319d})$	X: calculated from L-M
Wilson et al. (2003)	$\left(\frac{dP}{dL}\right)_L = \left(\frac{dP}{dL}\right)_{LO} \phi_{LO}^2 \phi_{Lo}^2 = 12.82 X_u^{-1.47} (1-x)^{1.8} \quad X_u = \left(\frac{\rho_G}{\rho_L}\right)^{0.5} \left(\frac{\mu_L}{\mu_G}\right)^{0.1} \left(\frac{1-x}{x}\right)^{0.9}$	
Tran et. al. (2000)	$\left(\frac{dP}{dL}\right)_L = \left(\frac{dP}{dL}\right)_{LO} \phi_{LO}^2 \phi_L^2 = 1 + (4.3Y^2 - 1)x^{0.875} La + x^{1.75} \quad La = \frac{\left[\frac{\sigma}{g(\rho_L - \rho_G)}\right]^{0.5}}{d}$	$\left(\frac{dP}{dL}\right)_{LO}$: Calculated from Chisholm
Souza et al. (1995)	$\left(\frac{dP}{dL}\right)_L = \left(\frac{dP}{dL}\right)_{LO} \phi_{LO}^2 \phi_L^2 = \left\{ \begin{array}{l} 1.376 + C_1 X_u^{-C_2}, \\ Fr_L < 0.7 \left\{ \begin{array}{l} C_1 = 4.172 + 5.48 Fr_L \\ C_2 = 1.773 - 0.169 Fr_L \end{array} \right\} \\ Fr \geq 0.7 \left\{ \begin{array}{l} C_1 = 7.242 \\ C_2 = 1.655 \end{array} \right\} \end{array} \right\} \quad Fr_L = \frac{G}{\rho_L \sqrt{gd}}$ $\left(\frac{dP}{dL}\right)_{LO} = \frac{f_L G^2 (1-x)^2}{2.d.\rho_L} \frac{1}{\sqrt{f_L}} = -2Log \left(\frac{\left(\frac{\varepsilon}{d}\right)}{3.7} + \frac{2.51}{Re_L \sqrt{f_L}} \right) \quad Re_L = \frac{Gd(1-x)}{\mu_L}$	
Wang et. al. (1997)	<p>-For $G > 200 \frac{kg}{m^2 \cdot sec}$, $C = 4.566 * 10^{-6} X^{0.128} Re_{Lo}^{0.938} \left(\frac{\rho_L}{\rho_G}\right)^{-2.15} \left(\frac{\mu_L}{\mu_G}\right)^{5.1}$, $Re_L = \frac{Gd}{\mu_L}$,</p> $\phi_L^2 = 1 + \frac{C}{X} + \frac{1}{X^2}, \quad \left(\frac{dP}{dL}\right)_L = \left(\frac{dP}{dL}\right)_{LO} \phi_{LO}^2$ <p>-For $G < 200 \frac{kg}{m^2 \cdot sec}$, $\phi_g^2 = 1 + 9.4 X^{0.62} + 0.564 X^{2.45}$, $\left(\frac{dP}{dL}\right)_L = \left(\frac{dP}{dL}\right)_{GO} \phi_{GO}^2$,</p>	$\left(\frac{dP}{dL}\right)_{go}$ & $\left(\frac{dP}{dL}\right)_{Lo}$ Calculated from L-M.

References	Frictional Pressure Drop Models/Correlations	Remarks
Garimella (2005)	$\left(\frac{dP}{dL}\right)_L = \frac{1}{2} f_{int} \frac{G^2 x^2}{\rho_g \alpha^{2.5}} \frac{1}{d}, \alpha = \left[1 + \left(\frac{\rho_G}{\rho_L}\right)^{0.65} \left(\frac{\mu_L}{\mu_G}\right)^{0.13} \left(\frac{1-x}{x}\right)^{0.74} \right], \text{Re}_L = \frac{Gd(1-x)}{\mu_L(1+\sqrt{\alpha})},$ $\text{Re}_g = \frac{Gdx}{\mu_g \sqrt{\alpha}}, f = \frac{64}{\text{Re}} \text{ (Laminor)}, \psi = \frac{j_L \mu_L}{\sigma}, f = \frac{0.316}{\text{Re}^{0.25}} \text{ (Turbulent)},$ $\left(\frac{dP}{dL}\right)_{Lo} = \frac{f_{Lo} G^2 (1-x)^2}{2.d_i \cdot \rho_L}, \left(\frac{dP}{dL}\right)_{go} = \frac{f_{go} G^2 x^2}{2.d_i \cdot \rho_G}, X = \left[\frac{\left(\frac{dP}{dL}\right)_{Lo}}{\left(\frac{dP}{dL}\right)_{Go}} \right]^{0.5}, j = \frac{G(1-x)}{\rho_L(1-\alpha)},$ $\frac{f_{int}}{f_L} = A x^a \text{Re}_L^b \psi^c, \text{ For } \text{Re}_L < 2100 \quad A = 1.308 * 10^{-0.3}, a = 0.4273, b = 0.9295,$ $c = -0.1211$	
Lee and Lee (2001)	$\left(\frac{dP}{dL}\right)_L = \left(\frac{dP}{dL}\right)_L \phi_L^2 \phi_L^2 = 1 + \frac{C}{X} + \frac{1}{X^2}, C = A \lambda^a \text{Re}_L^s \psi^r, \lambda = \frac{\mu_L^2}{\rho_L \sigma d}, \psi = \frac{\mu_L j}{\sigma}$	

2.4.Experimental Work Done on Two-Phase frictional Pressure Drop

McMillan [36] did a study of flow patterns and pressure drop in horizontal two-phase flow. An experiment was performed using R-11. The data obtained was used to verify the prediction of Lockhart and Martinelli correlations.

Kasturi et al.[37] run an experiment to measure the pressure drop and the void fraction for two-phase concurrent flow of air-water, air-corn-suger-water solution, air-glycerol-water solution, and air-butanol-water solution in a helical coil of 12.5 mm. Three correlations were chosen to compare data with (e.g. Lochkart-Martinelli, Dukler, and Hughmark correlations). The results of air-water showed good agreement with L-M correlation. Poor agreement was found comparing with Dukler, Hughmark correlation.

The data set obtained from Beggs et al. [38] was recorded using a test section with a diameter of 1.0- and 1.5-in, smooth, with liquid viscosity of 0.78-1.40 cp, using air and water as the working fluid. Void fraction measurements were conducted by using a pneumatically actuated, and quick closing ball valves. In their (1973) paper, Beggs et al. estimate their experimental standard deviation in void fraction measurements to be 7.98%. A total of 188 data points used for the purposes of direct comparison with inclination angle varies as (10, 5, 0,-5,-10) degree.

Mukherjee [39] recorded his experimental data using 1.5 in pipe with air-water, and air-kerosene as the working fluids. Once again, pneumatically actuated ball valves

served as the method of void fraction data collection. A total of 213 data points was recorded with inclination angles (-5, 0, 5) degree.

Hashizume [40] recorded his 170 data points with a 10 mm horizontal tube with R12 and R22 as the working fluid. He used quick closing valves to measure void fraction. Uncertainty analysis of the data obtained was not presented in this paper. Data on flow pattern, void fraction and pressure drop have been obtained for range of saturation pressure of 5.7 to 19.6 bar. For R12 and R22, the relation of mass quality with respect to void fraction and pressure drop at different values of flow rate is directly proportional.

Vijayarangan et al. [41] measured two-phase frictional pressure drop for R-134a in a vertical tube of 12.7 mm and 3 m length. They compared the experimental data with homogenous and separated flow model. Also they compared it with flow pattern method. They found that the flow pattern-based approach is the best model.

Andritsos et al. [42] recorded their 535 data points with a 0.99- and 3.75-in (2.52-9.53) cm horizontal pipe with air-water and air-Glycer as the working fluids. The liquid viscosity was varied from 1 to 80 cP.

Ebner et al. [43] run an experiment for horizontal air-water flow in a Perspex pipe having an inside diameter of 0.05 m and length of 5.08 m. Ebner et al. constructed flow pattern map and proposed an empirical pressure drop correlation.

Hashizume et al. [44] compared the data from paper of Hashizume [40] with air-water and water-steam system. They made a correction for the surface roughness equation and they made an interpolation in the small quality region. They found that a good agreement between this analyses and experimental data.

Klausner [45] studied the influence of gravity on pressure drop and heat transfer in flow boiling of R-11 in a vertical upflow, vertical down flow, and horizontal flow configurations. A mechanistic flow boiling heat transfer correlation was proposed.

Abdul-Majeed [46] conducted an experiment in order to simplify and improve the performance the mechanistic model developed by Taitel and Dukler and to come up with new model. Liquid hold up was estimated using an air-kerosene mixture flow through a test section consisting of a horizontal pipe 50.8 mm in diameter and 36 m long. The proposed model gives excellent results against 111 points.

Aube [47] studied the influence of surface heating on frictional pressure drop for single and two-phase flows by running an experiment for two different tube diameters and for pressure ranges of 10 and 45 bars.

Ekberg et al. [48] conducted an experiment to predict two-phase flow regimes, void fraction and pressure drop in horizontal, narrow, concentric annuli. Two transparent test sections, one with inner and outer diameters of 6.6 and 8.6 mm and an overall length of 46.0 cm; the other with 33.2 and 35.2 mm diameters and 43.0 cm length, respectively, were used. The correlation of Friedel was found to provide the best overall agreement with the data.

Triplett et al. [49] investigated the void fraction and the frictional pressure drop in circular channel of 1.1 and 1.45 mm inner diameters they found that after comparing the experimental data with available correlations that the Homogenous model provide best prediction in bubbly and slug flow.

Angeli et al. [50] conducted an experiment in horizontal test section made of steel with 24.3 mm ID and acrylic has 24 mm ID. Their main finding that the difference in tube material cannot be explained without the roughness term.

Spedding et al. [51] conducted an experiment for two-phase upflow in vertical and near vertical. Spedding et al. came up with new relations predicts holdup and transitions between flow regimes. They found that, the liquid holdup for near vertical flow was greater than for vertical upflow. And the total pressure drop was greater for near vertical flow compared with the vertical upflow case.

Ottens et al. [52] conducted an experiment for nearly-horizontal of 0.052 m internal diameter and 22 m length. Ottens et al. tested the predictive capability of new f -relation against several f -relations from the literature. And they recommended some of the correlations performed better than other. They found that the f . model based on the interfacial wave velocity gives best prediction of both the liquid hold-up and the frictional pressure gradient.

Warrier et al. [53] conducted an experiment for single-phase forced convection and subcooled and saturated nucleate boiling which performed in horizontal small rectangular channel of hydraulic diameter equal 0.75 mm. A correlation had been proposed for two-phase frictional pressure drop under subcooled and saturation nucleate boiling conditions.

Ould Didi et al. [1] run an experiment to measure two-phase frictional pressure drop for evaporation in two horizontal test sections of 10.92 and 12.00 mm diameter for five refrigerant. They manage to developed a new heat transfer model, and two-phase flow pattern map.

Pehlivan [54] performed an experiment to study the two-phase air-water flow regimes and frictional pressure drop in Mini- and Micro-channels. A three different circular test sections, with diameters of 3 mm, 1 mm and 800 μm , were used to study the two-phase frictional pressure drop and flow regime transition regions.

Nualboonrueng et al. [55] studied two-phase frictional pressure drop of R-134a during condensation in horizontal copper smooth tube of 9.52 mm diameter and 2.5 m long. Nualboonrueng et al. found that as average quality increase and mass flux the frictional pressure drop will increase. And as condensation temperature increase the pressure drop will decrease. Also, they came up with new correlation.

Recently, some of the literature, Chakrabarti et al. [56] seek to determine frictional pressure drop in Liquid-liquid two phase horizontal flow. Chakrabarti et al. run an experiment to investigate the frictional pressure drop characteristics for the flow of kerosene-water mixture through a horizontal pipe of 0.025 m diameter. Different combinations of flow regimes such that smooth stratified, wavy stratified, three layer flow, plug flow and oil dispersed in water, and water flow patterns. The superficial velocities were ranging from 0.03-2 m.s⁻¹. They developed a model to consider the energy minimization and pressure equalization of both phases. The results obtained from this model have yielded an accuracy of $\pm 10\%$ for regimes where fragmented droplets of one phase do not appear. For smooth stratified and stratified wavy regimens the results agree closely with the experimental data for Lovick and Angeli [57].

Vassallo et al. [14] conducted an experiment to predict an adiabatic two-phase frictional multipliers for R-134a flowing in 4.8 mm diameter. They compared their data with many correlations (Lockhart-Martenilli, Chisholm B-coefficient, Homogenous model) to assess their predictive capabilities. They found that the data was tended

towards homogenous flow as the pressure and flow rate are increased. Also, they found that the homogenous model is the best model among the other especially at the high pressure.

Field et al. [58] performed an experiment in a rectangular channel with $D_h = 148.0 \mu\text{m}$ with four refrigerants: R134a, R410A, propane (R290), and ammonia (R717). For validation, the measured frictional pressure drops have been compared to many published separated flow and homogeneous frictional pressure drop models. Field et al. proposed a new correlation for C , the Chisholm parameter, based on the Reynolds number of the vapor phase and the dimensionless grouping ψ for adiabatic two-phase frictional pressure drop of refrigerants in small channels.

Quiben et al. [59-60] conducted an experimental and analytical study, for diabatic and adiabatic flow condition in horizontal tubes, to obtain an accurate prediction for two-phase frictional pressure drop over a wide range of experimental conditions.

Saisorn et al. [61-62] performed an experiment for a channel of fused silica, 320 mm long, with an inside diameter of 0.53 mm. the data taken from the experiment was compared with homogenous model, and they found that the homogenous model is suitable. A new correlation produced of two-phase frictional multiplier from the micro channel case.

Shannak [63] conducted an experiment of air-water two-phase frictional pressure drop of vertical and horizontal smooth and rough pipes. He found that as the relative roughness increased, the frictional pressure drop increased. He also proposed a new prediction model for frictional pressure drop of two-phase flow in pipes.

Kawahara et al. [64] conducted an adiabatic experiment to investigate the effects of liquid (water-ethanol) properties on the characteristics of two-phase flow in horizontal circular microchannel of 250 and 500 μm .

Alizadehdakhel et al. [65] studied the two-phase flow regimes and frictional pressure drop by collecting a large number of experiments in a 20 mm diameter and 6 m length tube.

Dutkowski [66] run an experiment to investigate the frictional pressure drop in two-phase air-water adiabatic flow in minichannels made from stainless steel of 1.05-2.30 mm internal diameter and the length of test section of 300 mm. they found that the available prediction correlation gives poor results, and some corrections and modifications is needed for minichannels case.

Su et al. [67] investigated the frictional pressure drop for nitrogen in a three different kinds of stainless steel microchannels with diameter of 0.56, 1.00, and 1.80 mm. after testing the homogenous model and separated flow model, they found that those model

failed to predict the experimental results due to special operation condition. Therefore, a new correlation was developed in form of Lochkart-Martenilli.

Thome et al. [68] performed an experiment for studying two-phase frictional pressure drop in adiabatic horizontal circular smooth U-Bends and straight pipe for R-134a in 13.4 mm pipe diameter.

A summary of data collected from some of the above mentioned experimental work which used later on for the purposes of direct comparison in the horizontal, slightly inclined, and vertical pipe, as shown in Table 2.

Table 2 Data Collected

No.	Reference	Geometry	Data taken from	Channel Material	Length of test section	Working Fluids	Flow Orientation	Diameter (mm)	Pressure "P"(MPa)	Mass Flux "G" (Kg/m ² .sec)	Mass Quality "x"	No. of Data Point
1	McMillan (1963)	Circular	Table	Glass	8 ft	R-11	Hor.	46.66	0.1655	81.88- 401	0.13- 0.778	115
2	Hashizume (1983)	Circular	Table	Copper	2000 mm	R22, R12	Hor.	10	0.567-1.215	88-354	0.09-0.81	85
							Hor.	10	0.567-1.215	88- 354	0.08-0.81	85
3	Müller-Steinhagen and Heck (1986)	Circular	Figure	---	---	R12,	Hor.	14	0.30451	130-240	0.0-0.9923	17
						Water-Air	Ver.	26, 36, 50, 84	0.12-0.16	200	0.099-0.903	18
						Argon	Hor.	14	0.141-1.96	120-1000	0.01-0.91	56
4	Stanislav et al. (1986)	Circular	Figure	Acrylic	24 m	Air-Oil	Hor., Inclined	25.8	0.35	26-1180	0.0-0.173	151
5	Hashizume and Ogawa (1987)	Circular	Figure	---	---	Steam-Water	Hor.	29.5	3.00-11.00	340-920	0.0 - 0.53	69
6	Ebner et al. (1987)	Circular	Figure	Perspex	1.91 m	Air-Water	Hor.	50	0.06-0.25	12.00-2085	0.0-0.602	197
7	Klausner (1989)	Circular	Table	Copper	1.48 m	R-11	Ver.	19.1	0.134-0.25	123- 413	0.052-0.557	142
							Hor.	19.1	0.137-0.28	114- 407	0.065- 0.868	152
8	Aubé (1997)	Circular	Table	Inconel	3.59 m	Steam-Water	Ver.	13.4	3.59	4500-6050	0.02-0.2	84
9	Tran et al. (2000)	Circular	Figure	Brass	914 mm	R-134a	Hor.(Heated)	2.46	0.835	52-475	0.24-0.902	79
				Brass	914 mm	R-12	Hor.(Heated)	2.46	0.824	69-704	0.22-0.94	105
10	Ottens et al. (2001)	Circular	Table	Glass	22 m	Water-Air	Hor.(Heated)	52	0.1	150-1514	0.004-0.07	112
11	Ould Didi et al. (2002)	Circular	Figure	Copper	3.013 m	R134a	Hor.(Heated)	10-12	0.31-0.77	100-300	0.047-0.941	45
						R123	Hor.(Heated)	12	0.1123	300	0.0865-0.214	3
						R402A	Hor.(Heated)	12	0.71708	318	0.137-0.47	13
						R404A	Hor.(Heated)	12	0.659	318	0.142-0.597	10
						R502	Hor.(Heated)	12	0.609	300	0.129-0.614	7
12	Pehlivan (2003)	Circular	Table	Glass	200 mm	Air-Water	Hor.	3.00	0.0102-0.193	235.7-1209.8	0.012- 0.348	70
13	Nualboonrueng and Wongwises (2004)	Circular	Figure	Copper	2.5 m	R-134a	Hor. (Heated)	9.52	0.77-1.017	400-800	0.106-0.7811	34
							Hor. (Heated)	9.52	0.77-1.017	400-800	0.13-0.805	32

No.	Reference	Geometry	Data taken from	Channel Material	Length of test section	Working Fluids	Flow Orientation	Diameter (mm)	Pressure "P"(MPa)	Mass Flux "G" (Kg/m ² .sec)	Mass Quality "x"	No. of Data Point
14	Vassallo and Keller (2006)	Rec. Duct	Figure	Fused Silica	1.2 m	R-134a	Ver.	4.8	0.9-2.41	510- 2040	0.0- 0.716	143
15	Vijayarangan et al. (2007)	Circular	Figure	S. Steel	3.00 m	R-134a	Ver. (Heated)	12.7	0.416-0.964	1200-2000	0.111-0.972	114
16	Moreno Quibén and Thome (2007)	Circular	Figure	Copper	989 mm, 980 mm	R134a	Hor.(Heated)	13	0.352	150-300	0.018-0.956	85
						R22	Hor.(Heated)	13	0.585	150-600	0.014-0.994	218
						R410A	Hor.(Heated)	8.00-13.00	0.937	200-600	0.0232-0.987	228
17	Field and Hrnjak (2007)	Rectangular Duct	Figure	Aluminum	1.22 m	R-134a	Hor.	0.148	0.692	290	0.116- 0.732	7
						R410A	Hor.	0.148	1.75	450	0.034- 0.922	8
						Propane	Hor.	0.148	0.973	330	0.177- 0.865	10
						Ammonia	Hor.	0.148	1.0161	440	0.0723-0.961	10
18	Shannak (2008)	Circular	Figure	S. Steel	5.9 m	Air-Water	Ver.	52.5	0.8	480-930	0.0188-0.841	65
					9.6 m		Hor.	52.5	1.4	510- 700	0.0-0.879	77
19	Cavallini et al. (2009)	Square Cross Section	Figure	---	1.13 m	R-134a	Hor.	1.4	1.017	400-1000	0.252-0.77	13
						R236ea	Hor.	1.4	0.32	200-600	0.28- 0.809	10
						R410A	Hor.	1.4	2.43	600-1400	0.26- 0.744	9
20	Alizadehdakhel et al. (2009)	Circular	Figure	Glass	3.00 m	Air-Water	Hor.	19.3	0.1	64-654	0.0-0.6	53

2.5. Previous work done on Look-Up-Table

The application of the look-up table approach is widely recognized for both critical heat flux and film boiling heat transfer coefficient predictions. So, the LUT which predicts adiabatic two-phase frictional pressure drop does not exist. The LUT methodology is considered to be the same and the only variations between the tables are the values to be predicted and the dimensions of the table.

Groeneveld et al. [69] presented a LUT for predicting the critical heat flux of water. The CHF values for an 8-mm ID, water-cooled tube at 21 pressures, 20 mass fluxes, and 23 qualities for a vertical flow in single tube geometry. The prediction accuracy of the CHF-LUT is about 4% (based on root-mean square (RMS)) which is better than any other available prediction model. Correction factors were derived to account for different flow configurations.

In parallel to Groeneveld et al. work on the CHF-LUT, El Nakla et al. [70] established two versions of the look-up table to predict film boiling heat transfer coefficient for flow in 8 mm tubes. More than 70,000 experimental data points were used in deriving the tables. In one version, the heat transfer coefficient was expressed as a function of flow mass flux, pressure, quality and wall superheat and the other version the heat transfer coefficient was expressed as a function of flow mass flux, pressure, quality and wall heat flux. El Nakla et al. tables are currently implemented in CATHENA [71] code as a standard prediction technique due to their prediction accuracy (~10% RMS) and their wide range of flow conditions.

CHAPTER 3

Problem Statement and Objective of Study

3.1. Objectives of the Study

The objective of the proposed research thesis is to construct a look-up table for predicting the two-phase frictional pressure drop multiplier with accuracy superseding existing prediction techniques. The table covers wide range of flow conditions of pressure, mass fluxes, and qualities where different flow regimes exist.

The table is constructed as follows:

- 1- A skeleton table is made using available prediction techniques that best fit each sub range of the table. This will be done by assessing these models against experimental data and selecting the ones with least error.
- 2- The skeleton table is updated using all data banks. This procedure will result in reducing the error in regions where experimental data are available, by replacing the prediction value of the models with experimental values. This would result in improved accuracy of the table to supersede any other prediction techniques for the regions where experimental data are available. The table would predict other regions as good as best models.
- 3- Smoothing is applied on the table to remove discontinuities between sub regions and between the correlations and experimental data regions. This discontinuities

and irregularities are due to differences between data sets, data scattering, and other minor parameters such as surface roughness, flow instabilities, and pipe orientation.

- 4- Error assessment in terms of root mean square (RSM) error and average error is performed for the table against each data set. The table will also be assessing for each sub regions.

The values of the two-phase frictional pressure drop obtained from the look-up table can be used directly to predict the two-phase frictional pressure drop when used with a proper single phase frictional pressure drop correlation.

3.2. Parameters

In this research, adiabatic single component data has been considered in pipe diameter of 2.0-90.0 mm. The ranges of pressure, mass flux and mass quality were 0.10-20.5 MPa, 2.05-20,000 $\text{kg.m}^{-2}.\text{s}^{-1}$ and 0.0-1.0, respectively.

3.3. Methodology

- 1- An extensive survey was performed on the available literature. The main purpose of this task is to gather as much as possible of experimental data related to two-phase frictional pressure drop.
- 2- All data collected was tabulated in spread sheets with the same format and the same units of flow conditions.

- 3- Each data set assessed to remove the uncertainty in frictional pressure drop.
- 4- Each data set assessed with a leading models to know the best model.
- 5- Construct a skeleton table from leading models and correlations to assure correct parametric and asymptotic trends.
- 6- Updating the table with available experimental data. The updating procedure is done by removing a value of non-experimental point and replacing it with an experimental value for the same flow conditions.
- 7- Discontinuities appear between each sub ranges and between the models and experimental data regions. A smoothing program was applied to remove them.
- 8- Optimizing the table.
- 9- Analysis and performing uncertainty study on the final table.

CHAPTER 4

Comparison between Correlations and Experimental Data

Many correlations and models are available in the literature as previously mentioned in chapter two. As shown in Table 1, six correlations which are known for their high prediction accuracy are used to examine their performance among the experimental data collected from the literature as mentioned in table 2. In this section the flow parameters such as; pressure, mass flux, and mass quality are studied to show the effect on two-phase frictional pressure drop correlations.

To nominate the best correlations among of the chosen one, another check to their accuracy is needed. Average and root-mean squared errors are used to assess the predictions of the correlations.

4.1. Effect of Flow Parameters on Two-Phase Frictional Pressure Drop

Figure 1 shows the effect of mass flux (at high mass flux values) on two-phase frictional pressure drop at moderate constant pressure and by varying the mass quality. At a given mass quality, two-phase frictional pressure drop increases with increasing

mass flux. The increase in pressure drop is attributed to the increase in Reynolds number (turbulence). This is similar to the single-phase frictional pressure drop. Although the friction factor decreases with increasing mass flux but the increase in pressure drop due to turbulence is much higher.

Figure 1 also shows the effect of varying mass quality on frictional pressure drop. At a given mass flux, the frictional pressure drop increases with increasing mass quality. As the mass quality increases, the area between the liquid phase and the gas phase increases with an increase in the gas velocity. This would result in increasing the frictional pressure gradient at the interface which in turn will increase the total frictional pressure drop.

The same effect of mass flux and mass quality is observed by changing the working fluid from water-steam mixture to R-11 mixture at lower pressures and lower mass fluxes. This is demonstrated in Figures 2 and 3.

The effect of pressure on frictional pressure drop is shown in Figure 4 for a given mass flux and by varying the mass quality. At a given mass quality, the frictional pressure drop decreases with increasing flow pressure. There are two opposing effect occurring when increasing the pressure. The first is friction factor which increases slightly due to the increase in pressure. The other effect is the increase in density of the mixture. This increase in density will result in decreasing frictional pressure drop in an absolute value of greater than the increase due to friction factor.

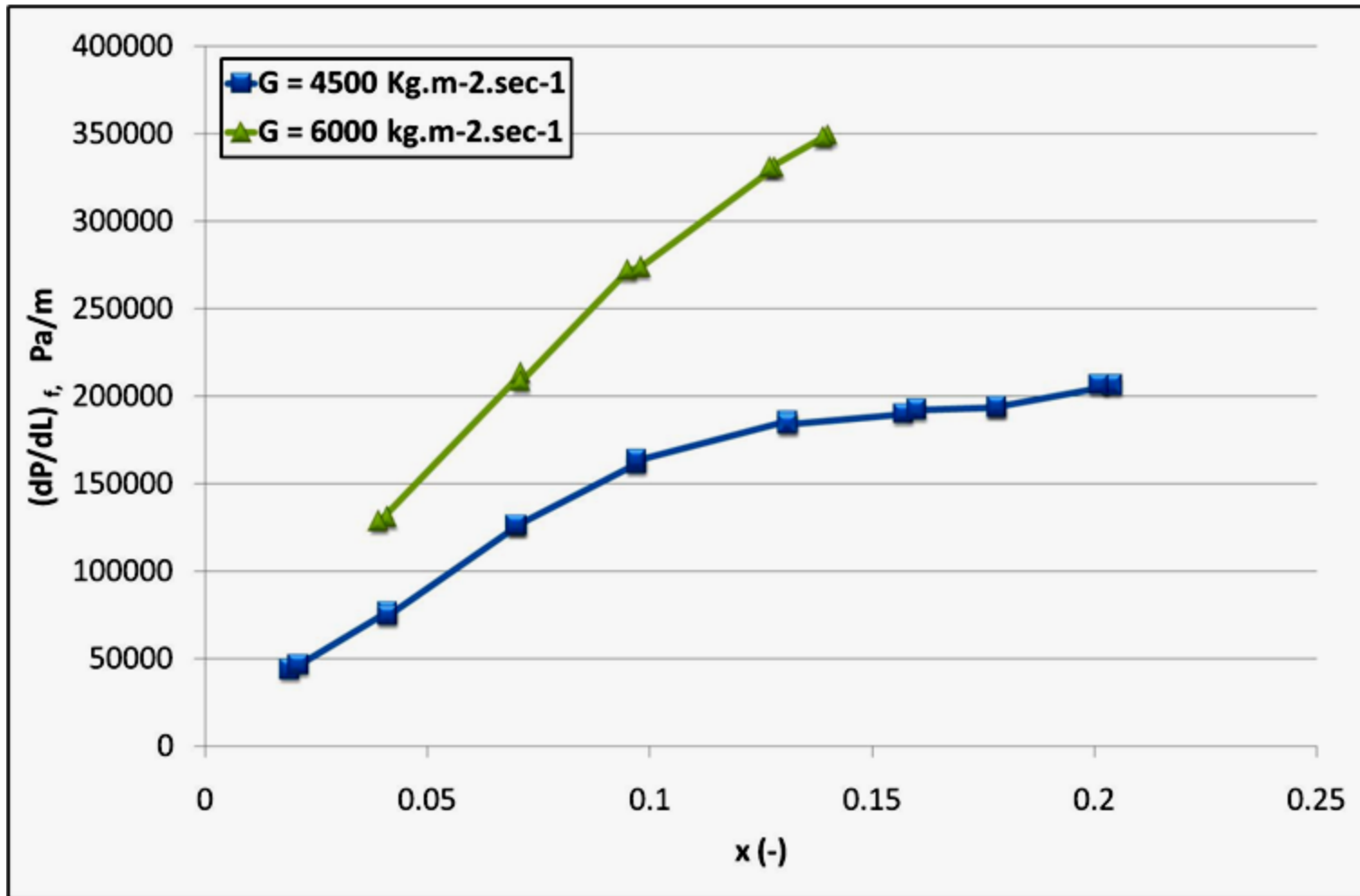


Figure 1 Two-phase frictional pressure gradient versus mass quality for Water-steam flow in 13.4 mm at system pressure equal to 2 MPa and variant mass flux for Aube [47]

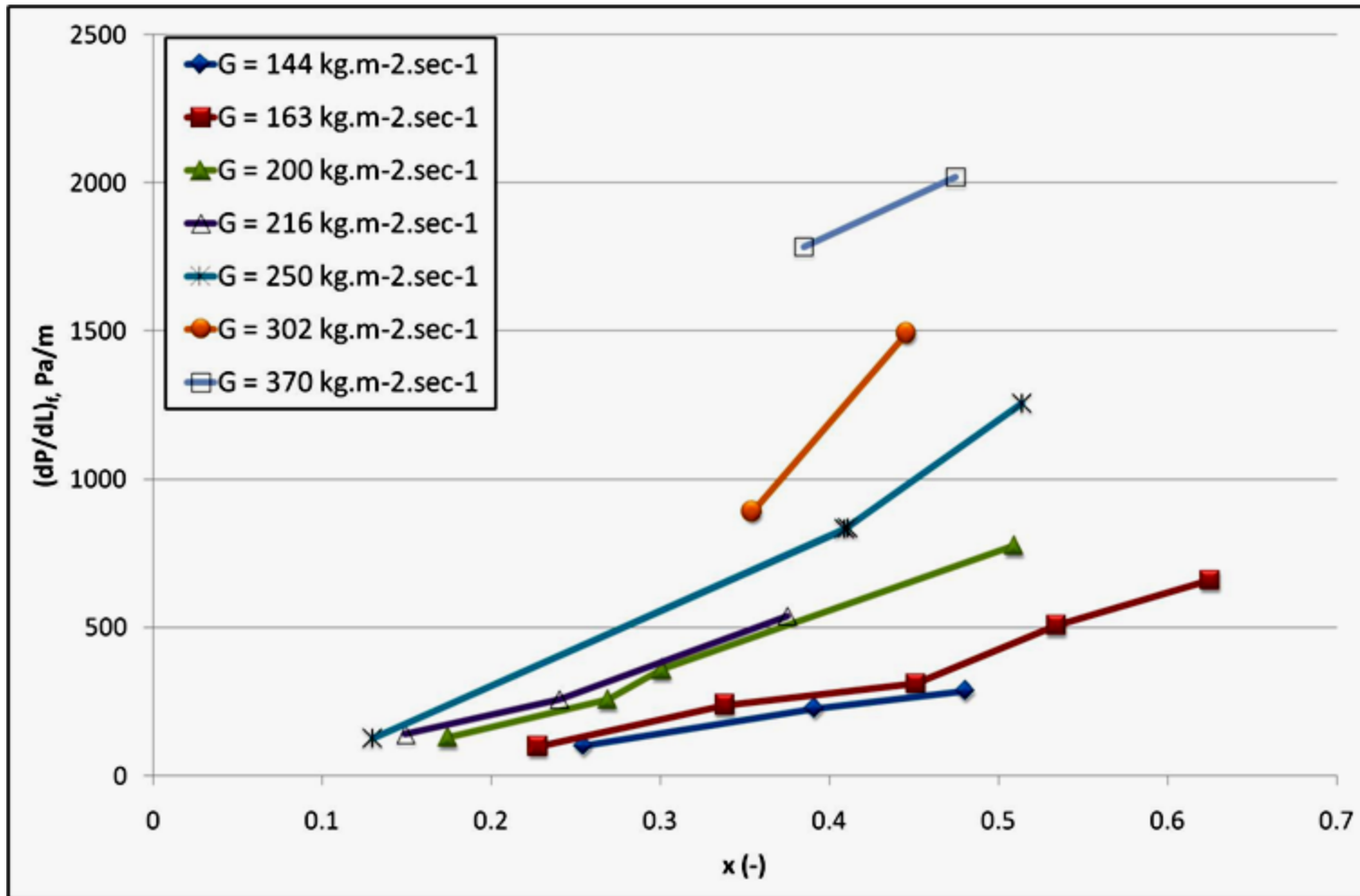


Figure 2 Two-phase frictional pressure gradient versus mass quality for R-11 flow in 46.6 mm at system pressure equal to 0.16 MPa and variant mass flux for McMillan [36]

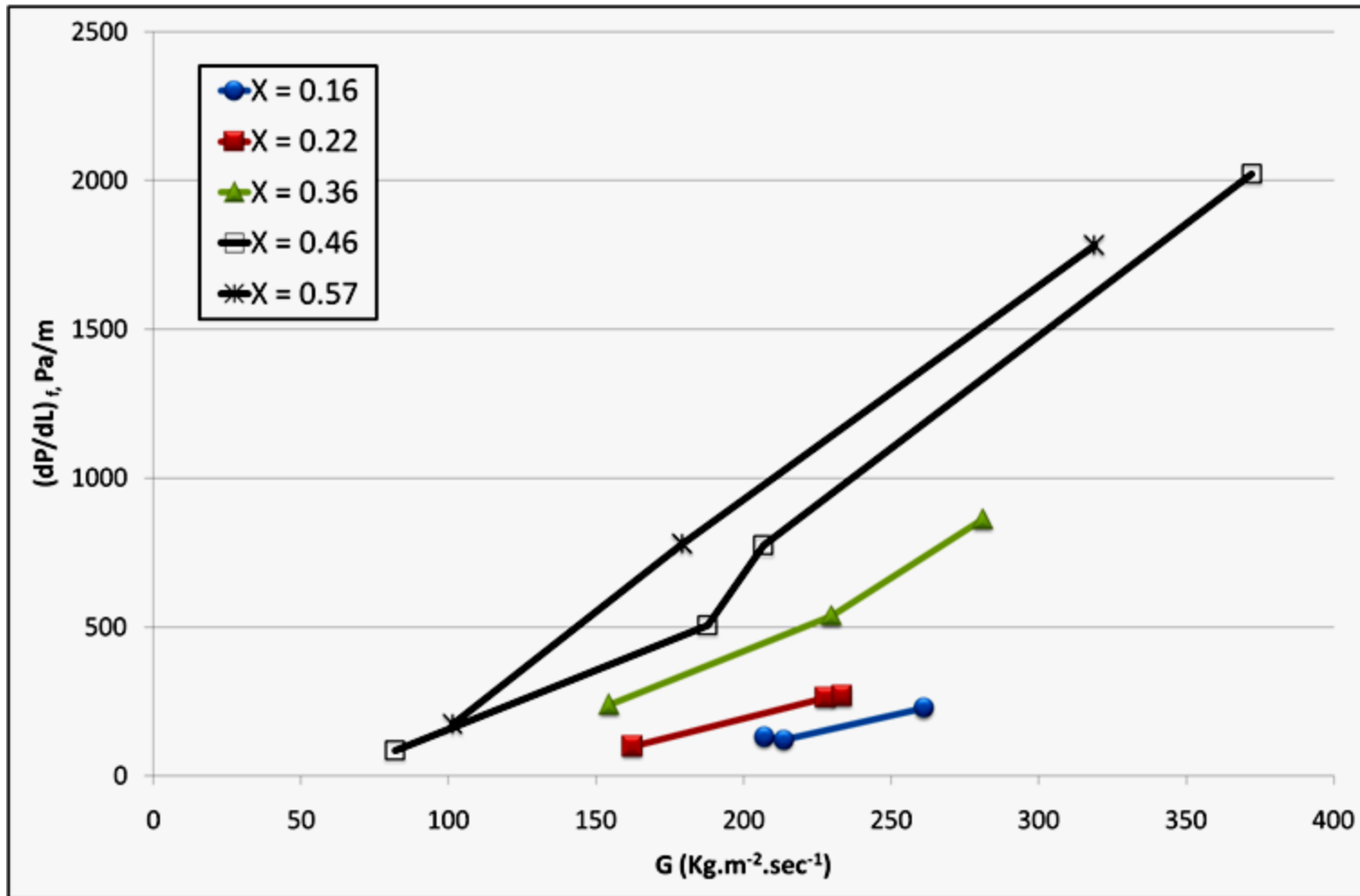


Figure 3 Two-phase frictional pressure gradient versus mass flux for R-11 flow in 46.6 mm at system pressure equal to 0.16 MPa and variant mass quality for McMillan [36]

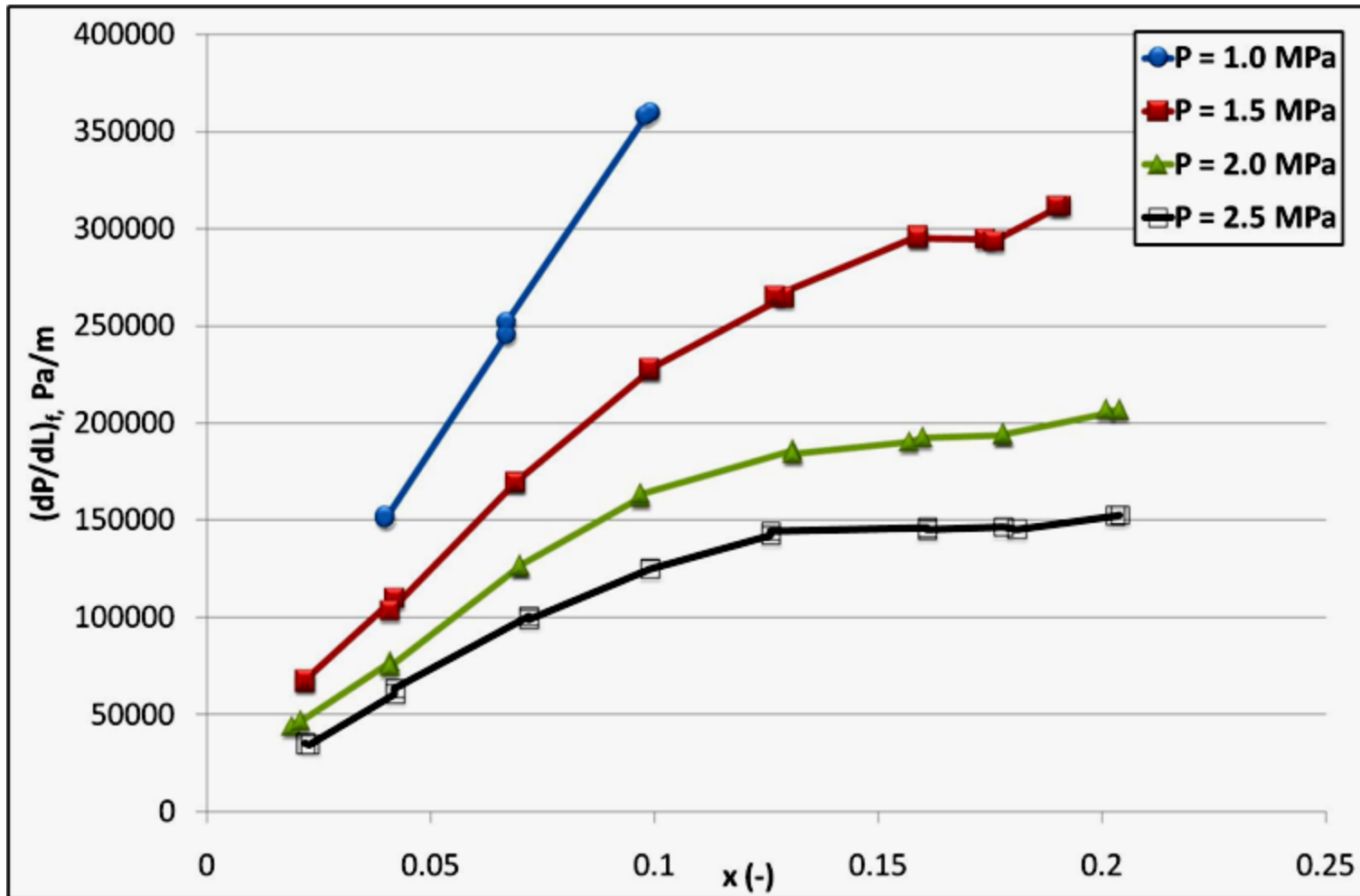


Figure 4 Two-phase frictional pressure gradient versus mass quality for Water-steam flow in 13.4 mm at mass flux equal to $4500 \text{ Kg.m}^{-2}.\text{sec}^{-1}$ and variant system pressure for Aube [47]

4.2. Assessment of Two-Phase Frictional Pressure Drop Correlations

The two-phase frictional pressure correlations listed in Table 1 have been assessed against collected data of Table 2. The error in prediction of each data point is

$$e_i = \left(\frac{Q_{cal,i} - Q_{exp,i}}{Q_{exp,i}} \right) \quad (20)$$

The average error (ε_1), and root-mean squared (RMS) error (ε_2) are, respectively, calculated in the prediction of each correlation is obtained from

$$\varepsilon_1 = \left[\frac{1}{N} \sum_{i=1}^N (e_i) \right] \times 100 \quad (21)$$

$$\varepsilon_2 = \left[\sqrt{\frac{\sum_{i=1}^N (e_i)^2}{N-1}} \right] \times 100 \quad (22)$$

The results of assessment are summarized in Table 3. It can be seen from the table that Gronnerud correlation shows the best overall prediction accuracy (least root-mean-squared error) among other correlations. Homogenous model and Friedel correlation come after with acceptable accuracy.

For purpose of choosing the accurate correlations for the look-up table, Table 4 is produced. This table (Table 4) acting as an error mapping, which has the same ranges of the skeleton table. The only difference between error mapping and skeleton table that the error mapping table is divided the skeleton table into sub-ranges for purpose of nominating the best correlations for each range of data.

Table 3 Statistical comparisons with experimental results in terms of percentage errors

Correlations Fluids		Homogeneous	Friedel	Lockhart- Martinelli	Gronnerud	Muller- Steinhagen	Chisholm	No. of Data	Reference
R-11	ε_1	24.1	-42	19.9	-72.1	26.6	41.6	115	McMillan (1963)
	ε_2	65.8	71.4	69.5	74.7	56.1	64.5		
R-12, R-22	ε_1	6.5	-21.2	163	-60.3	29.7	81.9	170	Hashizume (1983)
	ε_2	21.7	65	190.1	65.7	39.07	104.7		
Argon, Air- Water, R-12	ε_1	20.4	46	188.7	-34.4	29.5	152.4	84	Müller-Steinhagen and Heck (1986)
	ε_2	78.5	148	270.1	56	79.4	250.5		
Air-Oil	ε_1	-15.8	4.98	-41.5	-65.9	-59.4	-17.6	151	Stanislav et al. (1986)
	ε_2	60	64	56.6	71	66.4	70		
Steam-Water	ε_1	-16.7	7.06	134	-30.3	2.66	83.5	71	Hashizume and Ogawa (1987)
	ε_2	36.5	57.4	180	41.2	41.8	128		
Air-Water	ε_1	-32.8	-1.2	-56.1	-74.6	-36.2	-49.3	197	Ebner et al. (1987)
	ε_2	84.4	107.7	68.9	76.6	80.4	80.5		
R-11	ε_1	-4.34	-34.15	14.9	-68.16	-21.8	71.8	293	Klausner (1989)
	ε_2	35.5	50	51	70.1	35.1	102.2		
Steam-Water	ε_1	-36.3	-40.2	23.7	-49.3	-24.2	-47.8	84	Aubé (1997)
	ε_2	38.9	43.1	40.5	51.2	31	50.7		
R-134a	ε_1	-6.6	-65.8	44.5	-71.1	36.3	55.4	184	Tran et al. (2000)
	ε_2	23.6	71.5	72.2	73.6	46.4	80		
Air-Water	ε_1	-50.5	-34.9	-62.7	-78	-62.3	-64.3	112	Ottens et al. (2001)
	ε_2	57.6	57.1	67.1	79.6	66.1	69.7		
R-134a, R- 123, R-404, R-502	ε_1	-7.67	-66.1	17.7	-70	20.1	46.5	78	Ould Didi et al. (2002)
	ε_2	19	74.7	46.7	74.3	33	70.6		
Air-Water	ε_1	-14.1	-17.3	-18.8	-43.5	-11	-26.12	70	Pehlivan (2003)
	ε_2	22.8	37.4	23.3	44.7	18.2	33.7		
R-134a	ε_1	-49.9	-76	10.18	-75.6	-34.04	-20.2	66	Nualboonrueng and Wongwises (2004)
	ε_2	52.2	79	46.6	77.5	38.6	34.9		
R-134a	ε_1	-55.4	-73.9	8.8	-74.9	-44.8	-49.3	143	Vassallo and Keller (2006)
	ε_2	62.5	75.8	65.4	76.7	60.1	58.2		
R-134a	ε_1	101.9	-29.6	268.8	-11.1	171.5	64.4	114	Vijayarangan et al. (2007)
	ε_2	201.7	51	375.4	61.9	315.5	154.4		
R-410a	ε_1	-6.1	-28.7	122	-36.8	22.8	140	8	Field and Hrnjak (2007)
	ε_2	15	57.6	144	51.3	57	159		
Air-Water	ε_1	-71.3	-83	-32.1	-86.4	-63.9	-58.7	142	Shannak (2008)
	ε_2	72.6	85.6	37.3	88.1	65.4	60.6		
R-410a	ε_1	36.2	-38.1	329	-33.47	107	72.9	9	Cavallini et al. (2009)
	ε_2	43.8	62.6	382	52.2	120	90.5		
Total	ε_1	-10.3	-31.8	37.8	-62.7	-3.16	22.4	2091	
	ε_2	76.46	75.06	138.4	70.7	99.8	114.5		

Table 4 Error Mapping table

Density Ratio	Reynolds Number	Correlations		Mass Quality		
				0.0-0.3	0.35-0.6	0.65-1.0
2.0-10	10-1000	Homogenous	ϵ_1	--	--	--
			ϵ_2	--	--	--
		Friedel	ϵ_1	--	--	--
			ϵ_2	--	--	--
		Lockhart-Martinelli	ϵ_1	--	--	--
			ϵ_2	--	--	--
		Gronnerud	ϵ_1	--	--	--
			ϵ_2	--	--	--
		Muller	ϵ_1	--	--	--
			ϵ_2	--	--	--
		Chisholm`	ϵ_1	--	--	--
			ϵ_2	--	--	--
		No. of Data		--	--	--
	1000-10,000	Homogenous	ϵ_1	--	--	--
			ϵ_2	--	--	--
		Friedel	ϵ_1	--	--	--
			ϵ_2	--	--	--
		Lockhart-Martinelli	ϵ_1	--	--	--
			ϵ_2	--	--	--
		Gronnerud	ϵ_1	--	--	--
			ϵ_2	--	--	--
		Muller	ϵ_1	--	--	--
			ϵ_2	--	--	--
		Chisholm	ϵ_1	--	--	--
			ϵ_2	--	--	--
		No. of Data		--	--	--
	10,000-100,000	Homogenous	ϵ_1	41.77	56.67	29.16
			ϵ_2	63.25	81.21	42.51
		Friedel	ϵ_1	13.56	-42.4	-85.94
			ϵ_2	25.53	60.10	121.54
		Lockhart-Martinelli	ϵ_1	468.61	405.2	171.69
			ϵ_2	669.09	574.77	243.91
		Gronnerud	ϵ_1	4.83	-21.21	-76.04
			ϵ_2	18.59	30.87	107.56
		Muller	ϵ_1	75.26	132.46	145.04
			ϵ_2	109.85	188.26	205.98
		Chisholm	ϵ_1	70.70	72.08	30.93
			ϵ_2	100.05	102.11	43.75
		No. of Data		2.0	2.0	2.0
	100,000-1,000,000	Homogenous	ϵ_1	--	--	--
			ϵ_2	--	--	--
		Friedel	ϵ_1	--	--	--
			ϵ_2	--	--	--
		Lockhart-Martinelli	ϵ_1	--	--	--
			ϵ_2	--	--	--
		Gronnerud	ϵ_1	--	--	--
			ϵ_2	--	--	--
		Muller	ϵ_1	--	--	--
			ϵ_2	--	--	--
		Chisholm	ϵ_1	--	--	--
			ϵ_2	--	--	--
		No. of Data		--	--	--

Density Ratio	Reynolds Number	Correlations		Mass Quality		
				0.0-0.3	0.35-0.6	0.65-1.0
10-100	10-1000	Homogenous	ϵ_1	-9.74	3.03	-10.38
			ϵ_2	22.31	8.35	13.86
		Friedel	ϵ_1	18.31	-31.69	-88.61
			ϵ_2	25.35	45.26	109.3
		Lockhart-Martinelli	ϵ_1	115.5	178.22	75.84
			ϵ_2	152.02	219.03	105.7
		Gronnerud	ϵ_1	-21.27	-15.45	-79.05
			ϵ_2	30.27	23.71	99.57
		Muller	ϵ_1	-22.02	19.21	86.39
			ϵ_2	30.18	26.47	111.87
		Chisholm`	ϵ_1	126.24	189.36	111.46
			ϵ_2	163.46	232.48	140.5
		No. of Data		4	3	3
	1000-10,000	Homogenous	ϵ_1	8.12	16.19	-14.89
			ϵ_2	25.6	30.82	18.7
		Friedel	ϵ_1	22.35	-47.25	-93.46
			ϵ_2	46.16	52.74	94.81
		Lockhart-Martinelli	ϵ_1	201.17	144.6	7.54
			ϵ_2	213.34	166.27	21.8
		Gronnerud	ϵ_1	-52.12	-70.21	-94.76
			ϵ_2	54.12	71.68	96.11
		Muller	ϵ_1	10.38	38.59	46.52
			ϵ_2	28.17	50.15	52.01
		Chisholm	ϵ_1	113.93	86.73	-1.43
			ϵ_2	126.38	99.82	12.47
		No. of Data		44	43	36
	10,000-100,000	Homogenous	ϵ_1	-16.11	-35.24	-26.69
			ϵ_2	67.51	47.96	32.53
		Friedel	ϵ_1	-0.02	-72.44	-92.21
			ϵ_2	102.15	74.53	93.7
		Lockhart-Martinelli	ϵ_1	114.64	38.97	9
			ϵ_2	193.93	83.24	34.78
		Gronnerud	ϵ_1	-49.62	-70.54	-88.18
			ϵ_2	60.65	72.54	89.9
		Muller	ϵ_1	-14.58	-19.74	22.12
			ϵ_2	66.15	44.58	37.1
		Chisholm	ϵ_1	69.87	-5.6	-14.04
			ϵ_2	181.98	52.59	26.98
		No. of Data		179	104	32
	100,000-1,000,000	Homogenous	ϵ_1	-35.5	-66.74	-69.52
			ϵ_2	48.44	68.97	71.17
		Friedel	ϵ_1	-24.14	-85.67	-96.14
			ϵ_2	57.13	87.16	97.39
		Lockhart-Martinelli	ϵ_1	65.51	-19.75	-49.81
			ϵ_2	122.35	55.74	58.61
		Gronnerud	ϵ_1	-47.57	-83.94	-94.41
			ϵ_2	56.04	85.62	95.7
		Muller	ϵ_1	-24.61	-58.31	-51.03
			ϵ_2	48.08	63.89	55.77
		Chisholm	ϵ_1	4.96	-48.06	-62.64
			ϵ_2	90.14	64.31	66.94
		No. of Data		172	55	41

Density Ratio	Reynolds Number	Correlations		Mass Quality		
				0.0-0.3	0.35-0.6	0.65-1.0
100-1000	10-1000	Homogenous	ϵ_1	-18.04	--	--
			ϵ_2	71.19	--	--
		Friedel	ϵ_1	1.46	--	--
			ϵ_2	76.18	--	--
		Lockhart-Martinelli	ϵ_1	-53.88	--	--
			ϵ_2	64.4	--	--
		Gronnerud	ϵ_1	-78.05	--	--
			ϵ_2	80.52	--	--
		Muller	ϵ_1	-74.53	--	--
			ϵ_2	77.9	--	--
		Chisholm	ϵ_1	-10.31	--	--
			ϵ_2	83.61	--	--
		No. of Data		87	--	--
	1000-10,000	Homogenous	ϵ_1	-6	-14	-32.84
			ϵ_2	35.45	31.82	36.42
		Friedel	ϵ_1	-17.04	-68.79	-93.51
			ϵ_2	42.69	70.68	100.02
		Lockhart-Martinelli	ϵ_1	-0.36	-13.97	-48.47
			ϵ_2	44.52	33.06	52.92
		Gronnerud	ϵ_1	-57.5	-80.81	-95
			ϵ_2	61.18	82.01	101.59
		Muller	ϵ_1	-23.14	-21.25	-16.21
			ϵ_2	36.66	34.83	17.8
		Chisholm	ϵ_1	29.95	20.82	-31.06
			ϵ_2	83.73	46.58	36.35
		No. of Data		243	57	8
	10,000-100,000	Homogenous	ϵ_1	-18.66	0.91	-26.97
			ϵ_2	60.03	33.75	32.57
		Friedel	ϵ_1	-1.46	-65.36	-90.92
			ϵ_2	41.97	68.61	93.99
		Lockhart-Martinelli	ϵ_1	42.71	-5.09	-41.8
			ϵ_2	75.09	31.25	45.11
		Gronnerud	ϵ_1	-54.34	-78.37	-92.54
			ϵ_2	56.57	79.31	95.61
		Muller	ϵ_1	0.48	6.67	-2.73
			ϵ_2	51.9	32.9	19.68
		Chisholm	ϵ_1	84.07	37.31	-18.23
			ϵ_2	111.8	54.69	25.84
		No. of Data		149	71	16
	100,000-1,000,000	Homogenous	ϵ_1	-56.85	--	--
			ϵ_2	61.71	--	--
		Friedel	ϵ_1	-41.91	--	--
			ϵ_2	54.1	--	--
		Lockhart-Martinelli	ϵ_1	-57.1	--	--
			ϵ_2	64.54	--	--
		Gronnerud	ϵ_1	-75.55	--	--
			ϵ_2	76.97	--	--
		Muller	ϵ_1	-61.41	--	--
			ϵ_2	65.09	--	--
		Chisholm	ϵ_1	-62.31	--	--
			ϵ_2	68.29	--	--
		No. of Data		229	--	--

Density Ratio	Reynolds Number	Correlations		Mass Quality		
				0.0-0.3	0.35-0.6	0.65-1.0
1000-3000	10-1000	Homogenous	ϵ_1	--	--	--
			ϵ_2	--	--	--
		Friedel	ϵ_1	--	--	--
			ϵ_2	--	--	--
		Lockhart-Martinelli	ϵ_1	--	--	--
			ϵ_2	--	--	--
		Gronnerud	ϵ_1	--	--	--
			ϵ_2	--	--	--
		Muller	ϵ_1	--	--	--
			ϵ_2	--	--	--
		Chisholm	ϵ_1	--	--	--
			ϵ_2	--	--	--
		No. of Data		--	--	--
	1000-10,000	Homogenous	ϵ_1	122.14	-25.85	--
			ϵ_2	184.92	57.7	--
		Friedel	ϵ_1	126.81	-70.49	--
			ϵ_2	232.6	82.04	--
		Lockhart-Martinelli	ϵ_1	13.89	-61.86	--
			ϵ_2	72.54	72.36	--
		Gronnerud	ϵ_1	-49.16	-83.15	--
			ϵ_2	58.1	92.21	--
		Muller	ϵ_1	109.55	-18.84	--
			ϵ_2	167.15	55.07	--
		Chisholm	ϵ_1	102.79	-27.77	--
			ϵ_2	158.87	68.52	--
		No. of Data		13	6	--
	10,000-100,000	Homogenous	ϵ_1	-20.59	--	--
			ϵ_2	75.68	--	--
		Friedel	ϵ_1	29.11	--	--
			ϵ_2	120.13	--	--
		Lockhart-Martinelli	ϵ_1	-51.38	--	--
			ϵ_2	65.62	--	--
		Gronnerud	ϵ_1	-72.74	--	--
			ϵ_2	75.03	--	--
		Muller	ϵ_1	-26.43	--	--
			ϵ_2	71.88	--	--
		Chisholm	ϵ_1	-53.29	--	--
			ϵ_2	75.08	--	--
		No. of Data		95	--	--
	100,000-1,000,000	Homogenous	ϵ_1	--	--	--
			ϵ_2	--	--	--
		Friedel	ϵ_1	--	--	--
			ϵ_2	--	--	--
		Lockhart-Martinelli	ϵ_1	--	--	--
			ϵ_2	--	--	--
		Gronnerud	ϵ_1	--	--	--
			ϵ_2	--	--	--
		Muller	ϵ_1	--	--	--
			ϵ_2	--	--	--
		Chisholm	ϵ_1	--	--	--
			ϵ_2	--	--	--
		No. of Data		--	--	--

Figures 5-a, 5-b, and 5-c show the assessment result in graphical form for better visualization for selected data sets. As seen from the figures, there is a large scatter in the prediction with the experimental data mainly underpredicted by the correlations (negative average error).

Figures 6 – 11 present visual presentation of the correlation predictions' compared with data at different flow conditions. This is done in order to determine the regions at which each correlation can predict better as well as Table 4. For instance at low-to-moderate pressures and high mass fluxes, both Lockhart-Martinelli and Muller correlations apply better than other correlations, as demonstrated in Figure 6. For low pressure and low mass flux, the performance of correlations is acceptable for certain flow conditions and mass quality, but in other locations it is not, as indicated in Figure 7 - 9.

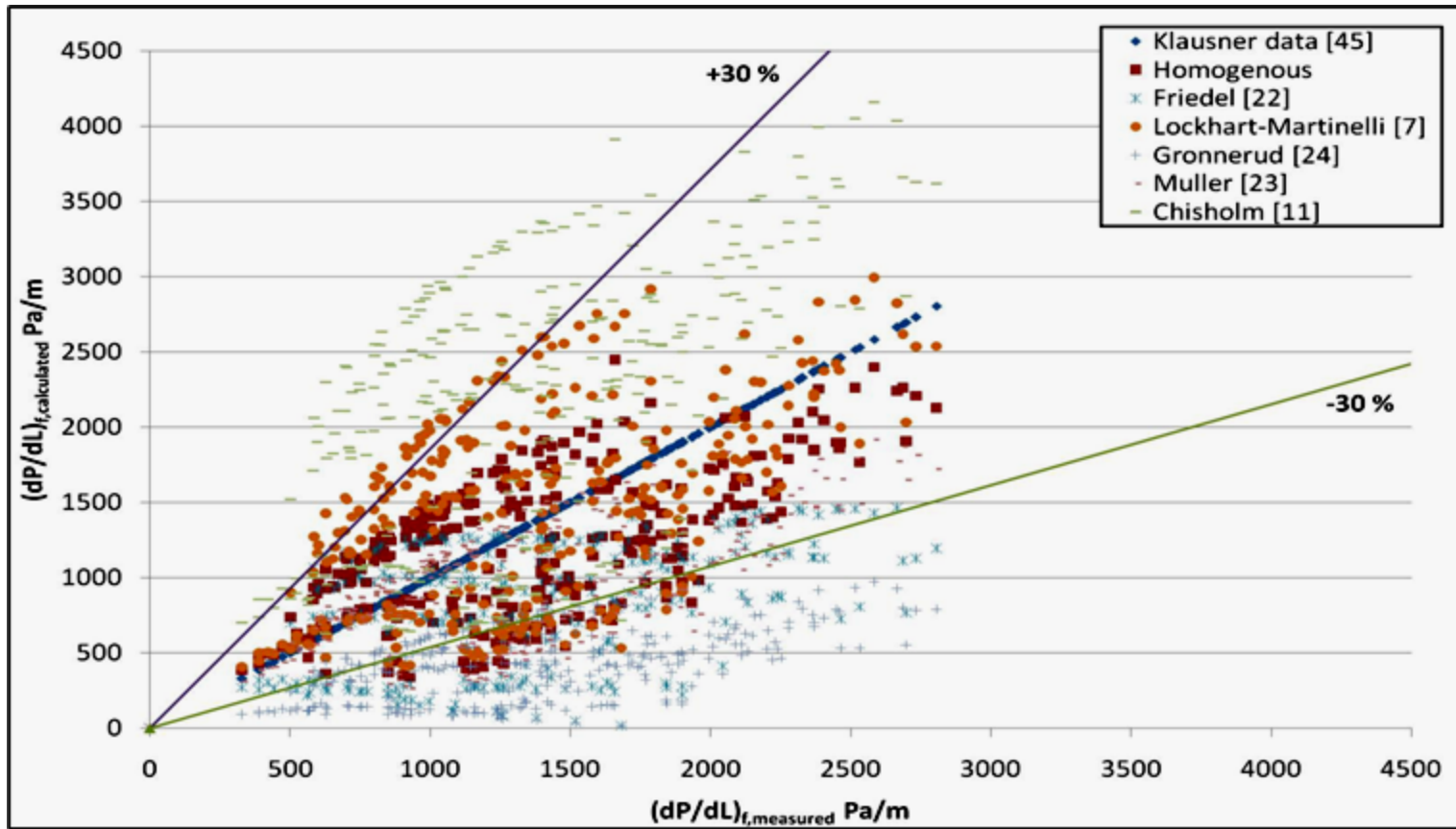


Figure 5-a Comparison of two-phase frictional pressure gradient with six correlations for Klausner [45] with six correlations.

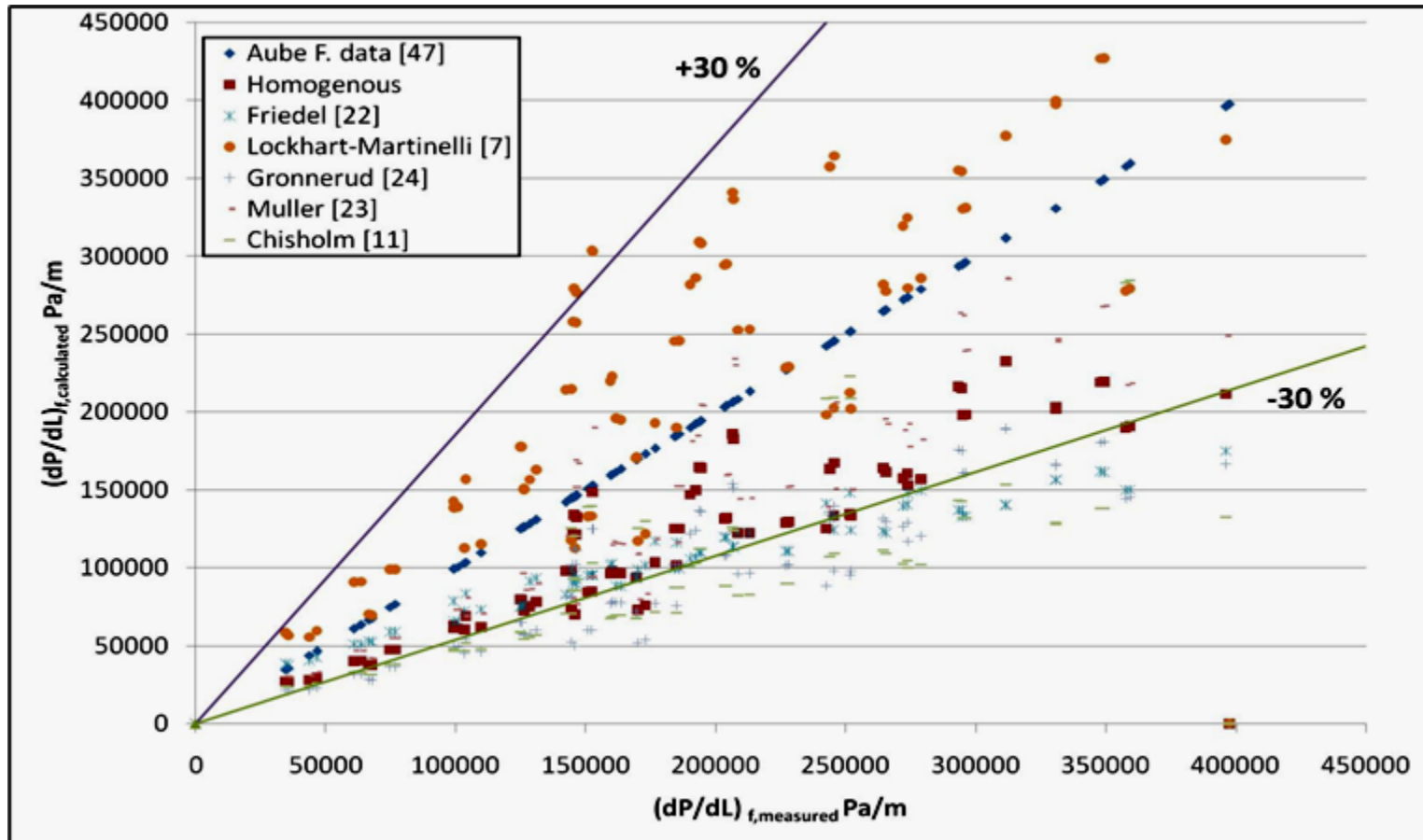


Figure 5-b Comparison of two-phase frictional pressure gradient with six correlations for Aube F.[47] with six correlations.

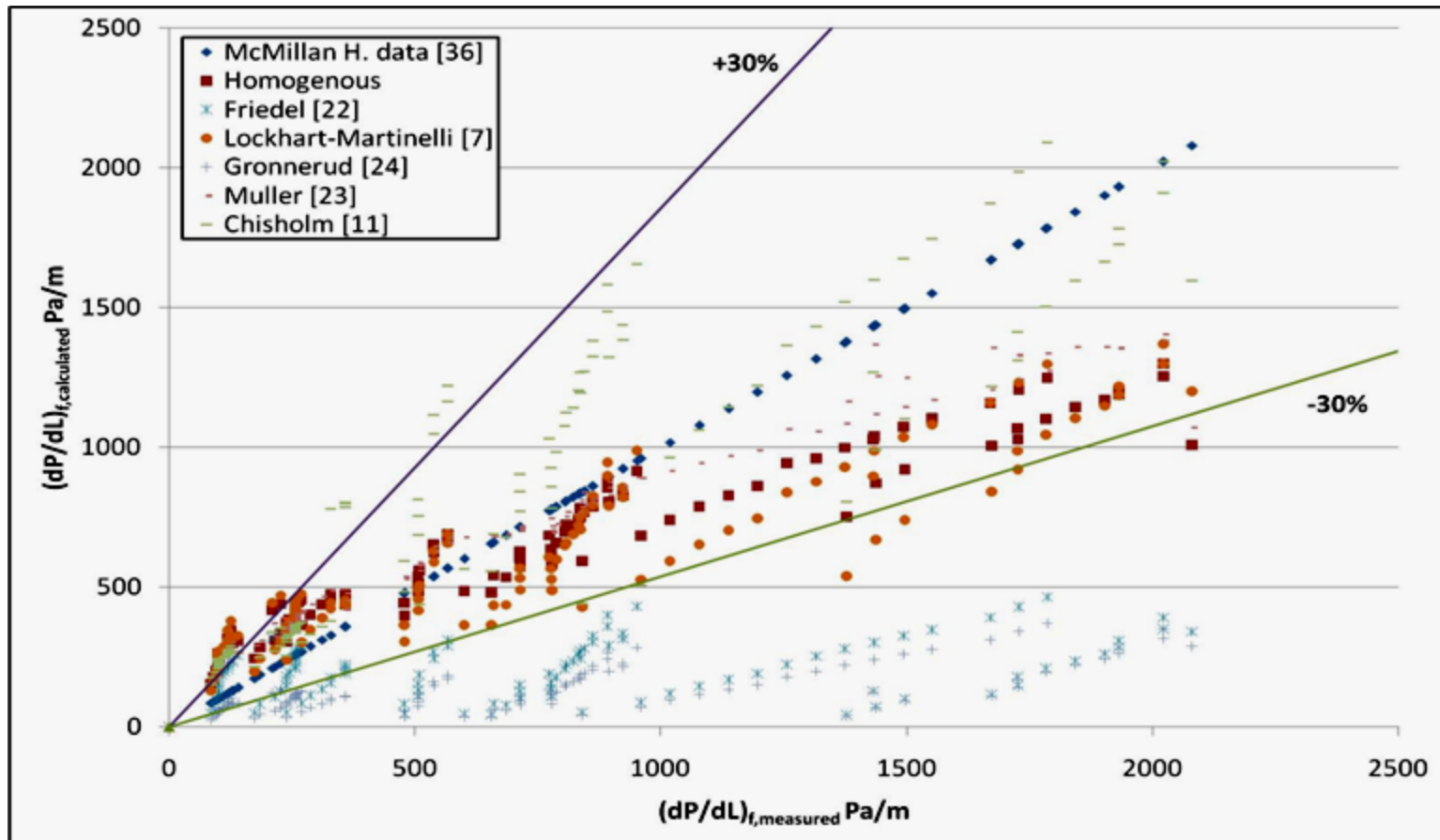


Figure 5-c Comparison of two-phase frictional pressure gradient with six correlations for McMillan H.[36] with six correlations.

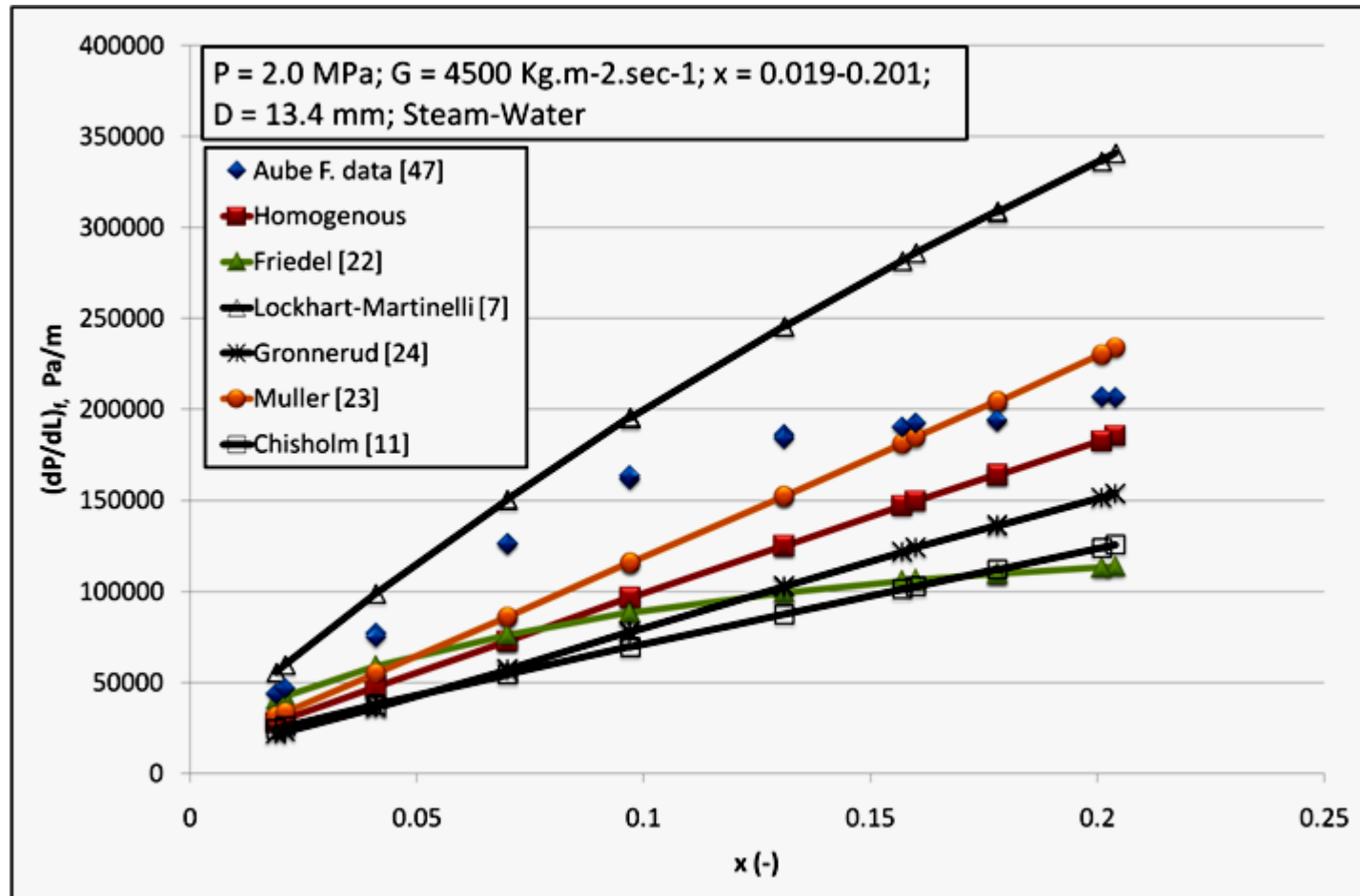


Figure 6-a Comparison for calculated and measured two-phase frictional pressure gradient for Aube [47] and several correlations at low pressure-high mass flux.

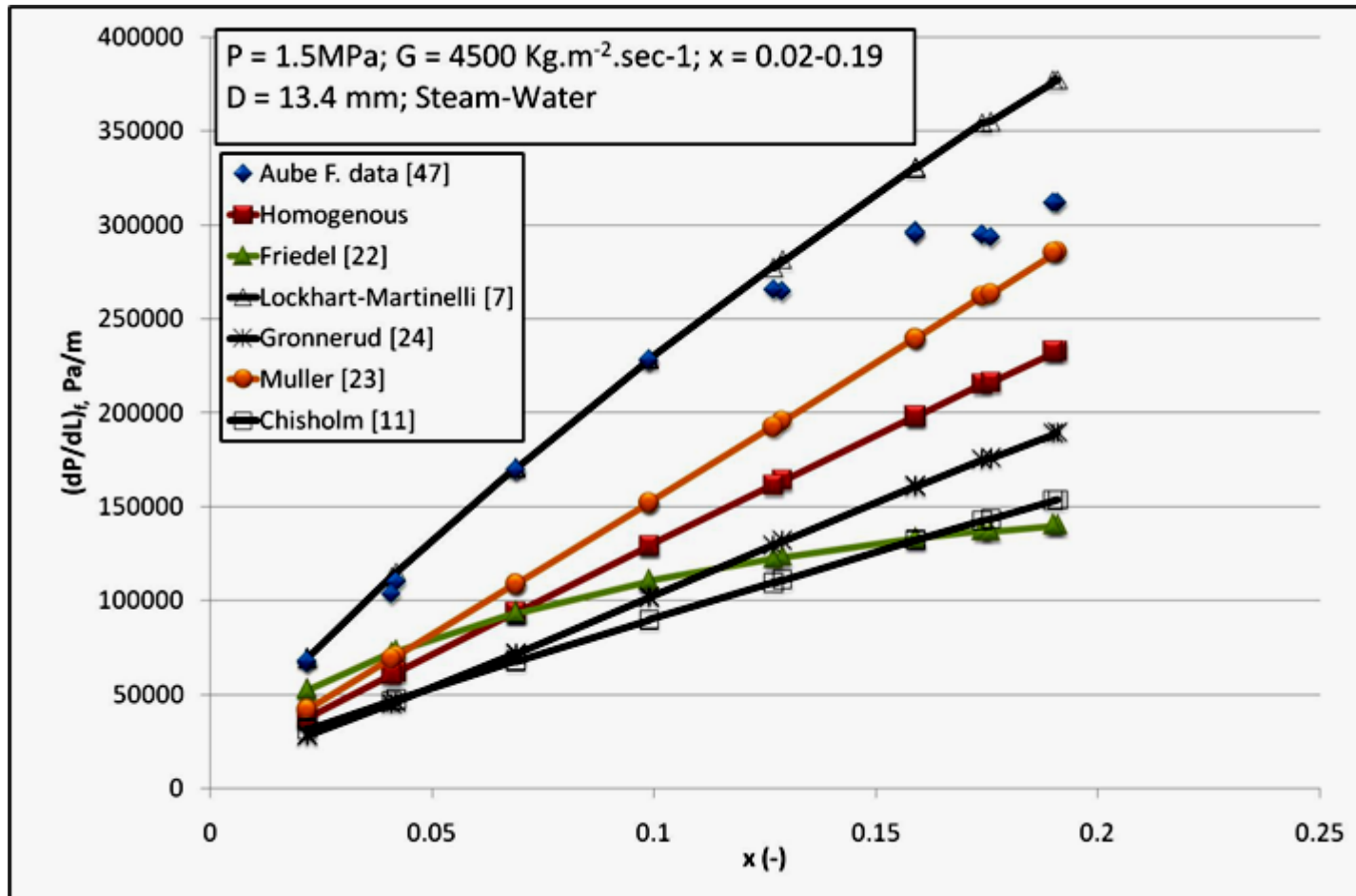


Figure 6-b Comparison for calculated and measured two-phase frictional pressure gradient for Aube [47] and several correlations, low pressure-high mass flux.

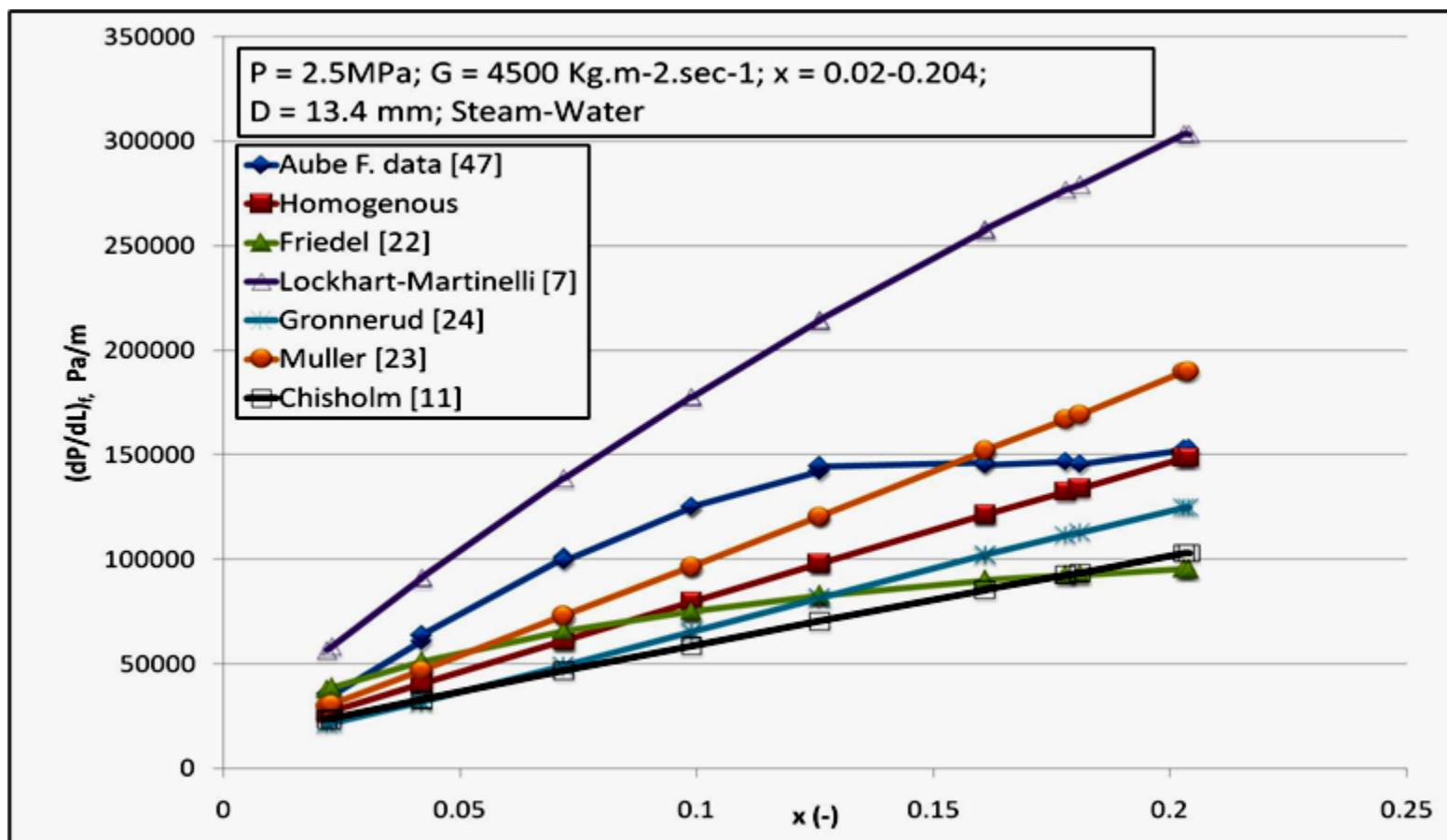


Figure 6-c Comparison for calculated and measured two-phase frictional pressure gradient for Aube [47] and several correlations at medium pressure-high mass flux.

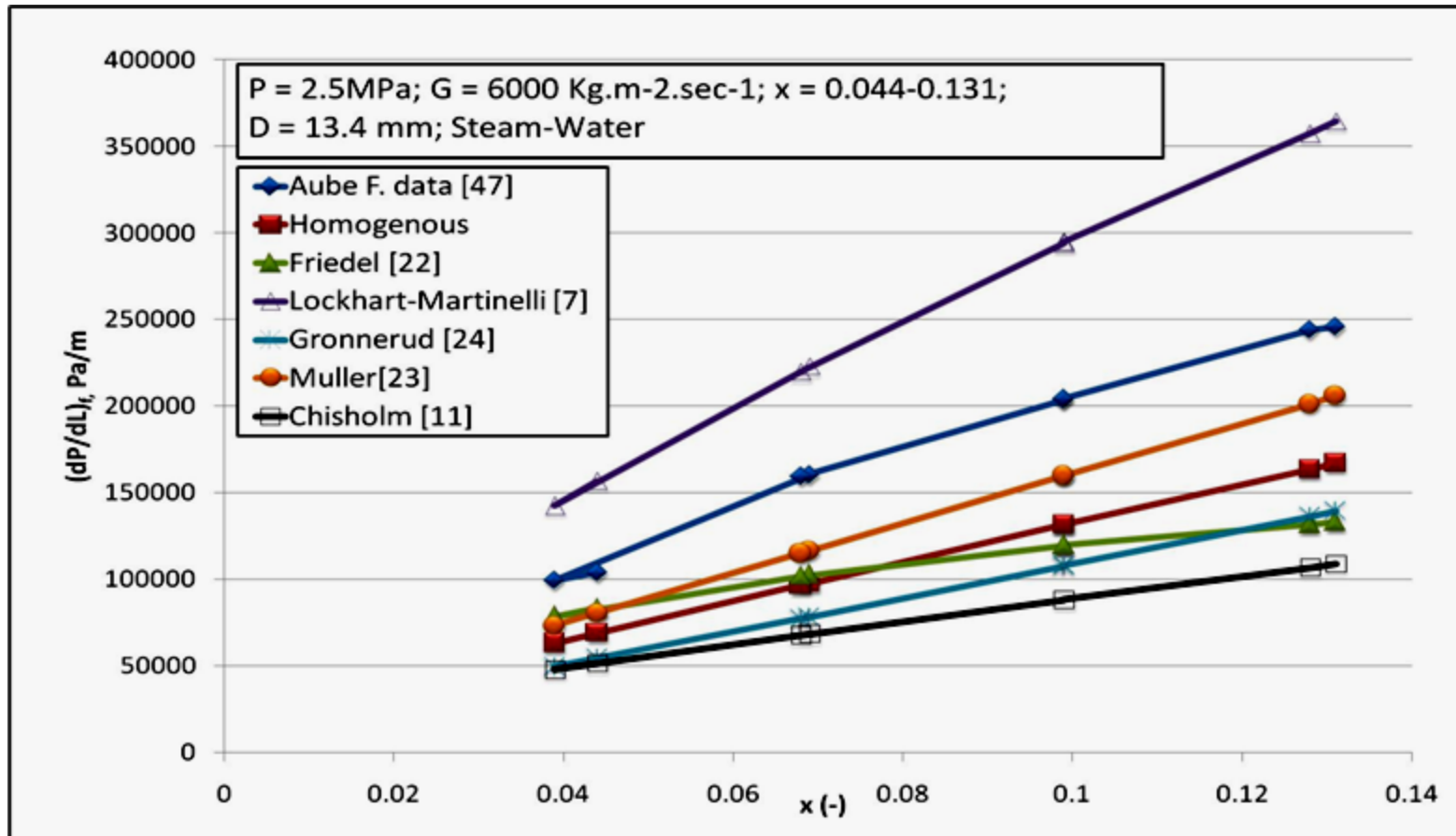


Figure 6-d Comparison for calculated and measured two-phase frictional pressure gradient for Aube [47] and several correlations at medium pressure-high mass flux.

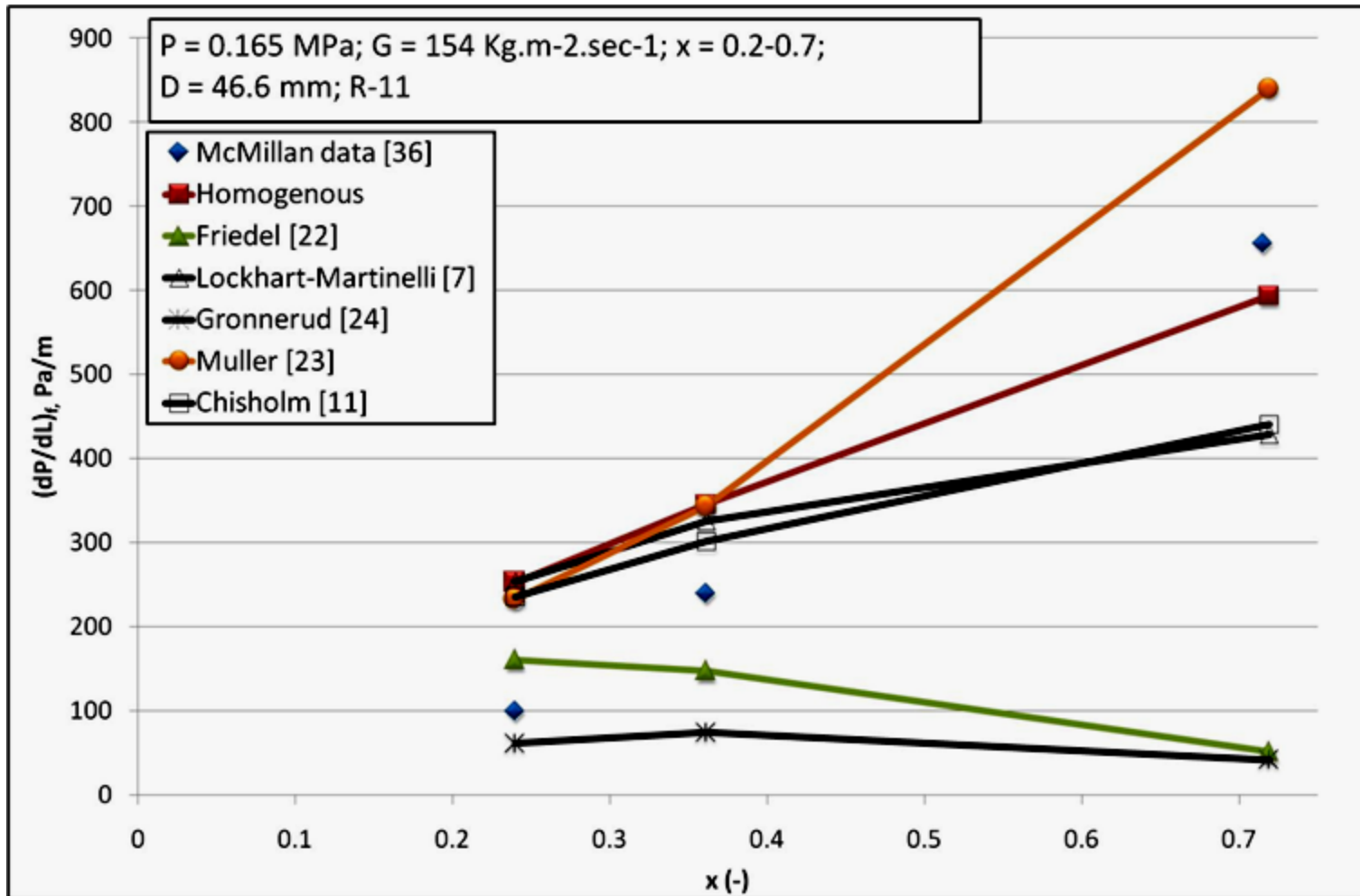


Figure 7 Comparison for calculated and measured two-phase frictional pressure gradient for McMillan [36] and several correlations at low pressure-low mass flux.

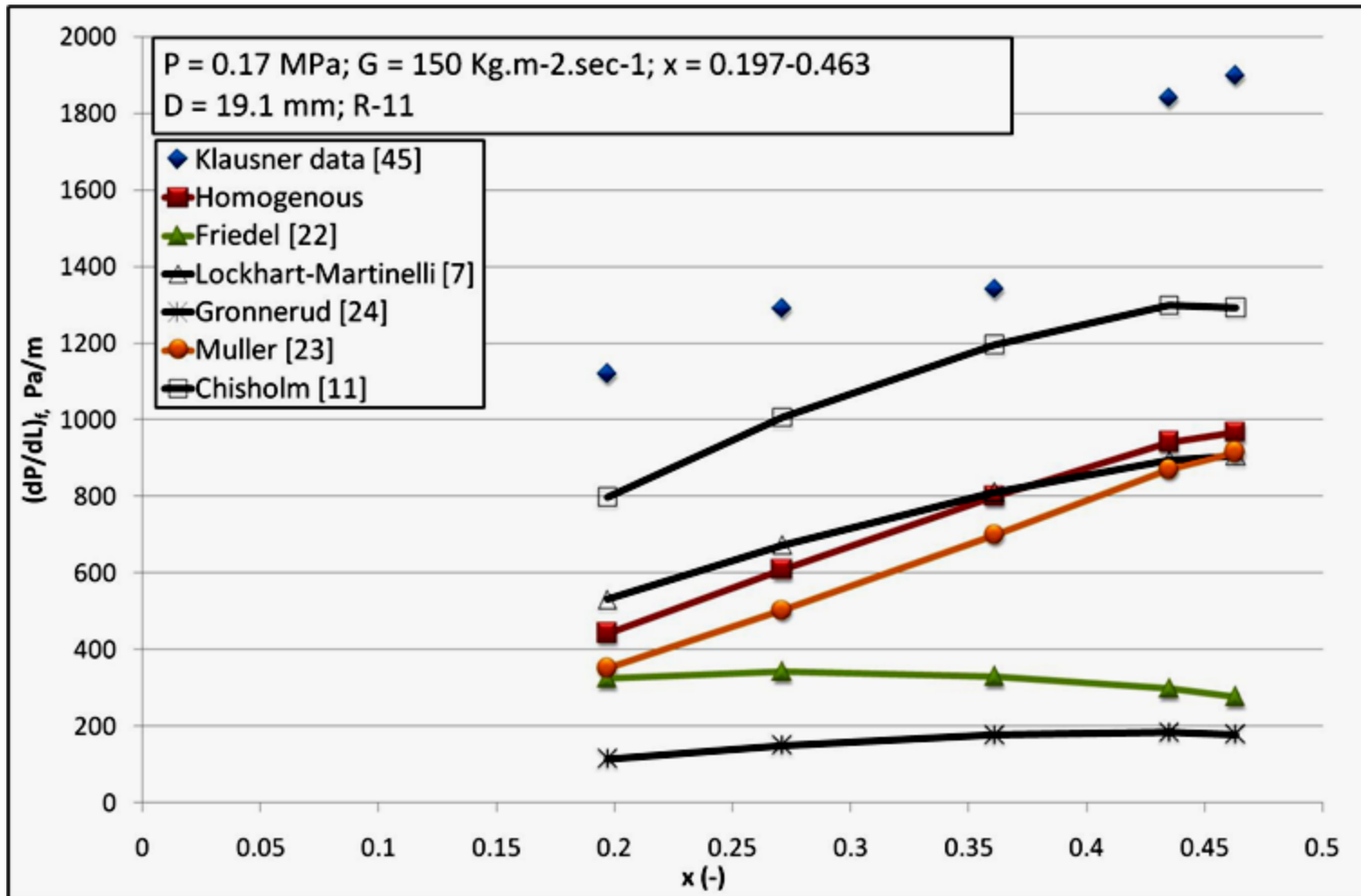


Figure 8 Comparison for calculated and measured two-phase frictional pressure gradient for Klausner [45] and several correlations at low pressure-low mass flux.

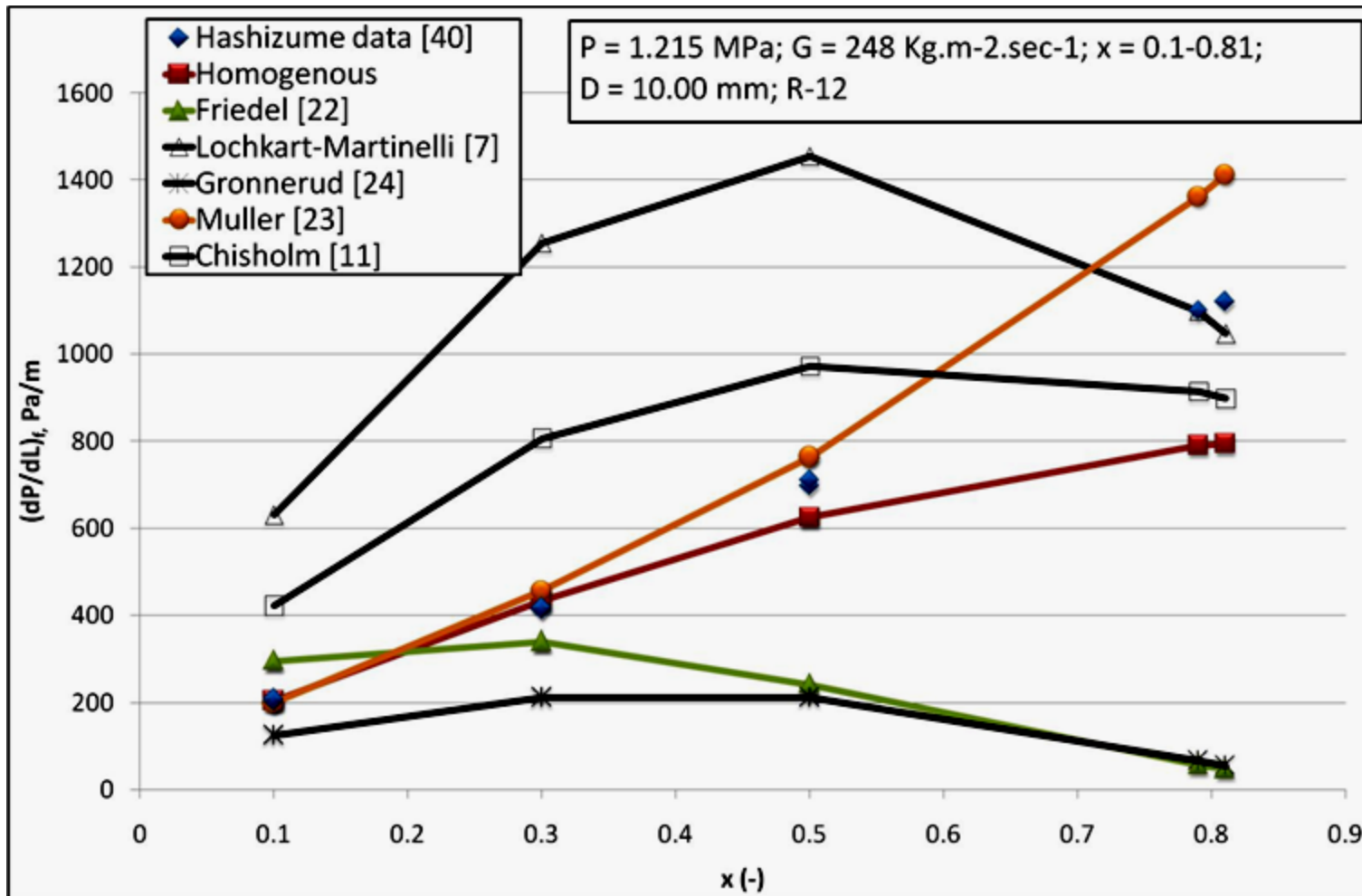


Figure 9 Comparison for calculated and measured two-phase frictional pressure gradient for Hashizume [40] and several correlations at low pressure-low mass flux.

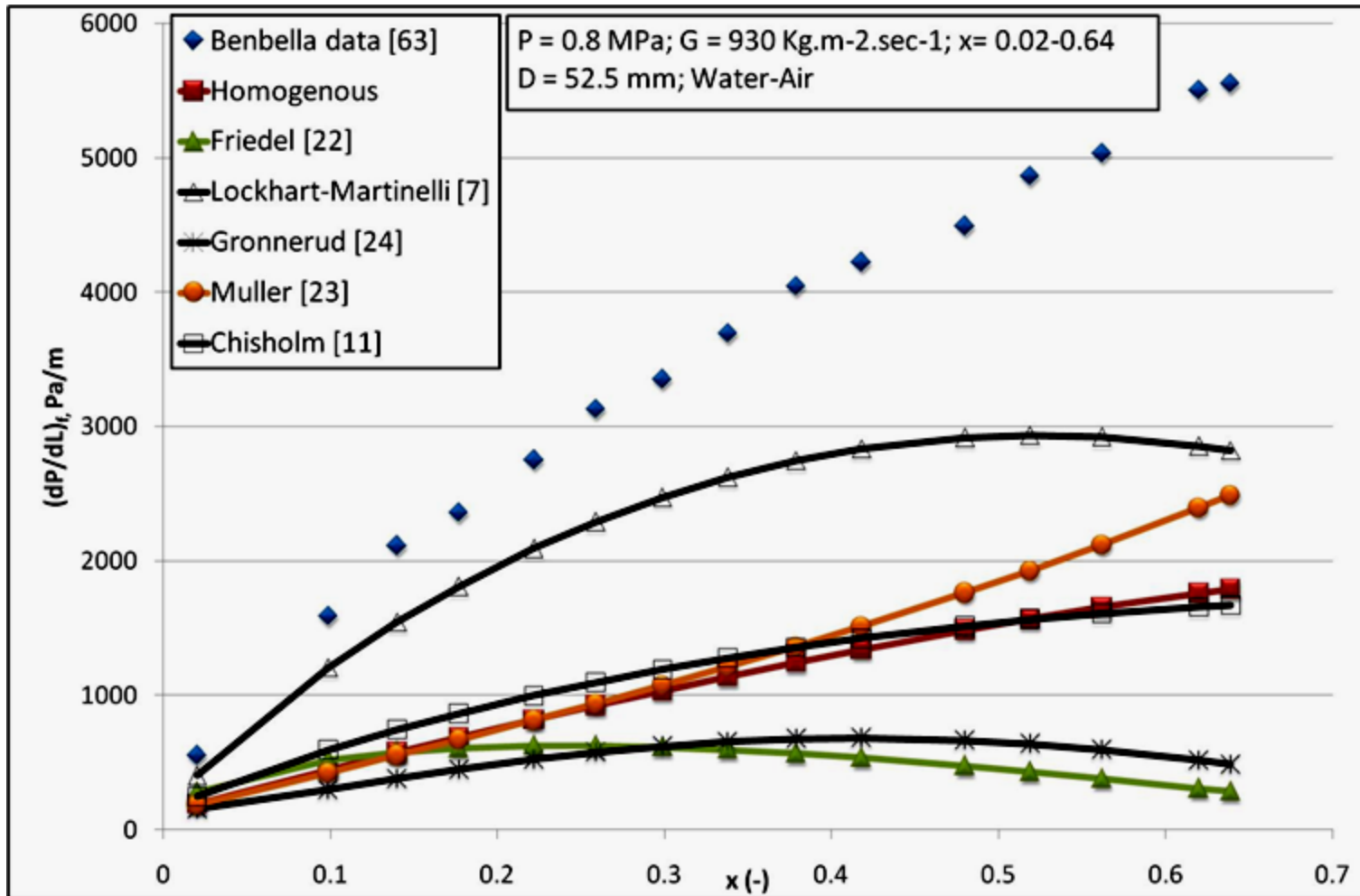


Figure 10 Comparison for calculated and measured two-phase frictional pressure gradient for Benbella [63] and several correlations at low pressure-medium mass flux.

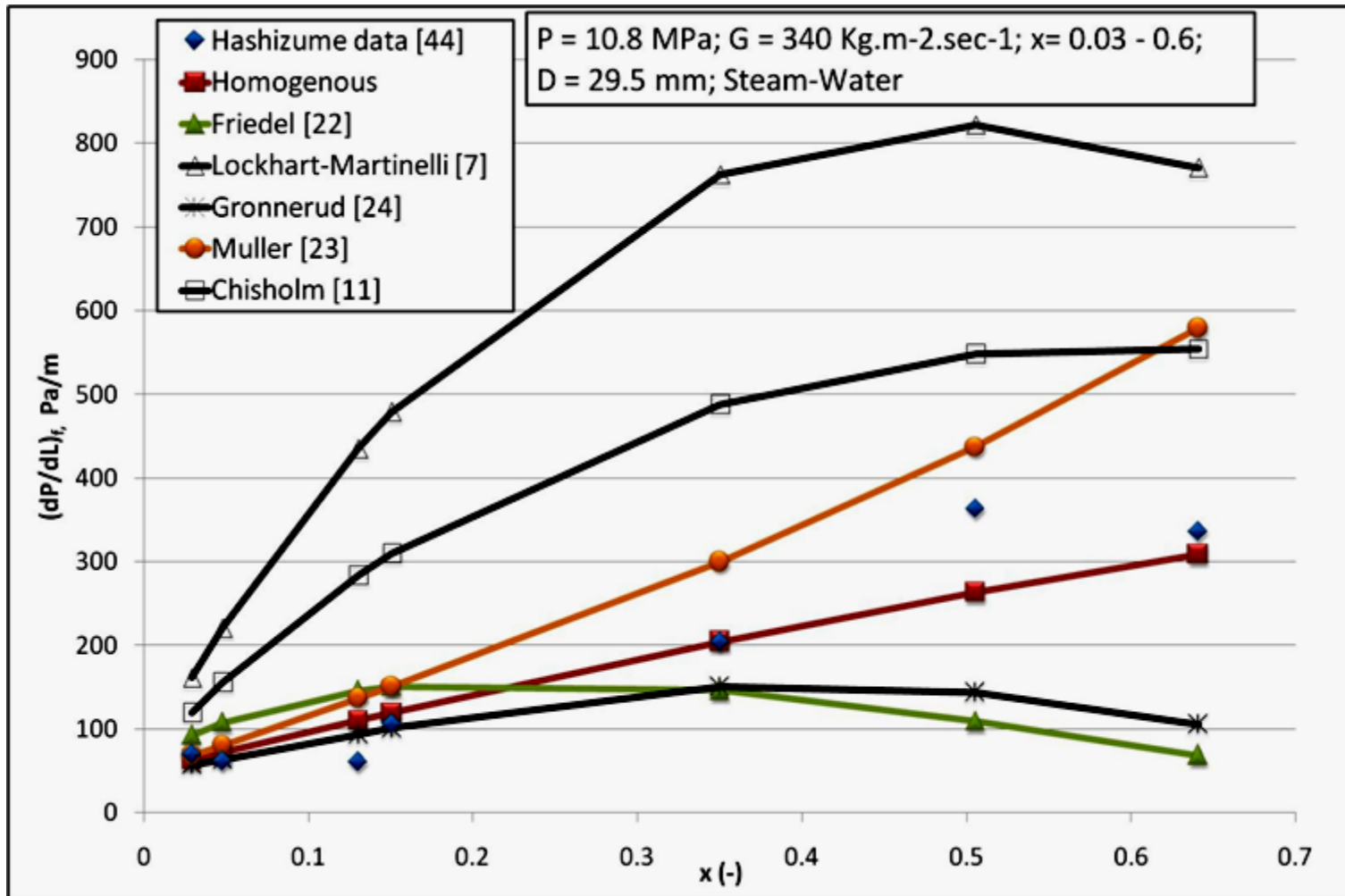


Figure 11-a Comparison for calculated and measured two-phase frictional pressure gradient for Hashizume [44] and several correlations at high pressure-medium mass flux.

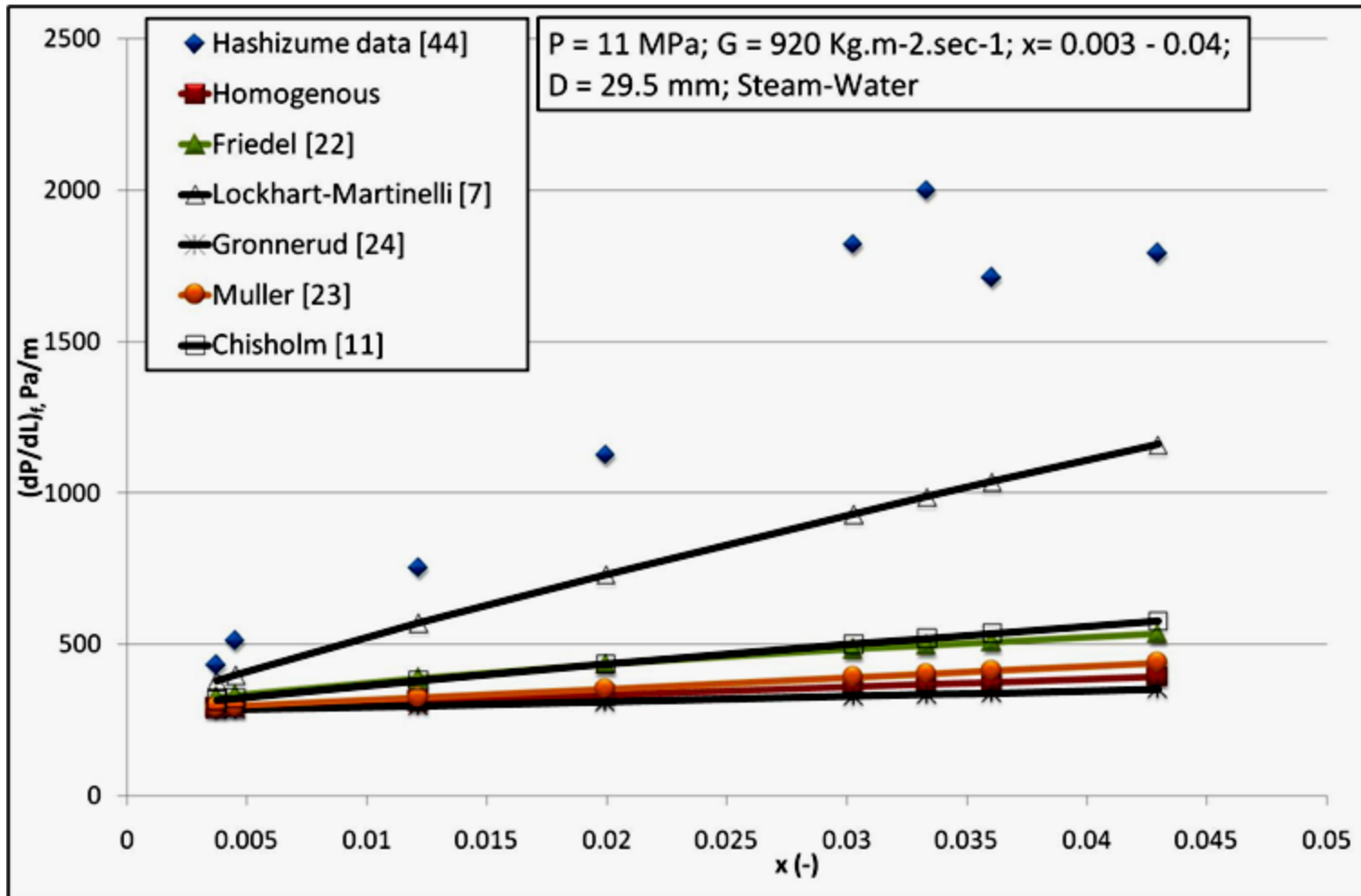


Figure 11-b Comparison for calculated and measured two-phase frictional pressure gradient for Hashizume [44] and several correlations at high pressure-low mass flux.

CHAPTER5

Look-Up-Table

5.1. General

The LUT is basically a normalized data bank of experimental data collected from different resources. It was approved, as mentioned in the literature review chapter, that the LUT technique is the most powerful tool of predicting available with (~4-10 % RMS). The current LUT have wide range of flow conditions and engineering applications such as; oil transport, electric power generation, designing heat exchangers...etc. Moreover, the usage of this table is very easy to handle and its prediction supersedes any correlations available. More information of the construction, usage...etc will be presents in this chapter.

5.2. Selecting Dimension, Parameters and Ranges of the Look-up Table

5.2.1. Dimension and Flow Parameters

The selection of the dimension of the table has been determined as

$$\phi_{Lo}^2 = f(x, y, z) \quad (23)$$

where x, y and z represent flow parameters. A closer look at the prediction techniques for two-phase frictional pressure drop multiplier, and regardless of the working fluid

used, it was concluded that ϕ_{Lo}^2 is a unique function (local condition function) of pressure (p), mass flux (G) and mass quality (x).

Selecting these three parameters will take care of all other parameters not listed. All saturated properties can be handled by saturated pressure for single component fluid (heated or unheated). For two components fluids, pressure is also a main parameter to determine all properties such as density and viscosity. The mass flux is a good measure as the flow channel hydraulic diameter effect is reduced. However a separate correction factor might be needed to predict the diameter effect on pressure drop. The selection of mass quality gives an indication of the fractions of each phase which is necessary to calculate the average properties of the fluids.

Looking at ϕ_{Lo}^2 , one can see that as dimensionless number, its value is universal which makes it applicable using any fluid. The final frictional pressure drop value will depend then on the single phase frictional pressure drop which depends on the fluid itself and the three parameters selected for predicting the multiplier. The problem lies in calculating the multiplier itself as the working fluids should be determined to get the properties. This might affect its use for different fluids which requires a correction to generalize its use. As a result of that and with the scarcity of water pressure drop experimental data it was decided to make a look-up table with dimensionless flow parameters. For example in fluid modeling, El Nakla (2011) used dimensional analysis to find that a good representative of pressure is the density ratio between

liquid and gas and Reynolds number denotes the mass flux. The results of El Nakla (2011) are consistent with the results of Bruce (1972) for modeling pressure for two-phase pressure drop.

The skeleton table was then constructed such that

$$\phi_{Lo}^2 = f(DR, Re_L, x) \quad (24)$$

where

$$DR = \frac{\rho_L}{\rho_G} \quad (25)$$

$$Re_L = \frac{GD}{\mu_L} \quad (26)$$

$$x = \frac{\dot{m}_g}{\dot{m}_{total}} \quad (27)$$

5.2.2. Range of Application of the Look-up Table

The look-up table was subdivided based on the selected flow parameters as the following,

Density ratio:	1500;	900;	600;	300;	200;	150;	100;	80;	60;
	40;	30;	20;	13;	10;	7;	5.5;	4;	2.5.
Reynolds No.:	100;	200;	400;	600;					
	1,000;	2,000;	4,000;	6,000;					
	8,000;	10,000;	20,000;	40,000;					
	60,000;	80,000;	100,000;	150,000;					
	200,000;	400,000;	600,000;	800,000;					
	1,000,000.								

Mass quality: 0.00; 0.05; 0.10; 0.15; 0.20; 0.25; 0.30; 0.35;
 0.40; 0.45; 0.50; 0.55; 0.60; 0.65; 0.70; 0.75;
 0.80; 0.85; 0.90; 0.95; 1.00

The corresponding saturated equivalent pressures of the above density ratio values for water and R134a are shown in Table 5. These values are just for reference and one can get the actual values of pressure by applying iteration techniques for the fluid under consideration.

As for mass qualities of 0.00 and 1.00 the flow is single phase liquid and single phase gas, respectively, the table entries of the frictional pressure drop multiplier corresponding to these values were set to unity. Table 6 shows a part of the skeleton table generated from best prediction correlations.

Table 5 Equivalent saturated pressures corresponding to water and R134a

Density ratio	Water equivalent pressure, MPa	R134a equivalent pressure, MPa
1500	0.103	0.015
900	0.185	0.029
600	0.28	0.044
300	0.57	0.088
200	0.86	0.133
150	1.15	0.175
100	1.7	0.263
80	2.11	0.327
60	2.76	0.428
40	3.98	0.625
30	5.09	0.805
20	7.07	1.37
13	9.69	1.59
10	11.51	1.913
7	14.15	2.41
5.5	15.925	2.755
4	18.12	3.2
2.5	20.625	3.735

Steps of building a LUT start with constructing a skeleton table from best available prediction methods based on Error Mapping table. Then experimental data are used to update the skeleton table. The updating process results in improving the prediction accuracy of the table by bringing the table values closer to actual values. As a final step, the updated table is smoothed to eliminate discontinuities between the regions of the correlations and experimental regions. The following steps are summarizing the construction of the Look-Up-Table;

1. A FORTRAN program, which is the most accurate computer language and most used in the industry, for each correlation has been done. Each one of them represents a skeleton table.
2. Around two thousands and ninety one experimental data points have been collected from the literature for variant pipe diameters and fluid flow condition.
3. First usage of the experimental data points is to assess which one of the correlations predicted better than other. For this purpose, an Error Mapping has been built and divided into sub-regions to obtain best accuracy of results.
4. Based on Error Mapping table, a new skeleton table has been built which guarantee using the suitable correlations in the suitable regions.
5. Second usage of the experimental data points is to update the new skeleton table. This action modified the entries of the table and makes them more actual.
6. Smoothing program is needed to eliminate the discontinuities and irregularities between regions. More details will explain later on.

7. An error assessment between Look-Up-Table and experimental data is needed to judge on the performance of this new techniques.

5.3. Constructing skeleton Table

The correlations explained in chapter 4 were used along the error mapping of Table 4 to assign a correlation for each sub-range of the table. The selection was based on the best prediction of the available data in that sub-range. The final skeleton table was constructed based on homogeneous model, Chisholm (1973) correlation, Muller-Steinhagen and Heck (1986) correlation, Grönnerud (1972) correlation, and Friedel (1979) correlation

Six-skeleton tables were constructing by using a standard programming language (e.g. FORTRAN software). Each one of these skeleton tables represents one of the two-phase pressure drop multipliers (Φ_{LO}^2) correlations, and the prediction accuracy of these skeleton tables was examined against the experimental data and error mapping table was generated as shown earlier. Only one skeleton table, which predicts the value of two-phase pressure drop multiplier (Φ_{LO}^2), is resulted from this comparison which is a combination of the six-skeleton tables. The important of the resulted skeleton table is to provide the initial estimate of the LUT two-phase frictional pressure drop multiplier values.

The two-phase frictional pressure drop multiplier (Φ_{LO}^2) presented as a function of dimensionless flow parameters which are density ratio (DR) at 1500.0– 2.5, Reynolds

Number (RE) at 100.0-1,000,000.0, and mass quality (x) at 0.0 – 1.00 for pipe diameter of ranges 2.0-90.0 mm. These flow parameters and the ranges of flow conditions both will assure the generality of the LUT for any kind of flow distribution, pipe diameter, physical properties, pipe orientation...etc. The LUT is based on database of two thousands and ninety one were collected from 18, data sets and provides the LUT values at 21 density ratios, 21 Reynolds number, and 21 mass qualities. So, the skeleton tables were constructed based on these flow parameters, and the regions were chosen to cover the existing experimental data and any experimental data available in the future. Figure 12 demonstrates the mechanism of constructing the skeleton table program.

In order to obtain one skeleton table out of six skeleton tables an error mapping table was used. The results of the assessment between these tables and the experimental data were presented in Table 4. This table is divided density ratio into four ranges, Reynolds number into four ranges, and mass quality into three ranges. Two types of error relations used to distinguish between correlations. One of them is the relative error which gives an indication of the data scattered around the correlations. The other one is the root-mean squared error which gives the error between LUT entries and the actual values. The methodology followed to construct the error mapping program is presented in Figure 13.

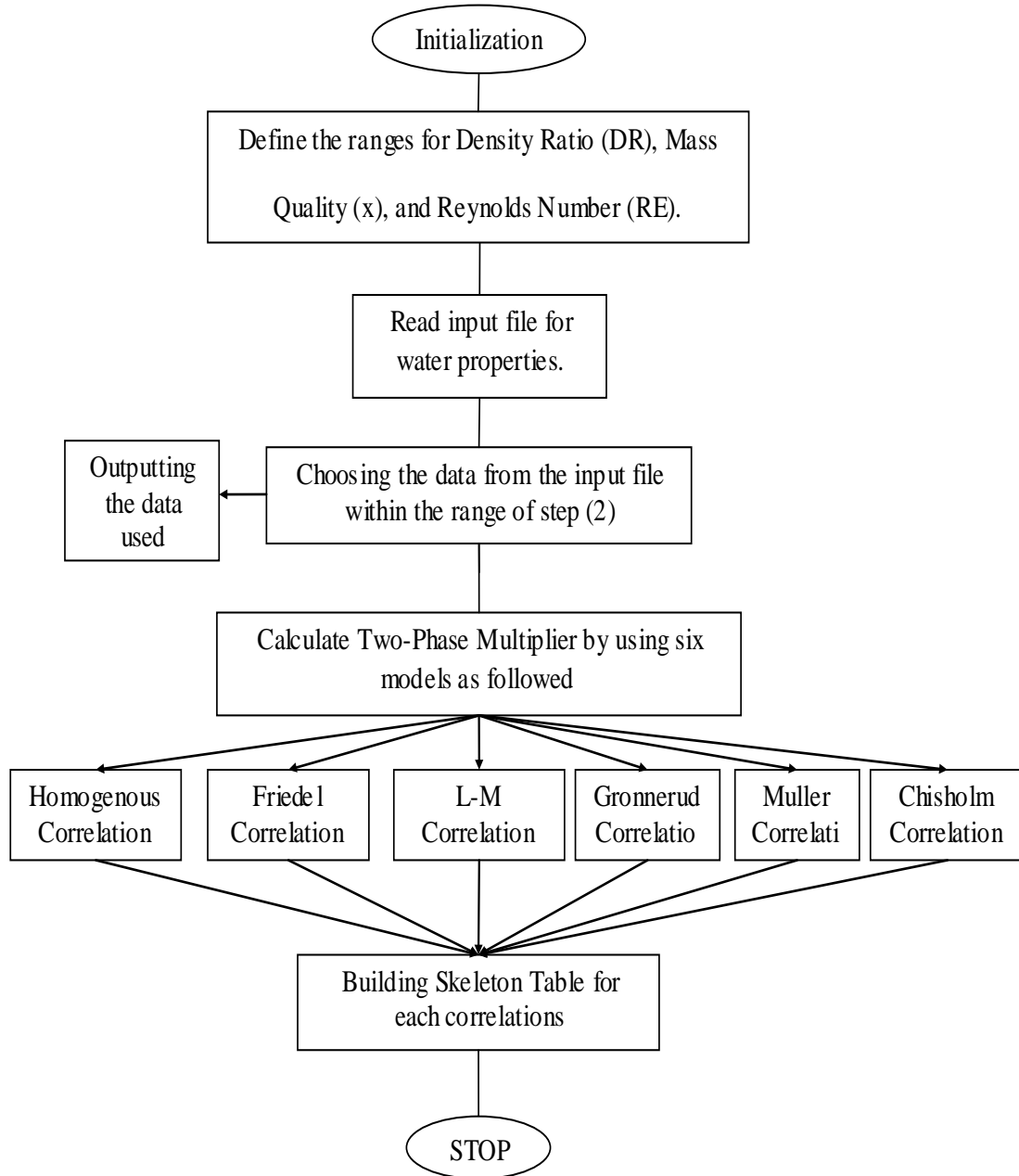


Figure 12 flow chart shown the Constructing skeleton tables from best correlations

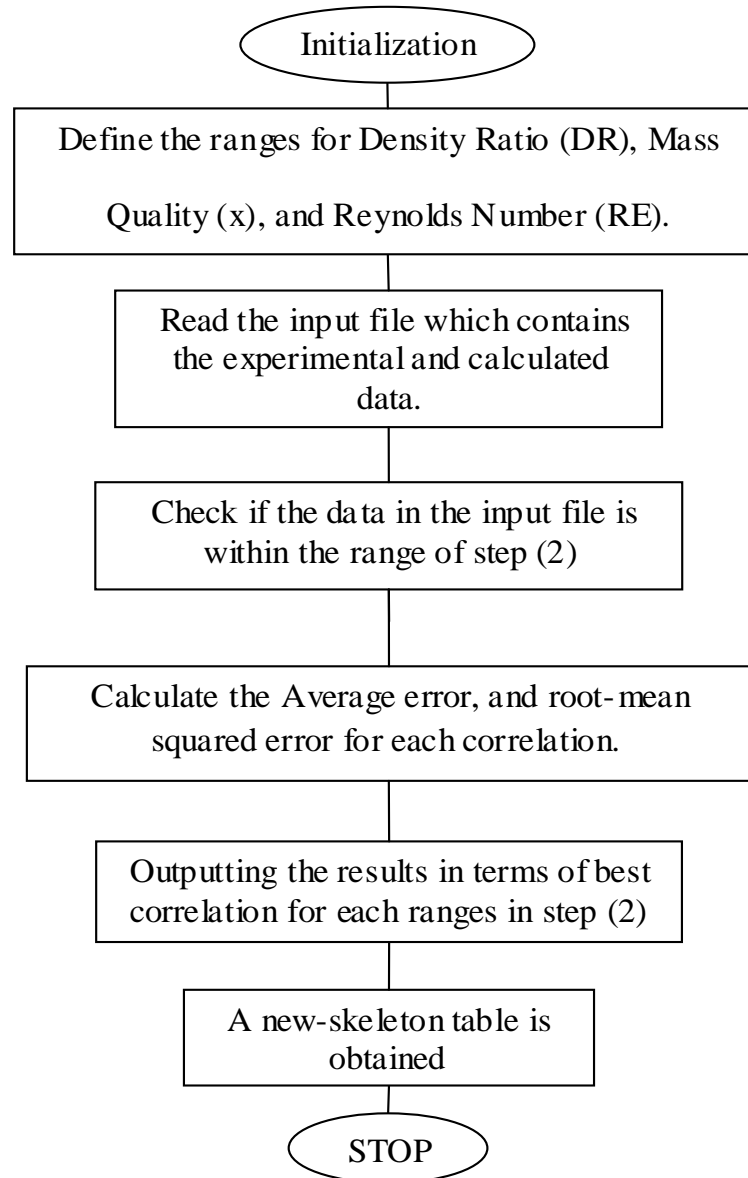


Figure 13flow chart Error Mapping Program

Now, for each ranges of density ratio, Reynolds number, and mass quality, one correlation with least error for the two-phase frictional pressure drop multiplier is nominated to be used in the skeleton table. Moreover, the values of the skeleton table were used for evaluating the slopes of two-phase frictional pressure drop multiplier versus density ratio, mass flux, and mass quality. For the ranges with no experimental data, Homogenous model is chosen.

Table 6 represents a sample of the skeleton table which is a combination of best correlations. This table presented is a result of error mapping table (table 4). Values in the skeleton table for density ratio of 1000-3000, Reynolds Number of 2000-10000, and mass quality of 0.0 - 0.3 are predicted using Gronnerud correlation [24] with green color. For same ranges of density ratio and Reynolds number but for mass quality of 0.35 - 0.6 are predicted using Muller correlation [23] with pink color. It is clearly shown in this table that the discontinuity and irregularities are there due to different behaviors of the chosen correlations. These irregularities will be tackled next.

Table 6 New Ske leton Table

Density Ratio (DR)	Reynolds Number (RE)	Mass Quality (x)																				
		0	0.05	0.1	0.15	0.2	0.25	0.3	0.35	0.4	0.45	0.5	0.55	0.6	0.65	0.7	0.75	0.8	0.85	0.9	0.95	1
1500	100	1	59.91	107.25	149.18	187.75	223.97	258.39	291.38	323.20	354.02	383.98	413.19	441.74	469.68	497.09	524.01	550.47	576.52	602.18	627.49	0
1500	200	1	59.91	107.25	149.18	187.75	223.97	258.39	291.38	323.20	354.02	383.98	413.19	441.74	469.68	497.09	524.01	550.47	576.52	602.18	627.49	0
1500	400	1	59.91	107.25	149.18	187.75	223.97	258.39	291.38	323.20	354.02	383.98	413.19	441.74	469.68	497.09	524.01	550.47	576.52	602.18	627.49	0
1500	600	1	59.91	107.25	149.18	187.75	223.97	258.39	291.38	323.20	354.02	383.98	413.19	441.74	469.68	497.09	524.01	550.47	576.52	602.18	627.49	0
1500	1000	1	59.91	107.25	149.18	187.75	223.97	258.39	291.38	323.20	354.02	383.98	413.19	441.74	469.68	497.09	524.01	550.47	576.52	602.18	627.49	0
1500	2000	1	17.80	41.25	70.34	104.64	143.83	187.71	716.03	832.63	955.01	1083.89	1220.00	1364.06	469.68	497.09	524.01	550.47	576.52	602.18	627.49	0
1500	4000	1	21.75	50.70	86.63	128.98	177.37	231.55	485.00	563.93	646.77	734.02	826.16	923.69	469.68	497.09	524.01	550.47	576.52	602.18	627.49	0
1500	6000	1	25.92	60.69	103.85	154.72	212.85	277.93	485.00	563.93	646.77	734.02	826.16	923.69	469.68	497.09	524.01	550.47	576.52	602.18	627.49	0
1500	8000	1	29.91	70.27	120.35	179.37	246.82	322.33	485.00	563.93	646.77	734.02	826.16	923.69	469.68	497.09	524.01	550.47	576.52	602.18	627.49	0
1500	10000	1	33.70	79.34	135.97	202.72	279.01	364.41	485.00	563.93	646.77	734.02	826.16	923.69	469.68	497.09	524.01	550.47	576.52	602.18	627.49	0
1500	20000	1	59.91	107.25	149.18	187.75	223.97	258.39	291.38	323.20	354.02	383.98	413.19	441.74	469.68	497.09	524.01	550.47	576.52	602.18	627.49	0
1500	40000	1	59.91	107.25	149.18	187.75	223.97	258.39	291.38	323.20	354.02	383.98	413.19	441.74	469.68	497.09	524.01	550.47	576.52	602.18	627.49	0
1500	60000	1	59.91	107.25	149.18	187.75	223.97	258.39	291.38	323.20	354.02	383.98	413.19	441.74	469.68	497.09	524.01	550.47	576.52	602.18	627.49	0
1500	80000	1	59.91	107.25	149.18	187.75	223.97	258.39	291.38	323.20	354.02	383.98	413.19	441.74	469.68	497.09	524.01	550.47	576.52	602.18	627.49	0
1500	100000	1	59.91	107.25	149.18	187.75	223.97	258.39	291.38	323.20	354.02	383.98	413.19	441.74	469.68	497.09	524.01	550.47	576.52	602.18	627.49	0
1500	150000	1	59.91	107.25	149.18	187.75	223.97	258.39	291.38	323.20	354.02	383.98	413.19	441.74	469.68	497.09	524.01	550.47	576.52	602.18	627.49	0
1500	200000	1	59.91	107.25	149.18	187.75	223.97	258.39	291.38	323.20	354.02	383.98	413.19	441.74	469.68	497.09	524.01	550.47	576.52	602.18	627.49	0
1500	400000	1	59.91	107.25	149.18	187.75	223.97	258.39	291.38	323.20	354.02	383.98	413.19	441.74	469.68	497.09	524.01	550.47	576.52	602.18	627.49	0
1500	600000	1	59.91	107.25	149.18	187.75	223.97	258.39	291.38	323.20	354.02	383.98	413.19	441.74	469.68	497.09	524.01	550.47	576.52	602.18	627.49	0
1500	800000	1	59.91	107.25	149.18	187.75	223.97	258.39	291.38	323.20	354.02	383.98	413.19	441.74	469.68	497.09	524.01	550.47	576.52	602.18	627.49	0
1500	1000000	1	59.91	107.25	149.18	187.75	223.97	258.39	291.38	323.20	354.02	383.98	413.19	441.74	469.68	497.09	524.01	550.47	576.52	602.18	627.49	0
1300	100	1	50.17	89.93	125.20	157.66	188.15	217.13	244.91	271.70	297.65	322.87	347.47	371.50	395.04	418.11	440.78	463.06	484.99	506.60	527.91	0
1300	200	1	50.17	89.93	125.20	157.66	188.15	217.13	244.91	271.70	297.65	322.87	347.47	371.50	395.04	418.11	440.78	463.06	484.99	506.60	527.91	0
1300	400	1	50.17	89.93	125.20	157.66	188.15	217.13	244.91	271.70	297.65	322.87	347.47	371.50	395.04	418.11	440.78	463.06	484.99	506.60	527.91	0
1300	600	1	50.17	89.93	125.20	157.66	188.15	217.13	244.91	271.70	297.65	322.87	347.47	371.50	395.04	418.11	440.78	463.06	484.99	506.60	527.91	0
1300	1000	1	50.17	89.93	125.20	157.66	188.15	217.13	244.91	271.70	297.65	322.87	347.47	371.50	395.04	418.11	440.78	463.06	484.99	506.60	527.91	0
1300	2000	1	15.01	34.57	58.85	87.46	120.15	156.75	602.46	700.54	803.49	911.91	1026.40	1147.59	395.04	418.11	440.78	463.06	484.99	506.60	527.91	0
1300	4000	1	18.14	42.07	71.76	106.75	146.74	191.51	408.09	474.48	544.16	617.55	695.05	777.09	395.04	418.11	440.78	463.06	484.99	506.60	527.91	0
1300	6000	1	21.51	50.13	85.65	127.52	175.36	228.92	408.09	474.48	544.16	617.55	695.05	777.09	395.04	418.11	440.78	463.06	484.99	506.60	527.91	0
1300	8000	1	24.75	57.89	99.03	147.51	202.91	264.93	408.09	474.48	544.16	617.55	695.05	777.09	395.04	418.11	440.78	463.06	484.99	506.60	527.91	0
1300	10000	1	27.83	65.27	111.74	166.50	229.08	299.14	408.09	474.48	544.16	617.55	695.05	777.09	395.04	418.11	440.78	463.06	484.99	506.60	527.91	0
1300	20000	1	50.17	89.93	125.20	157.66	188.15	217.13	244.91	271.70	297.65	322.87	347.47	371.50	395.04	418.11	440.78	463.06	484.99	506.60	527.91	0
1300	40000	1	50.17	89.93	125.20	157.66	188.15	217.13	244.91	271.70	297.65	322.87	347.47	371.50	395.04	418.11	440.78	463.06	484.99	506.60	527.91	0
1300	60000	1	50.17	89.93	125.20	157.66	188.15	217.13	244.91	271.70	297.65	322.87	347.47	371.50	395.04	418.11	440.78	463.06	484.99	506.60	527.91	0
1300	80000	1	50.17	89.93	125.20	157.66	188.15	217.13	244.91	271.70	297.65	322.87	347.47	371.50	395.04	418.11	440.78	463.06	484.99	506.60	527.91	0
1300	100000	1	50.17	89.93	125.20	157.66	188.15	217.13	244.91	271.70	297.65	322.87	347.47	371.50	395.04	418.11	440.78	463.06	484.99	506.60	527.91	0
1300	150000	1	50.17	89.93	125.20	157.66	188.15	217.13	244.91	271.70	297.65	322.87	347.47	371.50	395.04	418.11	440.78	463.06	484.99	506.60	527.91	0
1300	200000	1	50.17	89.93	125.20	157.66	188.15	217.13	244.91	271.70	297.65	322.87	347.47	371.50	395.04	418.11	440.78	463.06	484.99	506.60	527.91	0
1300	400000	1	50.17	89.93	125.20	157.66	188.15	217.13	244.91	271.70	297.65	322.87	347.47	371.50	395.04	418.11	440.78	463.06	484.99	506.60	527.91	0
1300	600000	1	50.17	89.93	125.20	157.66	188.15	217.13	244.91	271.70	297.65	322.87	347.47	371.50	395.04	418.11	440.78	463.06	484.99	506.60	527.91	0

5.4. Updating the Skeleton Table

All experimental data were tabulated having the same format. The flow conditions were presented in non-dimensional form (density ratio (DR), Re, x) to be consistent with the skeleton table. The updating process was performed by replacing the two-phase frictional pressure drop multiplier from the skeleton table by a weighted experimental value for the same flow conditions and leaving the table values unchanged where there are no experimental values. This process is the main step in improving the prediction accuracy of the table. The resulting updated table will have a better prediction for the regions where experimental data exist and will predict as good as correlations in the regions where experimental data are scarce.

5.4.1. Procedure of Updating

Each experimental frictional multiplier value $\phi_{Lo}^2(DR_o, Re_{Lo}, x_o)$ was used to generate the table ϕ_{Lo}^2 values at eight matrix conditions surrounding (DR_o, Re_{Lo}, x_o) . Figure 6 illustrates the definition of the matrix conditions surrounding the experimental data point. The following steps were required in generating the new table ϕ_{Lo}^2 values:

1. Correction for differences in DR, Re, and x conditions. The experimental ϕ_{Lo}^2 values $\phi_{Lo}^2(DR_o, Re_{Lo}, x_o)$ were extrapolated to the surrounding matrix conditions as follows:

$$\phi_{Lo}^2 \left(DR_i, (Re_L)_j, x_k \right)_n = \phi_{Lo}^2 \left(DR_o, (Re_L)_o, x_o \right) + \Delta \phi_{Lo}^2 \quad (28)$$

where

$$\Delta \phi_{Lo}^2 = \frac{\partial \phi_{Lo}^2}{\partial DR} (DR_i - DR_o) + \frac{\partial \phi_{Lo}^2}{\partial Re} (Re_j - Re_o) + \frac{\partial \phi_{Lo}^2}{\partial x} (x_k - x_o) \quad (29)$$

where:

$DR_i, (Re_L)_j, x_k$: are adjacent matrix conditions and the differential values are obtained from the skeleton table.

2. Calculation of weight factor. Figure 14 shows the conditions of an experimental ϕ_{Lo}^2 value enclosed in a box with corner points represent the ϕ_{Lo}^2 table conditions. Weight factors were assigned to the experimental ϕ_{Lo}^2 value, extrapolated to each of the surrounding eight corner points. The table point closest to the experimental conditions should receive more weight than the more distant ones. In order to account for that the weight contribution to the ϕ_{Lo}^2 table value at each corner of the box was made proportional cube root of the volume of the diagonally opposite sub-box. After the proportions of all eight weights had been calculated, the final weight factors $W_{i,j,k}$ were obtained by normalizing so that their sum was unity.

3. Evaluation of the new table ϕ_{Lo}^2 value. Using the extrapolated experimental ϕ_{Lo}^2 values and weight factors, the new ϕ_{Lo}^2 table values were found from

$$\phi_{Lo}^2(DR_i, (Re_L)_j, x_k) = \frac{\sum_{n=1}^{n=N} [(w_{i,j,k})_n \phi_{Lo}^2(DR_i, (Re_L)_j, x_k)_n]}{\sum_{n=1}^{n=N} (w_{i,j,k})_n} \quad (30)$$

where N is the total number of data points adjacent to the table point (DR_i, Re_j, x_k) , i.e., the number of data points falling in the range $DR_{i-1} - DR_{i+1}$, $Re_{j-1} - Re_{j+1}$, $x_{k-1} - x_{k+1}$, and n refers to the individual data points in that range.

4. The weighted average ϕ_{Lo}^2 thus calculated replaced the skeleton table ϕ_{Lo}^2 value at matrix conditions adjacent to experimental ϕ_{Lo}^2 values. In the regions of the ϕ_{Lo}^2 table where matrix conditions did not have adjacent data points, the original ϕ_{Lo}^2 table value (correlation value) was maintained.

Table 7 shows statistics on the experimental data used to perform updating of the skeleton table. An updating program is constructed, as shown in Figure 15.

Table 7 Summary of experimental data used in updating the skeleton table

Parameter	Selection Criteria
Total number of experimental data	2091
Number of data sets	18
Pipe diameter (mm)	$2.0 < D < 90.0$
Pressure Range (MPa)	$0.1 < P < 21$
Density Ratio (DR)	$2.5 < DR < 1,500$
Mass flux G (Kg.m ⁻² .sec ⁻¹)	$2.05 < G < 20,000$
Reynolds Number (Re)	$100 < Re < 1,000,000$
Mass quality (x)	$0.0 < x < 1.00$
Flow circumstances	Single component-Adiabatic only
Total Number of data used to after removal criteria	1177
Total number of data used for constructing LUT	940

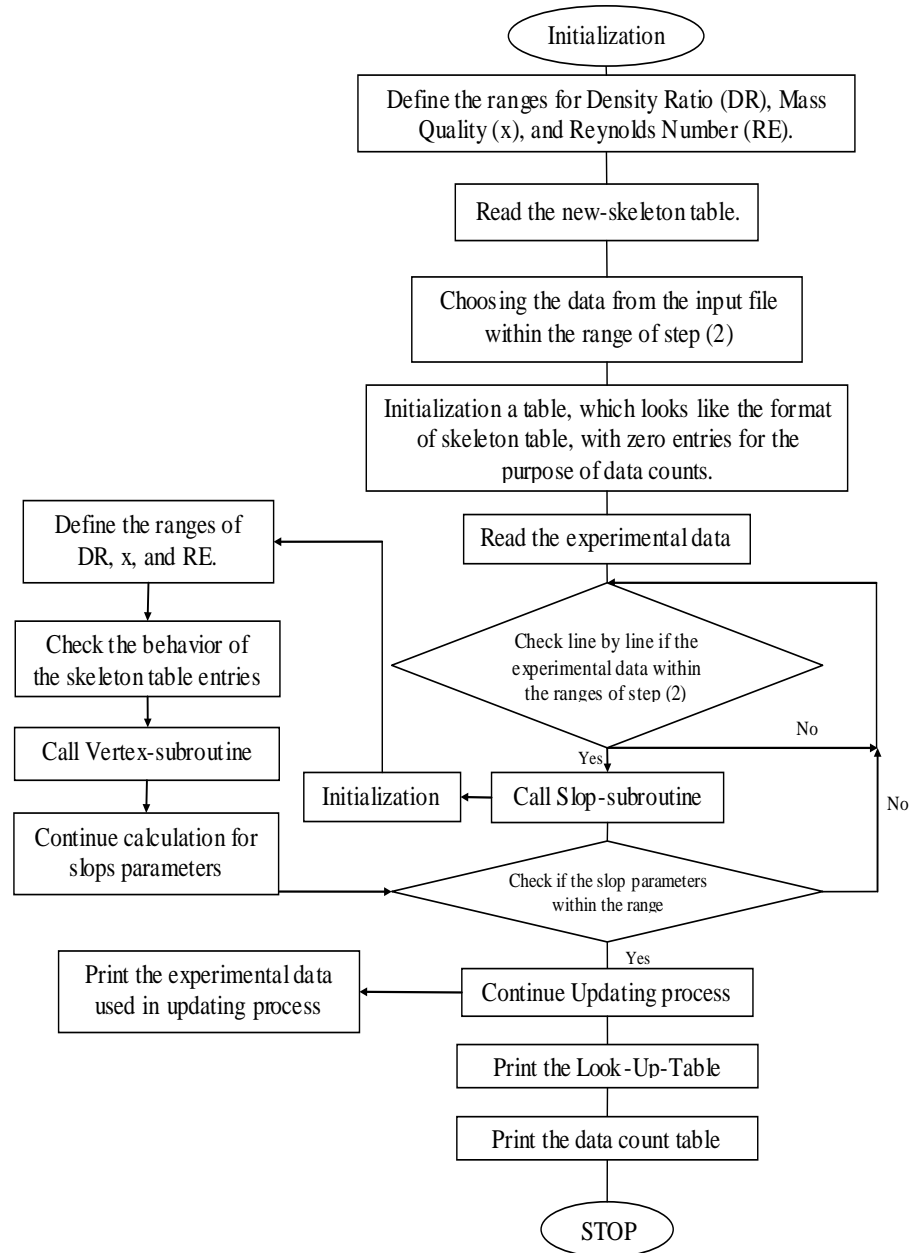


Figure 15 flow chart for updating the skeleton table with experimental data

5.5. Smoothing the Updated Table

The three-dimensional table-smoothing method by Huang and Cheng (1992) was employed to smooth table entries after updating. The smoothing procedure corrected table entries in question considering the adjacent table entries and concept of weighting factor. Although, this procedure modifies slightly the table entries established by experimental data, it creates continuous smooth multidimensional surface (see Figure 8). The slight deterioration of accuracy brings benefits in trouble-free application of the ϕ_{Lo}^2 look-up table in iteration procedures during calculations.

The smoothing process is performed by fitting the table's grid points in a polynomial. This can be controlled by three parameters, which are (i) number of points in each smoothing step, (ii) order of the polynomial, and (iii) a weight factor to control smoothing. Optimizing the table requires several updating and smoothing steps to be performed to minimize the error in prediction and to reduce discontinuities. After each time smoothing is performed (by controlling the three above mentioned parameters), visual inspection of the whole table is performed to assure consistency which is followed by calculating the error in prediction (see Section 5.6.).

A smoothing program was prepared in order to eliminate the discontinuities and irregularities between correlations and experimental regions in the three parametric ranges: density ratio, Reynolds number, and mass quality. This discontinuities and irregularities are due to differences between data sets, data scattering...etc. Also, the

boundary which located between regions shows discontinuities and irregularities. This regions happen due to the presence of the correlations data points and the experimental data points adjacent to each other, and other regions contains the experimental data sets adjacent each other.

Smoothing program, which developed by Huang and Cheng [72], aimed to strengthen the experimental data entries in the updated table by considering their weights, comparing with correlation data points entries which have zero weight. The principle of the smoothing method which described by D.C.Groeneveld [73]“is to fit three polynomials to six table entries in each parametric direction. The three polynomials intersect each other at the table entry, where the two-phase frictional pressure drop multiplier value is then adjusted. This resulted in a significant improvement in the smoothness of the LUT”.Furthermore, the correlations data points are modified to eliminate as much as possible the discontinuities and irregularities occurring due to updating process. At this stage, a look-up-table with its final shape is resulted. Figure 16 shows the procedure of constructing the smooth program. The smoothed table is shown in Appendix A.

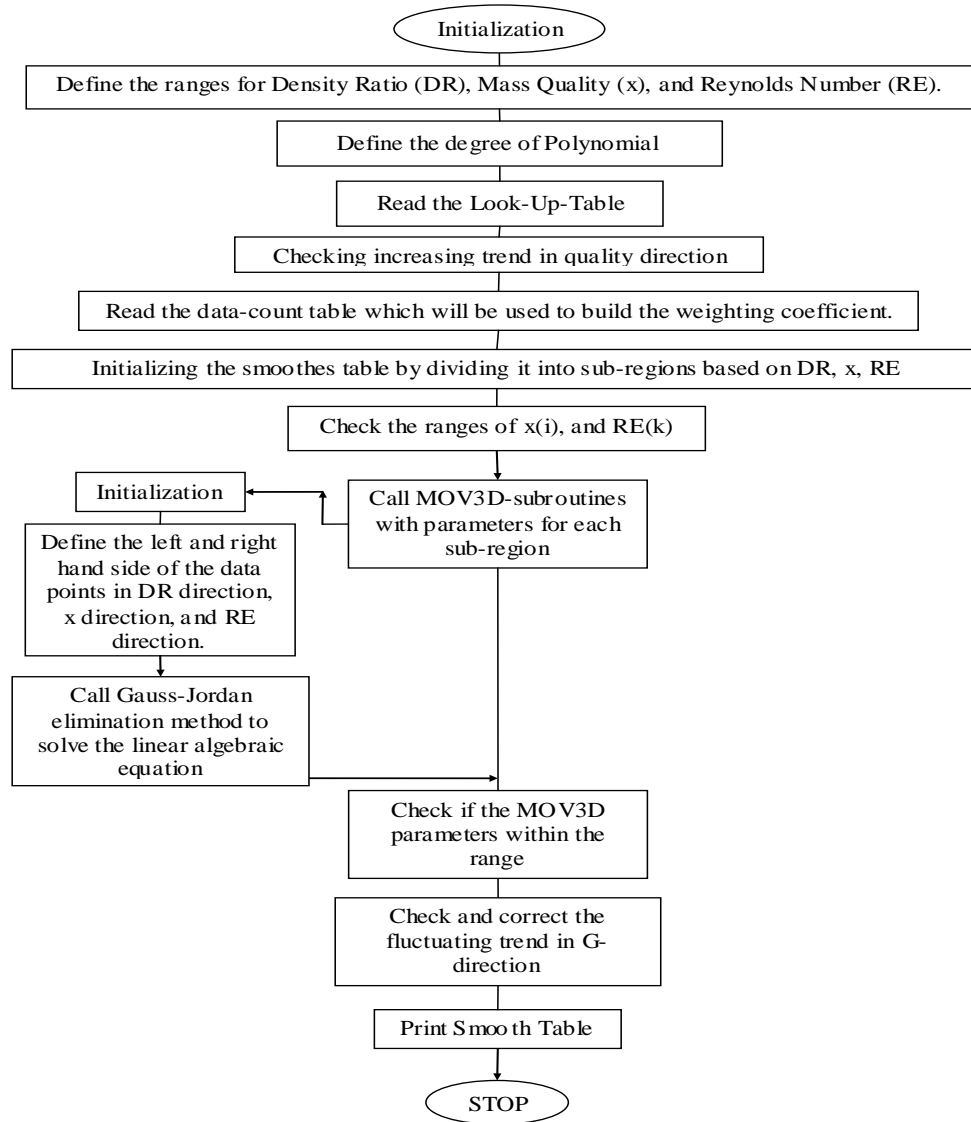


Figure 16 flow chart for Smoothing the Look-Up-Table

5.6. Look-Up-Table Assessment

After the look-up-table being smoothed, the LUT entries are ready to be used in the error assessment program. The beginning of the program, as previous ones, starts with initialization of the parameters and defining the ranges of density ratio, mass quality and Reynolds number. The error program aimed to calculate the percentage error

between the LUT entry and the experimental data which have same flow conditions.

The percentage error in prediction of each data point is calculated as presented previously in Equation 16.

The program then calculated the average error (ε_1), and root-mean-squared (RMS) error (ε_2), as presented previously in Equations 17 and 18. The results of assessment are summarized in Table 8. More detailed table is presented in the appendix B. The algorithm of this program is shown in Figure 17.

Table 8 Part of the data assessment of LUT

D	DR	Re _L	x	Total Mass Flux	Pressure	$\phi^2_{LO,exp}$	$\phi^2_{LO,pred}$	Percentage Error
m	--	--	--	Kg.m-2.sec-1	KPa	--	--	%
0.04666	239.69	8954.2	0.46677	81.8784	165.474	57.10	63.98	12.054
0.04666	237.4	10920.7	0.37686	99.5813	165.474	42.48	42.54	0.137
0.04666	237.4	12469.1	0.32959	113.7011	165.474	35.98	40.67	13.055
0.04666	235.11	13792.3	0.29701	125.4588	165.474	31.38	38.42	22.440
0.04666	230	14895.2	0.27091	135.4913	165.474	27.47	35.71	30.017
0.04666	232.93	16019.7	0.25443	145.3115	165.474	24.85	34.46	38.658
0.04666	232.93	16982.4	0.23949	154.0435	165.474	21.92	32.48	48.194
0.04666	232.05	17908.3	0.22751	162.2712	165.474	20.01	30.46	52.229
0.04666	230.72	18752.7	0.21561	169.6231	165.474	20.07	28.13	40.142
0.04666	230.72	19556.7	0.20645	176.8953	165.474	19.68	26.21	33.150
0.04666	230.72	20319.6	0.19841	183.796	165.474	19.38	24.78	27.886
0.04666	230.72	21050.2	0.19138	190.4047	165.474	18.21	24.23	33.016
0.04666	228.56	21728.8	0.18221	196.0579	165.474	17.63	23.01	30.527
0.04666	228.56	22349.5	0.17452	201.6581	165.474	17.88	22.23	24.297
0.04666	230.82	22811	0.16649	206.9132	165.474	17.09	21.61	26.468
0.04666	239.13	22458.5	0.16289	213.6016	165.474	14.97	22.18	48.117
0.04666	239.33	22682.1	0.14922	216.8131	165.474	17.01	20.42	20.054
0.04666	226.55	11233.3	0.57023	101.4654	165.474	79.47	89.18	12.219
0.04666	224.54	13224.9	0.48042	119.3275	165.474	63.96	62.75	-1.898
0.04666	223.62	14758	0.42654	132.7838	165.474	61.60	57.19	-7.173
0.04666	220.33	16122.5	0.39105	144.7007	165.474	55.91	54.44	-2.617

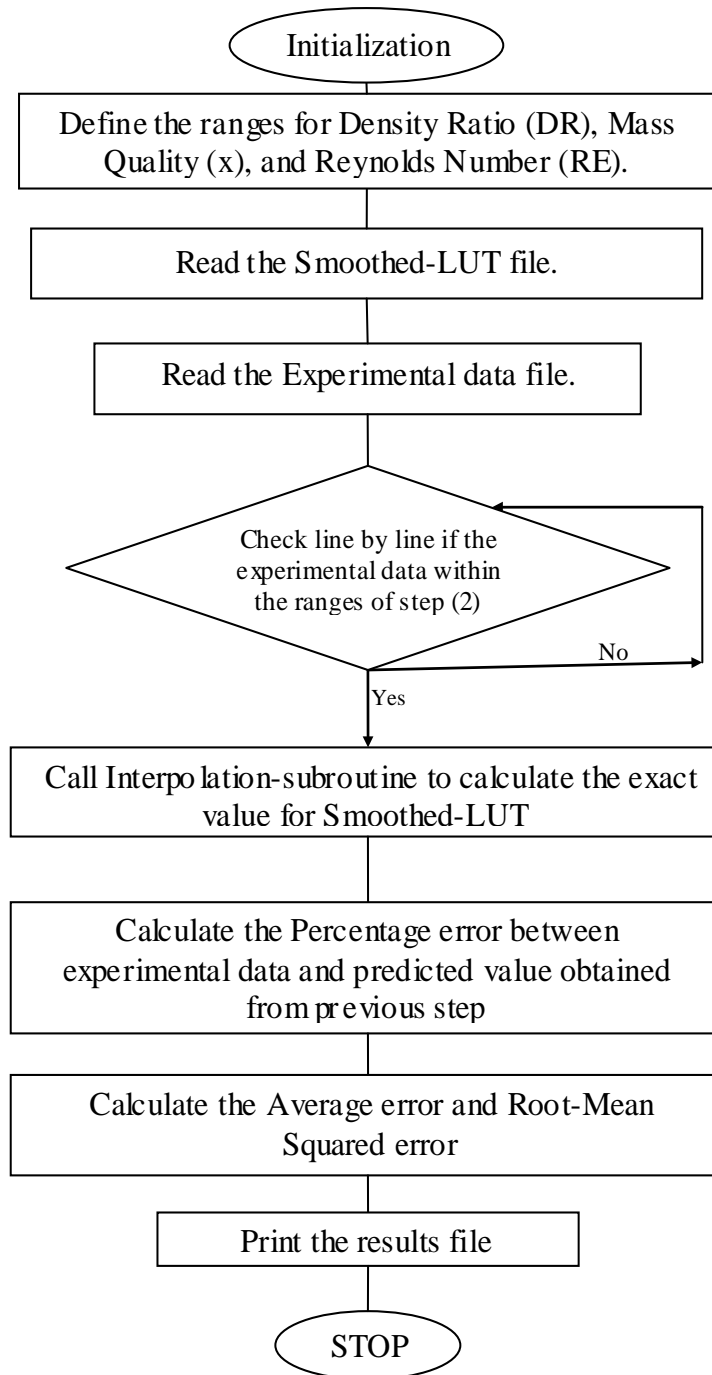


Figure 17 Flow chart shown Error assessments for Look-Up-Table

In accordance to Chapter 3, the LUT entries were processed and assessed against experimental data points. In addition to that LUT entries were compared with the prediction of six leading correlations. This step was necessary to judge whether the LUT is predicting better than the correlations or not. Average error and Root-Mean-Squared error was calculated to resolve the result. Moreover, visual presentation was presented to obtain an idea of the effectiveness of the LUT against the experimental data and the correlations.

Figure 18 shows the assessment result in graphical form for better visualization for selected data sets. As seen from the figure, there is a small scatter in the prediction with the experimental data within percentage error $\pm 30\%$.

The results of assessment for the LUT and the correlations against all data sets are summarized in Table 9. It can be seen from the table that LUT shows the best overall prediction accuracy (least root-mean-squared error) among other correlations.

Figures 19-23 show the capability of the LUT to predict in all flow conditions circumstances. Also, these figures show that the LUT has a very good trend and the irregularities and discontinuities are disappeared.

Figures 24-26 give a visual presentation of the performance of the LUT against the correlations at different flow conditions. These figures show that the LUT is better in prediction than the best correlations considered in this study.

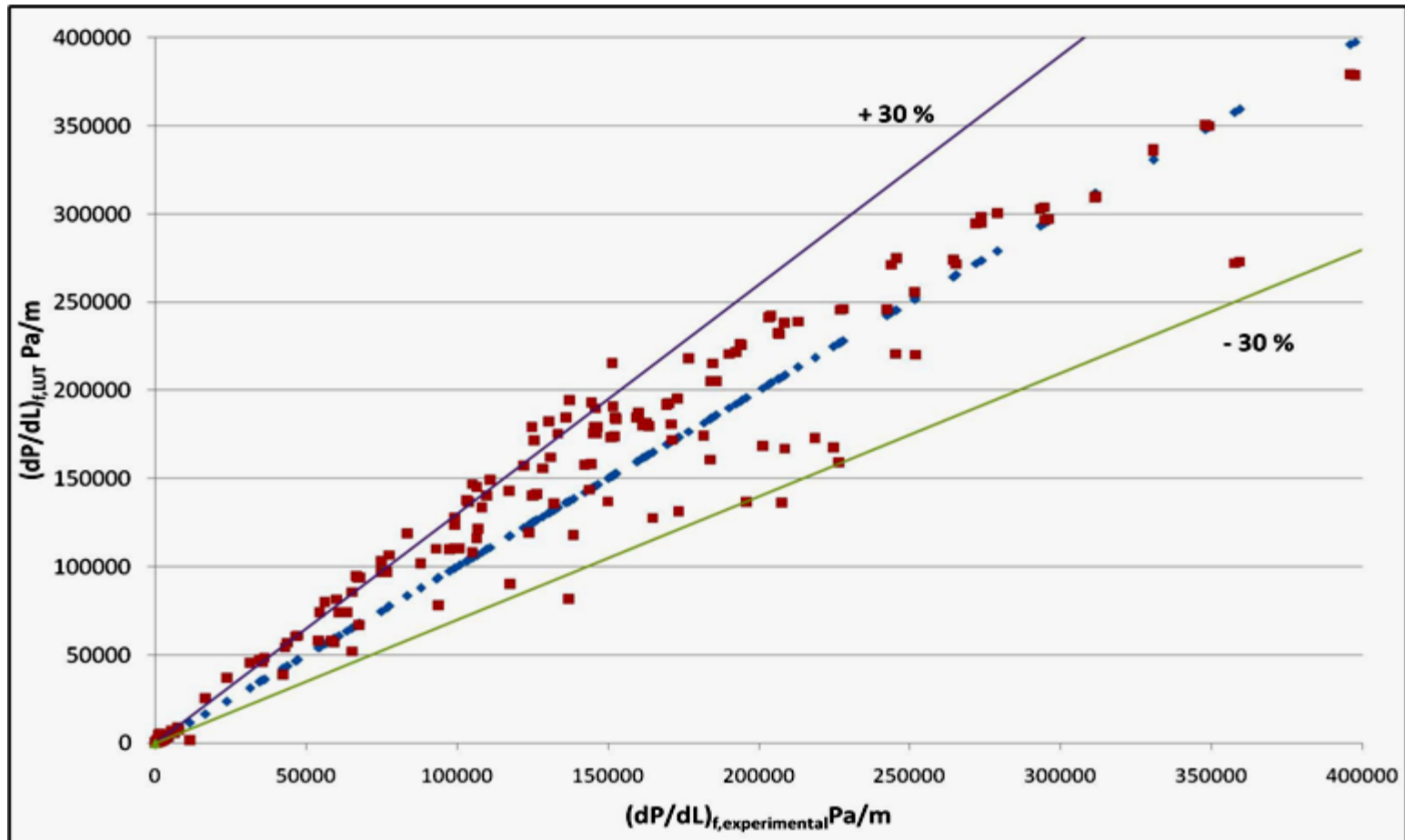


Figure 18 Comparison of two-phase frictional pressure gradient between LUT and experimental data sets.

Table 9 Statistical comparison Between LUT, Correlations, and experimental results
in terms of percentage errors

Correlations Fluids		LUT	Homogenous	Friedel	Lockhart- Martinelli	Gronnerud	Muller- Steinhagen	Chisholm	No. of Data	Reference
R-11	ε_1	6.9	24.1	-42	19.9	-72.1	26.6	41.6	115	[36]
	ε_2	17.88	65.8	71.4	69.5	74.7	56.1	64.5		
R-12	ε_1	8.72	6.5	-21.2	163	-60.3	29.7	81.9	170	[40]
	ε_2	18.56	21.7	65	190.1	65.7	39.07	104.7		
Argon	ε_1	30.8	20.4	46	188.7	-34.4	29.5	152.4	84	[23]
	ε_2	73.62	78.5	148	270.1	56	79.4	250.5		
Steam- Water	ε_1	42.75	-16.7	7.06	134	-30.3	2.66	83.5	50	[44]
	ε_2	77.19	36.5	57.4	180	41.2	41.8	128		
R-11	ε_1	13.96	-4.34	-34.15	14.9	-68.16	-21.8	71.8	293	[45]
	ε_2	40.54	35.5	50	51	70.1	35.1	102.2		
Steam- Water	ε_1	6.87	-36.3	-40.2	23.7	-49.3	-24.2	-47.8	84	
	ε_2	17.11	38.9	43.1	40.5	51.2	31	50.7		
Air- Water	ε_1	11.88	-14.13	-17.36	-18.87	-43.48	-11.02	-26.12	64	[54]
	ε_2	28.86	22.83	37.3	23.28	44.77	18.17	33.68		
Air- Water	ε_1	-9.38	-71.3	-83	-32.1	-86.4	-63.9	-58.7	80	[63]
	ε_2	17.85	72.6	85.6	37.3	88.1	65.4	60.6		
Total	ε_1	12.38	-11.4	-32.2	47.8	-62.3	-8.33	40.22	940	
	ε_2	38.87	47.29	68.3	114.6	67.4	45.91	103.26		

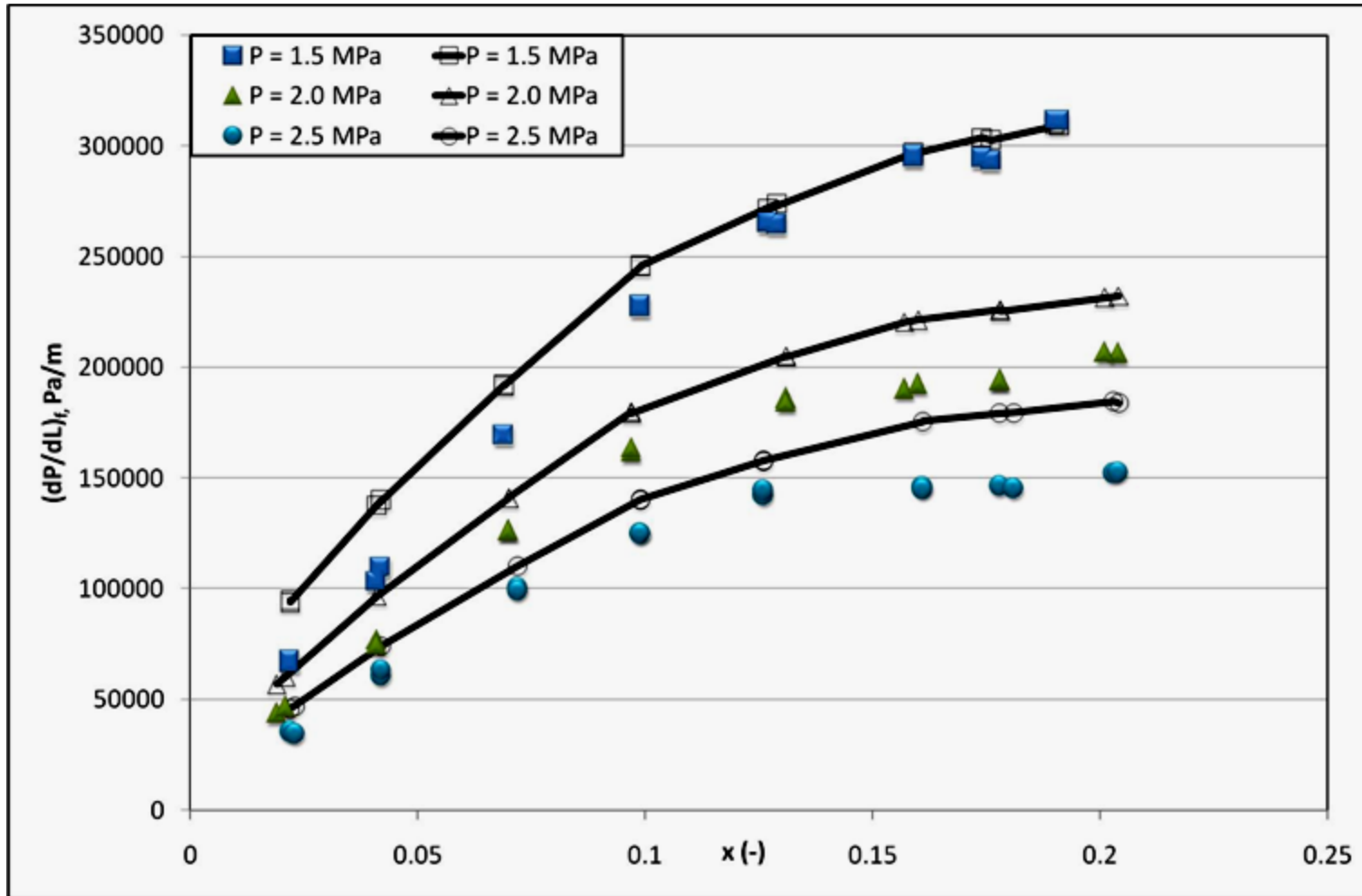


Figure 19 Comparison for calculated and measured two-phase frictional pressure gradient for Aube [47] and LUT at low to medium pressure and at mass flux equal to $4500 \text{ Kg.m}^{-2}.\text{s}^{-1}$; solid symbols, represent experimental data; open symbols, represent LUT data.

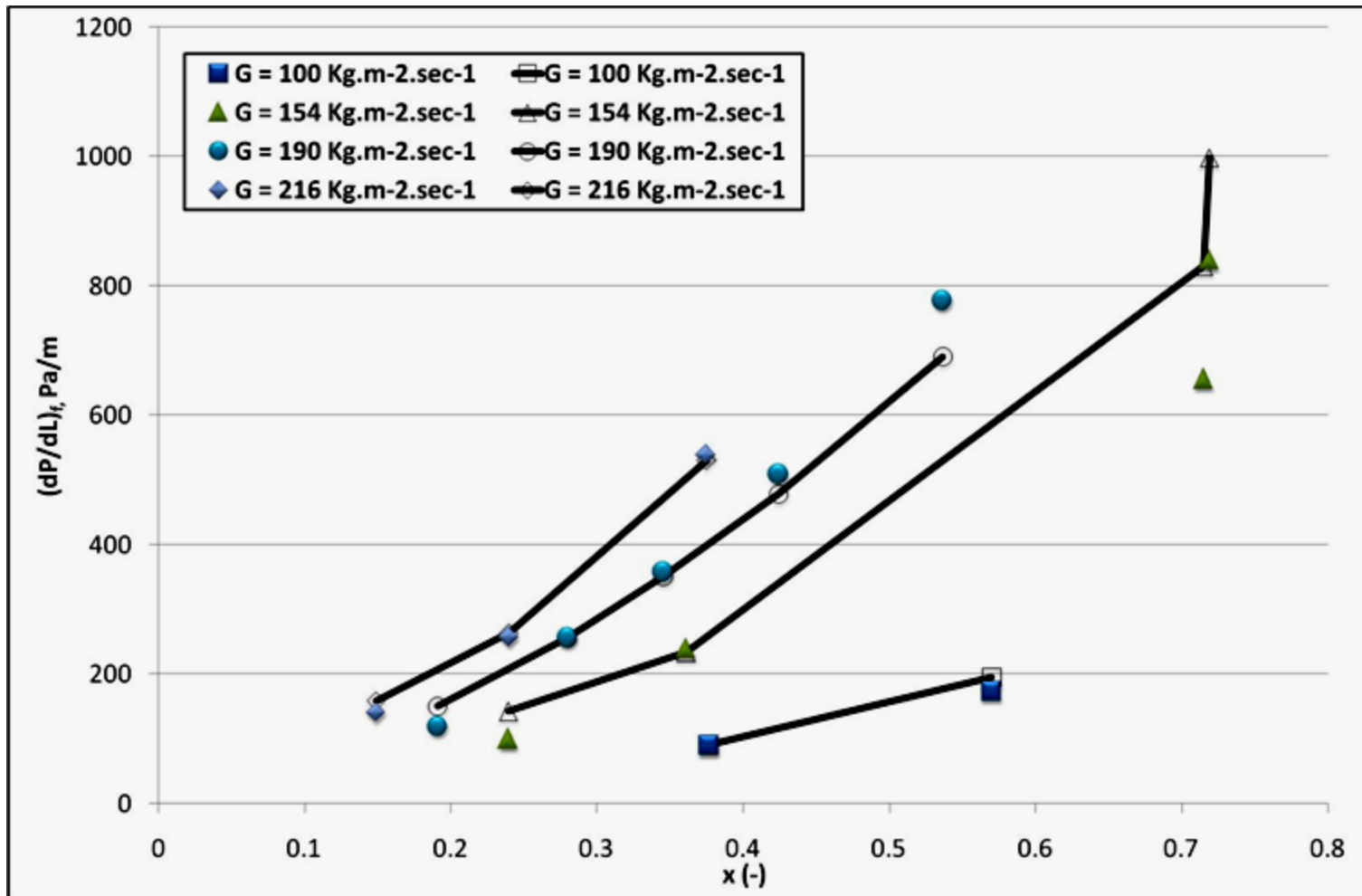


Figure 20 Comparison for calculated and measured two-phase frictional pressure gradient for McMillan [36] and LUT at low pressure equal to 0.165 MPa and at low mass flux; solid symbols, represent experimental data; open symbols, represent LUT data.

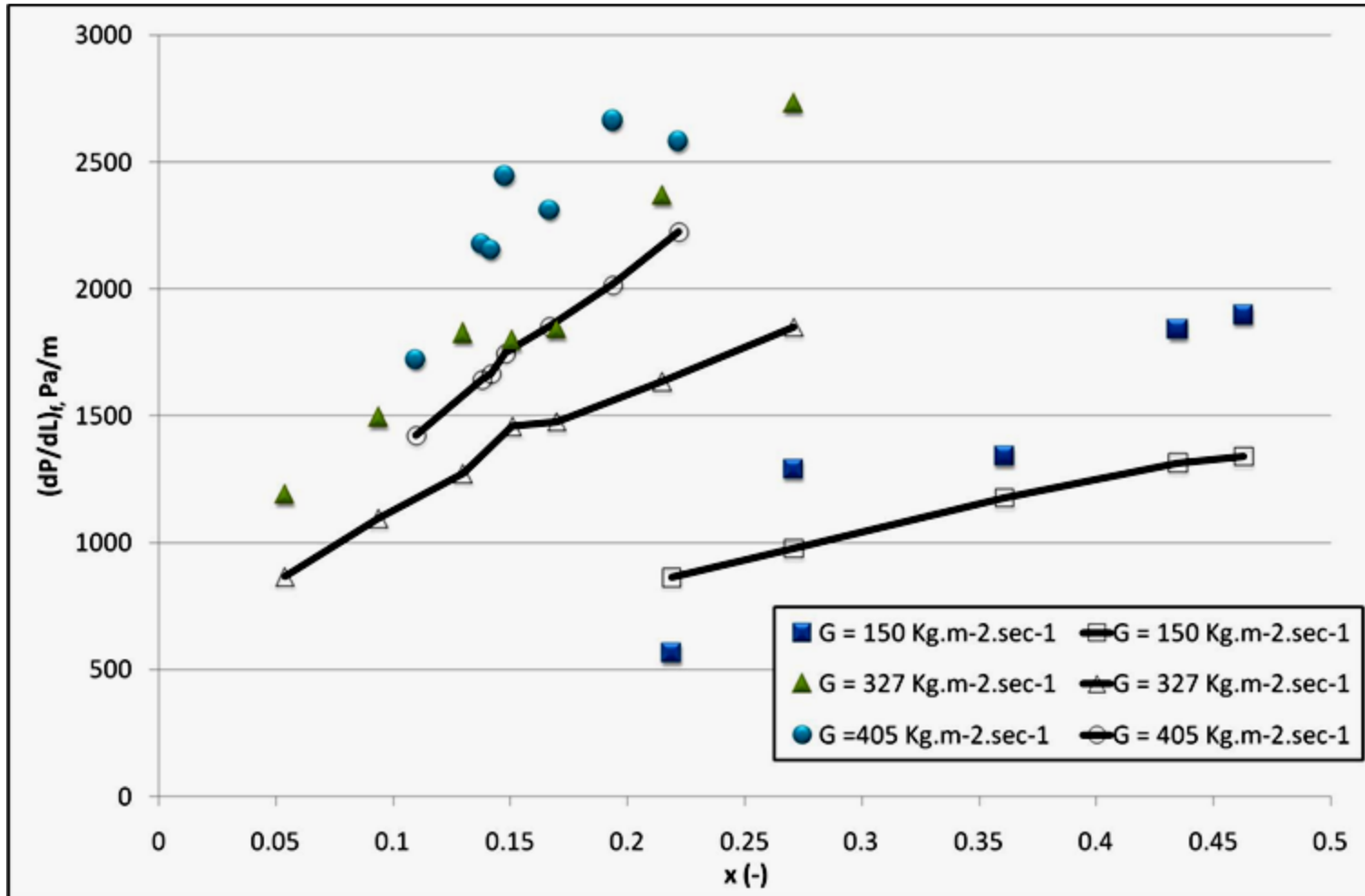


Figure 21 Comparison for calculated and measured two-phase frictional pressure gradient for Klausner [45] and LUT at low pressure equal to 0.17 MPa and at low mass flux; solid symbols, represent experimental data; open symbols, represent LUT data.

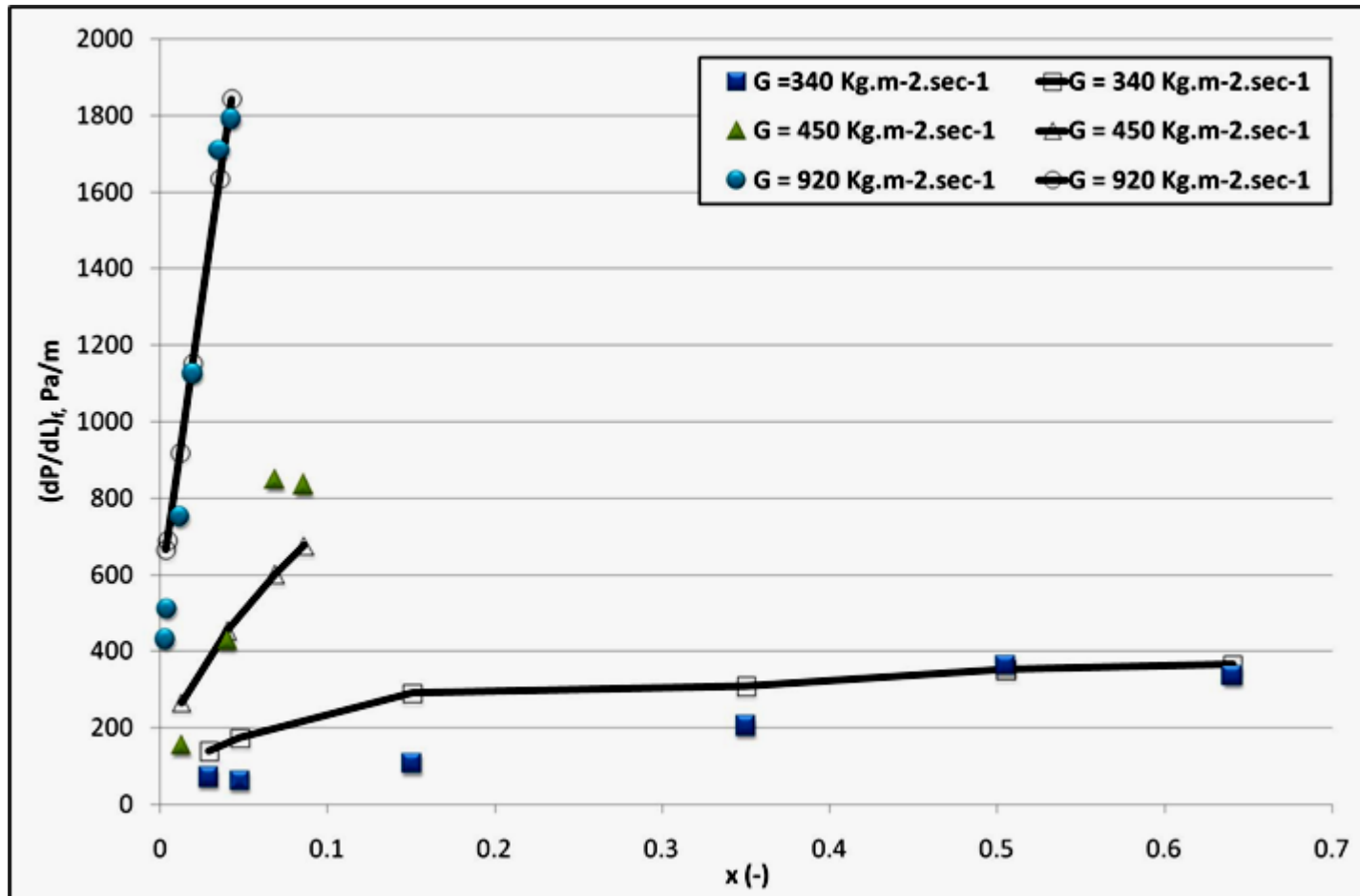


Figure 22 Comparison for calculated and measured two-phase frictional pressure gradient for Hashizume [44] and LUT at high pressure equal to 11.0 MPa and at medium to low mass flux; solid symbols, represent experimental data; open symbols, represent LUT data.

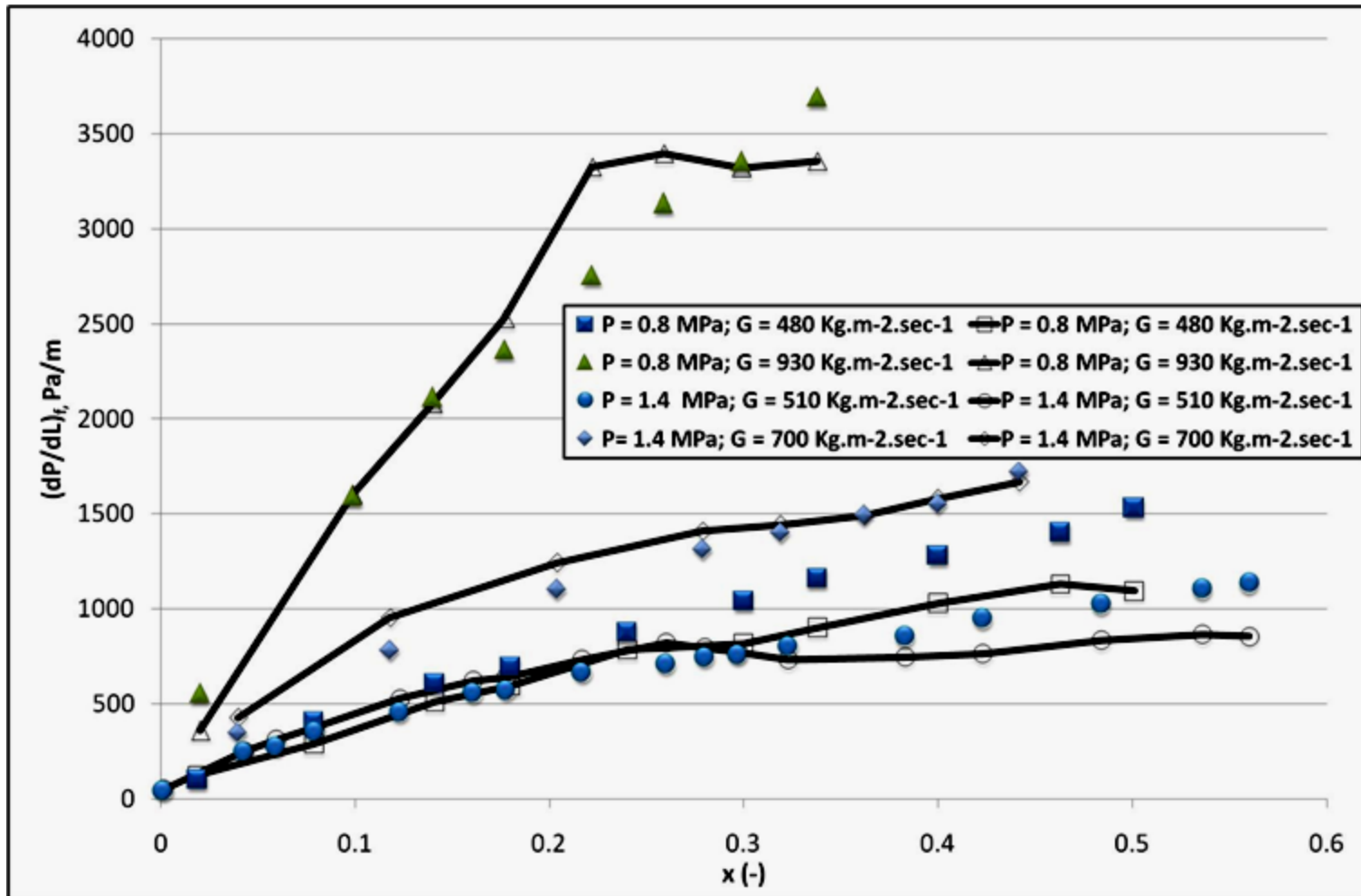


Figure 23 Comparison for calculated and measured two-phase frictional pressure gradient for Benbella [63] and LUT at low pressure-medium mass flux; solid symbols, represent experimental data; open symbols, represent LUT data.

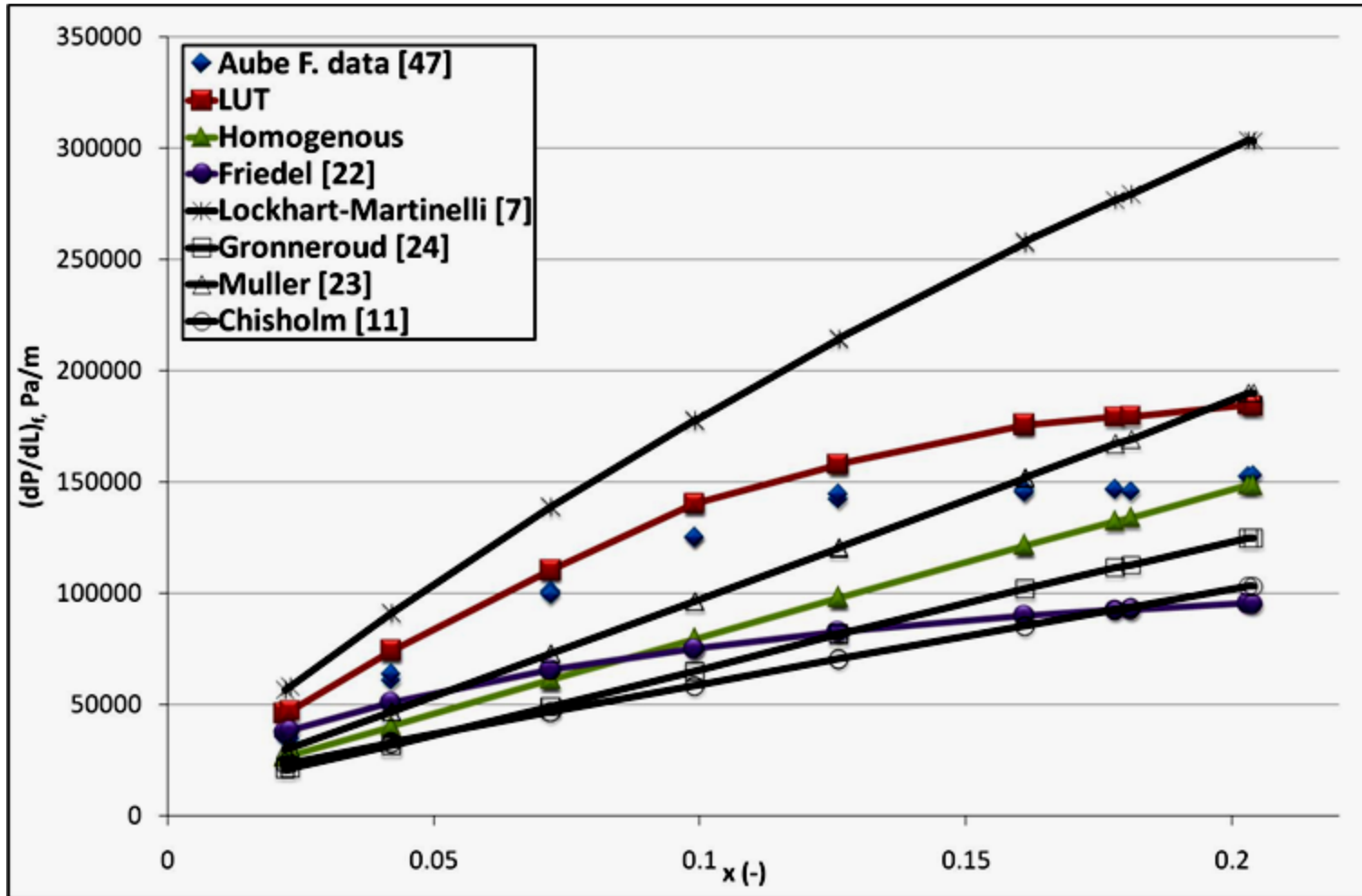


Figure 24 Comparison between measured two-phase frictional pressure gradient for Aube [47], LUT and six correlations at medium pressure equal to 2.5 MPa and at high mass flux equal to $4500 \text{ Kg.m}^{-2}.\text{sec}^{-1}$.

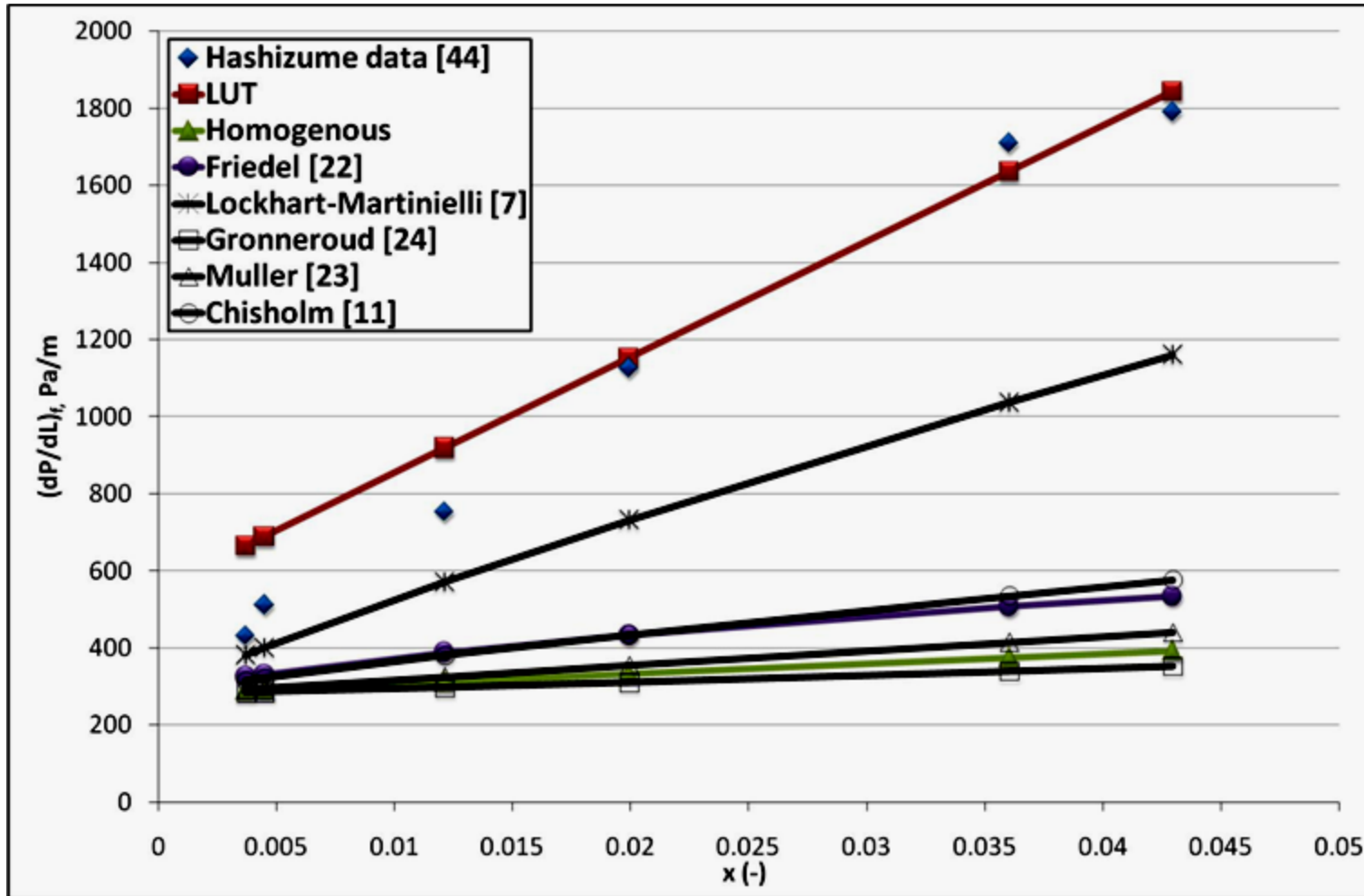


Figure 25 Comparison between measured two-phase frictional pressure gradient for Hashizume [44], LUT and six correlations at medium pressure equal to 11.0 MPa and at high mass flux equal to $920 \text{ kg} \cdot \text{m}^{-2} \cdot \text{sec}^{-1}$.

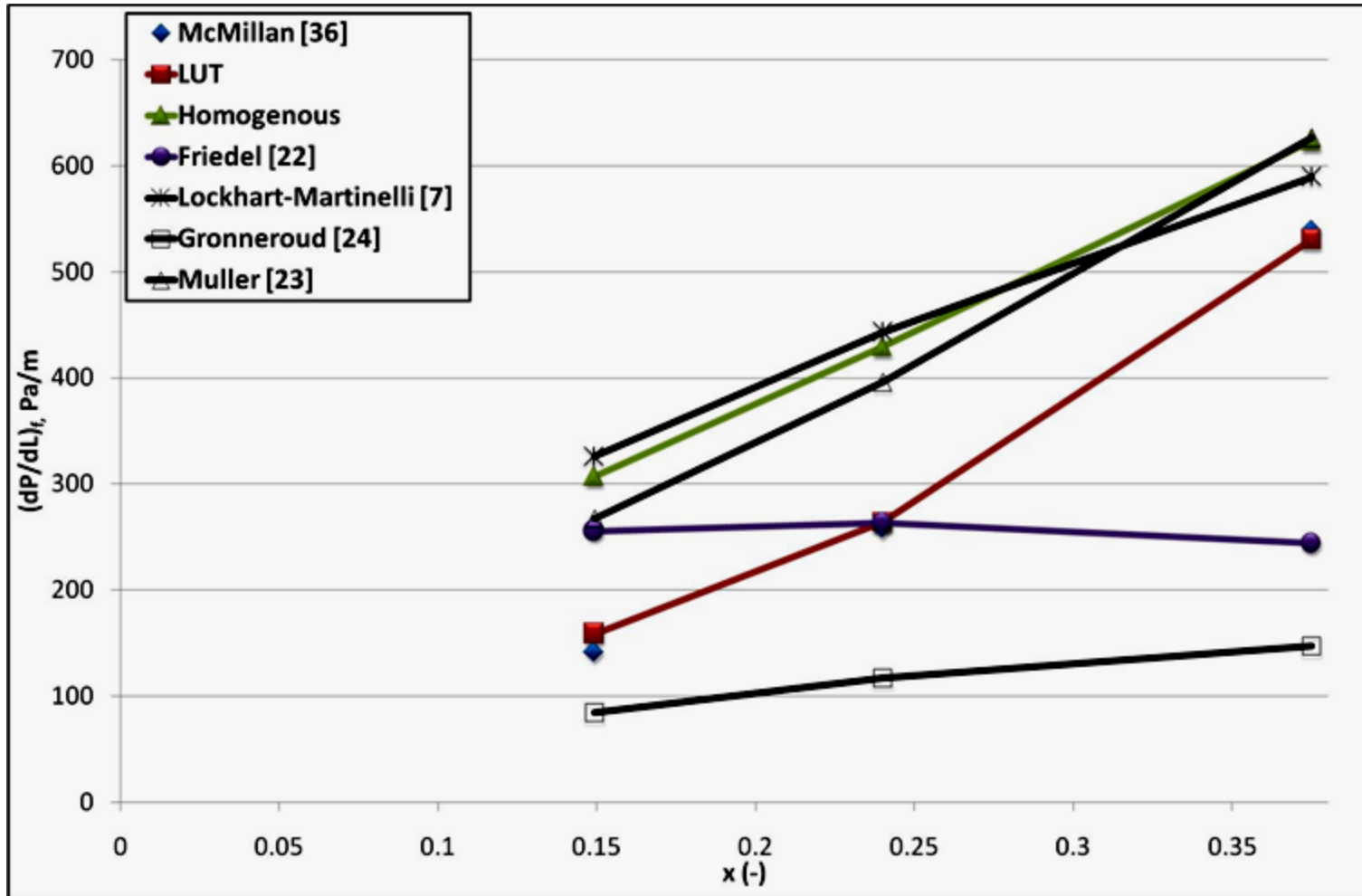


Figure 26 Comparison between measured two-phase frictional pressure gradient for McMillan [36], LUT and six correlations at medium pressure equal to 0.165 MPa and at high mass flux equal to $216 \text{ kg} \cdot \text{m}^{-2} \cdot \text{sec}^{-1}$.

As indicated early in this chapter that the RMS-error for the smooth LUT is 38.87 %. So, the LUT prediction is superseding the skeleton table and any existing correlation with RMS-error equal to 7.0 % lower. For more details, Figures 27-29 give a visual presentation of the performance of the smooth-LUT against the updated-LUT, skeleton-LUT, and experimental data sets at different flow conditions. These figures show that the LUT is better in prediction than the skeleton-LUT, which represent the correlations considered in this research. Moreover, these figures provide an indication that the discontinuities and irregularities which existed in the updated-LUT have been removed in the smooth-LUT.

Table 11 presents the amount of LUT's cells occupied by experimental data comparing with the LUT's cells occupied by correlations.

Figures 30-32 give a visual presentation of the performance of the LUT against the experimental data, which taken from different references, at different flow conditions. These figures show the effect of density ratio, Reynolds number, and mass quality on the two-phase frictional pressure drop multiplier. As mass quality increases the two-phase frictional pressure drop multiplier will increase, as shown in Figure 30. Same effect shown in Figure 32 for density ratio. Figure 31 shows an inverse relation between Reynolds number and two-phase frictional pressure drop multiplier.

Table 10 Statistical Comparisons between LUTs, and experimental results in terms of percentage errors

Correlations Fluids		Smoothed- LUT	Updated- LUT	Skeleton- LUT	No. of Data	Reference
R-11	ε_1	6.9	0.901	4.26	115	[36]
	ε_2	17.88	7.7	52.82		
R-12	ε_1	8.72	-0.31	10.06	170	[40]
	ε_2	18.56	6.26	23.1		
Argon	ε_1	30.8	7.06	21.03	84	[23]
	ε_2	73.62	26.52	73.3		
Steam-Water	ε_1	42.75	33.6	-15.8	50	[44]
	ε_2	77.19	62.1	36.3		
R-11	ε_1	13.96	11.32	-21.44	293	[45]
	ε_2	40.54	35.21	36.84		
Steam-Water	ε_1	6.87	0.68	-27.61	84	
	ε_2	17.11	5.89	34.04		
Air-Water	ε_1	11.88	0.48	-29.18	64	[54]
	ε_2	28.86	7.03	34.07		
Air-Water	ε_1	-9.38	-2.96	-70.58	80	[63]
	ε_2	17.85	13.94	72.24		
Total	ε_1	12.38	5.8	-13.78	940	
	ε_2	38.87	26.18	44.95		

Table 11 Summary of experimental data used in LUT

Parameters	Items
Total Number of data used for purpose of Updating	1170 data Points
Total Number of Experimental data used in LUT after applying Updating Program	7520 data points
Total Number of cells occupied by experimental data	1341 cells
Total Number of LUT's cells	9261 cells
Percentage of Cells occupied by experimental data	(1341/9261) = 14.5 %

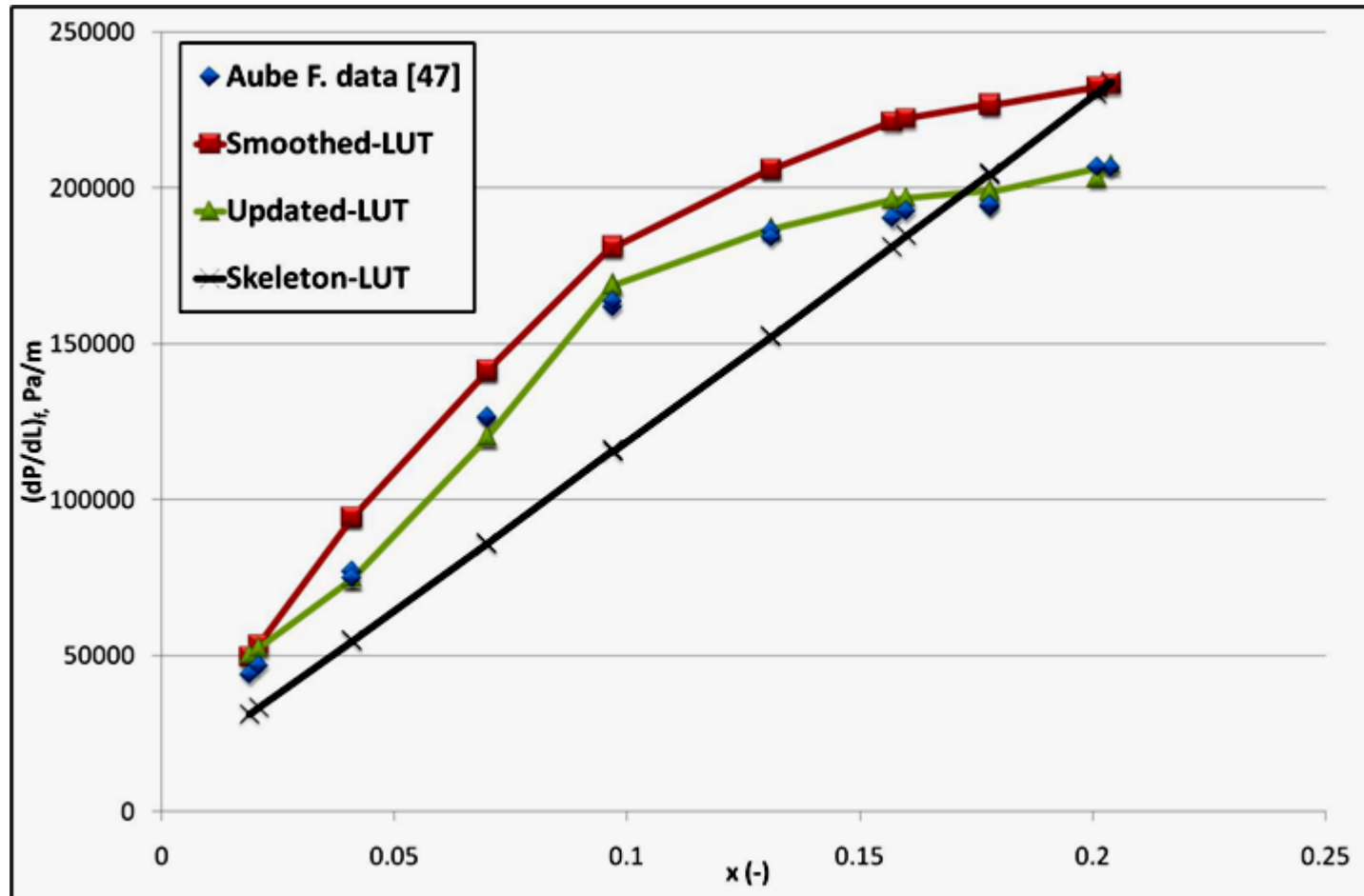


Figure 27 comparison between experimental, smoothed-LUT, updated-LUT, and skeleton-LUT for two-phase frictional pressure drop gradient for Aube [47] at density ratio (DR) = 84.62, Reynolds Number (Re) = 480,000, pressure (P) = 2.0 MPa, and mass flux (G) = 4500 Kg.m⁻².sec⁻¹.

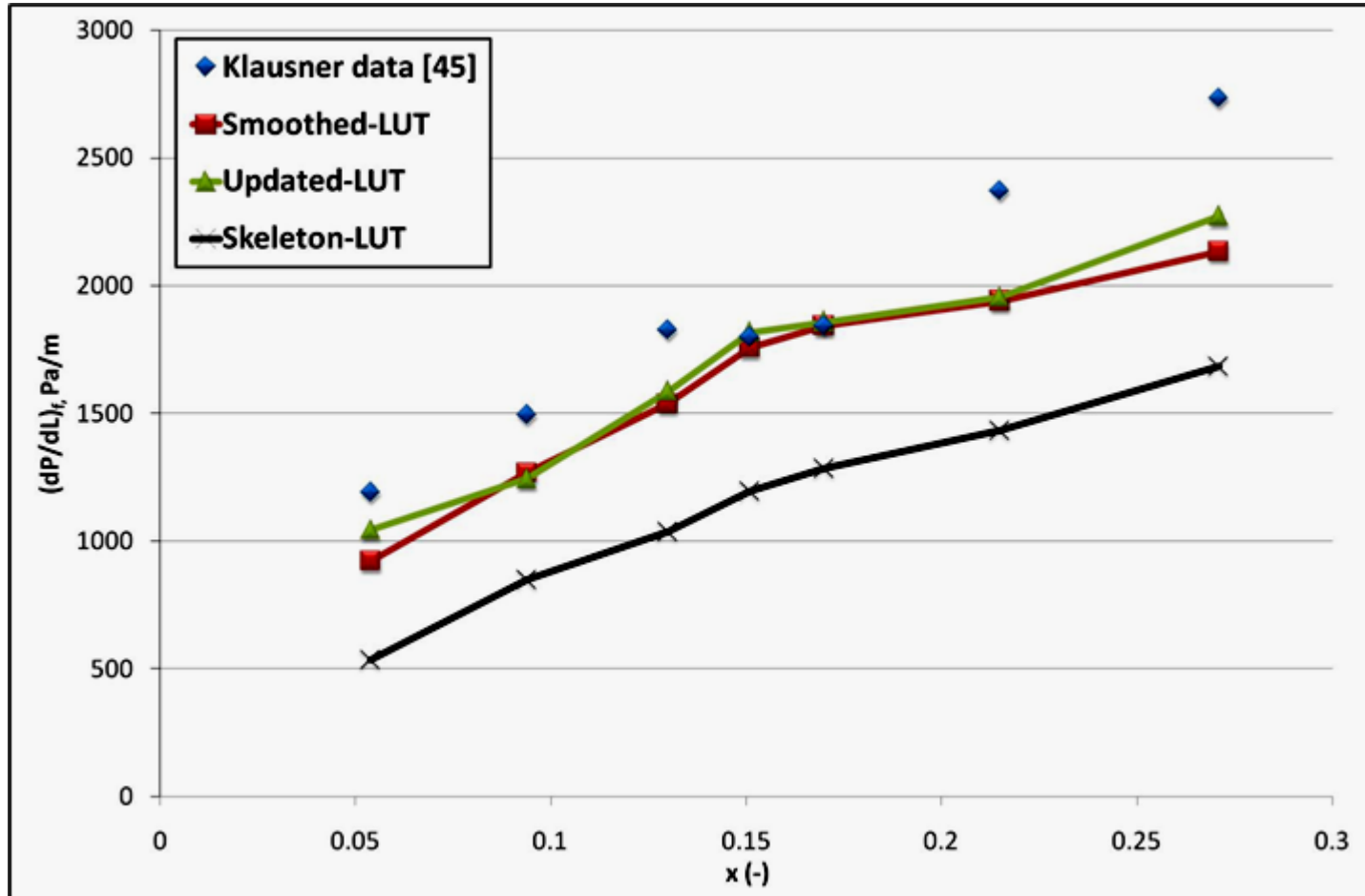


Figure 28 comparison between experimental, smoothed-LUT, updated-LUT, and skeleton-LUT for two-phase frictional pressure drop gradient for Klausner[45] at density ratio (DR) = 145.39, Reynolds Number (Re)= 10,000, pressure (P) = 0.17 MPa, and mass flux (G) = 327 K g.m⁻².sec⁻¹.

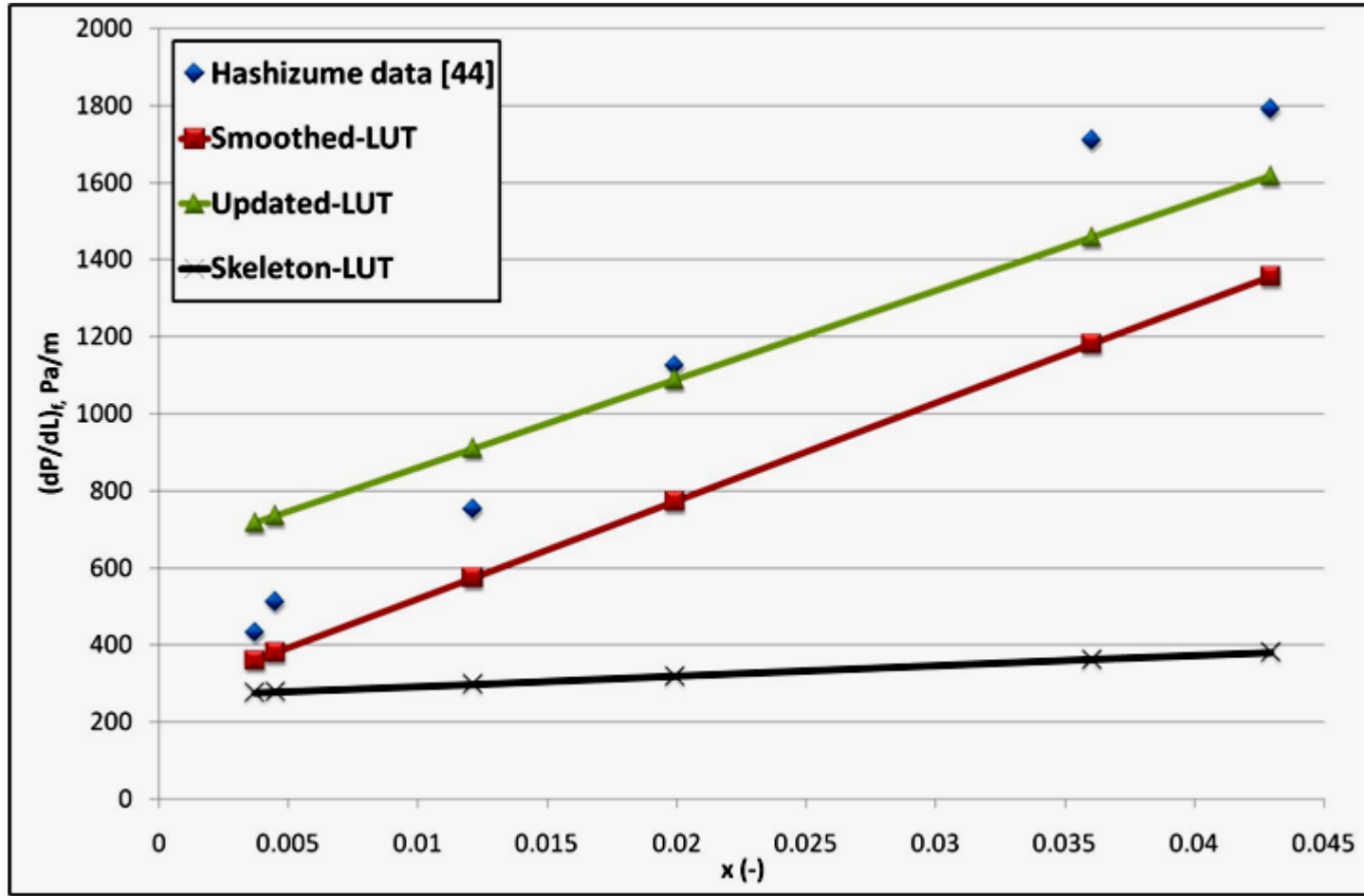


Figure 29 comparison between experimental, smoothed-LUT, updated-LUT, and skeleton-LUT for two-phase frictional pressure drop gradient for Hashizume[44] at density ratio (DR) = 10.74, and Reynolds Number (Re)= 342,953.9021, pressure (P) = 11.0 MPa, and mass flux (G) = 920 Kg.m⁻².sec⁻¹.

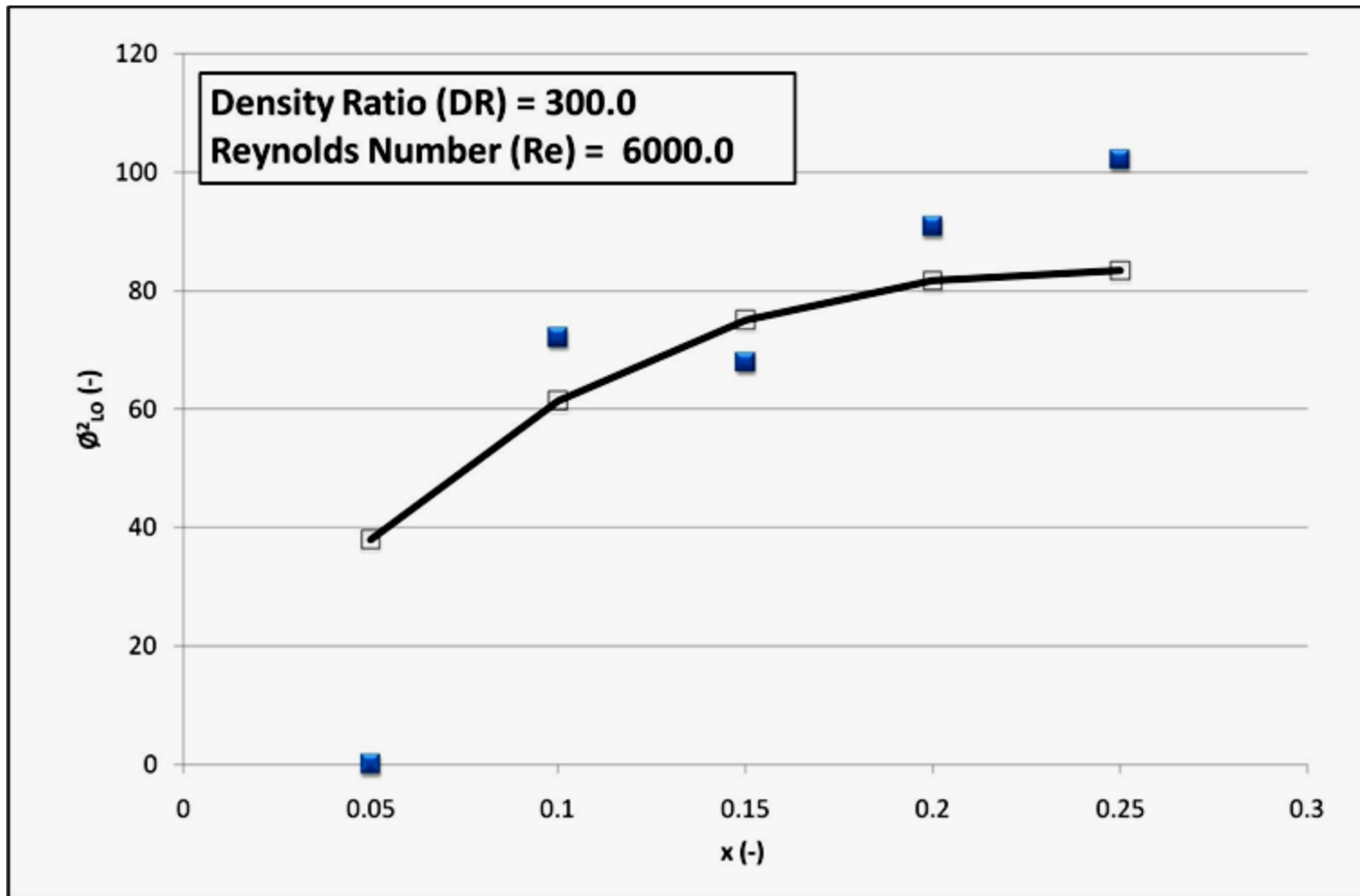


Figure 30 comparison between experimental and LUT for two-phase frictional pressure drop multiplier; solid symbols, represent experimental data; open symbols, represent LUT data.

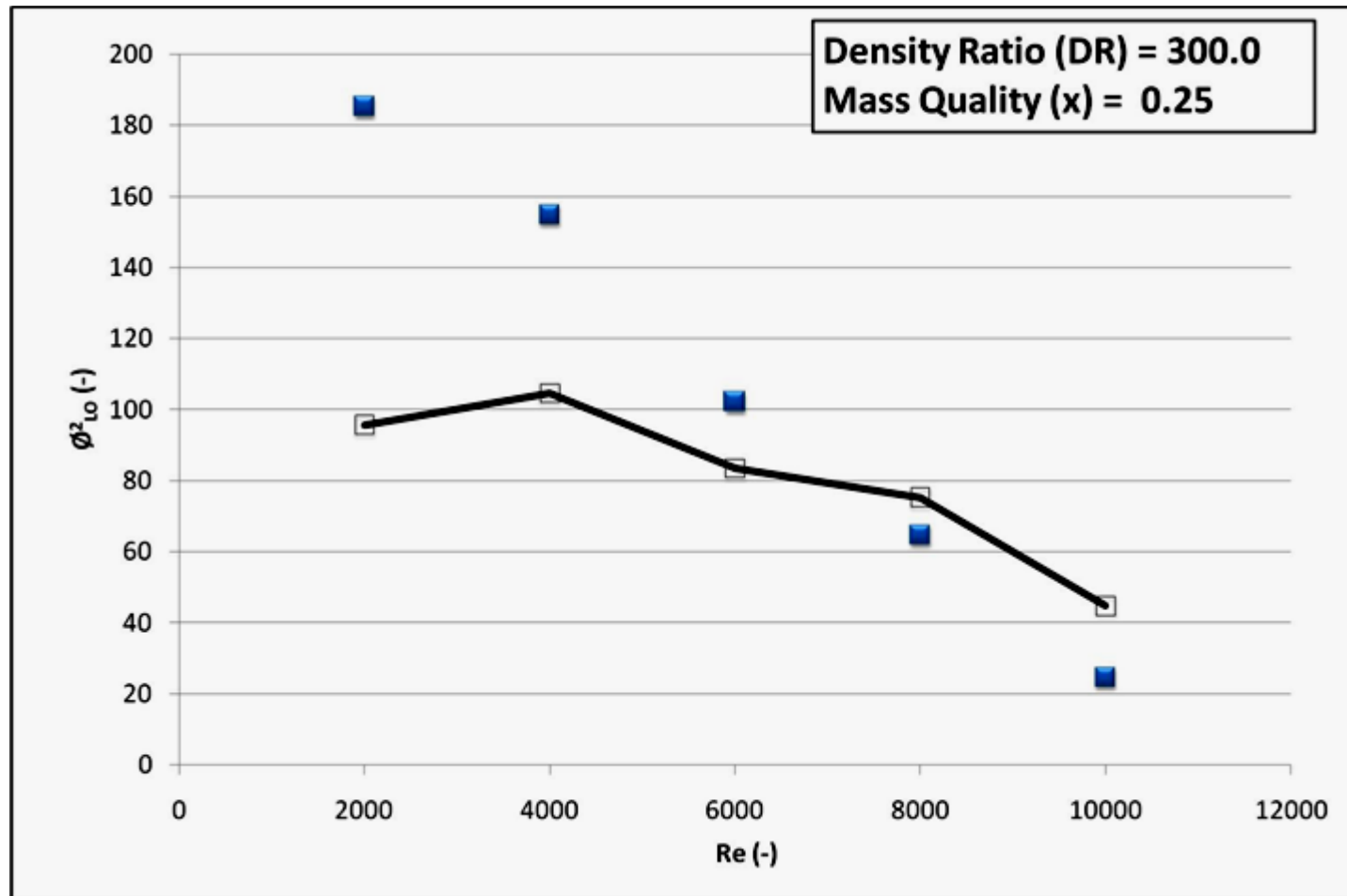


Figure 31 comparison between experimental and LUT for two-phase frictional pressure drop multiplier; solid symbols, represent experimental data; open symbols, represent LUT data.

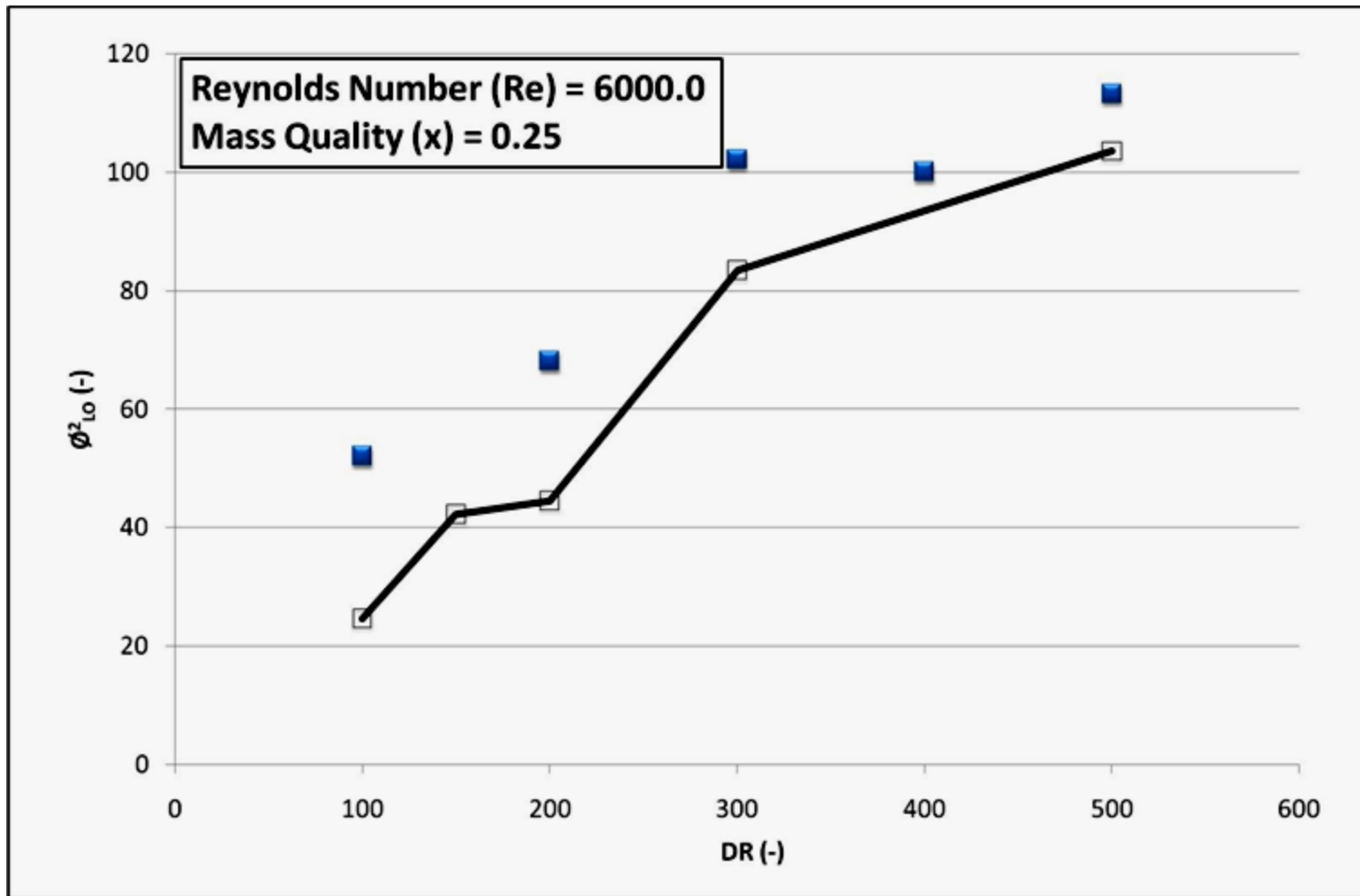


Figure 32 comparison between experimental and LUT for two-phase frictional pressure drop multiplier; solid symbols, represent experimental data; open symbols, represent LUT data.

CHAPTER 6

Look-Up-Table Procedure

6.1. Procedures of using the LUT

The following steps give an explanation on how to use the LUT;

- 1- For each experimental data sets mass quality (x), pressure (P), density for liquid and gas (ρ_L & ρ_G), Viscosity for liquid and gas (μ_L & μ_G), Pipe diameter (D), total mass flux ($G_{Tot.}$), and total two-phase frictional pressure

drop $\left(\frac{dP}{dL}\right)_{TP,exp.}$ are giving. Now, the two-phase multiplier was calculated as

following;

$$a- \phi_{LO,exp}^2 = \left(\frac{dP}{dL}\right)_{TP,exp} \bigg/ \left(\frac{dP}{dL}\right)_{SP,exp} \quad (31)$$

where:

$\left(\frac{dP}{dL}\right)_{TP,exp}$: Total two-phase frictional pressure drop.

$\left(\frac{dP}{dL}\right)_{SP,exp}$: Single-phase frictional pressure drop.

$$\text{b- } \left(\frac{dP}{dL} \right)_{SP, \exp} = \frac{2}{D} f \frac{G_{Tot}^2}{\rho_L} \quad (32)$$

where:

f : Friction factor.

G_{Tot} : Total mass flux.

ρ_L : Density for liquid-phase.

$$\text{c- } \text{Re}_L = \frac{DG_{Tot}}{\mu_L} \quad (33)$$

where:

μ_L : Viscosity for liquid-phase.

d- If $\text{Re}_L \leq 2000$, then;

$$f = \frac{16}{\text{Re}_L} \quad (34)$$

If $\text{Re}_L > 2000$, then;

$$f = \frac{0.079}{\text{Re}_L^{0.25}} \quad (35)$$

- 2- The LUT two-phase frictional multiplier $\phi_{LO,LUT}^2$ can be obtained by knowing the three parameters which are: density ratio (DR), Re_L , x , which can be calculated based on the experimental data as following;

$$DR = \frac{\rho_L}{\rho_G} \quad (36)$$

$$Re_L = \frac{G_{Tot} D}{\mu_L} \quad (37)$$

$$x = \frac{\dot{m}_g}{\dot{m}_{total}} \quad (38)$$

6.2. Examples on how to use the LUT

Example 1: Calculate average error between $\left(\frac{dP}{dL}\right)_{TP,exp}$ and $\left(\frac{dP}{dL}\right)_{TP,LUT}$ for

McMillan's experimental data [36] in a horizontal flow of an R-11 in a 46.66 mm pipe diameter. The total mass flux of Freon flow is $81.87 \text{ Kg.m}^{-2}.\text{sec}^{-1}$, and the mass quality is 0.4667, and the total two-phase frictional pressure drop is 85.76 Pa.m^{-1} , the relevant physical prosperities are:

$$\rho_L = 1475 \text{ Kg.m}^{-3}$$

$$\rho_G = 6.15 \text{ Kg.m}^{-3}$$

$$\mu_L = 0.000427 \text{ N.sec.m}^{-2}$$

$$\mu_G = 0.000013085 \text{ N.sec.m}^{-2}$$

Also compare the results with Homogenous correlation, Friedel correlation, Lochkart-Martinelli correlation, Grönnerud correlation, Muller Correlation, and Chisholm correlation.

Solution:

First calculate the Reynolds number as follow;

$$\text{Re}_L = \frac{DG_{Tot}}{\mu_L} = \frac{0.04667 \times 81.87}{0.000427} = 8946.26$$

Reynolds number greater than 2000 that's means the flow is turbulent and the friction

factor calculated as following;

$$f = \frac{0.079}{\text{Re}_L^{0.25}} = \frac{0.079}{(8946.26)^{0.25}} = 0.008123$$

The experimental single-phase frictional pressure drop $\left(\frac{dP}{dL}\right)_{SP,exp}$ is calculated as

following;

$$\left(\frac{dP}{dL}\right)_{SP,exp} = \frac{2}{D} f \frac{G_{Tot}^2}{\rho_L} = \frac{2}{0.04667} \times 0.008123 \times \frac{(81.87)^2}{1475} = 1.5 Pa.m^{-1}$$

Then, the experimental two-phase multiplier will be;

$$\phi_{LO,exp}^2 = \frac{\left(\frac{dP}{dL}\right)_{TP,exp}}{\left(\frac{dP}{dL}\right)_{SP,exp}} = \frac{85.76}{1.5} = 57.173$$

Now, the LUT two-phase multiplier obtained as following;

$$x = 0.4667,$$

$$\text{Re} = 8946.26$$

$$\text{DR} = \frac{\rho_L}{\rho_G} = \frac{1475}{6.15} = 239.84$$

Using the table in Appendix A, and doing three dimensional interpolations. The LUT two-phase multiplier is:

$$\phi_{Lo,LUT}^2 = f(DR, Re_L, x) = 63.98$$

$$\blacktriangleright \left(\frac{dP}{dL} \right)_{TP,LUT} = \phi_{Lo,LUT}^2 \left(\frac{dP}{dL} \right)_{SP,LUT} = 63.98 \times 1.5 = 95.97$$

Relative error

$$e_i = \left(\frac{95.97 - 85.76}{85.76} \right) \times 100 = 11.905\%$$

Comparisons between Experimental, correlations, and LUT:

Table 12 Summary of single-phase flow example

Correl. Items	Experimental	LUT	Homogenous	Friedel	Lockhart- Martinelli	Gronnerud	Muller- Steinhagen	Chisholm
$\left(\frac{dP}{dL} \right)_{TP}$	85.76	95.97	108.13	140.4	150.3	158.1807	202.38	154.01
% Error	--	11.905%	26.08 %	63.71%	75.256	84.45%	136.0 %	79.58%

Example 2: Calculate average error between $\left(\frac{dP}{dL} \right)_{TP,exp}$ and $\left(\frac{dP}{dL} \right)_{TP,LUT}$ for Zhang et al. unified model[74] in horizontal flow of an Air-Water in a 76.2 mm pipe diameter. The total mass flux of the flow is 701.5 Kg.m⁻².sec⁻¹, and the mass quality is 0.00214, and the total two-phase frictional pressure drop is 90.02 Pa.m⁻¹, the relevant physical prosperities are:

$$\rho_L = 1000.0 \text{ Kg.m}^{-3}$$

$$\rho_G = 3.00 \text{ Kg.m}^{-3}$$

$$\mu_L = 0.001 \text{ N.sec.m}^{-2}$$

$$\mu_G = 0.000018 \text{ N.sec.m}^{-2}$$

Also compare the results with Homogenous correlation, Friedel correlation, Lochkart-Martinelli correlation, Grönnerud correlation, Muller Correlation, and Chisholm correlation.

Solution:

First calculate the Reynolds number as follow;

$$\text{Re}_L = \frac{DG_{Tot}}{\mu_L} = \frac{0.0762 \times 701.5}{0.001} = 53,454.3$$

Reynolds number greater than 2000 that's means the flow is turbulent and the friction factor calculated as following;

$$f = \frac{0.079}{\text{Re}_L^{0.25}} = \frac{0.079}{(53,454.3)^{0.25}} = 0.0051955$$

The experimental single-phase frictional pressure drop $\left(\frac{dP}{dL}\right)_{SP,exp}$ is calculated as

following;

$$\left(\frac{dP}{dL}\right)_{SP,exp} = \frac{2}{D} f \frac{G_{Tot}^2}{\rho_L} = \frac{2}{0.0762} \times 0.0051955 \times \frac{(701.5)^2}{1000.0} = 67.1051 \text{ Pa.m}^{-1}$$

Then, the experimental two-phase multiplier will be;

$$\phi_{LO,exp}^2 = \frac{\left(\frac{dP}{dL}\right)_{TP,exp}}{\left(\frac{dP}{dL}\right)_{SP,exp}} = \frac{90.02}{67.1051} = 1.342$$

Now, the LUT two-phase multiplier obtained as following;

$$x = 0.00214$$

$$Re = 53,454.3$$

$$DR = \frac{\rho_L}{\rho_G} = \frac{1000.0}{3.00} = 333.333$$

Using the table in Appendix A, and doing three dimensional interpolations. The LUT two-phase multiplier is:

$$\phi_{Lo,LUT}^2 = f(DR, Re_L, x) = 1.71$$

$$\left(\frac{dP}{dL}\right)_{TP,LUT} = \phi_{Lo,LUT}^2 \left(\frac{dP}{dL}\right)_{SP,LUT} = 1.7 \times 67.1051 = 114.07$$

Relative error

$$e_i = \left(\frac{114.08 - 90.02}{90.02}\right) \times 100 = 26.73\%$$

Comparisons between correlations and LUT:

Table 13 Summary of two-phase flow example

Correl. Items	Zhang et al. (2006)	LUT	Homogenous	Friedel	Lockhart- Martinelli	Gronnerud	Muller- Steinhagen	Chisholm
$\left(\frac{dP}{dL}\right)_{TP}$	90.02	114.07	108.92	114.07	126.83	101.156	117.10	114.75
% Error	--	26.73%	21.00 %	26.73 %	40.9 %	12.37 %	30.08 %	27.5 %

CHAPTER 7

CONCLUSIONS AND RECOMMENDATIONS

This research topic focuses on constructing a look-up table to predict two-phase frictional pressure drop multiplier with accuracy superseding existing prediction techniques.

The LUT covers wide range of flow conditions of density ratio, Reynolds number, and mass qualities where different flow regimes exist.

The study is accomplished as follows:

- Wide literature survey was performed in order to better understand the way available prediction techniques are performing.
- Along with literature survey, data collection process was initiated and categorized according to the flow conditions. Many of the data are shown as graphical form which required scanning and extracting the data using precession extraction software.
- Data were tested and compared together as they come from different sources. Also a comparison between data and available prediction techniques was performed in order to determine the flow conditions at which each model performs better. This would help in constructing the skeleton table.

- Skeleton table was constructed based on homogeneous model, Chisholm (1973) correlation, Muller-Steinhagen and Heck (1986) correlation, Grönnerud (1972) correlation, and Friedel (1979) correlation.
- Updating skeleton table was done by replacing the experimental data point with skeleton table entries.
- Smooth program was applied on the updated table in order to remove the irregularities and discontinuities between experimental data points and correlations data points.
- Error assessments between the LUT and experimental data points were applied. Error assessment between the correlations and LUT was generated.
- The results of assessment for the LUT and the correlations against all data sets are summarized in Table 7. It can be seen from the table that LUT shows the best overall prediction accuracy (least root-mean-squared error) among other correlations.

The LUT technique has many advantages over the correlations chosen for the comparisons, e.g., the LUT is simple to use, wide range of application, and it constructed based on a quit large database. Future work built on this study can do by updating the LUT with new experimental data available in the literature.

REFERENCES

- [1] M. Ould Didi, N. Kattan, and J. Thome, "Prediction of two-phase pressure gradients of refrigerants in horizontal tubes," *International journal of refrigeration*, vol. 25, pp. 935-947, 2002.
- [2] J. G. Collier and J. R. Thome, *Convective boiling and condensation*: Oxford University Press, USA, 1996.
- [3] J. Nikuradse, "Investigation of Turbulent Flow in Tubes of Non-Circular Cross Section," *Ingen.-Arch*, vol. 1, pp. 306-332, 1930.
- [4] C. F. Colebrook, "Turbulent flow in pipes with particular reference to the transition region between the smooth and rough pipe laws," *J. Inst. Civ. Eng*, vol. 11, pp. 133-156, 1939.
- [5] L. F. Moody, "Friction factors for pipe flow," *Trans. ASME*, vol. 66, pp. 671-684, 1944.
- [6] R. Martinelli and D. Nelson, "Prediction of pressure drop during forced-circulation boiling of water," *Trans. ASME*, vol. 70, pp. 695-702, 1948.
- [7] R. Lockhart and R. Martinelli, "Proposed correlation of data for isothermal two-phase, two-component flow in pipes," *Chemical Engineering Progress*, vol. 45, pp. 39-48, 1949.
- [8] J. Thom, "Prediction of pressure drop during forced circulation boiling of water," *International Journal of Heat and Mass Transfer*, vol. 7, pp. 709-724, 1964.
- [9] A. E. Dukler, et al, "Pressure Drop and Hold-up in Two-Phase Flow Part A - A Comparison of Existing Correlations," and "Part B - An Approach Through Similarity Analysis", *AIChE Journal*, vol. 10, pp. 38-51, 1964.
- [10] C. Baroczy, "A systematic correlation for two-phase pressure drop," *Atomics International*, Canoga Park, Calif. 1966.
- [11] D. Chisholm, "Pressure gradients due to friction during the flow of evaporating two-phase mixtures in smooth tubes and channels," *International Journal of Heat and Mass Transfer*, vol. 16, pp. 347-358, 1973.

- [12] D. Reddy, S. Sreepada, A. N. Nahavandi, E. P. R. Institute, and C. U. H. T. R. Facility, "Two-Phase Friction Multiplier Correlation for High-Pressure Steam-Water Flow," ed: Electric Power Research Institute, 1982.
- [13] P. Whalley, "Boiling, condensation, and gas-liquid flow," 1987.
- [14] P. Vassallo and K. Keller, "Two-phase frictional pressure drop multipliers for SUVA R-134a flowing in a rectangular duct," *International Journal of Multiphase Flow*, vol. 32, pp. 466-482, 2006.
- [15] W. Davis, "The effect of Froude number in estimating vertical two phase gas-liquid friction losses," *British Chemical Engineering*, vol. 8, pp. 462-468, 1963.
- [16] B. Cou t, P. Brown, and A. Hunt, "Two-phase bubbly-droplet flow through a contraction: experiments and a unified model," *International Journal of Multiphase Flow*, vol. 17, pp. 291-307, 1991.
- [17] D. A. L. Souza and M. D. M. Pimenta, "Prediction of pressure drop during horizontal two-phase flow of pure and mixed refrigerants," 1995.
- [18] G. F. Woerlee, J. Berends, Z. Olujic, and J. de Graauw, "A comprehensive model for the pressure drop in vertical pipes and packed columns," *Chemical Engineering Journal*, vol. 84, pp. 367-379, 2001.
- [19] H. S. Isbin, R. Moen, and D. Mosher, "Two-Phase Pressure Drops," Minnesota. Univ., Minneapolis. Inst. of Tech. 1954.
- [20] I. Owen, A. Abdul-Ghani, and A. Amini, "Diffusing a homogenized two-phase flow," *International Journal of Multiphase Flow*, vol. 18, pp. 531-540, 1992.
- [21] A. Cicchitti, C. Lombardi, M. Silvestri, G. Soldaini, and R. Zavattarelli, "Two-Phase Cooling Experiments-Pressure Drop," *Heat Transfer, and Burnout Measurements, Energia Nucleare*, vol. 7, pp. 407-425, 1960.
- [22] L. Friedel, "Improved friction pressure drop correlations for horizontal and vertical two-phase pipe flow," 1979.
- [23] H. Müller-Steinhagen and K. Heck, "A simple friction pressure drop correlation for two-phase flow in pipes," *Chemical Engineering and Processing: Process Intensification*, vol. 20, pp. 297-308, 1986.

- [24] R. Grönnerud, "Investigation of liquid hold-up, flow-resistance and heat transfer in circulation type evaporators, part iv: two-phase flow resistance in boiling refrigerants," *Bull. De l'Inst. Du Froid, Annexe*, vol. 1, 1972.
- [25] W. Zhang, T. Hibiki, and K. Mishima, "Correlations of two-phase frictional pressure drop and void fraction in mini-channel," *International Journal of Heat and Mass Transfer*, vol. 53, pp. 453-465, 2010.
- [26] D. Beattie, "A note on the calculation of two-phase pressure losses," *Nuclear Engineering and Design*, vol. 25, pp. 395-402, 1973.
- [27] I. Y. Chen, K. S. Yang, Y. J. Chang, and C. C. Wang, "Two-phase pressure drop of air-water and R-410A in small horizontal tubes," *International Journal of Multiphase Flow*, vol. 27, pp. 1293-1299, 2001.
- [28] A. Cavallini, G. Censi, D. D. Col, L. Doretto, G. A. Longo, and L. Rossetto, "Condensation of halogenated refrigerants inside smooth tubes," *HVAC & R Research*, vol. 8, pp. 429-451, 2002.
- [29] K. Mishima and T. Hibiki, "Some characteristics of air-water two-phase flow in small diameter vertical tubes," *International Journal of Multiphase Flow*, vol. 22, pp. 703-712, 1996.
- [30] M. Wilson, T. Newell, J. Chato, and C. Infante Ferreira, "Refrigerant charge, pressure drop, and condensation heat transfer in flattened tubes," *International journal of refrigeration*, vol. 26, pp. 442-451, 2003.
- [31] T. Tran, M. C. Chyu, M. Wambsganss, and D. France, "Two-phase pressure drop of refrigerants during flow boiling in small channels: an experimental investigation and correlation development* 1," *International Journal of Multiphase Flow*, vol. 26, pp. 1739-1754, 2000.
- [32] C. C. WangChing-Shan, "Visual observation of two-phase flow pattern of R-22, R-134a, and R-407C in a 6.5-mm smooth tube," *Experimental thermal and fluid science*, vol. 15, pp. 395-405, 1997.
- [33] S. Garimella, J. Killion, and J. Coleman, "An experimentally validated model for two-phase pressure drop in the intermittent flow regime for circular microchannels," *Journal of fluids engineering*, vol. 124, p. 205, 2002.

- [34] S. Garimella, A. Agarwal, and J. Killion, "Condensation pressure drop in circular microchannels," *Heat transfer engineering*, vol. 26, pp. 28-35, 2005.
- [35] H. Ju Lee and S. Yong Lee, "Pressure drop correlations for two-phase flow within horizontal rectangular channels with small heights," *International Journal of Multiphase Flow*, vol. 27, pp. 783-796, 2001.
- [36] H. K. McMillan, "A study of flow patterns and pressure drop in horizontal two-phase flow," PH.D., Engineering, Mechanical, Purdue University, Michigan, 1963.
- [37] G. Kasturi and J. Stepanek, "Two phase flow--I. Pressure drop and void fraction measurements in concurrent gas-liquid flow in a coil," *Chemical Engineering Science*, vol. 27, pp. 1871-1880, 1972.
- [38] D. H. Beggs and J. P. Brill, "A study of two-phase flow in inclined pipes," *Journal of Petroleum technology*, vol. 25, pp. 607-617, 1973.
- [39] H. Mukherjee, *An experimental study of inclined two-phase flow*: University of Tulsa, 1979.
- [40] K. Hashizume, "Flow pattern, void fraction and pressure drop of refrigerant two-phase flow in a horizontal pipe--I. Experimental data," *International Journal of Multiphase Flow*, vol. 9, pp. 399-410, 1983.
- [41] B. Vijayarangan, S. Jayanti, and A. Balakrishnan, "Pressure drop studies on two-phase flow in a uniformly heated vertical tube at pressures up to the critical point," *International Journal of Heat and Mass Transfer*, vol. 50, pp. 1879-1891, 2007.
- [42] N. Andritsos, "Effect of pipe diameter and liquid viscosity on horizontal stratified flow," ed: University of Illinois at Urbana-Champaign, 1986.
- [43] L. Ebner, J. Draho, and G. Ebner, "Characterization of hydrodynamic regimes in horizontal two-phase flow Part I: Pressure drop measurements," *Chemical engineering and processing*, vol. 22, pp. 39-43, 1987.
- [44] K. Hashizume and N. Ogawa, "Flow pattern, void fraction and pressure drop of refrigerant two-phase flow in a horizontal pipe. III: Comparison of the analysis with existing pressure drop data on air/water and steam/water systems," *International Journal of Multiphase Flow*, vol. 13, pp. 261-267, 1987.

- [45] J. F. Klausner, "The influence of gravity on pressure drop and heat transfer in flow boiling," Ph.D., Mechanical Engineering, University of Illinois, Champaign, 1989.
- [46] G. Abdul-Majeed, "Liquid holdup in horizontal two-phase gas--liquid flow," *Journal of Petroleum Science and Engineering*, vol. 15, pp. 271-280, 1996.
- [47] F. Aubé, "Effets du flux de chaleur sur les pertes de pression par frottement dans des écoulements monophasiques et diphasiques," These presentee en vue de l'obtention du diplome de philosophi/e doctor (Ph.D.), Departement De Genie Mechanique, Ecole Polytechnique De Montreal, Montreal, 1996.
- [48] N. Ekberg, S. Ghiaasiaan, S. Abdel-Khalik, M. Yoda, and S. Jeter, "Gas-liquid two-phase flow in narrow horizontal annuli," *Nuclear Engineering and Design*, vol. 192, pp. 59-80, 1999.
- [49] K. Triplett, S. Ghiaasiaan, S. Abdel-Khalik, A. LeMouel, and B. McCord, "Gas-liquid two-phase flow in microchannels:: Part II: void fraction and pressure drop," *International Journal of Multiphase Flow*, vol. 25, pp. 395-410, 1999.
- [50] P. Angeli and G. Hewitt, "Pressure gradient in horizontal liquid-liquid flows," *International Journal of Multiphase Flow*, vol. 24, pp. 1183-1203, 1999.
- [51] P. Spedding, G. Woods, R. Raghunathan, and J. Watterson, "Flow Pattern, Holdup and Pressure Drop in Vertical and Near Vertical Two-and Three-Phase Upflow," *Chemical Engineering Research and Design*, vol. 78, pp. 404-418, 2000.
- [52] M. Ottens, H. C. J. Hoefsloot, and P. J. Hamersma, "Transient gas-liquid flow in horizontal T-junctions," *Chemical Engineering Science*, vol. 56, pp. 43-55, 2001.
- [53] G. R. Warrier, V. K. Dhir, and L. A. Momoda, "Heat transfer and pressure drop in narrow rectangular channels," *Experimental thermal and fluid science*, vol. 26, pp. 53-64, 2002.
- [54] K. K. Pehlivan, "Experimental study on two-phase flow regimes and frictional pressure drop in mini-and micro-channels," Master of Applied Science,

Mechanical and Industrial Engineering, Concordia University, Montreal, Quebec, Canada, 2003.

- [55] T. Nualboonrueng and S. Wongwises, "Two-phase flow pressure drop of HFC-134a during condensation in smooth and micro-fin tubes at high mass flux," *International Communications in Heat and Mass Transfer*, vol. 31, pp. 991-1004, 2004.
- [56] D. Chakrabarti, G. Das, and S. Ray, "Pressure Drop in Liquid liquid Two Phase Horizontal Flow: Experiment and Prediction," *Chemical engineering & technology*, vol. 28, pp. 1003-1009, 2005.
- [57] S. Cull, J. Lovick, G. Lye, and P. Angeli, "Scale-down studies on the hydrodynamics of two-liquid phase biocatalytic reactors," *Bioprocess and biosystems engineering*, vol. 25, pp. 143-153, 2002.
- [58] B. S. Field and P. Hrnjak, "Adiabatic two-phase pressure drop of refrigerants in small channels," *Heat Transfer Engineering*, 28, vol. 8, pp. 704-712, 2007.
- [59] J. Moreno Quibén and J. R. Thome, "Flow pattern based two-phase frictional pressure drop model for horizontal tubes. Part I: Diabatic and adiabatic experimental study," *International Journal of Heat and Fluid Flow*, vol. 28, pp. 1049-1059, 2007.
- [60] J. Moreno Quibén and J. R. Thome, "Flow pattern based two-phase frictional pressure drop model for horizontal tubes, Part II: New phenomenological model," *International Journal of Heat and Fluid Flow*, vol. 28, pp. 1060-1072, 2007.
- [61] S. Saisorn and S. Wongwises, "Flow pattern, void fraction and pressure drop of two-phase air-water flow in a horizontal circular micro-channel," *Experimental thermal and fluid science*, vol. 32, pp. 748-760, 2008.
- [62] S. Saisorn and S. Wongwises, "An experimental investigation of two-phase air-water flow through a horizontal circular micro-channel," *Experimental thermal and fluid science*, vol. 33, pp. 306-315, 2009.
- [63] B. A. Shannak, "Frictional pressure drop of gas liquid two-phase flow in pipes," *Nuclear Engineering and Design*, vol. 238, pp. 3277-3284, 2008.

- [64] A. Kawahara, M. Sadatomi, K. Nei, and H. Matsuo, "Experimental study on bubble velocity, void fraction and pressure drop for gas-liquid two-phase flow in a circular microchannel," *International Journal of Heat and Fluid Flow*, vol. 30, pp. 831-841, 2009.
- [65] A. Alizadehdakhel, M. Rahimi, J. Sanjari, and A. A. Alsairafi, "CFD and artificial neural network modeling of two-phase flow pressure drop," *International Communications in Heat and Mass Transfer*, vol. 36, pp. 850-856, 2009.
- [66] K. Dutkowski, "Two-phase pressure drop of air-water in minichannels," *International Journal of Heat and Mass Transfer*, vol. 52, pp. 5185-5192, 2009.
- [67] H. Su, H. Niu, L. Pan, S. Wang, A. Wang, and Y. Hu, "The Characteristics of Pressure Drop in Microchannels," *Industrial & Engineering Chemistry Research*, vol. 49, pp. 3830-3839, 2010.
- [68] J. R. Thome and R. J. Da Silva Lima, "Two-Phase Pressure Drops in Adiabatic Horizontal Circular Smooth U-Bends and Contiguous Straight Pipes (RP-1444)," 2010.
- [69] D. C. Groeneveld, Leung, L.K.H., Guo Y.J., Vasic, A.Z, El Nakla, M., Peng, S.W., Yang, J., and Cheng, S.C., "Look-up Tables for Predicting CHF and Film Boiling Heat Transfer: Past, Present and Future," *Nuclear Technology*, vol. 152, pp. 87-104, 2005.
- [70] M. El Nakla, Cheng, S. C., and Groeneveld, D. C, "Improvements of Prediction Accuracy and Parametric Trends of the Film Boiling Look-up Tables at ACR Conditions of Interest," *Technical Report for Atomic Energy of Canada Limited (Protected)*, UO-MCG-TH-2004-001-Rev.1, March, 2004.
- [71] A. E. o. C. L. CATHENA Code, 2007 (Protected).
- [72] X. Huang and S. Cheng, "Simple method for smoothing multidimensional experimental data with application to the CHF and postdryout look-up tables," *Numerical Heat Transfer*, vol. 26, pp. 425-438, 1994.

- [73] D. Groeneveld, J. Shan, A. Vasić, L. Leung, A. Durmayaz, J. Yang, S. Cheng, and A. Tanase, "The 2006 CHF look-up table," *Nuclear Engineering and Design*, vol. 237, pp. 1909-1922, 2007.
- [74] H. Q. Zhang and C. Sarica, "Unified Modeling of Gas/Oil/Water-Pipe Flow—Basic Approaches and Preliminary Validation," *SPE Proj Fac & Constl*, vol. 2, pp. 1-7, 2006.

Appendix A

LOOK UP TABLE

DR	Re	Mass Quality (x)																						
		0	0.05	0.1	0.15	0.2	0.25	0.3	0.35	0.4	0.45	0.5	0.55	0.6	0.65	0.7	0.75	0.8	0.85	0.9	0.95	1		
1500	100	1	56.0598	102.7293	145.7425	185.1947	223.9028	259.127	297.9428	330.2861	361.1154	393.082	424.3879	454.0168	514.1696	551.8805	574.6682	577.772	554.2448	498.9505	413.2216	1		
1500	200	1	56.0599	102.7294	145.7428	185.2104	223.905	259.1496	298.0416	330.458	361.3381	393.252	424.5697	454.3527	514.1127	551.8062	574.5922	577.678	554.2362	499.0527	413.5829	1		
1500	400	1	56.0603	102.7296	145.7433	185.2171	223.8826	259.1719	298.2414	330.8088	361.7947	393.5953	424.9331	455.0384	513.9976	551.6552	574.4354	577.4824	554.2161	499.2547	414.303	1		
1500	600	1	56.0607	102.7298	145.7439	185.2157	223.8461	259.1841	298.4424	331.1674	362.2665	393.9413	425.2948	455.7403	513.8813	551.502	574.2769	577.2785	554.1926	499.4529	415.0171	1		
1500	1000	1	56.0615	102.7303	145.7435	185.2122	223.7576	259.2023	298.8449	331.9019	363.2473	394.6335	426.0033	457.1805	513.6472	551.1951	573.9595	576.8463	554.1322	499.833	416.408	1		
1500	2000	1	56.0634	102.7314	145.7479	114.8945	264.9319	440.2334	631.9788	758.4268	848.9355	902.6346	919.7193	902.4994	859.3716	774.8469	677.2904	577.1952	483.8961	405.964	364.8693	1		
1500	4000	1	56.0671	102.7336	145.7536	136.1022	230.2383	338.0634	456.7236	542.2582	607.5932	648.5313	672.9164	685.7589	685.8201	663.2185	626.7832	576.9901	520.9301	455.3424	393.8775	1		
1500	6000	1	56.0709	102.7359	145.7593	157.5187	250.8535	357.1038	471.2577	554.6851	617.0746	651.6891	671.7596	684.5527	684.7783	663.05	627.6946	577.2147	522.1182	455.4605	389.7217	1		
1500	8000	1	56.0747	102.7381	145.765	176.6838	269.5558	373.7704	484.9541	564.6869	623.6454	654.4746	670.8609	680.9583	681.8899	661.3709	627.3698	578.605	524.7832	458.1794	391.0937	1		
1500	10000	1	56.0785	102.7403	145.7707	171.3874	240.7689	315.4851	396.3809	463.1318	526.4817	554.1774	565.9307	583.7577	576.8683	561.6962	533.451	487.5701	435.4453	367.1711	298.825	1		
1500	20000	1	56.0974	102.7515	145.7991	141.4917	174.1062	209.9579	252.6062	290.739	341.9972	371.8412	400.2585	443.8543	467.9579	493.3184	505.0291	494.0044	467.4122	410.6048	333.8776	1		
1500	40000	1	56.1352	102.7738	145.856	154.3133	199.4287	247.8055	301.4966	343.8914	387.462	409.0357	431.1185	476.5637	527.0011	564.3622	587.3999	589.17	572.2825	521.4949	440.713	1		
1500	60000	1	56.1731	102.7961	145.913	116.5033	158.7359	204.9379	259.2458	306.3754	352.3892	389.1265	424.7508	462.6177	517.6097	552.4868	572.2734	570.9456	549.2664	496.3111	417.1443	1		
1500	80000	1	56.2109	102.8184	145.9699	116.6889	159.0009	205.0163	256.5028	302.7624	348.1135	385.0878	420.282	456.4305	517.9529	552.9088	572.6846	571.559	549.2542	495.6679	415.2247	1		
1500	100000	1	56.2487	102.8407	146.0269	184.7925	222.2237	258.1901	293.7875	325.9199	357.9676	385.8561	414.3984	445.9707	513.2989	550.7776	573.4021	575.3596	553.4543	498.4836	412.5926	1		
1500	150000	1	57.0235	102.8965	146.1692	185.7527	223.2573	258.6663	292.3851	323.2556	354.1418	383.3322	411.9798	440.6115	514.8458	552.7708	575.5941	578.0863	554.3013	497.169	406.6796	1		
1500	200000	1	57.3206	103.4248	146.3115	186.1723	223.7093	258.8999	291.9446	322.4059	352.8738	382.5617	411.2798	438.8952	515.3263	553.4039	576.2537	578.8088	554.2117	496.1159	403.3293	1		
1500	400000	1	57.6291	103.9939	147.0673	186.7568	224.3032	259.3088	291.7771	322.0231	352.1422	382.3117	411.1983	438.1605	515.5319	553.6748	576.5372	579.1789	554.1392	495.6773	402.0542	1		
1500	600000	1	57.4294	103.7822	146.9077	187.0881	224.6375	259.799	292.8298	323.8398	354.3013	384.1902	413.3773	441.8259	515.8593	554.1071	576.9883	578.8627	553.3856	494.099	398.2577	1		
1500	800000	1	57.4107	103.7379	146.8673	187.1621	224.6984	259.9612	293.3295	324.7193	355.3912	385.0477	414.3266	443.5794	515.973	554.2571	577.1465	578.655	553.0617	493.4643	396.7604	1		
1500	1000000	1	57.392	103.6936	146.8269	186.9859	224.5142	259.6824	292.6827	323.6016	354.0423	383.8565	412.9526	441.2876	516.3427	554.7451	577.6591	579.2882	553.181	492.8084	394.1482	1		
x →		0	0.05	0.1	0.15	0.2	0.25	0.3	0.35	0.4	0.45	0.5	0.55	0.6	0.65	0.7	0.75	0.8	0.85	0.9	0.95	1		
1300	100	1	47.3081	86.5067	122.611	155.8495	188.4572	217.978	250.4858	277.72	303.5334	330.6494	357.0584	381.8905	432.112	463.7071	482.9158	485.9557	466.9232	421.7396	352.9321	1		
1300	200	1	47.3083	86.5068	122.6111	155.7886	188.3833	217.9324	250.5723	277.8626	303.7217	330.7922	357.2067	382.1688	432.0655	463.6459	482.8523	485.8712	466.9097	421.8126	353.2041	1		
1300	400	1	47.3088	86.5069	122.6111	155.7264	188.2904	217.8921	250.747	278.1532	304.1078	331.0809	357.5029	382.7368	431.9709	463.5221	482.7234	485.6913	466.8801	421.9571	353.7451	1		
1300	600	1	47.3093	86.5071	122.6111	155.6923	188.2214	217.8786	250.9234	278.4506	304.5079	331.3719	357.797	383.3184	431.8755	463.3978	482.5958	485.504	466.8459	422.0963	354.2792	1		
1300	1000	1	47.3103	86.5075	122.6112	155.6551	188.0995	217.8765	251.2783	279.0596	305.3417	331.9548	358.3713	384.5117	431.6831	463.1452	482.3357	485.1024	466.7651	422.3594	355.3099	1		
1300	2000	1	47.3127	86.5085	122.6114	96.108	220.8671	366.9706	531.4728	637.8967	714.2537	760.2003	775.7763	762.9964	721.2685	651.7742	571.6607	489.6528	413.8762	350.3532	321.2389	1		
1300	4000	1	47.3176	86.5104	122.6117	112.7416	191.2183	281.8167	383.1876	455.1335	510.5705	545.7845	566.7811	578.7083	576.1926	557.887	528.1314	486.93	441.631	388.1623	340.7234	1		
1300	6000	1	47.3225	86.5123	122.6121	130.1235	207.9582	297.6569	395.126	465.1035	518.2983	548.2775	565.6996	577.8486	575.2939	557.6961	528.8616	486.847	442.5079	388.1513	337.119	1		
1300	8000	1	47.3274	86.5142	122.6124	145.6486	222.9971	311.1658	406.072	473.2704	524.0301	550.7585	565.4733	575.4315	572.9809	556.3511	528.6496	488.1975	444.8454	390.4264	338.2886	1		
1300	10000	1	47.3323	86.516	122.6128	144.5223	204.3608	269.7326	340.7701	398.3864	454.3996	476.4883	484.9246	499.3663	484.3679	467.6259	440.6025	398.0633	353.9686	297.1696	246.1227	1		
1300	20000	1	47.3569	86.5255	122.6145	114.6669	139.98	170.3423	206.7759	238.6466	284.1655	308.9273	333.0989	371.2618	389.4668	409.1843	417.7666	406.5139	384.8757	337.6968	278.423	1		
1300	40000	1	47.406	86.5445	122.618	127.5847	165.3309	208.1624	255.8125	291.7512	329.9248	346.4509	364.3674	404.4585	447.7714	478.9056	498.3138	499.9987	487.7972	446.5545	382.4467	1		
1300	60000	1	47.455	86.5634	122.6216	90.7779	126.0736	166.357	214.3324	255.2706	295.3402	326.8231	356.8493	390.0272	437.0229	466.3109	483.1744	482.2698	465.1443	421.9985	359.9513	1		
1300	80000	1	47.5041	86.5824	122.6251	90.8812	126.3254	166.3955	212.2196	252.6124	291.8521	323.5235	353.1636	384.9058	437.313	466.666	483.5242	482.8607	465.1949	421.5546	358.5725	1		
1300	100000	1	47.5532	86.6014	122.6286	155.0874	186.0474	216.5841	247.119	274.1004	301.2924	324.6621	348.5735	375.2226	432.8433	464.5637	484.1171	486.4657	469.2787	424.5534	357.0137	1		
1300	150000	1	47.6759	86.6488	122.6373	155.8778	187.1518	217.0904	245.8778	271.91	298.028	322.5392	346.644	370.8026	432.7103	464.4884	483.7371	486.2455	467.1591	420.4559	347.7585	1		
1300	200000	1	47.9692	86.6962	122.6461	156.2468	187.6456	217.3777	245.5093	271.1997	296.9258	321.8777	346.08	369.3766	433.105	465.0067	484.2772	486.9013	467.122	419.6589	345.2061	1		
1300	400000	1	48.2226	87.118	123.282	156.6945	188.2708	217.768	245.3939	270.9403	296.3178	321.652	346.0279	368.7606	433.2735	465.2286	484.5078	487.2449	467.0694	419.3267	344.2658	1		
1300	600000	1	48.1294	86.9745	123.2845	156.9951	188.5821	218.1999	246.3481	272.5181	298.1737	323.311	347.8313	371.7955	433.5421	465.5819	484.8783	486.8913	466.3773	417.9456	341.1031	1		
1300	800000	1	48.119	86.9567	123.1894	157.0193	188.5807	218.2957	246.7846	273.2674	299.1266	324.1433	348.7248	373.2903	433.6354	465.7048	485.0068	486.671	466.0761	417.3818	339.8349	1		
1300	1000000	1	48.1086	86.9388	123.0943	156.7962	188.3994	218.0647	246.2147	272.2608	298.0007	323.151	347.6058	371.4055	433.9386	466.1049	485.4258	487.2499	466.2313	416.9233	337.8612	1		

DR	Re	Mass Quality (x)																				
		0	0.05	0.1	0.15	0.2	0.25	0.3	0.35	0.4	0.45	0.5	0.55	0.6	0.65	0.7	0.75	0.8	0.85	0.9	0.95	1
1100	150000	1	41.4259	74.9298	106.1808	135.451	162.7047	188.3353	212.6631	235.2875	257.4944	279.1695	300.3329	321.0221	374.7832	402.3569	419.0334	421.0798	404.224	363.6255	300.2097	1
1100	200000	1	41.4249	74.9276	106.1743	135.5599	162.7329	188.2777	212.1982	234.6698	256.7412	278.269	299.2706	319.7827	375.1268	402.8088	419.5035	421.3516	404.011	362.6407	297.3506	1
1100	400000	1	41.4207	74.9185	106.1483	135.5841	162.7204	188.212	212.0216	234.4481	256.4566	277.8801	298.8124	319.2487	375.2737	403.0018	419.7052	421.4682	403.9201	362.2184	296.1155	1
1100	600000	1	41.4165	74.9095	106.1223	135.3555	162.6258	188.3274	213.117	235.8262	258.115	279.8529	301.0768	321.89	375.5075	403.3104	420.028	421.6553	403.7748	361.5438	294.1325	1
1100	800000	1	41.4124	74.9005	106.0963	135.1363	162.5334	188.3534	213.6293	236.4786	258.9207	280.8531	302.2459	323.1924	375.5886	403.4169	420.1392	421.7194	403.7244	361.3094	293.4389	1
1100	1000000	1	41.4082	74.8914	106.0703	135.1783	162.529	188.2592	212.968	235.5994	257.9088	279.6623	300.8454	321.5524	375.8526	403.7655	420.5043	421.932	403.5588	360.5438	291.1658	1
x →		0	0.05	0.1	0.15	0.2	0.25	0.3	0.35	0.4	0.45	0.5	0.55	0.6	0.65	0.7	0.75	0.8	0.85	0.9	0.95	1
900	100	1	77.3299	126.6642	164.4049	190.3403	209.4555	222.2777	226.2164	232.9279	241.4731	251.2788	263.1935	278.1027	332.1637	360.3065	380.2403	387.2907	376.1907	342.7475	294.6746	1
900	200	1	69.1168	114.0684	149.7641	175.3823	195.5206	210.4455	217.5808	227.1678	238.2912	250.3011	263.829	279.5549	333.7175	361.3517	380.6956	387.2353	375.8454	342.5589	295.6609	1
900	400	1	61.9289	103.2429	137.2809	162.6711	183.7303	200.4857	210.3237	222.3944	235.7047	249.5529	264.3984	280.7666	335.3156	362.6021	381.585	387.8561	376.3627	343.3764	298.0872	1
900	600	1	58.3163	98.0566	131.4283	156.7783	178.3338	195.9961	207.0825	220.358	234.674	249.3233	264.703	281.2953	336.31	363.5282	382.4918	388.8085	377.4125	344.726	300.7604	1
900	1000	1	45.1591	87.4781	124.4339	151.0952	174.4955	193.7465	206.1064	222.3255	235.4216	247.2107	265.0588	281.727	337.8005	365.1457	384.3948	391.097	380.0913	348.0129	306.4788	1
900	2000	1	63.2894	113.9096	140.3903	146.0857	143.72	138.0474	138.0773	174.3926	234.8331	321.2807	434.3153	566.5389	849.6549	1043.496	1197.853	1294.459	1317.657	1238.618	1020.231	1
900	4000	1	48.2398	87.5928	113.8349	129.0729	139.6573	148.3057	158.323	188.1162	230.0159	286.2379	354.5919	433.4664	623.8397	744.5468	841.3376	901.3564	913.1351	861.1591	735.7059	1
900	6000	1	45.0395	85.636	112.5233	128.0132	138.7448	147.3879	158.075	188.1976	230.1293	286.6128	355.3413	434.6658	627.8948	749.8741	848.5172	910.2319	922.1807	869.7325	746.0303	1
900	8000	1	43.3841	84.3998	111.615	127.3895	138.3316	147.2204	158.5139	188.6911	230.4172	286.7473	355.3738	434.6011	628.5006	750.5549	848.824	910.507	923.1814	871.2345	748.5883	1
900	10000	1	45.3119	86.2821	113.3366	128.5499	139.1304	147.8099	158.9428	187.5887	230.3262	286.5102	354.8913	434.3996	631.5746	754.4018	853.0968	914.702	928.473	877.4284	758.3887	1
900	20000	1	40.6972	76.6131	100.8952	115.3303	126.0774	136.1969	150.0728	180.3652	225.5709	283.5452	353.1455	432.8294	636.4803	759.4568	858.4731	920.3802	934.4672	884.8654	771.6301	1
900	40000	1	36.787	69.8783	92.7456	107.0581	118.3405	129.5457	146.1196	177.532	220.0717	282.9079	352.9881	432.607	634.8004	756.5586	853.9083	915.6179	930.2372	880.8809	767.311	1
900	60000	1	34.8209	66.5244	87.9629	102.3547	113.8573	125.4872	143.7349	175.8874	222.8709	282.5951	353.356	433.4494	633.3297	754.9275	851.9935	913.3406	927.0577	876.1579	758.5701	1
900	80000	1	33.5324	64.2257	84.8541	99.4476	111.0075	122.9267	141.964	174.7238	222.2546	282.5998	354.0652	434.7596	629.8707	751.021	847.0844	907.1204	919.5156	866.7844	742.4447	1
900	100000	1	32.7864	62.7701	83.0934	97.3822	108.9229	120.9224	140.1059	173.4171	221.7114	282.9696	355.452	437.2033	629.0606	750.7877	846.9824	906.4263	917.2899	861.8284	730.0901	1
900	150000	1	21.0668	39.5219	61.1909	85.1877	110.9594	138.0602	168.4111	194.2086	219.9722	244.5654	267.3618	287.8332	340.2635	364.615	379.7404	382.1491	367.7001	333.3682	286.8256	1
900	200000	1	19.6752	37.3414	58.6238	82.5662	108.6008	136.1251	166.8296	193.1135	219.342	244.3513	267.4655	288.1092	337.5592	361.1685	375.0656	376.0599	360.4323	324.7371	272.6264	1
900	400000	1	16.5737	32.6299	53.0806	76.8625	103.336	131.644	163.5968	190.9032	218.0756	243.9165	267.6696	288.6619	334.7533	357.4063	369.8489	369.3429	352.6399	315.9308	258.9319	1
900	600000	1	14.8475	30.3111	50.4984	74.3362	101.0451	129.7562	161.73	189.6054	217.3393	243.6707	267.7865	288.9794	335.4799	358.121	370.4933	369.7787	352.7571	315.6382	257.9321	1
900	800000	1	13.9656	28.9184	48.8624	72.6802	99.4267	128.3969	160.5496	188.7837	216.8637	243.5159	267.8766	289.1902	336.4129	359.1455	371.6525	371.0364	353.9919	316.8573	259.7266	1
900	1000000	1	13.2684	27.6905	47.3486	71.1011	98.0253	127.2776	159.5183	188.0742	216.4434	243.3694	267.9445	289.3724	336.5379	359.2091	371.5422	370.6069	353.1206	315.4055	256.6825	1
x →		0	0.05	0.1	0.15	0.2	0.25	0.3	0.35	0.4	0.45	0.5	0.55	0.6	0.65	0.7	0.75	0.8	0.85	0.9	0.95	1
600	100	1	61.9011	100.5497	129.3169	147.7519	160.6858	167.654	165.8448	168.4456	172.4579	177.5827	184.6124	194.3788	232.3691	252.6548	267.3045	272.9103	265.6491	242.4144	208.7138	1
600	200	1	55.2953	90.4625	117.5437	135.6553	149.3662	157.9777	163.8385	169.8908	176.7731	185.1017	195.5365	233.5934	253.4625	267.6275	272.8094	265.3023	242.1783	209.3629	1	
600	400	1	49.5271	81.8414	107.5733	125.4452	139.8677	149.9043	153.2554	160.0505	167.8229	176.1602	185.54	196.4951	234.8154	254.3959	268.2519	273.1941	265.5822	242.6683	211.0201	1
600	600	1	46.5993	77.6596	102.8334	120.6309	135.4476	146.1968	150.634	158.3818	166.9611	175.9506	185.7748	196.9252	235.5679	255.0755	268.887	273.8321	266.2709	243.5657	212.8602	1
600	1000	1	42.3174	77.1114	105.5751	123.3729	138.4606	148.8242	152.416	160.5563	165.97	172.4218	186.0494	197.299	236.6784	256.2446	270.2183	275.3986	268.0862	245.805	216.8131	1
600	2000	1	50.8392	90.8357	112.0741	116.0534	114.0396	107.8298	103.1977	124.5239	164.4281	223.7423	301.8741	392.2927	602.2369	739.07	848.0266	917.6061	936.2789	882.6412	737.677	1
600	4000	1	42.5517	76.0609	98.0658	108.7339	115.411	118.1177	120.6905	137.3592	163.7267	199.8673	246.3225	301.067	441.1196	526.2761	594.3485	637.3885	647.514	612.3723	529.0552	1
600	6000	1	41.2047	72.774	92.6195	102.2447	108.2854	110.8171	114.7039	133.0599	159.7611	197.7673	248.8409	304.0719	444.2482	530.3947	599.7182	643.7297	653.8837	618.5494	536.4003	1
600	8000	1	31.2548	60.6854	80.1588	90.761	98.5727	103.8281	110.9298	131.6648	160.7763	200.1297	247.8841	303.123	444.6691	530.8661	600.1947	644.3463	654.7426	619.5908	538.1642	1
600	10000	1	30.0349	59.7863	79.7181	89.7078	97.5968	103.4489	110.9725	131.7349	160.7708	200.3524	248.3757	302.9592	445.1922	531.6224	601.7004	648.0596	658.9911	624.3188	545.451	1
600	20000	1	31.3767	58.8139	76.9485	86.4805	94.2204	100.1265	108.615	128.9631	159.745	199.9314	248.565	303.6229	448.4088	535.0914	605.6423	652.2712	663.6755	629.7977	554.6453	1
600	40000	1	28.5604	53.717	70.5864	80.1538	88.397	95.2203	105.867	127.334	159.1429	199.9732	248.9194	304.232	448.187	534.4606	604.0279	649.0216	659.9821	626.3577	551.1445	1
600	60000	1	27.1921	50.9851	66.8668	76.8371	84.8125	91.9898	104.0175	126.0467	157.8129	198.979	247.9505	303.7931	447.6207	533.6767	602.8864	647.1558	657.8439	623.3126	545.1733	1
600	80000	1	26.1622	49.0832	64.3975	74.4527	82.4351	90.0671	102.2949	124.5448	157.1749	198.8506	248.4501	304.721	445.2382	530.9794	599.4909	642.8546	652.6212	616.819	534.0819	1
600	100000	1	25.4389	47.7142	62.5886	72.5587	80.4718	88.3051	100.9363	123.6002	156.7736	199.1023	249.4183	306.4291	444.7286	530.8781	599.4982	642.467				

DR	Re	Mass Quality (x)																				
		0	0.05	0.1	0.15	0.2	0.25	0.3	0.35	0.4	0.45	0.5	0.55	0.6	0.65	0.7	0.75	0.8	0.85	0.9	0.95	1
500	8000	1	36.56	63.2599	80.5214	91.0636	96.6244	98.7302	102.0419	115.7566	138.295	168.9634	207.5857	254.0246	377.1749	450.3786	509.2291	546.8157	555.8641	526.1308	457.7991	1
500	10000	1	30.5516	53.5283	69.1559	78.758	84.9851	89.3205	95.2842	110.8299	135.4336	168.5461	209.6433	255.7651	377.1666	450.463	510.102	550.1008	559.5162	530.1577	464.0099	1
500	20000	1	26.7689	48.5715	63.5745	73.5589	80.6702	86.0508	93.8114	110.8322	136.6275	169.5048	210.5379	256.9811	379.7784	453.3405	513.5153	553.7805	563.6685	534.9696	471.848	1
500	40000	1	25.7793	46.9433	61.1824	70.8614	77.9895	83.5187	92.2927	108.8994	135.5119	169.7722	211.0563	257.7903	379.8675	453.2173	512.5844	551.1281	560.4304	531.9796	468.8294	1
500	60000	1	24.42	44.7067	58.4956	67.836	74.5578	80.3385	90.2582	107.6363	134.0393	168.6021	209.8505	257.0664	379.4819	452.6467	511.6475	549.478	558.6552	529.418	463.7836	1
500	80000	1	23.4768	43.1994	56.5527	65.5672	72.2363	78.1826	88.0269	106.0833	133.4125	168.4509	210.2778	257.862	377.464	450.3636	508.7729	545.8337	554.2309	523.9175	454.3928	1
500	100000	1	22.7198	42.0543	54.9565	63.6221	70.1686	76.4151	86.5975	105.2683	133.0638	168.6632	211.1029	259.3177	377.0444	450.2929	508.8037	545.5332	553.035	521.124	447.4064	1
500	150000	1	15.3953	27.8328	41.362	55.6444	70.5841	86.0081	102.9713	117.499	131.9611	145.8449	158.8521	170.7603	201.9851	216.7316	226.065	227.8454	219.5428	199.3028	171.8715	1
500	200000	1	14.4293	26.3435	39.5687	53.7419	68.7876	84.448	101.7938	116.7946	131.5609	145.7108	158.9254	170.9462	200.3979	214.6992	223.2988	224.2391	215.2365	194.1918	163.5041	1
500	400000	1	12.556	23.4276	35.8933	49.9066	65.04	81.254	99.4871	115.1922	130.6135	145.424	159.0714	171.3282	198.778	212.4948	220.2128	220.2361	210.5953	188.9523	155.4181	1
500	600000	1	11.4539	21.7924	33.9669	48.1185	63.5177	79.887	98.4143	114.1946	129.9971	145.1356	159.151	171.5415	199.231	212.9309	220.5966	220.4978	210.6519	188.7678	154.8364	1
500	800000	1	10.6454	20.5382	32.8319	46.8331	62.4591	78.9713	97.7365	113.6102	129.5957	144.8347	159.0146	171.6109	199.8002	213.5471	221.2844	221.2349	211.3717	189.479	155.8963	1
500	1000000	1	10.0607	19.6084	31.6636	45.7117	61.2708	78.0351	96.9426	113.3	129.3575	144.7277	159.0289	171.7106	199.8844	213.5911	221.221	220.9802	210.8536	188.6191	154.1136	1
x →		0	0.05	0.1	0.15	0.2	0.25	0.3	0.35	0.4	0.45	0.5	0.55	0.6	0.65	0.7	0.75	0.8	0.85	0.9	0.95	1
300	100	1	41.3448	65.5778	82.777	94.2316	100.408	102.1925	97.6029	95.5357	95.3592	96.195	98.4984	102.9241	124.1623	135.5628	144.1763	147.6681	144.1966	131.7739	113.3116	1
300	200	1	37.0064	58.8588	74.8982	86.1088	92.795	95.6612	93.0479	92.4465	93.6188	95.6267	98.8145	103.7033	124.9239	136.0363	144.3143	147.5495	143.9022	131.5406	113.6225	1
300	400	1	33.2629	53.1681	68.2807	79.3292	86.4846	90.2829	89.3025	89.9368	92.236	95.2021	99.1065	104.3521	125.6052	136.5117	144.5696	147.7066	143.9692	131.7214	114.4799	1
300	600	1	31.366	50.3661	65.0653	76.0682	83.4841	87.7533	87.5461	88.7841	91.6271	95.038	99.2718	104.6656	125.9787	136.8177	144.8238	148.0217	144.2926	132.1574	115.4476	1
300	1000	1	28.948	47.4293	62.4036	72.8271	80.5638	85.3393	85.8789	87.7317	91.1201	94.9459	99.4855	104.9878	126.4499	137.2837	145.3468	148.8286	145.2109	133.3034	117.5401	1
300	2000	1	27.1367	62.1305	83.2682	93.2722	95.7039	92.961	87.1208	93.456	111.0849	126.0809	167.0643	208.8023	321.7474	396.8556	457.7718	498.6371	511.746	484.4771	409.3861	1
300	4000	1	33.6545	65.4815	87.079	99.0079	104.589	103.9951	100.5182	101.7545	110.0804	121.4383	139.159	161.8846	231.9838	278.8468	317.6367	345.5181	353.8709	336.3797	292.6247	1
300	6000	1	38.0072	61.4041	75.1143	81.6972	83.4165	80.099	76.5223	80.0052	91.2066	106.7723	130.5674	159.9466	238.1921	284.5912	322.1299	349.0789	355.3565	336.9586	294.9673	1
300	8000	1	43.9089	62.3563	71.6945	75.3039	75.2094	71.5681	68.5184	73.3794	84.5416	101.7517	125.7902	155.8693	235.8499	283.8292	322.7711	350.48	357.3145	338.8792	296.3955	1
300	10000	1	33.327	38.4499	41.488	42.879	44.7572	45.9894	48.6789	52.411	54.0124	65.8105	89.4466	115.4623	189.7077	235.3098	275.7459	309.7979	324.8224	319.9288	298.6809	1
300	20000	1	22.1665	24.5586	28.8182	34.9033	43.3071	52.7457	64.7733	77.082	87.4362	103.8621	125.5417	150.4738	221.2239	262.018	297.1141	325.1079	334.722	325.0722	301.7796	1
300	40000	1	11.8092	20.1424	30.2187	42.0039	56.0352	70.9912	88.6116	105.506	126.4828	148.6453	172.8566	197.5149	265.6947	302.5373	331.1772	350.3437	351.3438	332.7418	299.16	1
300	60000	1	18.1863	31.7715	40.5771	46.1343	50.3083	53.5704	59.5316	70.5759	86.5898	107.9434	134.11	164.0892	240.6299	287.5536	325.5804	351.6497	357.9122	339.7662	299.7263	1
300	80000	1	17.3806	30.6006	39.1945	44.5762	48.6862	52.1171	57.6871	68.8337	85.9112	107.7	134.3029	164.5283	239.746	286.4979	324.0688	349.3078	355.088	336.3081	293.8356	1
300	100000	1	16.5814	29.6115	37.9817	43.3472	47.3576	51.0271	56.7523	68.2599	85.6234	107.8164	134.6857	165.3077	240.1242	287.1224	324.7073	349.1185	354.3437	334.5707	289.5319	1
300	150000	1	11.5957	20.2415	29.0986	38.2266	47.6185	57.1855	67.2511	76.0224	84.8321	93.2396	101.2362	108.6971	128.2326	137.8705	144.0991	145.6285	140.5808	127.8912	110.9108	1
300	200000	1	10.8275	19.1435	27.8376	36.9685	46.4124	56.0991	66.4281	75.4955	84.4842	93.0804	101.155	108.6722	127.5591	136.9101	142.6449	143.3535	137.8626	124.6666	105.6629	1
300	400000	1	9.6091	17.267	25.3802	34.4081	43.8197	53.8491	64.7938	74.311	83.7177	92.7733	101.1043	108.7654	126.8221	135.7717	140.9078	140.8167	134.9159	121.3431	100.5752	1
300	600000	1	8.9829	16.2268	24.1157	33.0998	42.6442	52.7188	63.9781	73.5746	83.2085	92.4695	101.115	108.8703	126.8148	135.6971	140.8042	140.9811	134.9481	121.2247	100.2239	1
300	800000	1	8.3609	15.2492	23.3102	32.1116	41.8369	51.9739	63.463	73.1474	82.9086	92.261	101.053	108.9336	126.998	135.8868	141.0438	141.4446	135.3982	121.6698	100.8953	1
300	1000000	1	7.7977	14.4247	22.3246	31.2628	40.9904	51.3493	62.9724	72.9462	82.8021	92.2542	101.0849	109.0218	127.241	136.135	141.2205	141.2863	135.0736	121.1311	99.7921	1
x →		0	0.05	0.1	0.15	0.2	0.25	0.3	0.35	0.4	0.45	0.5	0.55	0.6	0.65	0.7	0.75	0.8	0.85	0.9	0.95	1
200	100	1	31.7158	50.1174	62.9485	70.2148	74.2204	74.8314	69.7087	68.3324	67.1831	66.746	68.9471	71.7847	85.1585	93.3964	99.599	102.323	100.3136	92.0087	79.6208	1
200	200	1	28.3809	44.8903	56.8201	63.9087	68.2953	69.7217	66.2262	65.9637	65.8471	66.3053	69.2104	72.4088	85.7442	93.7528	99.6963	102.2125	100.0681	91.8047	79.8124	1
200	400	1	25.5046	40.4719	51.6919	58.6586	63.4017	65.5351	63.3683	64.0568	64.8025	65.9847	69.4848	72.9614	86.267	94.1018	99.8748	102.2923	100.0786	91.8919	80.3721	1
200	600	1	24.0336	38.2698	49.1715	56.0945	61.0401	63.5379	61.9988	63.1692	64.34	65.8612	69.6669	73.2657	86.5606	94.3235	100.0524	102.4885	100.2783	92.167	81.0113	1
200	1000	1	22.1333	35.9521	47.091	53.4781	58.6807	61.5831	60.6453	62.3387	63.954	65.7963	69.9493	73.6517	86.945	94.6579	100.4192	103.0084	100.8762	92.9182	82.4007	1
200	2000	1	17.6073	25.7659	29.7676	29.2833	27.6447	25.3205	22.9113	31.1002	48.8758	73.8333	109.2326	145.105	229.9915	282.8002	324.3856	350.8901	358.2151	338.3487	288.7041	1
200	4000	1	19.8036	31.5957	43.2215	50.4769	57.8525	62.9839	68.4329	77.3786	88.3411	99.2187	121.3462	138.9389	187.6791	213.5967	233.2871	245.2606	245.717	230.7628	202.8414	1
200	6000	1	11.2649	16.2415	24.7533	33.5277	44.4838	55.192	68.0749	84.556	101.5614	116.6201	136.2828	153.8453	202.0758	223.8101	239.663	248.57	245.9011	229.5954	203.3235	1
200	8000	1	25.9836	42.3854	52.2697	56.3467	58.1843	56.2312	53.8127	56.5465	64.1108	75.2864	92.3252	110.4309	162.9307	195.7321	223.5507	243.3775	249.189			

DR	Re	Mass Quality (x)																				
		0	0.05	0.1	0.15	0.2	0.25	0.3	0.35	0.4	0.45	0.5	0.55	0.6	0.65	0.7	0.75	0.8	0.85	0.9	0.95	1
150	200	1	23.0094	36.4829	45.7591	51.7474	55.1198	56.2572	53.13	52.1121	51.6259	51.3964	52.4806	55.0887	65.1202	71.4927	76.2698	77.9267	76.7935	70.2072	61.5379	1
150	400	1	20.7616	33.0526	41.7836	47.7011	51.3693	53.0827	50.9901	50.704	50.8867	51.1999	52.6922	55.5132	65.504	71.7546	77.9933	76.8058	70.2674	61.965	1	
150	600	1	19.5734	31.2545	39.713	45.606	49.4479	51.4728	49.8983	49.9948	50.5333	51.1223	52.8296	55.7671	65.7372	71.9336	76.5667	78.1401	76.9448	70.4542	62.4468	1
150	1000	1	18.3207	29.4947	37.6784	43.4607	47.5328	49.9089	48.849	49.3513	50.271	51.1203	53.0398	56.0691	66.0391	72.2041	76.8773	78.5419	77.3848	70.9915	63.4975	1
150	2000	1	13.309	25.546	32.9822	37.0306	38.2967	37.7955	35.2225	34.1522	38.7597	47.2827	62.489	75.7239	126.882	160.0846	188.6031	209.4572	220.2487	215.1942	195.4696	1
150	4000	1	17.4412	38.959	57.0552	68.7507	78.6204	84.0737	87.3787	88.7583	89.6606	86.1156	91.6612	98.6433	128.3831	145.3443	159.8653	169.9647	173.3148	166.5309	152.3535	1
150	6000	1	6.4066	11.0521	19.6857	30.11	42.1855	53.3855	66.808	79.6141	92.8089	103.3856	115.261	125.814	155.7479	169.7663	180.2445	185.5439	182.8236	170.9162	152.7586	1
150	8000	1	15.2329	26.1004	33.6155	38.0309	41.2311	41.4611	42.8722	46.1965	52.7877	61.8034	73.5008	88.0653	125.9156	149.7363	169.9869	183.8304	187.2322	177.968	157.5538	1
150	10000	1	13.7411	21.432	28.7099	32.8919	37.9157	41.087	44.6581	48.514	51.0601	54.6597	63.4348	76.8334	112.0408	133.472	153.5909	169.7108	174.9922	169.9493	156.8768	1
150	20000	1	6.8643	10.2761	16.1102	22.276	30.0926	38.8582	49.1171	58.9324	67.9407	77.9344	90.4701	105.0011	139.2243	156.6578	172.3963	183.2215	183.4563	174.1551	158.8034	1
150	40000	1	7.0357	10.9536	18.2908	28.4964	40.7112	54.3854	69.5203	83.3095	95.7308	110.1629	123.4266	136.1881	166.4549	181.1296	191.819	197.3726	193.1407	179.3534	159.1283	1
150	60000	1	7.2912	18.3014	28.2122	36.9426	45.1803	52.7124	61.534	69.564	76.0099	84.2374	93.1426	103.1733	136.0674	154.1805	169.1933	179.373	181.2547	173.363	158.1577	1
150	80000	1	10.5446	18.3522	23.3516	26.4134	28.34	29.9628	32.9815	38.9132	47.6614	58.7676	72.1496	87.8166	127.4421	151.6223	171.3833	184.5607	187.4975	177.9223	155.9323	1
150	100000	1	10.4452	18.1478	23.0856	26.0737	27.9884	29.6645	32.2436	38.1434	46.9389	58.3127	71.906	87.7349	127.3634	151.7784	171.4984	184.2665	186.9712	176.97	153.68	1
150	150000	1	7.9839	13.2612	18.3967	23.3596	28.0736	32.8607	37.5408	41.8324	46.0436	50.2192	54.0474	57.828	68.7865	74.0748	77.7545	79.0868	76.6757	70.4209	62.8283	1
150	200000	1	7.6086	12.7238	17.7057	22.6328	27.3458	32.2034	36.9058	41.2537	45.5351	49.8322	53.7461	57.5332	68.394	73.5743	76.9897	77.8951	75.2931	68.8039	60.2204	1
150	400000	1	16.7214	22.715	26.7055	30.2872	33.1922	36.2073	39.0752	41.5982	44.1544	48.121	52.4821	57.3775	67.9631	72.9844	76.0725	76.5342	73.7773	67.1037	57.6585	1
150	600000	1	15.1507	20.8104	24.8861	28.6134	31.8508	35.247	38.4944	41.3421	44.3707	48.6236	52.6827	57.9793	72.9444	76.0309	76.5708	73.8254	67.0322	57.5219	1	
150	800000	1	6.1296	10.389	14.8927	19.6706	24.5964	29.8088	35.2127	40.0612	44.995	49.6755	54.0067	57.9453	68.0982	73.045	76.1628	76.7947	74.0658	67.2504	57.8763	1
150	1000000	1	5.5917	9.625	14.1038	18.9101	24.0914	29.4069	34.8347	39.6643	44.78	49.6443	53.955	57.8584	68.2289	73.1871	76.2596	76.7603	73.8968	67.0054	57.3663	1
x →		0	0.05	0.1	0.15	0.2	0.25	0.3	0.35	0.4	0.45	0.5	0.55	0.6	0.65	0.7	0.75	0.8	0.85	0.9	0.95	1
100	100	1	6.1911	10.1641	14.2219	18.0859	21.544	24.5561	26.6496	29.1261	32.1701	34.6869	36.8989	39.4882	46.4724	50.0925	51.9724	52.5006	50.6811	46.2481	39.2963	1
100	200	1	6.0965	10.0502	14.0752	17.9069	21.3576	24.3701	26.6662	29.1449	32.1887	34.6985	36.8998	39.4904	46.4855	50.1064	51.9993	52.5295	50.7099	46.2816	39.3411	1
100	400	1	6.0116	9.9503	13.9568	17.767	21.2238	24.2425	26.7005	29.1844	32.2273	34.7223	36.9018	39.4953	46.5126	50.1349	52.0552	52.5895	50.7695	46.3501	39.4322	1
100	600	1	5.9651	9.8954	13.8973	17.6962	21.1617	24.1834	26.736	29.2266	32.2673	34.747	36.9041	39.5008	46.5407	50.164	52.1146	52.652	50.8313	46.4204	39.5249	1
100	1000	1	6.2608	10.0359	13.5147	17.6222	21.1093	24.1346	26.8101	29.3191	32.3516	34.7986	36.9101	39.5137	46.5997	50.2233	52.2419	52.7845	50.9607	46.5649	39.7138	1
100	2000	1	8.2431	18.9383	26.2499	31.13	33.5558	34.3282	34.9663	34.2066	36.0075	40.5683	45.4784	55.9871	71.2368	84.2217	93.5992	98.3639	96.9708	86.7074	67.5545	1
100	4000	1	8.6318	26.3304	43.9501	56.3929	67.9924	75.8574	83.0304	84.5343	82.6	76.091	72.075	69.3857	69.3168	67.4867	65.6072	63.0902	60.5359	56.4534	52.4467	1
100	6000	1	3.9744	6.9405	12.1715	17.8885	24.6455	30.3551	38.9449	46.8986	54.653	60.1757	67.1397	81.8963	82.0879	82.0479	82.0079	79.6876	74.1046	64.6953	52.5254	1
100	8000	1	6.834	10.3126	13.4428	15.0974	17.0765	17.8201	20.8508	26.2602	31.8437	39.2629	46.5956	81.79	82.1566	82.127	82.0974	82.0678	79.7896	70.0807	54.4922	1
100	10000	1	5.3106	10.6981	16.6303	19.9798	24.4608	27.9027	32.6623	39.5301	44.8567	49.721	55.4093	80.1967	80.4549	80.407	80.3591	80.3112	76.6222	67.5115	53.4759	1
100	20000	1	3.8685	6.6228	10.7817	13.798	18.1687	22.1766	26.9269	29.5743	32.2872	35.9545	41.1892	71.8916	72.2114	72.1944	72.1775	72.1605	70.8548	64.6135	53.7688	1
100	40000	1	2.948	6.5988	12.4387	19.5423	28.0395	36.6809	45.4185	51.698	55.7325	59.5728	62.9236	74.8268	74.9814	74.9679	74.9545	74.1746	68.9613	62.1186	54.187	1
100	60000	1	4.6738	10.7193	16.5495	21.601	26.6399	31.3372	36.7689	44.0021	46.8654	51.1869	55.3134	75.7097	75.9745	76.2394	76.2347	76.0498	72.1432	64.4514	54.6245	1
100	80000	1	6.1127	10.5314	14.3233	17.2621	19.8851	22.3636	24.8362	29.8132	33.8397	38.4431	43.3827	70.8398	71.1258	71.1036	71.0813	71.0591	69.3467	62.3025	53.0235	1
100	100000	1	5.9224	10.2096	13.9858	17.1235	20.0596	22.8642	25.1919	29.5056	33.067	37.127	41.4856	66.2878	66.5462	66.5279	66.5096	66.4914	65.0853	58.942	51.3416	1
100	150000	1	8.7152	16.3382	21.6396	25.2913	27.6215	29.6675	30.7398	34.7484	39.4862	45.9361	54.1178	122.2616	122.8542	122.8013	122.7485	122.6956	122.6428	117.5687	98.9511	1
100	200000	1	9.3004	17.1605	22.1435	25.0922	26.5219	27.484	27.3277	30.569	35.145	41.741	50.318	123.3126	123.9473	123.8961	123.8449	123.7936	123.7424	118.8245	99.6758	1
100	400000	1	13.1057	21.5396	25.4975	27.1984	27.2613	26.6796	24.956	27.0098	30.9418	37.4494	46.5105	124.4569	125.1347	125.0865	125.0383	124.9901	124.9419	120.315	101.0604	1
100	600000	1	12.845	21.0102	25.0328	26.3502	26.1233	25.2583	23.3938	25.4006	29.5761	36.2302	45.0034	124.669	125.3617	125.3125	125.2634	125.2142	125.165	120.4452	100.4805	1
100	800000	1	14.7221	22.3936	26.0063	27.0556	26.4115	24.9494	22.7396	24.4551	28.5656	35.4291	44.5276	124.7036	125.4008	125.3511	125.3014	125.2516	125.2019	120.4287	100.0616	1
100	1000000	1	10.0057	18.0207	22.3636	24.0533	24.1974	23.3206	21.4549	23.5118	28.2836	35.2535	44.0687	124.728	125.4293	125.3783	125.3273	125.2762	125.2252	120.3254	99.4349	1
x →		0	0.05	0.1	0.15	0.2	0.25	0.3	0.35	0.4	0.45	0.5	0.55	0.6	0.65	0.7	0.75	0.8	0.85	0.9	0.95	1
80	100	1	5.2655	8.4897	11.7175	14.7239	17.4582	19.9177	21.1945	23.6534	25.7861	28.0292	30.3087	42.0725	42.1951	42.1824	42.1697	42.1571	41.1811	37.5125	32.2052	1
80	200	1	5.16	8.3653	11.5562	14.53	17.2542	19.7203	21.1944	23.662	25.7988	28.0375	30.3081	42.0972	42.22	42.2073	42.1945	42.1818	41.2011	37.5348	32.2411	1
80	400	1	5.0648	8.2553	11.4192	14.3705	17.0939	19.5773	21.1944	23.68	25.8258	28.0552	30.3066	42.1488	42.2722	42.2593	42.2464	42.2336	41.2426	37.5808	32.3142	1
80	600	1	5.0124	8.194																		

DR	Re	Mass Quality (x)																				
		0	0.05	0.1	0.15	0.2	0.25	0.3	0.35	0.4	0.45	0.5	0.55	0.6	0.65	0.7	0.75	0.8	0.85	0.9	0.95	1
80	200000	1	7.6824	14.0197	18.0599	20.55	21.8982	22.8921	22.9507	25.2586	29.2311	34.6266	41.4456	100.9138	101.4309	101.3902	101.3496	101.3089	101.2682	97.3653	82.2479	1
80	400000	1	9.7161	15.9594	18.849	20.1815	20.5729	20.5839	19.8024	21.6207	25.3463	31.0243	38.4884	101.8813	102.4325	102.3944	102.3563	102.3181	102.28	98.6184	83.3909	1
80	600000	1	9.6174	15.674	18.7461	19.6868	19.7356	19.4957	18.417	20.4441	24.1863	29.8685	37.201	102.0539	102.6178	102.5788	102.5398	102.5008	102.4618	98.7164	82.9321	1
80	800000	1	11.2449	17.5892	20.6175	21.598	21.3223	20.4349	18.7448	20.4011	23.794	29.3629	36.5996	102.0753	102.6446	102.6052	102.5657	102.5262	102.4868	98.6986	82.5974	1
80	1000000	1	8.2305	14.7104	18.2353	19.6445	19.8893	19.2967	17.8291	19.4512	23.4534	29.178	36.2338	102.1055	102.6783	102.6378	102.5974	102.5569	102.5165	98.6338	82.1069	1
x →		0	0.05	0.1	0.15	0.2	0.25	0.3	0.35	0.4	0.45	0.5	0.55	0.6	0.65	0.7	0.75	0.8	0.85	0.9	0.95	1
60	100	1	4.0337	6.4206	8.8213	11.0355	13.0962	14.9735	16.2691	18.0848	19.7695	21.3217	23.1435	32.1299	32.2235	32.2159	32.2083	32.2008	31.6163	28.7868	24.6506	1
60	200	1	3.9825	6.36	8.7426	10.9425	12.9977	14.8759	16.2699	18.0867	19.7758	21.3292	23.1457	32.1442	32.238	32.2304	32.2228	32.2152	31.6308	28.8072	24.6829	1
60	400	1	3.9358	6.3066	8.6772	10.8711	12.9275	14.8118	16.2716	18.0909	19.7894	21.3455	23.1506	32.1746	32.2686	32.261	32.2534	32.2458	31.661	28.8492	24.749	1
60	600	1	3.9092	6.2765	8.6415	10.8344	12.8927	14.7812	16.2737	18.0956	19.8043	21.3637	23.156	32.2074	32.3017	32.2941	32.2865	32.2789	31.6928	28.893	24.817	1
60	1000	1	3.7261	6.2246	8.8485	10.7969	12.8606	14.7571	16.2789	18.1062	19.8383	21.4061	23.1689	32.2811	32.376	32.3683	32.3607	32.353	31.7607	28.9853	24.9577	1
60	2000	1	4.2844	7.3682	9.8085	10.8138	11.9791	12.9344	13.5399	17.5227	21.352	24.7396	28.6538	47.7424	47.9412	47.929	47.9168	47.9046	46.966	41.6308	34.9086	1
60	4000	1	4.157	7.0701	10.6183	11.6862	13.2478	13.2783	14.4771	19.1269	23.0502	25.9059	29.4625	45.5308	45.5188	45.5067	45.4947	44.5669	39.7586	32.6433	1	
60	6000	1	2.6217	5.1461	7.4168	9.2201	11.0293	13.0519	15.3336	19.7059	24.7521	28.2368	32.7502	49.1617	49.3749	49.588	49.5488	49.5096	47.2359	41.7287	33.5501	1
60	8000	1	3.0329	5.8324	8.0915	10.0764	11.8074	13.8194	15.9094	19.383	23.6234	27.8767	31.4381	51.2239	51.43	51.406	51.3819	51.3579	49.5065	43.507	34.5164	1
60	10000	1	2.4959	4.7178	7.5378	10.4187	13.4409	15.9345	18.8917	22.1636	25.6116	30.0714	32.8712	54.3838	54.6079	54.5843	54.5607	54.5371	52.7207	47.6056	38.9497	1
60	20000	1	2.8564	5.2693	8.6717	11.9038	15.8778	20.0397	24.1254	27.0978	31.1308	36.5017	39.3648	55.5246	55.6929	55.6557	55.6185	55.5813	52.7169	47.2023	38.5708	1
60	40000	1	2.4054	5.5522	9.1016	13.2941	17.6399	22.4477	26.8023	32.0152	36.4521	40.8506	43.5305	53.5849	53.7154	53.6986	53.6818	52.7058	47.99	41.8266	34.3399	1
60	60000	1	3.4761	7.0704	9.6655	11.6183	13.1093	14.5777	16.2897	20.3529	22.6005	26.5979	30.3353	51.68	51.9024	51.8803	51.8582	51.8361	50.1343	44.323	35.8087	1
60	80000	1	5.3379	8.5256	10.8193	12.5773	13.8997	15.289	16.0672	18.0966	21.1302	24.6107	27.9851	46.5879	46.7816	46.7648	46.7479	46.731	45.4309	40.7338	34.33	1
60	100000	1	4.9548	9.6989	13.233	15.8226	17.9091	19.6983	20.231	21.765	23.7593	25.8087	27.6012	43.6035	43.7702	43.7611	43.7519	43.7427	43.0376	38.9922	33.3274	1
60	150000	1	4.444	10.0456	14.3109	17.5241	19.9184	22.2912	23.3297	25.6859	28.8661	32.5202	36.6416	78.3147	78.6771	78.6453	78.6135	78.5817	78.5499	75.4955	64.4934	1
60	200000	1	6.0105	10.9434	14.179	16.204	17.4319	18.5541	18.4494	20.2246	23.2227	27.417	32.5595	78.4777	78.877	78.8459	78.8148	78.7837	78.7525	75.7655	64.7225	1
60	400000	1	7.134	12.1302	14.6241	15.7636	16.248	16.5165	15.761	17.1838	20.0263	24.2126	29.862	79.2565	79.686	79.6569	79.6278	79.5988	79.5697	76.78	65.6113	1
60	600000	1	7.1627	11.8671	14.5938	15.4538	15.5958	15.539	14.6062	16.2287	19.111	23.3297	28.7954	79.3793	79.8192	79.79	79.7608	79.7317	79.7025	76.9021	65.3292	1
60	800000	1	8.0412	13.0386	15.5431	16.5593	16.5168	15.9679	14.6518	16.0578	18.7897	23.1115	28.4537	79.4011	79.8441	79.8149	79.7856	79.7563	79.727	76.915	65.1108	1
60	1000000	1	6.5581	11.5486	14.298	15.4375	15.7365	15.3934	14.0246	15.2165	18.4195	22.8838	28.182	79.4508	79.8966	79.8662	79.8359	79.8056	79.7752	76.8623	64.7321	1
x →		0	0.05	0.1	0.15	0.2	0.25	0.3	0.35	0.4	0.45	0.5	0.55	0.6	0.65	0.7	0.75	0.8	0.85	0.9	0.95	1
40	100	1	2.8656	4.4413	5.987	7.4659	8.8424	10.1282	11.2873	12.5963	13.5946	14.7512	16.0153	22.1389	22.2027	22.1979	22.1932	22.1884	21.8215	19.8804	17.0808	1
40	200	1	2.8566	4.4298	5.9711	7.4472	8.8219	10.1062	11.2876	12.5962	13.5962	14.7539	16.0142	22.144	22.2079	22.2032	22.1985	22.1938	21.8317	19.8953	17.1037	1
40	400	1	2.8488	4.4201	5.9587	7.4365	8.8128	10.0977	11.2883	12.5959	13.5999	14.76	16.0119	22.1552	22.2192	22.2146	22.21	22.2054	21.8532	19.9263	17.1507	1
40	600	1	2.8442	4.414	5.9506	7.4301	8.8076	10.0919	11.2893	12.5955	13.6044	14.7671	16.0097	22.1674	22.2315	22.2271	22.2226	22.2182	21.8756	19.9586	17.1991	1
40	1000	1	2.8383	4.4057	5.9392	7.4239	8.8045	10.0877	11.2921	12.5946	13.6158	14.7845	16.0054	22.1955	22.26	22.2558	22.2516	22.2474	21.9238	20.027	17.2997	1
40	2000	1	3.4199	5.5717	7.0706	7.6416	8.1401	8.485	8.5565	11.2168	13.6217	15.6283	18.0357	30.6728	30.8044	30.7999	30.7953	30.7908	30.4404	26.8073	21.5567	1
40	4000	1	3.2325	5.025	7.1859	7.8878	8.7244	8.5965	9.3076	12.5476	15.1077	16.9638	18.7608	29.0976	29.2318	29.3661	29.3586	29.3511	28.9161	25.8333	20.9001	1
40	6000	1	2.2464	3.5886	4.8149	6.0128	7.08	8.4145	9.9657	12.7346	16.3609	19.0189	21.7794	33.3142	33.464	33.4623	33.4605	33.3587	32.042	28.1844	22.0311	1
40	8000	1	2.6156	4.4143	5.7607	6.9149	7.8356	8.9689	10.1947	12.3226	15.363	18.458	20.7926	35.2521	35.4399	35.6277	35.6068	35.5859	34.3738	30.0188	22.9859	1
40	10000	1	2.2245	3.6703	5.2627	7.0838	8.8184	9.9606	11.4899	13.2118	15.2858	17.0037	17.6774	33.7077	33.8747	33.8715	33.8683	33.8651	33.6173	31.2453	26.1789	1
40	20000	1	2.399	3.947	6.2344	8.4527	11.1285	13.8287	16.4716	17.9349	20.1148	22.2162	22.5258	33.2604	33.3998	33.5392	33.5155	33.4917	32.1128	29.8533	25.6818	1
40	40000	1	2.3102	4.9204	7.3329	9.9175	12.2322	14.7738	16.8989	19.9766	22.5004	25.3505	27.0057	36.0766	36.1944	36.1859	36.1774	35.6846	32.8643	28.5565	22.6349	1
40	60000	1	2.9465	5.7971	7.6887	9.0896	10.0132	10.8802	11.7152	14.4198	15.806	18.3927	20.9392	35.3951	35.5457	35.5305	35.5154	35.5002	34.3346	30.125	23.5919	1
40	80000	1	4.6332	7.202	8.8299	10.0244	10.6742	11.3654	11.6023	12.6924	14.697	17.0636	19.5363	32.2973	32.4302	32.418	32.4059	32.3937	31.4576	27.9386	22.6834	1
40	100000	1	4.4011	8.6803	11.6348	13.6566	15.075	16.1044	15.9464	16.5038	17.5767	18.6109	19.5398	30.1517	30.2622	30.256	30.2498	30.2436	29.7656	26.755	21.9481	1
40	150000	1	3.9985	8.8695	12.5626	15.3622	17.1167	18.9013	19.275	20.4796	22.2942	24.1752	26.3409	54.8143	55.0619	55.0416	55.0213	55.001	54.9807	53.0327	46.042	1
40	200000	1	5.0877	8.468	10.7584	12.2855	13.0597	13.9957	13.6656	14.5851	16.6255	19.6139	23.0494	54.674	54.949	54.9291	54.9091	54.8891	54.8692	52.9533	46.1018	1
40	400000	1	5.6501	9.243	11.1828	12.0702	12.4615	12.7236	11.8497	12.5353	14.3374	17.0061	20.6671	55.2356	55.5362	55.5179	55.4997	55.4814	55.4631	53.7098	46.737	1
40	600000	1	4.8336	8.3679	10.83	11.6619	11.9163	12.0607	11.1827	12.2937	14.091	16.5162	19.8305	55.3239	55.6326	55.6144	55.5962	55.578	55.5598	53.8128	46.5745	1
40																						

DR	Re	Mass Quality (x)																					
		0	0.05	0.1	0.15	0.2	0.25	0.3	0.35	0.4	0.45	0.5	0.55	0.6	0.65	0.7	0.75	0.8	0.85	0.9	0.95	1	
30	10000	1	1.8522	3.0912	4.1904	5.3017	6.5668	7.6867	8.8013	11.2842	13.6036	15.508	17.1483	26.8623	26.9885	26.9849	26.9813	26.7751	24.7584	21.3869	15.6462	1	
30	20000	1	1.8571	3.0995	4.3851	5.5224	6.7923	8.2043	9.7199	12.0233	14.6531	17.0456	18.526	27.2012	27.3139	27.308	26.9611	24.6321	21.1992	15.5195	1		
30	40000	1	2.2578	4.2945	5.821	7.152	7.8817	8.9013	9.5522	12.1512	13.742	15.9038	17.557	27.1018	27.2258	27.222	27.2182	26.9971	25.5372	21.9155	16.0852	1	
30	60000	1	2.9498	5.4824	6.9292	8.2405	9.0254	9.8081	9.7106	11.6886	13.0723	15.1908	17.0407	26.6127	26.737	26.8613	26.8407	26.8201	25.6255	22.1932	16.562	1	
30	80000	1	2.9692	4.923	6.1024	6.9988	7.573	8.2884	8.555	9.6595	11.2343	13.2428	15.2576	24.7941	24.918	25.0418	25.0337	25.8378	20.8329	15.9721	1		
30	100000	1	2.9909	4.805	6.0551	6.988	7.9154	8.9252	9.1288	9.9954	11.3816	12.926	14.6379	22.6908	22.7954	22.9	22.8828	22.8656	21.8693	19.2211	15.1428	1	
30	150000	1	5.6197	7.7886	9.3462	10.5103	11.2626	12.4505	12.5902	13.2388	14.943	17.0039	19.8657	42.1925	42.3866	42.3708	42.355	42.3392	42.3234	40.8069	36.2895	1	
30	200000	1	8.2345	13.4186	16.4976	18.0018	18.3727	18.408	16.5965	15.7682	15.9132	16.7639	18.3017	43.8068	44.0286	44.0136	43.9987	43.9838	43.9689	42.5371	37.0107	1	
30	400000	1	10.1434	17.2419	21.59	23.3816	23.9262	23.5547	20.9744	19.3581	18.2434	17.6751	18.2801	44.0012	44.2249	44.2135	44.2022	44.1908	44.1795	43.0903	37.7616	1	
30	600000	1	7.6943	19.2497	27.9379	32.9471	35.8543	37.4018	35.9656	34.659	31.7943	27.5346	25.7976	41.1945	41.3284	41.3206	41.3128	41.305	41.2972	40.548	37.2633	1	
30	800000	1	2.257	9.1478	16.3571	23.7914	30.5254	37.1521	41.9342	44.3741	45.0289	43.8491	41.286	41.2418	41.1976	40.813	40.255	39.4645	38.2454	36.4568	35.2593	1	
30	1000000	1	1.6812	6.5187	11.8879	17.5537	23.7326	29.6511	33.7061	35.7136	38.0415	38.7994	41.5043	41.5278	41.5193	41.5108	41.5023	41.4937	40.6758	38.2795	35.3011	1	
x →		0	0.05	0.1	0.15	0.2	0.25	0.3	0.35	0.4	0.45	0.5	0.55	0.6	0.65	0.7	0.75	0.8	0.85	0.9	0.95	1	
20	100	1	1.7689	2.5403	3.2483	3.9497	4.6464	5.3229	6.1894	6.7979	7.3956	8.0358	11.7777	11.8102	11.8081	11.8061	11.8041	11.802	11.6054	10.5875	9.1135	1	
20	200	1	1.788	2.5625	3.2765	3.9834	4.6825	5.3579	6.1895	6.7985	7.3945	8.0363	11.7796	11.8122	11.8102	11.8081	11.8061	11.8041	11.6102	10.5934	9.1232	1	
20	400	1	1.8052	2.5817	3.2999	4.0106	4.7113	5.3848	6.1898	6.7999	7.3923	8.0372	11.7838	11.8164	11.8145	11.8125	11.8105	11.8086	11.6202	10.6057	9.143	1	
20	600	1	1.8146	2.5917	3.3115	4.0239	4.7255	5.3974	6.1901	6.8014	7.39	8.0381	11.7885	11.8211	11.8192	11.8173	11.8154	11.8134	11.6306	10.6183	9.1631	1	
20	1000	1	1.8255	2.6029	3.3232	4.0368	4.74	5.409	6.1909	6.8051	7.3853	8.0403	11.7989	11.8316	11.8298	11.8281	11.8263	11.8245	11.6528	10.6445	9.204	1	
20	2000	1	2.6251	3.6046	4.0702	4.9053	5.351	5.558	5.9859	7.0279	8.2611	9.4098	15.8572	15.9244	15.9915	15.9905	15.9895	15.9308	15.3267	13.2339	9.3348	1	
20	4000	1	2.6134	3.5005	3.9334	4.7324	5.1536	5.3921	5.9934	7.396	8.4644	9.6847	15.4498	15.5247	15.5996	15.5993	15.5867	15.3157	14.7737	13.0183	9.9184	1	
20	6000	1	2.0397	2.8665	3.471	3.8425	4.1103	4.3675	4.7828	6.216	7.4411	8.925	16.3578	16.4353	16.5127	16.5115	16.5104	16.4433	15.9059	13.767	10.2371	1	
20	8000	1	1.8582	2.8141	3.4996	4.067	4.5462	5.0949	5.5074	6.9581	8.2958	9.8953	17.5714	17.6514	17.6498	17.6483	17.6468	17.528	16.7921	14.3305	10.5078	1	
20	10000	1	1.5873	2.3783	2.9958	3.6812	4.4096	5.1771	5.9092	7.722	9.1272	10.4545	17.6582	17.7332	17.7328	17.7324	17.7324	17.7319	17.6996	16.4474	14.2898	10.595	1
20	20000	1	1.5531	2.3963	3.1151	3.8602	4.6031	5.5021	6.318	8.2391	9.8605	11.4566	17.8532	17.9199	17.9186	17.9173	17.916	17.8179	16.3598	14.1625	10.4701	1	
20	40000	1	1.8153	3.2719	4.3839	5.4329	6.0154	6.8647	7.4173	8.8727	9.9038	11.6372	18.5464	18.6184	18.6162	18.614	18.6119	18.4458	17.4542	14.946	10.9652	1	
20	60000	1	2.4555	4.3613	5.381	6.4668	7.0646	7.7409	7.7139	8.7715	9.5275	10.7785	18.0614	18.1248	18.1183	18.1119	18.1054	18.0989	17.4796	15.1517	11.3242	1	
20	80000	1	2.3789	3.7223	4.4489	5.1342	5.5323	6.0793	6.3864	7.1725	8.101	9.387	17.4392	17.523	17.6069	17.5976	17.5883	17.579	16.863	14.644	11.108	1	
20	100000	1	2.2757	3.4603	4.2162	4.9045	5.6275	6.3887	6.6915	7.3461	8.1846	9.0995	15.9234	15.9945	16.0655	16.0568	16.0481	16.0394	15.369	13.4618	10.505	1	
20	150000	1	3.6247	4.9904	6.1525	7.3439	7.9543	9.1134	9.6309	10.245	11.3766	12.569	28.6586	28.7786	28.7707	28.7627	28.7548	28.7468	28.7388	27.8237	24.9216	1	
20	200000	1	4.4455	8.6226	11.6925	13.7296	14.7868	15.783	15.1774	14.6626	14.7954	14.758	29.6881	29.7995	29.7929	29.7863	29.7798	29.7732	29.7666	29.0094	25.5962	1	
20	400000	1	4.2098	9.7769	14.4891	17.8909	20.7429	23.2524	23.9171	23.4879	22.9536	21.5559	27.6299	27.6752	27.6711	27.6669	27.6628	27.6586	27.6545	27.178	25.6099	1	
20	600000	1	6.3134	15.8126	23.6817	28.9161	32.6089	35.5249	36.0186	35.3142	32.7085	28.1481	26.471	26.5464	26.4418	26.4273	26.4127	26.3981	26.3302	25.6346	24.9586	1	
20	800000	1	1.4001	6.5234	12.5577	19.2402	25.6376	32.2776	37.517	40.5691	41.4799	40.4462	36.6516	34.008	33.9402	33.8175	29.6547	27.6023	25.6949	23.9788	23.5182	1	
20	1000000	1	0	3.5044	8.8135	15.2974	22.9582	30.797	37.0529	40.5001	42.8639	43.2206	40.6144	36.059	35.6731	33.2097	30.6911	28.2732	25.9898	23.9295	23.1419	1	
x →		0	0.05	0.1	0.15	0.2	0.25	0.3	0.35	0.4	0.45	0.5	0.55	0.6	0.65	0.7	0.75	0.8	0.85	0.9	0.95	1	
13	100	1	1.5293	2.0166	2.4719	2.9343	3.391	3.8386	4.3154	4.7358	5.0978	5.5068	5.9298	8.046	8.0681	8.066	8.0639	8.0618	7.9006	7.157	6.129	1	
13	200	1	1.5368	2.025	2.4819	2.9468	3.4043	3.8522	4.3154	4.7358	5.0974	5.5066	5.9304	8.0469	8.069	8.0669	8.0648	8.0628	7.9037	7.161	6.1357	1	
13	400	1	1.5441	2.0326	2.4897	2.9565	3.4144	3.8624	4.3155	4.7359	5.0966	5.5062	5.9315	8.0488	8.0708	8.0688	8.0668	8.0648	7.9099	7.1692	6.1493	1	
13	600	1	1.5486	2.0369	2.4932	2.9614	3.4195	3.8678	4.3157	4.7361	5.0958	5.5058	5.9326	8.0507	8.0728	8.0708	8.0689	8.0669	7.9164	7.1777	6.1631	1	
13	1000	1	1.555	2.0423	2.4959	2.9664	3.4244	3.8739	4.3161	4.7363	5.0944	5.5052	5.9351	8.0617	8.0893	8.1169	8.1138	8.1107	7.9298	7.1952	6.1911	1	
13	2000	1	2.4278	3.1272	3.4257	3.7227	3.8558	3.9128	3.9938	4.5749	5.315	6.1372	7.1146	11.5208	11.578	11.6352	11.6306	11.6259	11.3561	9.8413	7.1187	1	
13	4000	1	2.2849	2.8566	3.0512	3.3575	3.4768	3.6321	3.8069	4.6376	5.3796	6.2078	7.169	10.9417	10.9907	10.9904	10.9901	10.9734	10.6304	9.3695	7.1658	1	
13	6000	1	1.752	2.3232	2.6695	2.9677	3.1291	3.2369	3.337	4.0626	4.9344	5.9354	7.0443	11.553	11.6115	11.6701	11.6697	11.6538	11.3261	9.8166	7.2957	1	
13	8000	1	1.5859	2.1601	2.5622	2.9727	3.2194	3.5493	3.7764	4.6567	5.704	6.4878	7.3703	11.2081	11.258	11.2563	11.2547	11.1586	10.808	9.3586	7.147	1	
13	10000	1	1.5555	1.9113	2.2233	2.6171	3.1709	3.7254	4.2657	5.0558	5.872	6.5638	7.044	10.3897	10.4332	10.4327	10.4322	10.4039	9.9176	8.8327	7.066	1	
13	20000	1	1.5229	1.9824	2.3327	2.869	3.4117	4.0446	4.6117	5.4078	6.1121	6.7448	7.0298	9.8332	9.8697	9.9061	9.9054	9.8815	9.4158	8.4953	6.9483	1	
13	40000	1	1.9003	2.5627	2.9622	3.5201	3.6395	3.9262	4.0258	4.6198	5.4862	6.7797	7.7553	12.2074	12.2652	12.323	12.3217	12.2711	11.7259	10.1527	7.6537	1	
13	60000	1	1.8874	2.5976	3.0642	3.6866	3.6619	3.9651	4.0127	4.661	5.5515	6.619	7.8744	12.2877	12.3451	12.4024	12.3928	12.3833	11.8308	10.272	7.8256	1	
13	80000	1	1.9892	2.6673	3.23	3.8918																	

DR	Re	Mass Quality (x)																				
		0	0.05	0.1	0.15	0.2	0.25	0.3	0.35	0.4	0.45	0.5	0.55	0.6	0.65	0.7	0.75	0.8	0.85	0.9	0.95	1
10	400	1	1.3967	1.7717	2.1455	2.4995	2.8295	3.1617	3.4869	3.8174	4.1461	4.4276	4.7381	6.3152	6.3316	6.3299	6.3282	6.3265	6.1945	5.6228	4.8048	1
10	600	1	1.3973	1.7723	2.1457	2.5002	2.8295	3.1613	3.4862	3.8179	4.1475	4.428	4.7407	6.3133	6.3297	6.328	6.3264	6.3247	6.1968	5.626	4.8135	1
10	1000	1	1.3981	1.7728	2.1455	2.5007	2.8284	3.1596	3.485	3.819	4.1507	4.429	4.7464	6.3095	6.3258	6.3242	6.3227	6.3211	6.2015	5.6324	4.8309	1
10	2000	1	1.4501	1.8107	2.1571	2.4528	2.7516	3.093	3.4237	3.8165	4.0728	4.4482	4.784	6.4066	6.4277	6.4273	6.4269	6.4037	6.357	5.7302	4.8475	1
10	4000	1	1.4057	1.5662	1.7762	2.1055	2.4813	3.0076	3.5236	4.2141	4.6051	4.7901	5.2381	6.0425	6.0564	6.0504	5.817	5.5448	5.3887	4.9807	4.6279	1
10	6000	1	1.153	1.31	1.5751	1.9846	2.3943	2.7637	3.1952	3.8073	4.2541	4.4149	4.9669	6.156	6.1765	6.1757	6.1431	5.9274	5.8021	5.2369	4.6837	1
10	8000	1	1.3453	1.5334	1.8039	2.2031	2.4973	2.8984	3.3201	3.599	4.1214	4.434	5.1238	7.0675	7.0928	7.0918	7.0908	7.0325	6.9228	6.1333	5.1186	1
10	10000	1	1.3643	1.5192	1.7244	1.9877	2.3698	2.7995	3.2898	3.7092	4.2459	4.6393	5.2193	7.0346	7.0582	7.0818	7.0816	7.0739	6.8758	6.1825	5.2269	1
10	20000	1	1.2587	1.4421	1.6247	2.1939	3.1112	3.9162	4.7405	5.4092	5.9455	6.3377	6.6204	7.1207	7.1335	6.9953	6.8038	6.5032	6.1324	5.4967	4.8275	1
10	40000	1	1.3628	1.661	2.5529	3.8623	4.6161	6.0553	7.3702	8.273	8.965	9.4068	9.4228	9.1601	8.9015	8.2956	7.4961	6.6638	5.9425	5.0863	4.5281	1
10	60000	1	1.3669	1.6158	2.639	4.0649	4.5974	6.1164	7.4361	8.4327	9.1065	9.4483	9.557	9.2713	8.9842	8.3495	7.5769	6.7272	5.9237	5.0577	4.4941	1
10	80000	1	1.456	1.6184	2.7022	4.1616	4.5919	6.0458	7.4768	8.4812	9.1688	9.4876	9.5592	9.2735	8.9767	8.3385	7.5626	6.7103	5.8934	5.0298	4.4572	1
10	100000	1	0.8836	1.0222	2.1016	3.405	3.6635	4.8386	5.9495	6.701	7.2902	7.6482	7.7628	7.428	7.4221	7.1808	6.8171	6.3485	5.8116	5.1535	4.5874	1
10	150000	1	5.9108	7.7749	9.1801	10.0966	8.7463	8.1702	7.1891	6.9657	6.9643	6.9628	6.9613	6.9599	6.9584	6.957	6.9555	6.908	6.5967	6.0321	5.5368	1
10	200000	1	9.7109	13.0769	14.9939	15.4412	13.5062	11.8563	9.2217	7.0221	7.0093	6.9965	6.9838	6.971	6.9582	6.9454	6.9326	6.9198	6.7064	6.1766	5.6007	1
10	400000	1	3.4633	3.1408	3.3462	3.6326	3.4336	3.8268	4.013	6.795	6.8111	6.8105	6.8098	6.8092	6.8085	6.8079	6.8072	6.8065	6.7056	6.1739	5.5912	1
10	600000	1	1.4496	1.796	2.5616	2.9713	3.3949	3.9563	4.325	6.8046	6.819	6.8184	6.8177	6.8171	6.8164	6.8158	6.8152	6.8145	6.7172	6.1698	5.5759	1
10	800000	1	1.3912	1.7735	2.0941	2.7439	3.2016	3.6713	4.2046	6.7964	6.8115	6.8109	6.8104	6.8098	6.8093	6.8087	6.8081	6.8076	6.7225	6.1683	5.5706	1
10	1000000	1	1.4215	1.8128	2.2088	2.596	3.1757	3.7456	3.9921	6.7999	6.8162	6.8156	6.815	6.8144	6.8138	6.8132	6.8126	6.812	6.7197	6.1636	5.5532	1
x →		0	0.05	0.1	0.15	0.2	0.25	0.3	0.35	0.4	0.45	0.5	0.55	0.6	0.65	0.7	0.75	0.8	0.85	0.9	0.95	1
7	100	1	1.2932	1.548	1.8003	2.0442	2.2769	2.501	2.6805	4.6118	4.623	4.6223	4.6217	4.621	4.6204	4.6198	4.6191	4.6185	4.5195	4.0926	3.4693	1
7	200	1	1.2894	1.5436	1.7948	2.0377	2.2703	2.4947	2.6806	4.6115	4.6227	4.622	4.6214	4.6208	4.6201	4.6195	4.6188	4.6182	4.5197	4.0937	3.4725	1
7	400	1	1.2859	1.5397	1.7897	2.0318	2.2643	2.4891	2.6809	4.6109	4.6221	4.6214	4.6208	4.6202	4.6195	4.6189	4.6183	4.6176	4.5202	4.0961	3.4789	1
7	600	1	1.284	1.5376	1.7872	2.029	2.2617	2.4869	2.6813	4.6103	4.6215	4.6209	4.6202	4.6196	4.619	4.6183	4.6177	4.6171	4.5207	4.0984	3.4854	1
7	1000	1	1.2818	1.5352	1.7845	2.0263	2.2594	2.4852	2.6821	4.6091	4.6203	4.6197	4.619	4.6184	4.6178	4.6172	4.6166	4.616	4.5218	4.1032	3.4984	1
7	2000	1	1.3069	1.5474	1.8095	1.8828	2.0715	2.3341	2.546	4.7369	4.7513	4.7656	4.7799	4.777	4.7741	4.7713	4.7684	4.7655	4.7626	4.3775	3.9264	1
7	4000	1	1.2982	1.539	1.7367	1.8057	1.9669	2.2342	2.3688	4.6695	4.6845	4.6996	4.6991	4.6987	4.6982	4.6978	4.6973	4.6969	4.6363	4.2778	3.7877	1
7	6000	1	1.2521	1.4927	1.7291	2.0251	2.3007	2.4482	2.5777	4.6649	4.6771	4.677	4.6767	4.6769	4.6768	4.6768	4.6767	4.6767	4.6684	4.2782	3.7708	1
7	8000	1	1.3239	1.5539	1.7874	2.0537	2.3118	2.5547	2.7644	4.7245	4.7373	4.7501	4.7498	4.7494	4.7491	4.7487	4.7484	4.7481	4.702	4.2788	3.7726	1
7	10000	1	1.2891	1.5292	1.7455	2.005	2.1665	2.4202	2.6588	4.6594	4.671	4.6826	4.6802	4.6778	4.6755	4.6731	4.6707	4.6683	4.6659	4.3009	3.8011	1
7	20000	1	1.1043	1.2673	1.5505	2.0782	2.6524	3.3024	3.9514	5.4093	5.4219	5.4209	5.4198	5.4187	5.4177	5.3152	5.0226	4.7853	4.528	4.0796	3.6589	1
7	40000	1	1.1025	1.2984	1.7846	2.5491	3.4345	4.4462	5.3503	6.7121	6.7298	6.7293	6.7287	6.6986	6.4312	6.0155	5.4326	4.9449	4.4027	3.846	3.5121	1
7	60000	1	1.0993	1.3429	1.8289	2.606	3.4806	4.5498	5.5173	6.8431	6.8603	6.8589	6.8574	6.7725	6.4584	6.036	5.5264	4.9799	4.4048	3.83	3.4925	1
7	80000	1	1.0949	1.3289	1.8322	2.6167	3.4787	4.4865	5.4903	6.846	6.8636	6.8621	6.8605	6.7711	6.4964	6.0699	5.5558	5.0017	4.4162	3.8308	3.4818	1
7	100000	1	1.0614	1.2906	1.811	2.5732	3.5152	4.5161	5.5221	6.8768	6.8943	6.892	6.8897	6.7554	6.514	6.0861	5.5637	4.9987	4.4019	3.806	3.4399	1
7	150000	1	1.4868	1.6482	1.9621	2.4936	2.29	2.5078	2.7636	4.669	4.6801	4.6794	4.6787	4.6781	4.6774	4.6768	4.6761	4.6754	4.5744	4.1426	3.5282	1
7	200000	1	1.6097	1.7597	2.242	2.6569	2.5758	2.9226	3.0277	4.6839	4.6936	4.6928	4.6921	4.6913	4.6905	4.6898	4.689	4.6883	4.573	4.1335	3.5023	1
7	400000	1	1.4378	1.6839	1.9891	2.304	2.6183	2.9775	3.2167	4.6937	4.7023	4.7015	4.7007	4.6999	4.6991	4.6982	4.6974	4.6966	4.5724	4.1297	3.4911	1
7	600000	1	1.2623	1.5178	2.0676	2.3439	2.643	3.0249	3.3605	4.7023	4.7101	4.7092	4.7084	4.7075	4.7066	4.7058	4.7049	4.704	4.5715	4.1235	3.4732	1
7	800000	1	1.24	1.4766	1.7231	2.26	2.4634	2.7911	3.2731	4.6992	4.7075	4.7066	4.7058	4.7049	4.7041	4.7032	4.7024	4.7015	4.5712	4.1213	3.4669	1
7	1000000	1	1.2691	1.521	1.7671	2.0072	2.4388	2.8454	3.097	4.6939	4.7032	4.7023	4.7015	4.7007	4.6998	4.699	4.6982	4.6973	4.5701	4.1143	3.4464	1
x →		0	0.05	0.1	0.15	0.2	0.25	0.3	0.35	0.4	0.45	0.5	0.55	0.6	0.65	0.7	0.75	0.8	0.85	0.9	0.95	1
5.5	100	1	1.2388	1.4312	1.6265	1.8151	1.9922	2.161	2.2656	3.7576	3.7662	3.7656	3.765	3.7644	3.7639	3.7633	3.7627	3.7621	3.6713	3.317	2.8021	1
5.5	200	1	1.2328	1.4244	1.6178	1.8049	1.9817	2.151	2.2657	3.7573	3.766	3.7654	3.7648	3.7642	3.7636	3.763	3.7624	3.7618	3.6715	3.3179	2.8047	1
5.5	400	1	1.2275	1.4184	1.6101	1.7959	1.9725	2.1423	2.2659	3.7568	3.7655	3.7649	3.7643	3.7637	3.7631	3.7626	3.762	3.7614	3.6719	3.3198	2.8099	1
5.5	600	1	1.2246	1.4152	1.6062	1.7916	1.9684	2.1387	2.2662	3.7563	3.765	3.7644	3.7638	3.7632	3.7627	3.7621	3.7615	3.7609	3.6723	3.3218	2.8152	1
5.5	1000	1	1.2212	1.4116	1.6019	1.7871	1.9644	2.1357	2.2668	3.7553	3.7639	3.7634	3.7628	3.7622	3.7617	3.7611	3.7605	3.76	3.6731	3.3256	2.8258	1
5.5	2000	1	1.2352	1.4128	1.6307	1.6045	1.7302	1.9477	2.0986	3.9119	3.9224	3.933	3.9314	3.9297	3.9281	3.9265	3.9249	3.9232	3.9216	3.673	3.425	1
5.5	4000	1	1.2239	1.4022	1.5567	1.528	1.6319	1.8529	1.9138	3.8329	3.8454	3.8579	3.8577	3.8574	3.8571	3.8568	3.8565	3.8562	3.8171	3.5339	3.1926	1
5.5	6000	1	1.1838	1.3621	1.5321	1.7736	1.9986	2.0889	2.1567	3.8206	3.8302	3.8399	3.8399	3.8398	3.8398	3.8398	3.8398	3.8397	3.8354	3.538	3.1806	1
5.5	8000	1	1.2712																			

DR	Re	Mass Quality (x)																				
		0	0.05	0.1	0.15	0.2	0.25	0.3	0.35	0.4	0.45	0.5	0.55	0.6	0.65	0.7	0.75	0.8	0.85	0.9	0.95	1
5.5	400000	1	1.3589	1.5355	1.7623	2.0138	2.2463	2.5246	2.7461	3.6913	3.6975	3.7036	3.7024	3.7011	3.6999	3.6986	3.6974	3.6961	3.5277	3.1417	2.5048	1
5.5	600000	1	1.192	1.3824	1.8376	2.0518	2.2723	2.568	2.8764	3.6987	3.7041	3.7095	3.7095	3.7094	3.7094	3.7094	3.7085	3.5254	3.135	2.4865	1	
5.5	800000	1	1.1592	1.3249	1.5039	1.9543	2.0992	2.3567	2.8034	3.6961	3.702	3.7078	3.7065	3.7052	3.7039	3.7026	3.7013	3.7	3.5245	3.1326	2.4801	1
5.5	1000000	1	1.1948	1.3788	1.5568	1.7303	2.0764	2.4032	2.6448	3.6912	3.698	3.7048	3.7035	3.7022	3.7009	3.6996	3.6983	3.697	3.5219	3.1249	2.4591	1
x →		0	0.05	0.1	0.15	0.2	0.25	0.3	0.35	0.4	0.45	0.5	0.55	0.6	0.65	0.7	0.75	0.8	0.85	0.9	0.95	1
4	100	1	1.1829	1.3128	1.4502	1.5826	1.7031	1.8158	1.8476	2.8973	2.9042	2.911	2.9103	2.9096	2.9088	2.9081	2.9074	2.9066	2.8082	2.5291	2.1279	1
4	200	1	1.1752	1.3039	1.4388	1.5691	1.6892	1.8025	1.8477	2.897	2.9038	2.9107	2.91	2.9092	2.9085	2.9078	2.907	2.9063	2.8083	2.5298	2.1299	1
4	400	1	1.1683	1.2961	1.4288	1.5574	1.6773	1.7914	1.8479	2.8963	2.9032	2.91	2.9093	2.9086	2.9078	2.9071	2.9064	2.9057	2.8086	2.5313	2.1339	1
4	600	1	1.1646	1.292	1.4237	1.5518	1.6719	1.7865	1.848	2.8956	2.9025	2.9093	2.9086	2.9079	2.9072	2.9065	2.9057	2.905	2.8089	2.5327	2.138	1
4	1000	1	1.1602	1.2873	1.4182	1.5458	1.6666	1.7824	1.8485	2.8942	2.9011	2.9079	2.9072	2.9065	2.9058	2.9051	2.9044	2.9037	2.8095	2.5357	2.1461	1
4	2000	1	1.1641	1.2788	1.4498	1.3307	1.3943	1.5641	1.6537	3.1012	3.1088	3.1079	3.107	3.1061	3.1052	3.1043	3.1033	3.1024	3.1015	2.9449	2.8914	1
4	4000	1	1.1507	1.2665	1.3763	1.2557	1.3029	1.4748	1.464	2.9799	2.9898	2.9997	2.9996	2.9994	2.9993	2.9991	2.999	2.9988	2.979	2.7722	2.5772	1
4	6000	1	1.1161	1.2319	1.3361	1.5214	1.6938	1.727	1.734	2.9599	2.967	2.9741	2.9729	2.9717	2.9705	2.9693	2.9681	2.9668	2.9656	2.7796	2.5702	1
4	8000	1	1.2167	1.3129	1.4165	1.5665	1.7111	1.8384	1.9524	2.9784	2.9851	2.9918	2.9985	2.997	2.9954	2.9939	2.9923	2.9907	2.9892	2.7798	2.5709	1
4	10000	1	1.1632	1.2738	1.3646	1.5032	1.5252	1.6625	1.7827	2.9516	2.9577	2.9566	2.9556	2.9545	2.9535	2.9524	2.9514	2.9503	2.9493	2.7682	2.5522	1
4	20000	1	1.0509	1.134	1.2422	1.5514	1.8469	2.1875	2.5302	3.3564	3.3651	3.3737	3.3729	3.3721	3.3713	3.31	3.043	2.9307	2.9068	2.6509	2.4767	1
4	40000	1	1.062	1.1482	1.3926	1.8058	2.2902	2.8288	3.2726	4.0554	4.0636	4.0615	4.0595	4.0574	3.8988	3.6815	3.3248	3.1422	2.8473	2.5517	2.4322	1
4	60000	1	1.0599	1.189	1.4338	1.8559	2.3072	2.8953	3.4517	4.1158	4.1244	4.1238	4.1231	4.0869	3.8488	3.6572	3.4195	3.1578	2.8643	2.5532	2.4299	1
4	80000	1	1.0416	1.1701	1.4286	1.8567	2.3111	2.8439	3.3747	4.1156	4.1252	4.1246	4.1239	4.0869	3.9176	3.7226	3.4819	3.212	2.9036	2.5766	2.4414	1
4	100000	1	1.0188	1.1439	1.4108	1.8135	2.316	2.8233	3.3768	4.1374	4.1472	4.146	4.1447	4.0715	3.9492	3.7545	3.5097	3.2324	2.9136	2.5758	2.4303	1
4	150000	1	1.3134	1.3555	1.5252	1.8984	1.6065	1.6779	1.8536	2.6874	2.6929	2.6927	2.6925	2.6923	2.6921	2.6919	2.6917	2.6665	2.5048	2.1887	1.5978	1
4	200000	1	1.4134	1.432	1.7523	2.0113	1.8437	2.0417	2.1174	2.6992	2.703	2.7027	2.7025	2.7022	2.7019	2.7017	2.7014	2.6647	2.4996	2.1785	1.5718	1
4	400000	1	1.2809	1.3889	1.5391	1.7266	1.8795	2.0791	2.2746	2.7062	2.709	2.7087	2.7084	2.7081	2.7077	2.7074	2.7071	2.664	2.4975	2.1741	1.5606	1
4	600000	1	1.1226	1.2482	1.6107	1.7623	1.9059	2.1183	2.393	2.7116	2.7137	2.7133	2.7129	2.7126	2.7122	2.7118	2.7115	2.6627	2.4939	2.167	1.5426	1
4	800000	1	1.0808	1.1768	1.2889	1.6537	1.7403	1.9282	2.333	2.8947	2.9044	2.9022	2.817	2.7296	2.7285	2.7274	2.7262	2.6623	2.4927	2.1646	1.5363	1
4	1000000	1	1.1219	1.2385	1.3491	1.4567	1.7187	1.9672	2.1905	2.3202	2.6561	3.0259	2.9528	2.759	2.7275	2.727	2.7264	2.6609	2.4887	2.1566	1.5157	1
x →		0	0.05	0.1	0.15	0.2	0.25	0.3	0.35	0.4	0.45	0.5	0.55	0.6	0.65	0.7	0.75	0.8	0.85	0.9	0.95	1
2.5	100	1	1.1263	1.1936	1.2725	1.3475	1.4104	1.4659	1.4266	1.4845	1.5416	1.5981	1.6539	1.7092	2.0299	2.0355	2.0351	2.0217	1.9221	1.7213	1.4403	1
2.5	200	1	1.1171	1.1831	1.2589	1.3314	1.3937	1.4499	1.4266	1.4845	1.5417	1.5982	1.654	1.7093	2.0297	2.0352	2.0349	2.0215	1.9222	1.7218	1.4417	1
2.5	400	1	1.1088	1.1738	1.2469	1.3175	1.3796	1.4367	1.4267	1.4846	1.5418	1.5984	1.6543	1.7096	2.0292	2.0347	2.0344	2.0212	1.9223	1.7227	1.4443	1
2.5	600	1	1.1044	1.1689	1.2409	1.3106	1.373	1.4308	1.4268	1.4847	1.542	1.5986	1.6545	1.7099	2.0287	2.0342	2.0339	2.0209	1.9225	1.7237	1.447	1
2.5	1000	1	1.0992	1.1633	1.2342	1.3035	1.3665	1.4256	1.427	1.4851	1.5424	1.5991	1.6552	1.7106	2.0278	2.0332	2.0329	2.0203	1.9229	1.7256	1.4524	1
2.5	2000	1	1.0943	1.1465	1.2681	1.0622	1.1835	1.2109	1.4027	1.4107	1.6325	1.7711	1.7917	2.2961	2.2999	2.2807	2.2616	2.2424	2.2232	2.2041	1	
2.5	4000	1	1.0794	1.1327	1.1961	0.9893	0.9797	1.0996	1.0186	1.154	1.2441	1.3907	1.9457	1.9807	2.1474	2.1503	2.1501	2.1437	2.1138	1.9848	1.9349	1
2.5	6000	1	1.0496	1.1031	1.1419	1.2695	1.3872	1.3626	1.3092	1.4429	1.441	1.4104	1.9281	2.0643	2.1091	2.1097	2.1103	2.1103	2.1098	1.9953	1.9328	1
2.5	8000	1	1.1608	1.1913	1.2306	1.321	1.4067	1.4744	1.5373	1.4551	1.5009	1.5428	1.681	1.7352	2.1072	2.1111	2.1096	2.1082	2.1067	1.9953	1.9331	1
2.5	10000	1	1.1004	1.1467	1.1748	1.2517	1.2057	1.2831	1.3425	1.2797	1.3122	1.5406	1.7368	1.7624	2.1151	2.1188	2.1169	2.1151	2.1132	1.9704	1.8958	1
2.5	20000	1	1.0244	1.0665	1.0862	1.281	1.4332	1.6148	1.7995	1.9153	1.9362	2.0362	2.2552	2.3397	2.3117	2.2728	2.0287	1.9801	1.9783	1.9077	1.8554	1
2.5	40000	1	1.0409	1.0728	1.1929	1.425	1.6998	1.9947	2.2017	2.2054	2.4734	2.6157	2.6792	2.7341	2.5925	2.4769	2.2399	2.2073	2.0388	1.8741	1.8583	1
2.5	60000	1	1.0394	1.1113	1.2297	1.4649	1.6928	2.0274	2.36	2.4108	2.5092	2.6608	2.6985	2.681	2.4956	2.4246	2.3281	2.2133	2.0641	1.8866	1.866	1
2.5	80000	1	1.0161	1.091	1.2213	1.4615	1.6985	1.981	2.2627	2.4624	2.5984	2.6755	2.7005	2.6817	2.5746	2.5006	2.4021	2.2793	2.114	1.9191	1.8872	1
2.5	100000	1	0.998	1.0702	1.2051	1.4187	1.6899	1.9395	2.2513	2.4659	2.6113	2.6987	2.7183	2.666	2.6091	2.5366	2.4363	2.3084	2.134	1.929	1.8909	1
2.5	150000	1	1.2296	1.2125	1.3109	1.6039	1.2694	1.2702	1.3992	1.4842	1.5606	1.6104	1.6772	1.7593	1.7465	1.7462	1.718	1.6272	1.4819	1.2327	0.6859	1
2.5	200000	1	1.3192	1.2747	1.5149	1.6968	1.7446	1.7449	1.7452	1.7456	1.7459	1.7453	1.7448	1.7443	1.7035	1.7022	1.7009	1.6233	1.4755	1.2225	0.6615	1
2.5	400000	1	1.2046	1.2452	1.3203	1.4432	1.5189	1.6412	1.8032	1.8027	1.747	1.7461	1.7451	1.745	1.745	1.7153	1.6216	1.4727	1.2182	0.651	1	
2.5</																						

Appendix B

ERROR ASSESSMENT TABLE

D	DR	Re	X	Mass Flux	Pressure	$\bar{\phi}_{LO,asp}^2$	$\bar{\phi}_{LO,let}^2$	Relative Error
m	--	--	--	Kg.m ⁻² .sec ⁻¹	KPa	--	--	%
0.04666	239.69	8954.2	0.46677	81.8784	165.474	57.101	63.984	12.0536
0.04666	237.4	10920.7	0.37686	99.5813	165.474	42.477	42.535	0.1367
0.04666	237.4	12469.1	0.32959	113.7011	165.474	35.976	40.673	13.0551
0.04666	235.11	13792.3	0.29701	125.4588	165.474	31.381	38.423	22.4393
0.04666	230	14895.2	0.27091	135.4913	165.474	27.468	35.713	30.0156
0.04666	232.93	16019.7	0.25443	145.3115	165.474	24.849	34.455	38.6564
0.04666	232.93	16982.4	0.23949	154.0435	165.474	21.917	32.48	48.1957
0.04666	232.05	17908.3	0.22751	162.2712	165.474	20.011	30.462	52.2292
0.04666	230.72	18752.7	0.21561	169.6231	165.474	20.072	28.13	40.1439
0.04666	230.72	19556.7	0.20645	176.8953	165.474	19.684	26.209	33.1492
0.04666	230.72	20319.6	0.19841	183.796	165.474	19.375	24.778	27.8865
0.04666	230.72	21050.2	0.19138	190.4047	165.474	18.214	24.227	33.0158
0.04666	228.56	21728.8	0.18221	196.0579	165.474	17.63	23.012	30.5261
0.04666	228.56	22349.5	0.17452	201.6581	165.474	17.881	22.225	24.2958
0.04666	230.82	22811	0.16649	206.9132	165.474	17.086	21.608	26.469
0.04666	239.13	22458.5	0.16289	213.6016	165.474	14.971	22.175	48.1141
0.04666	239.33	22682.1	0.14922	216.8131	165.474	17.006	20.417	20.0544
0.04666	226.55	11233.3	0.57023	101.4654	165.474	79.468	89.178	12.2187
0.04666	224.54	13224.9	0.48042	119.3275	165.474	63.96	62.746	-1.8978
0.04666	223.62	14758	0.42654	132.7838	165.474	61.604	57.185	-7.1733
0.04666	220.33	16122.5	0.39105	144.7007	165.474	55.905	54.442	-2.6168
0.04666	220.33	17207.8	0.36105	154.4413	165.474	52.538	50.9	-3.1164
0.04666	220.24	18274	0.3382	163.5448	165.474	47.509	48.145	1.3388
0.04666	219.03	19230.6	0.31886	171.7991	165.474	43.568	45.24	3.8372
0.04666	218.2	20140.5	0.3033	179.7349	165.474	41.265	42.555	3.1261
0.04666	218.39	20839.2	0.28906	187.0337	165.474	40.392	40.317	-0.1852
0.04666	218.3	21399.8	0.28021	191.5191	165.474	38.738	39.046	0.7944
0.04666	217.25	22072.4	0.269	198.3136	165.474	36.456	37.202	2.0467
0.04666	218.39	22805.7	0.25881	204.6835	165.474	34.495	35.84	3.8989
0.04666	217.98	23447.4	0.24845	210.4429	165.474	32.86	34.116	3.8215
0.04666	217.61	24115.1	0.24003	216.2819	165.474	31.329	32.915	5.0629
0.04666	217.16	24816.3	0.23373	222.3333	165.474	29.835	32.098	7.5826
0.04666	217.18	25405.7	0.22636	227.6946	165.474	29.282	31.008	5.894
0.04666	216.77	26061.3	0.22113	233.3213	165.474	28.696	30.3	5.5891
0.04666	228.96	12239.1	0.60903	111.6039	165.474	92.889	116.233	25.1305
0.04666	224.73	14518.6	0.52902	131.6954	165.474	78.168	83.987	7.4441
0.04666	221.44	16208.6	0.48026	146.6114	165.474	69.109	73.414	6.2293
0.04666	217.06	17796	0.45107	160.572	165.474	63.814	70.948	11.1798
0.04666	216.51	19055.5	0.42383	171.268	165.474	60.275	68.962	14.4124
0.04666	212.67	20082.1	0.39935	180.2389	165.474	55.099	65.477	18.8356
0.04666	210.68	20895.6	0.37411	187.0069	165.474	56.361	59.877	6.2386
0.04666	208.76	21446.1	0.34572	191.3862	165.474	54.091	52.996	-2.0245
0.04666	208.76	21782.2	0.31622	194.3854	165.474	52.639	46.182	-12.2673
0.04666	206.77	22568.9	0.30095	200.543	165.474	49.837	42.991	-13.7367
0.04666	211.07	14583	0.66941	131.9074	165.474	138.539	172.628	24.6063
0.04666	207.84	16586.6	0.58311	148.6548	165.474	112.291	109.496	-2.4894
0.04666	204.94	18407	0.53427	163.3851	165.474	101.041	97.592	-3.4139
0.04666	196.69	20067.1	0.50322	177.1598	165.474	87.62	90.806	3.6365
0.04666	194.49	21371.7	0.47504	187.7231	165.474	79.165	84.655	6.9348
0.04666	218.8	20812.4	0.42457	188.7849	165.474	78.637	73.645	-6.3479
0.04666	212.47	24043.1	0.375	216.7857	165.474	65.328	64.824	-0.7719
0.04666	207.86	25627.3	0.35947	229.8439	165.474	58.93	62.076	5.3389
0.04666	204	26999.4	0.34358	240.8584	165.474	57.28	58.931	2.8816
0.04666	201.05	28339.6	0.33168	251.8198	165.474	52.962	56.937	7.5066
0.04666	190.99	17319.3	0.71515	152.901	165.474	146.739	189.875	29.3963
0.04666	187.84	19206.8	0.63575	169.9934	165.474	127.468	149.09	16.9622
0.04666	184.67	20971.5	0.5869	184.0071	165.474	115.695	116.673	0.8455
0.04666	181.71	22425.6	0.5507	195.7648	165.474	103.748	106.448	2.6021
0.04666	179.75	23659.2	0.52184	205.93	165.474	94.928	98.695	3.9678
0.04666	209.13	22930.3	0.47484	206.7529	165.474	101.941	89.77	-11.9394
0.04666	205.41	24642.8	0.44577	221.722	165.474	94.161	83.909	-10.8875
0.04666	196.47	26479.8	0.42748	236.9831	165.474	86.854	80.763	-7.0132
0.04666	192.18	28112.9	0.41107	250.2536	165.474	78.903	78.221	-0.8638
0.04666	184.78	29618.6	0.39963	263.6567	165.474	77.15	76.231	-1.1908
0.04666	184.28	30920.3	0.38388	273.3708	165.474	74.801	73.498	-1.741
0.04666	180.93	32351.5	0.3733	283.9606	165.474	69.935	71.875	2.7737
0.04666	235.22	25730	0.13563	234.6221	165.474	12.646	18.887	49.3523
0.04666	235.22	27706.3	0.12984	252.6434	165.474	11.678	18.48	58.2556
0.04666	232.62	26896	0.17129	244.6544	165.474	20.582	23.928	16.2574
0.04666	230.74	28869.9	0.16323	261.1364	165.474	20.143	23.018	14.2724
0.04666	202.3	16429.7	0.70748	149.3446	165.474	140.049	193.275	38.0047
0.04666	200.81	18014.4	0.6251	165.5877	165.474	128.106	142.687	11.3826
0.04666	198.11	19592.6	0.57483	179.2829	165.474	131.515	114.854	-12.6684
0.04666	196.75	21081.6	0.53662	190.2178	165.474	118.565	104.604	-11.7752
0.04666	194.01	22522.6	0.50917	200.9934	165.474	107.567	96.677	-10.1244
0.04666	191.09	23797.8	0.48651	210.6278	165.474	100.565	91.288	-9.2246
0.04666	189.43	25438.2	0.45608	225.1458	165.474	91.511	85.27	-6.8191
0.04666	184.36	27165.7	0.43277	238.4428	165.474	84.536	80.969	-4.2189
0.04666	184.06	28345	0.40911	248.7938	165.474	79.618	76.698	-3.6672
0.04666	177.71	30108.7	0.39937	262.834	165.474	73.315	75.696	3.2482
0.04666	178.91	31096	0.38057	271.3537	165.474	70.79	72.002	1.7116
0.04666	177.62	32304	0.36822	281.1739	165.474	66.509	69.892	5.086
0.04666	170.64	34678.4	0.35437	302.7251	165.474	60.459	67.897	12.3027
0.04666	172.09	36393.1	0.33258	317.6942	165.474	55.572	63.55	14.3561
0.04666	170.64	38059.3	0.31714	332.2387	165.474	54.805	60.361	10.137
0.04666	187.15	21538.4	0.77784	196.401	165.474	198.5	216.799	9.2187
0.04666	170.16	25048.7	0.72823	228.3296	165.474	159.052	188.885	18.7565
0.04666	168.96	26443.6	0.6831	240.5385	165.474	151.191	173.644	14.8509
0.04666	150.41	29915	0.67507	271.3523	165.474	136.907	161.095	17.6681

D	DR	Re	X	Mass Flux	Pressure	$\phi^2_{LO,asp}$	$\phi^2_{LO,let}$	Relative Error
m	--	--	--	Kg.m-2.sec-1	KPa	--	--	%
0.04666	137.3	32457.7	0.66126	291.311	165.474	103.514	137.933	33.2502
0.04666	137.11	33306.6	0.63416	295.6373	165.474	121.821	128.427	5.4232
0.04666	136.97	34882.1	0.60234	307.9524	165.474	113.362	115.185	1.6086
0.04666	136.97	36149.8	0.57573	318.9138	165.474	110.245	108.944	-1.1794
0.04666	136.96	37481.1	0.55508	330.5388	165.474	107.014	105.218	-1.6779
0.04666	136.96	38504.3	0.53478	339.5628	165.474	105.394	102.152	-3.0761
0.04666	136.96	39428.3	0.51629	347.7109	165.474	102.696	99.591	-3.0237
0.04666	136.96	40286	0.49947	355.2751	165.474	98.9	96.541	-2.3853
0.04666	136.94	42239.7	0.47458	372.2349	165.474	95.381	88.881	-6.8147
0.04666	136.96	43948.7	0.45326	387.5756	165.474	88.866	82.668	-6.975
0.04666	103.58	45474.4	0.43347	400.74	165.474	86.236	54.561	-36.7307
0.04666	228.96	17029.9	0.71902	155.2896	165.474	182.429	218.729	19.898
0.04666	217.02	19580.7	0.65234	178.4864	165.474	163.351	180.165	10.2929
0.04666	213.07	21341.9	0.60638	193.5882	165.474	150.486	137.544	-8.6001
0.04666	207.09	22921.3	0.57578	207.8407	165.474	140.681	124.146	-11.753
0.04666	202.09	24314.5	0.55206	220.4742	165.474	133.922	117.53	-12.2399
0.04666	198.47	25610.8	0.53189	231.3295	165.474	129.533	111.729	-13.7446
0.04666	191.7	27952.9	0.51373	252.2171	165.474	116.89	107.402	-8.1163
0.04666	188.41	29238.4	0.48605	263.6298	165.474	113.327	100.032	-11.7317
0.04666	185.02	30849.1	0.46817	276.8737	165.474	108.66	96.691	-11.0156
0.04666	178.82	32516.4	0.45768	291.6305	165.474	103.527	94.765	-8.4631
0.04666	175.81	33868.8	0.44561	303.7597	165.474	100.415	92.744	-7.6393
0.04666	172.71	35326	0.43542	315.252	165.474	97.806	91.502	-6.4454
0.04666	169.76	37585.2	0.41496	334.5738	165.474	94.864	88.639	-6.5625
0.04666	166.87	39702.6	0.3984	352.4093	165.474	89.663	86.371	-3.6706
0.04666	164.02	41703.3	0.38469	369.1036	165.474	85.492	80.686	-5.6217
0.01	42.19	3350.9	0.5	88.4643	567	13.248	17.516	32.2165
0.01	42.19	3350.9	0.5	88.4643	567	14.065	17.516	24.5295
0.01	42.19	3350.9	0.79	88.4643	567	24.451	31.622	29.3286
0.01	42.19	3350.9	0.79	88.4643	567	24.042	31.622	31.5281
0.01	42.19	4691.3	0.31	123.85	567	8.351	9.257	10.8591
0.01	42.19	4691.3	0.31	123.85	567	8.351	9.257	10.8591
0.01	42.19	4691.3	0.5	123.85	567	16.247	18.664	14.8725
0.01	42.19	4691.3	0.51	123.85	567	15.567	19.128	22.88
0.01	42.19	4691.3	0.8	123.85	567	25.596	32.504	26.988
0.01	42.19	4691.3	0.81	123.85	567	26.141	32.342	23.7217
0.01	42.19	6701.8	0.3	176.9285	567	9.846	9.125	-7.3258
0.01	42.19	6701.8	0.3	176.9285	567	9.846	9.125	-7.3258
0.01	42.19	6701.8	0.5	176.9285	567	17.894	19.839	10.8727
0.01	42.19	6701.8	0.5	176.9285	567	17.894	19.839	10.8727
0.01	42.19	6701.8	0.79	176.9285	567	32.821	35.908	9.405
0.01	42.19	6701.8	0.81	176.9285	567	32.821	35.62	8.5265
0.01	42.19	9382.6	0.3	247.6999	567	10.916	10.271	-5.9083
0.01	42.19	9382.6	0.3	247.6999	567	10.916	10.271	-5.9083
0.01	42.19	13403.7	0.1	353.8571	567	3.722	3.889	4.4864
0.01	42.19	13403.7	0.11	353.8571	567	3.903	4.281	9.6881
0.01	24.23	3670.7	0.1	88.4643	937	3.696	3.878	4.9148
0.01	24.23	3670.7	0.1	88.4643	937	3.688	3.878	5.1404
0.01	24.23	3670.7	0.3	88.4643	937	6.226	6.023	-3.2737
0.01	24.23	3670.7	0.3	88.4643	937	6.655	6.023	-9.4992
0.01	24.23	3670.7	0.5	88.4643	937	8.963	10.982	22.5304
0.01	24.23	3670.7	0.5	88.4643	937	9.756	10.982	12.5685
0.01	24.23	3670.7	0.79	88.4643	937	14.991	18.27	21.8708
0.01	24.23	3670.7	0.8	88.4643	937	15.387	18.236	18.511
0.01	24.23	5139	0.1	123.85	937	2.914	3.442	18.1094
0.01	24.23	5139	0.11	123.85	937	3.024	3.578	18.3146
0.01	24.23	5139	0.3	123.85	937	5.811	5.428	-6.5774
0.01	24.23	5139	0.31	123.85	937	5.811	5.55	-4.4781
0.01	24.23	5139	0.5	123.85	937	8.628	10.881	26.1109
0.01	24.23	5139	0.5	123.85	937	8.628	10.881	26.1109
0.01	24.23	5139	0.79	123.85	937	15.099	18.867	24.961
0.01	24.23	5139	0.79	123.85	937	15.099	18.867	24.961
0.01	24.23	7341.4	0.1	176.9285	937	2.9	3.119	7.5344
0.01	24.23	7341.4	0.3	176.9285	937	5.777	5.424	-6.1159
0.01	24.23	7341.4	0.3	176.9285	937	5.777	5.424	-6.1159
0.01	24.23	7341.4	0.5	176.9285	937	10.399	11.217	7.8592
0.01	24.23	7341.4	0.79	176.9285	937	20.233	20.389	0.7747
0.01	24.23	7341.4	0.79	176.9285	937	17.356	20.389	17.4791
0.01	24.23	10278	0.1	247.6999	937	2.696	2.68	-0.5813
0.01	24.23	10278	0.3	247.6999	937	6.426	6.25	-2.7349
0.01	24.23	10278	0.31	247.6999	937	6.74	6.43	-4.5971
0.01	24.23	10278	0.5	247.6999	937	11.229	12.626	12.4475
0.01	24.23	10278	0.5	247.6999	937	11.229	12.626	12.4475
0.01	24.23	10278	0.8	247.6999	937	20.808	21.543	3.5291
0.01	24.23	10278	0.8	247.6999	937	21.201	21.543	1.6119
0.01	24.23	14682.9	0.1	353.8571	937	2.748	2.686	-2.2496
0.01	24.23	14682.9	0.1	353.8571	937	2.923	2.686	-8.11
0.01	24.23	14682.9	0.3	353.8571	937	7.221	6.429	-10.968
0.01	17.68	3846.3	0.09	88.4643	1215	3.484	3.141	-9.8441
0.01	17.68	3846.3	0.1	88.4643	1215	3.6	3.299	-8.3542
0.01	17.68	3846.3	0.3	88.4643	1215	5.686	4.824	-15.1517
0.01	17.68	3846.3	0.5	88.4643	1215	7.007	8.516	21.5409
0.01	17.68	3846.3	0.5	88.4643	1215	7.277	8.516	17.025
0.01	17.68	3846.3	0.77	88.4643	1215	11.202	14.03	25.246
0.01	17.68	3846.3	0.81	88.4643	1215	11.588	13.829	19.3384
0.01	17.68	5384.8	0.1	123.85	1215	2.735	2.871	4.9637
0.01	17.68	5384.8	0.3	123.85	1215	5.145	4.244	-17.5161
0.01	17.68	5384.8	0.49	123.85	1215	4.33	7.868	81.688
0.01	17.68	5384.8	0.5	123.85	1215	4.33	8.118	87.4705

D	DR	Re	X	Mass Flux	Pressure	$\Phi^2_{LO,asp}$	$\Phi^2_{LO,let}$	Relative Error
m	--	--	--	Kg.m-2.sec-1	KPa	--	--	%
0.01	17.68	5384.8	0.79	123.85	1215	13.034	14.573	11.8083
0.01	17.68	5384.8	0.8	123.85	1215	13.034	14.555	11.6669
0.01	17.68	7692.5	0.1	176.9285	1215	2.253	2.611	15.8829
0.01	17.68	7692.5	0.11	176.9285	1215	2.481	2.727	9.9399
0.01	17.68	7692.5	0.3	176.9285	1215	5.076	4.492	-11.505
0.01	17.68	7692.5	0.3	176.9285	1215	4.961	4.492	-9.4565
0.01	17.68	7692.5	0.5	176.9285	1215	8.108	8.638	6.5411
0.01	17.68	7692.5	0.5	176.9285	1215	8.108	8.638	6.5411
0.01	17.68	7692.5	0.8	176.9285	1215	13.299	15.331	15.2814
0.01	17.68	7692.5	0.8	176.9285	1215	12.839	15.331	19.406
0.01	17.68	10769.6	0.1	247.6999	1215	2.562	2.226	-13.1082
0.01	17.68	10769.6	0.1	247.6999	1215	2.651	2.226	-16.0324
0.01	17.68	10769.6	0.3	247.6999	1215	5.252	4.721	-10.1083
0.01	17.68	10769.6	0.3	247.6999	1215	5.315	4.721	-11.1862
0.01	17.68	10769.6	0.5	247.6999	1215	8.885	9.221	3.7893
0.01	17.68	10769.6	0.5	247.6999	1215	9.063	9.221	1.7456
0.01	17.68	10769.6	0.79	247.6999	1215	14.021	15.281	8.9842
0.01	17.68	10769.6	0.81	247.6999	1215	14.276	15.073	5.5773
0.01	17.68	15385.1	0.1	353.8571	1215	2.445	2.243	-8.2589
0.01	17.68	15385.1	0.1	353.8571	1215	2.445	2.243	-8.2589
0.01	17.68	15385.1	0.3	353.8571	1215	5.19	4.87	-6.1601
0.01	17.68	15385.1	0.31	353.8571	1215	5.558	5.011	-9.8541
0.01	31.31	3717	0.49	88.4643	567	9.437	13.007	37.8317
0.01	31.31	3717	0.51	88.4643	567	9.437	13.524	43.3072
0.01	31.31	3717	0.8	88.4643	567	16.342	23.041	40.9934
0.01	31.31	3717	0.8	88.4643	567	16.956	23.041	35.8895
0.01	31.31	5203.8	0.3	123.85	567	5.748	6.537	13.7154
0.01	31.31	5203.8	0.3	123.85	567	5.748	6.537	13.7154
0.01	31.31	5203.8	0.51	123.85	567	12.008	13.981	16.4308
0.01	31.31	5203.8	0.51	123.85	567	11.497	13.981	21.6055
0.01	31.31	5203.8	0.79	123.85	567	19.842	24.012	21.0153
0.01	31.31	5203.8	0.81	123.85	567	19.331	23.81	23.1658
0.01	31.31	7434	0.1	176.9285	567	2.806	3.6	28.3145
0.01	31.31	7434	0.11	176.9285	567	2.806	3.803	35.5353
0.01	31.31	7434	0.3	176.9285	567	7.276	6.562	-9.8166
0.01	31.31	7434	0.31	176.9285	567	6.706	6.709	0.0448
0.01	31.31	7434	0.49	176.9285	567	11.747	13.692	16.5515
0.01	31.31	7434	0.5	176.9285	567	11.2	14.145	26.2991
0.01	31.31	7434	0.79	176.9285	567	22.377	26.169	16.9449
0.01	31.31	7434	0.8	176.9285	567	22.377	26.137	16.8031
0.01	31.31	10407.6	0.1	247.6999	567	2.798	3.169	13.2667
0.01	31.31	10407.6	0.11	247.6999	567	2.798	3.404	21.6603
0.01	31.31	10407.6	0.3	247.6999	567	8.077	8.024	-0.6559
0.01	31.31	10407.6	0.3	247.6999	567	8.077	8.024	-0.6559
0.01	31.31	10407.6	0.48	247.6999	567	14.938	15.027	0.5938
0.01	31.31	10407.6	0.49	247.6999	567	15.216	15.406	1.2491
0.01	31.31	14867.9	0.1	353.8571	567	3.33	3.188	-4.2497
0.01	31.31	14867.9	0.1	353.8571	567	3.33	3.188	-4.2497
0.01	17.21	3984.9	0.1	88.4643	937	3.219	3.245	0.8107
0.01	17.21	3984.9	0.29	88.4643	937	5.372	4.651	-13.4233
0.01	17.21	3984.9	0.3	88.4643	937	5.015	4.692	-6.431
0.01	17.21	3984.9	0.49	88.4643	937	6.978	8.085	15.8556
0.01	17.21	3984.9	0.5	88.4643	937	7.161	8.297	15.874
0.01	17.21	3984.9	0.5	88.4643	937	7.161	8.297	15.874
0.01	17.21	3984.9	0.79	88.4643	937	10.73	13.623	26.9642
0.01	17.21	3984.9	0.8	88.4643	937	10.73	13.59	26.6499
0.01	17.21	5578.8	0.1	123.85	937	2.435	2.775	13.9796
0.01	17.21	5578.8	0.3	123.85	937	4.578	4.08	-10.8756
0.01	17.21	5578.8	0.51	123.85	937	6.968	8.79	26.1558
0.01	17.21	5578.8	0.8	123.85	937	11.91	14.334	20.356
0.01	17.21	7969.8	0.11	176.9285	937	2.129	2.669	25.3786
0.01	17.21	7969.8	0.3	176.9285	937	5.317	4.47	-15.9204
0.01	17.21	7969.8	0.5	176.9285	937	6.923	8.525	23.1452
0.01	17.21	7969.8	0.8	176.9285	937	11.719	14.982	27.8505
0.01	17.21	11157.7	0.11	247.6999	937	2.072	2.298	10.9138
0.01	17.21	11157.7	0.3	247.6999	937	4.721	4.636	-1.807
0.01	17.21	11157.7	0.5	247.6999	937	7.684	8.982	16.892
0.01	17.21	11157.7	0.8	247.6999	937	13.609	14.776	8.5705
0.01	17.21	11157.7	0.8	247.6999	937	13.609	14.776	8.5705
0.01	17.21	15939.5	0.1	353.8571	937	2.213	2.215	0.1104
0.01	17.21	15939.5	0.27	353.8571	937	4.749	4.341	-8.5771
0.01	17.21	15939.5	0.29	353.8571	937	5.065	4.641	-8.3751
0.01	12.25	4153.3	0.08	88.4643	1215	2.674	2.311	-13.5894
0.01	12.25	4153.3	0.09	88.4643	1215	2.759	2.405	-12.836
0.01	12.25	4153.3	0.1	88.4643	1215	2.864	2.498	-12.7751
0.01	12.25	4153.3	0.3	88.4643	1215	4.145	3.449	-16.8058
0.01	12.25	4153.3	0.32	88.4643	1215	3.8	3.55	-6.5814
0.01	12.25	4153.3	0.5	88.4643	1215	5.004	5.831	16.5212
0.01	12.25	4153.3	0.51	88.4643	1215	5.004	5.999	19.8922
0.01	12.25	4153.3	0.79	88.4643	1215	7.601	9.679	27.3368
0.01	12.25	4153.3	0.8	88.4643	1215	7.601	9.663	27.1277
0.01	12.25	5814.6	0.1	123.85	1215	2.058	2.113	2.6516
0.01	12.25	5814.6	0.3	123.85	1215	3.687	3.152	-14.5192
0.01	12.25	5814.6	0.48	123.85	1215	4.765	5.271	10.62
0.01	12.25	5814.6	0.52	123.85	1215	4.765	5.966	25.1968
0.01	12.25	5814.6	0.8	123.85	1215	7.655	10.166	32.796
0.01	12.25	8306.5	0.1	176.9285	1215	1.693	1.974	16.6354
0.01	12.25	8306.5	0.29	176.9285	1215	3.494	3.328	-4.7534
0.01	12.25	8306.5	0.5	176.9285	1215	5.649	5.991	6.0476

D	DR	Re	X	Mass Flux	Pressure	$\phi^2_{LO,asp}$	$\phi^2_{LO,let}$	Relative Error
m	--	--	--	Kg.m ⁻² .sec ⁻¹	KPa	--	--	%
0.01	12.25	8306.5	0.79	176.9285	1215	8.62	10.057	16.6684
0.01	12.25	8306.5	0.81	176.9285	1215	8.725	9.98	14.384
0.01	12.25	11629.1	0.1	247.6999	1215	1.997	1.819	-8.9343
0.01	12.25	11629.1	0.1	247.6999	1215	1.823	1.819	-0.2338
0.01	12.25	11629.1	0.11	247.6999	1215	1.881	1.877	-0.2398
0.01	12.25	11629.1	0.3	247.6999	1215	3.646	3.578	-1.8584
0.01	12.25	11629.1	0.5	247.6999	1215	5.411	6.174	14.0962
0.01	12.25	11629.1	0.5	247.6999	1215	6.27	6.174	-1.5393
0.01	12.25	11629.1	0.73	247.6999	1215	8.256	9.522	15.3345
0.01	12.25	11629.1	0.8	247.6999	1215	8.825	9.484	7.4697
0.01	12.25	11629.1	0.8	247.6999	1215	8.825	9.484	7.4697
0.01	12.25	16613	0.09	353.8571	1215	1.984	1.763	-11.1324
0.01	12.25	16613	0.1	353.8571	1215	1.984	1.836	-7.4867
0.01	12.25	16613	0.1	353.8571	1215	1.984	1.836	-7.4867
0.01	12.25	16613	0.12	353.8571	1215	2.134	1.956	-8.3253
0.01	12.25	16613	0.3	353.8571	1215	3.813	3.837	0.6206
0.01	12.25	16363.8	0.49	348.5492	1215	6.202	6.322	1.9264
0.01	12.25	16613	0.5	353.8571	1215	5.978	6.453	7.9507
0.014	73.69	13917.5	0.1025	240	304.51	5.252	5.837	11.1402
0.014	73.69	13917.5	0.3001	240	304.51	21.98	20.16	-8.2818
0.014	73.69	13917.5	0.49997	240	304.51	48.845	39.745	-18.629
0.014	73.69	13917.5	0.79303	240	304.51	78.661	66.196	-15.8475
0.014	73.69	11018	0.10634	190	304.51	4.087	6.23	52.4084
0.014	73.69	11018	0.31124	190	304.51	19.203	20.989	9.3003
0.014	73.69	11018	0.50319	190	304.51	36.061	39.271	8.9027
0.014	73.69	7538.6	0.09711	130	304.51	2.564	6.335	147.0958
0.014	73.69	7538.6	0.30088	130	304.51	17.11	18.605	8.7365
0.014	73.69	7538.6	0.5049	130	304.51	35.024	37.291	6.4727
0.014	73.69	7538.6	0.79748	130	304.51	58.882	62.765	6.593
0.026	1368.72	19071.9	0.10411	200	160	44.619	95.266	113.5107
0.026	1368.72	19071.9	0.30552	200	160	182.755	198.001	8.3425
0.026	1368.72	19071.9	0.50235	200	160	266.523	347.701	30.4579
0.026	1368.72	19071.9	0.81002	200	160	361.148	430.739	19.2696
0.026	1368.72	19071.9	0.90309	200	160	382.026	354.909	-7.0981
0.036	1368.72	26407.3	0.10447	200	160	44.942	95.546	112.5981
0.036	1368.72	26407.3	0.30664	200	160	204.546	201.672	-1.4051
0.036	1368.72	26407.3	0.49777	200	160	321.144	341.464	6.3273
0.036	1368.72	26407.3	0.80582	200	160	439.342	464.347	5.6913
0.036	1368.72	26407.3	0.89301	200	160	472.538	404.634	-14.3702
0.05	1368.72	36676.8	0.10485	200	160	31.706	95.851	202.3153
0.05	1368.72	36676.8	0.29612	200	160	197.298	212.191	7.5486
0.05	1368.72	36676.8	0.50524	200	160	331.577	363.875	9.7408
0.05	1368.72	36676.8	0.80201	200	160	470.907	514.39	9.2338
0.084	1368.72	61617	0.09915	200	160	33.318	91.434	174.4314
0.084	1368.72	61617	0.15169	200	160	54.229	129.577	138.9451
0.084	1368.72	61617	0.19833	200	160	82.992	100.663	21.2922
0.084	1368.72	61617	0.26827	200	160	127.349	152.773	19.9643
0.014	50.23	89018.9	0.08722	1000	487	6.683	7.549	12.9566
0.014	50.23	89018.9	0.11453	1000	487	8.702	9.215	5.9039
0.014	50.23	71215.1	0.10036	800	487	6.917	7.266	5.0423
0.014	50.23	71215.1	0.15626	800	487	10.471	9.54	-8.8903
0.014	50.23	40058.5	0.01146	450	487	0.525	1.312	149.909
0.014	50.23	40058.5	0.12016	450	487	6.273	6.454	2.8732
0.014	50.23	40058.5	0.194	450	487	12.984	11.233	-13.4862
0.014	50.23	40058.5	0.23983	450	487	15.084	14.308	-5.1447
0.014	50.23	20474.3	0.11508	230	487	8.781	5.501	-37.3537
0.014	50.23	20474.3	0.23055	230	487	10.993	12.293	11.8278
0.014	50.23	20474.3	0.32261	230	487	18.017	18.574	3.0887
0.014	50.23	20474.3	0.409	230	487	23.371	23.269	-0.4348
0.014	50.23	20474.3	0.51212	230	487	38.664	30.007	-22.3893
0.014	50.23	10949.3	0.11557	123	487	1.703	4.956	191.0103
0.014	50.23	10949.3	0.26562	123	487	13.738	12.029	-12.4412
0.014	50.23	10949.3	0.50822	123	487	22.225	24.529	10.3675
0.014	50.23	10949.3	0.71606	123	487	35.112	44.498	26.7328
0.014	50.23	10949.3	0.91233	123	487	47.828	37.838	-20.8878
0.014	27	13167.5	0.6	117.0497	915.56	16.781	24.216	44.3077
0.014	27	25316.9	0.6	225.0495	915.56	19.495	24.454	25.4344
0.014	27	13473.3	0.4	119.7684	915.56	10.458	10.449	-0.0869
0.014	27	25586.1	0.4	227.4418	915.56	11.938	10.966	-8.1422
0.014	27	48014.7	0.4	426.8161	915.56	15.453	11.026	-28.65
0.014	27	13293.3	0.3	118.1676	915.56	7.616	7.085	-6.9652
0.014	27	25557.5	0.3	227.1883	915.56	8.733	7.643	-12.484
0.014	27	49184.7	0.3	437.2172	915.56	13.165	8.703	-33.8965
0.014	27	13597	0.2	120.8673	915.56	4.277	4.89	14.3559
0.014	27	26145.1	0.2	232.4111	915.56	5.099	5.519	8.2329
0.014	27	51572.7	0.2	458.4448	915.56	7.758	7.257	-6.4569
0.014	27	89832.3	0.2	798.5446	915.56	8.578	6.402	-25.3671
0.014	27	13564.1	0.1	120.5755	915.56	2.172	2.881	32.6403
0.014	27	25443.8	0.1	226.1768	915.56	2.501	3.188	27.4683
0.014	27	49608.3	0.1	440.9827	915.56	4.604	4.544	-1.3059
0.014	27	89623.7	0.1	796.691	915.56	4.472	4.485	0.2924
0.014	27	111874.5	0.1	994.4841	915.56	4.373	5.007	14.478
0.014	27	13381.6	0.05	118.9529	915.56	1.541	1.77	14.8739
0.014	27	51300.2	0.05	456.0221	915.56	1.757	2.507	42.6892
0.014	27	90341	0.05	803.0671	915.56	1.32	2.784	110.8355
0.014	27	110020.6	0.05	978.0047	915.56	1.28	3.226	152.1295
0.014	125.28	7748	0.1	120	188.419	13.229	17.126	29.4555
0.014	46.15	10999	0.1	120	542.968	1.325	4.028	203.9402
0.014	27	13499.4	0.1	120	914.288	1.329	2.881	116.7407

D	DR	Re	X	Mass Flux	Pressure	$\bar{\phi}_{LO,asp}^2$	$\bar{\phi}_{LO,let}^2$	Relative Error
m	--	--	--	Kg.m ⁻² .sec ⁻¹	KPa	--	--	%
0.014	166.61	13178.1	0.1	230	151.849	13.69	17.966	31.237
0.014	50.23	20474.3	0.1	230	488.872	5.175	4.638	-10.372
0.014	27	25873.8	0.1	230	943.717	1.788	3.211	79.5789
0.014	10.49	38358	0.1	230	1958.408	2.838	1.785	-37.0838
0.014	166.61	25783.2	0.1	450	141.409	12.714	10.255	-19.3386
0.014	50.23	40058.5	0.1	450	484.111	6.212	5.247	-15.5295
0.014	27	50622.7	0.1	450	879.937	4.262	4.603	7.9956
0.014	10.49	75048.2	0.1	450	1961.005	2.115	1.786	-15.5217
0.014	46.15	73326.7	0.1	800	524.9	6.968	7.135	2.4048
0.014	27	89996	0.1	800	924.512	4.402	4.482	1.8116
0.014	10.49	133419.1	0.1	800	1955.866	2.365	5.554	134.8673
0.014	27	112495	0.1	1000	950.479	4.384	5.038	14.9157
0.014	10.49	166773.9	0.1	1000	1960.897	2.193	9.563	336.022
0.0295	10.74	342953.9	0.00373	920	11000	1.627	1.357	-16.5397
0.0295	10.74	342953.9	0.00452	920	11000	1.929	1.433	-25.7066
0.0295	10.74	342953.9	0.01214	920	11000	2.839	2.165	-23.73
0.0295	10.74	342953.9	0.01995	920	11000	4.249	2.914	-31.4149
0.0295	10.74	342953.9	0.03605	920	11000	6.456	4.459	-30.9395
0.0295	10.74	342953.9	0.04296	920	11000	6.762	5.122	-24.2515
0.0295	10.74	167749.2	0.01322	450	11000	2.03	2.611	28.5983
0.0295	10.74	167749.2	0.04056	450	11000	5.652	5.943	5.1628
0.0295	10.74	167749.2	0.0689	450	11000	11.19	8.069	-27.8914
0.0295	10.74	167749.2	0.08609	450	11000	11.011	8.955	-18.6734
0.0295	10.74	167749.2	0.16096	450	11000	22.836	11.535	-49.4887
0.0295	54.79	238195.5	0.01061	920	3000	1.704	2.052	20.4436
0.0295	54.79	238195.5	0.01261	920	3000	1.309	2.251	71.9374
0.0295	54.79	238195.5	0.02101	920	3000	2.461	3.082	25.2497
0.0295	54.79	238195.5	0.05195	920	3000	4.275	6.134	43.491
0.0295	54.79	238195.5	0.07617	920	3000	7.218	8.337	15.5138
0.0295	54.79	106152.4	0.01087	410	3000	1.427	1.816	27.2748
0.0295	54.79	106152.4	0.02693	410	3000	3.536	3.021	-14.5691
0.0295	54.79	106152.4	0.08715	410	3000	5.176	8.258	59.5372
0.0295	54.79	106152.4	0.09005	410	3000	6.627	8.532	28.7481
0.0295	54.79	106152.4	0.10217	410	3000	5.944	9.622	61.8711
0.0295	54.79	106152.4	0.1073	410	3000	8.095	9.978	23.2588
0.0295	54.79	106152.4	0.15718	410	3000	11.354	13.307	17.2028
0.0295	54.79	106152.4	0.1842	410	3000	11.884	14.671	23.4483
0.0295	54.79	106152.4	0.21266	410	3000	14.975	15.962	6.5927
0.0295	54.79	106152.4	0.29755	410	3000	29.972	19.006	-36.5878
0.0295	54.79	106152.4	0.33224	410	3000	26.068	19.356	-25.7478
0.0295	25.11	252811.3	0.01252	820	5900	1.963	2.405	22.5301
0.0295	25.11	252811.3	0.01376	820	5900	1.579	2.544	61.13
0.0295	25.11	252811.3	0.11717	820	5900	4.956	12.925	160.7955
0.0295	25.11	252811.3	0.1309	820	5900	4.879	13.875	184.4144
0.0295	25.11	252811.3	0.14396	820	5900	4.878	14.778	202.9853
0.0295	25.11	252811.3	0.17703	820	5900	7.076	16.267	129.878
0.0295	25.11	252811.3	0.2041	820	5900	6.152	17.255	180.4942
0.0295	25.11	252811.3	0.21084	820	5900	8.79	17.384	97.7659
0.0295	25.11	252811.3	0.24309	820	5900	7.761	18.005	131.9776
0.0295	25.11	123322.6	0.02588	400	5900	1.988	2.333	17.3701
0.0295	25.11	123322.6	0.05718	400	5900	2.544	3.81	49.7788
0.0295	25.11	123322.6	0.0949	400	5900	2.175	5.041	131.7326
0.0295	25.11	123322.6	0.10118	400	5900	2.967	5.235	76.4547
0.0295	25.11	123322.6	0.10789	400	5900	4.174	5.393	29.197
0.0295	25.11	123322.6	0.12848	400	5900	5.027	5.877	16.9041
0.0295	25.11	123322.6	0.25024	400	5900	8.509	8.13	-4.4485
0.0295	25.11	123322.6	0.27078	400	5900	7.284	8.55	17.376
0.0295	25.11	123322.6	0.41576	400	5900	11.414	10.532	-7.7345
0.0295	11.05	125918	0.02945	340	10800	1.5	2.472	64.8186
0.0295	11.05	125918	0.0481	340	10800	1.323	3.404	157.1679
0.0295	11.05	125918	0.15083	340	10800	2.286	5.751	151.5959
0.0295	11.05	125918	0.35021	340	10800	4.404	6.535	48.401
0.0295	11.05	125918	0.50537	340	10800	7.847	7.458	-4.9574
0.0295	11.05	125918	0.64074	340	10800	7.258	10.133	39.62
0.0191	135.81	4321.8	0.38	147	197.222	112.554	83.576	-25.7458
0.0191	128.13	4188	0.318	144	208.941	86.867	78.999	-9.0572
0.0191	124.3	4164.7	0.239	144	215.318	88.442	67.523	-23.6519
0.0191	150.49	4317	0.153	144	178.067	66.457	51.712	-22.1868
0.0191	135.81	4145.4	0.205	141	197.222	84.899	63.474	-25.2364
0.0191	128.13	4100.7	0.233	141	208.941	85.192	68.387	-19.7269
0.0191	120.23	4053.5	0.265	141	222.503	63.613	73.283	15.201
0.0191	144.49	4105.1	0.347	138	185.435	88.893	85.429	-3.897
0.0191	137.92	4246	0.436	144	194.223	113.969	86.956	-23.7022
0.0191	137.92	4246	0.457	144	194.223	117.541	87.056	-25.9355
0.0191	145.4	4467.4	0.197	150	184.287	74.323	57.905	-22.0897
0.0191	139.21	4430.6	0.219	150	192.44	37.318	61.719	65.3851
0.0191	150.96	4499.6	0.271	150	177.51	85.974	72.121	-16.1129
0.0191	155.3	4524.2	0.361	150	172.554	89.687	81.656	-8.9553
0.0191	156.78	4532.4	0.435	150	170.926	123.177	89.089	-27.6737
0.0191	152.87	4510.5	0.463	150	175.294	126.699	90.729	-28.3902
0.0191	186.46	4685.9	0.261	150	143.57	96.636	58.322	-39.648
0.0191	192.66	4809.3	0.231	153	138.895	88.357	50.66	-42.6649
0.0191	178.17	10560.5	0.069	341	150.316	19.309	17.864	-7.4841
0.0191	161.31	10269.3	0.105	338	166.111	29.93	21.99	-26.527
0.0191	140.51	10149.2	0.149	343	190.67	31.253	26.108	-16.4615
0.0191	140.94	9622.3	0.247	325	190.083	41.123	35.464	-13.7608
0.0191	166.54	9965.7	0.094	326	160.884	33.883	21.136	-37.622
0.0191	161.31	10178.2	0.054	335	166.111	19.583	15.168	-22.5449
0.0191	159.28	10244.3	0.094	338	168.238	24.165	20.502	-15.1564

D	DR	Re	X	Mass Flux	Pressure	$\Phi^2_{LO,asp}$	$\Phi^2_{LO,let}$	Relative Error
m	--	--	--	Kg.m ⁻² .sec ⁻¹	KPa	--	--	%
0.0191	155.3	9983.4	0.13	331	172.554	30.545	25.736	-15.745
0.0191	145.4	10215.5	0.151	343	184.287	28.066	27.423	-2.2892
0.0191	147.68	10066.8	0.17	337	181.439	29.721	29.73	0.0289
0.0191	141.82	9722.5	0.215	328	188.913	39.902	32.665	-18.1378
0.0191	137.5	9665.7	0.271	328	194.82	45.856	35.817	-21.8916
0.0191	138.78	9682.7	0.254	328	193.033	39.732	35.263	-11.247
0.0191	161.83	10184.4	0.143	335	165.583	34.359	26.978	-21.4825
0.0191	167.6	9978	0.129	326	159.853	30.553	25.407	-16.8434
0.0191	176.45	10448.1	0.103	338	151.792	31.076	21.732	-30.0665
0.0191	182.26	10513.1	0.089	338	146.913	16.6	20.269	22.1019
0.0191	189.53	10403.6	0.077	332	141.218	24.877	19.489	-21.6607
0.0191	155.79	11981.3	0.111	397	172.01	25.134	20.746	-17.4595
0.0191	162.34	12259.2	0.084	403	165.055	18.809	17.114	-9.0095
0.0191	151.91	12103.6	0.114	403	176.399	26.096	21.026	-19.4284
0.0191	149.08	11880.4	0.122	397	179.747	25.29	22.233	-12.0908
0.0191	144.04	11862.1	0.134	399	186.011	24.089	22.884	-5.001
0.0191	141.82	11827.1	0.154	399	188.913	27.82	24.98	-10.206
0.0191	135.4	11724	0.175	399	197.826	25.231	25.433	0.7995
0.0191	127.74	11510.5	0.206	396	209.572	28.558	26.439	-7.4192
0.0191	153.84	12102.8	0.106	402	174.194	21.063	19.934	-5.3592
0.0191	129.71	11717.8	0.198	402	206.43	29.395	25.977	-11.6294
0.0191	160.29	12168.5	0.07	401	167.172	22.615	15.432	-31.7601
0.0191	155.79	12102	0.079	401	172.01	18.899	16.442	-13.0019
0.0191	159.28	12244.6	0.07	404	168.238	14.288	15.315	7.1873
0.0191	156.78	12207.3	0.074	404	170.926	17.061	15.741	-7.7371
0.0191	157.77	12222.2	0.087	404	169.847	17.072	17.397	1.9011
0.0191	151.43	11946.2	0.108	398	176.954	24.532	20.382	-16.9169
0.0191	152.39	11960.6	0.124	398	175.846	25.31	22.56	-10.8672
0.0191	178.75	12612.2	0.053	407	149.826	16.445	14.16	-13.8939
0.0191	153.84	7677.1	0.21	255	174.194	45.93	38.88	-15.3488
0.0191	174.75	8083.8	0.114	262	153.279	49.292	36.044	-26.8755
0.0191	179.33	8217	0.096	265	149.337	32.066	33.119	3.2843
0.0191	168.68	8029	0.085	262	158.828	21.811	28.182	29.21
0.0191	164.95	7719.9	0.172	253	162.439	45.051	38.918	-13.6147
0.0191	170.31	7951.8	0.14	259	157.3	45.896	39.028	-14.9638
0.0191	163.9	8137.1	0.21	267	163.481	44.741	42.884	-4.1498
0.0191	159.78	8097.3	0.223	267	167.704	51.638	42.512	-17.6723
0.0191	154.32	8043.3	0.258	267	173.646	54.517	42.592	-21.8735
0.0191	138.78	7616.2	0.366	258	193.033	63.019	43.972	-30.2242
0.0191	144.49	7883	0.095	265	185.435	20.743	22.583	8.8704
0.0191	154.81	7897.4	0.112	262	173.099	38.492	28.71	-25.4134
0.0191	152.87	7788.1	0.137	259	175.294	29.494	31.112	5.4851
0.0191	140.51	7486.2	0.171	253	190.67	39.764	29.068	-26.8977
0.0191	131.71	7746.4	0.185	265	203.325	33.872	27.911	-17.5972
0.0191	163.38	8253.9	0.099	271	164.005	27.295	29.114	6.664
0.0191	167.6	8111	0.093	265	159.853	34.384	29.531	-14.1161
0.0191	163.38	4477.2	0.257	147	164.005	87.18	66.784	-23.3951
0.0191	157.27	4444.5	0.293	147	170.385	99.244	73.992	-25.4446
0.0191	164.42	4025.3	0.371	132	162.959	132.694	83.279	-37.2397
0.0191	175.31	4167.9	0.433	135	152.782	150.064	87.386	-41.7673
0.0191	166.54	4218.6	0.356	138	160.884	127.006	80.193	-36.8593
0.0191	149.55	4042.4	0.329	135	179.186	105.719	85.407	-19.2132
0.0191	115.29	4109	0.212	144	231.91	43.701	60.694	38.8829
0.0191	107.36	4143.5	0.242	147	248.735	75.098	64.747	-13.7829
0.0191	137.92	4334.4	0.299	147	194.223	90.845	76.225	-16.0931
0.0191	147.22	3940.7	0.338	132	182.006	104.873	84.795	-19.1453
0.0191	133.33	4043.2	0.35	138	200.867	104.881	85.315	-18.6558
0.0191	167.6	3764.7	0.318	123	159.853	141.408	72.745	-48.5564
0.0191	144.04	3924.3	0.231	132	186.011	98.637	72.15	-26.8529
0.0191	151.91	3964.4	0.199	132	176.399	70.885	67.268	-5.1025
0.0191	156.28	4076.7	0.174	135	171.467	72.728	59.305	-18.4565
0.0191	134.15	3959.9	0.263	135	199.646	98.364	76.064	-22.671
0.0191	178.75	4369.3	0.557	141	149.826	143.603	114.039	-20.5876
0.0191	164.42	7989.6	0.1	262	162.959	25.583	30.702	20.01
0.0191	153.35	7762.7	0.136	258	174.743	36.574	30.925	-15.4454
0.0191	174.75	7960.4	0.163	258	153.279	48.727	43.572	-10.5787
0.0191	171.96	8304.9	0.168	270	155.783	41.243	41.081	-0.3934
0.0191	167.07	7800.1	0.199	255	160.368	44.282	42.887	-3.151
0.0191	162.34	7939.6	0.223	261	165.055	57.386	43.642	-23.9488
0.0191	155.3	7781.6	0.276	258	172.554	55.199	43.595	-21.0221
0.0191	150.49	7734.7	0.31	258	178.067	65.308	43.765	-32.9868
0.0191	166	8371	0.19	274	161.401	46.765	40.664	-13.0462
0.0191	158.27	8203.6	0.14	271	169.309	33.781	34.288	1.5015
0.0191	157.77	8107.8	0.099	268	169.847	26.621	28.022	5.2616
0.0191	160.29	8223.6	0.111	271	167.172	30.809	30.303	-1.6438
0.0191	167.07	8014.2	0.081	262	160.368	33.82	26.759	-20.8765
0.0191	171.96	8243.4	0.17	268	155.783	42.87	41.7	-2.7299
0.0191	162.86	7883.6	0.219	259	164.529	57.378	43.338	-24.4688
0.0191	156.28	7911.8	0.258	262	171.467	47.787	43.393	-9.1943
0.0191	139.21	7797.9	0.35	264	192.44	66.27	40.411	-39.021
0.0191	180.49	10369.4	0.08	334	148.364	26.27	19.404	-26.1354
0.0191	172.51	10556.8	0.099	343	155.28	27.351	21.086	-22.9082
0.0191	171.41	10359.3	0.103	337	156.287	20.535	21.771	6.0182
0.0191	168.14	10412.9	0.112	340	159.34	28.278	22.734	-19.6035
0.0191	161.83	10154	0.134	334	165.583	32.028	25.859	-19.2622
0.0191	155.79	9898.9	0.161	328	172.01	37.957	29.618	-21.9698
0.0191	148.15	9415.2	0.207	315	180.874	36.24	34.433	-4.985
0.0191	142.26	9787.6	0.222	330	188.33	37.969	33.358	-12.1447
0.0191	146.31	9929.5	0.196	333	183.144	37.473	31.764	-15.234

D	DR	Re	X	Mass Flux	Pressure	$\bar{\phi}_{LO,asp}^2$	$\bar{\phi}_{LO,LUT}^2$	Relative Error
m	--	--	--	Kg.m ⁻² .sec ⁻¹	KPa	--	--	%
0.0191	133.74	10113.9	0.242	345	200.256	42.977	32.678	-23.9651
0.0191	131.3	9728.6	0.283	333	203.943	43.693	34.695	-20.5943
0.0191	146.31	10227.7	0.192	343	183.144	37.032	31.039	-16.183
0.0191	154.32	10242.4	0.165	340	173.646	33.895	29.359	-13.3818
0.0191	163.38	10355.5	0.129	340	164.005	35.321	24.938	-29.397
0.0191	167.6	10222.9	0.121	334	159.853	31.551	24.046	-23.7857
0.0191	170.86	10353	0.111	337	156.793	29.256	22.696	-22.4211
0.0191	182.85	10488.5	0.079	337	146.432	29.11	19.27	-33.8044
0.0191	191.4	10893.9	0.052	347	139.821	23.372	16.716	-28.4785
0.0191	164.95	12205.3	0.072	400	162.439	16.916	15.846	-6.3243
0.0191	169.77	12672.1	0.061	413	157.808	16.043	14.399	-10.2496
0.0191	163.9	12220.8	0.085	401	163.481	19.415	17.318	-10.8014
0.0191	155.3	11883.5	0.1	394	172.554	26.034	19.389	-25.5219
0.0191	158.77	12388.6	0.09	409	168.773	20.543	17.615	-14.2532
0.0191	153.84	12253.3	0.11	407	174.194	20.057	20.3	1.2122
0.0191	145.85	12009.6	0.138	403	183.714	25.679	23.639	-7.9442
0.0191	143.6	11884.8	0.142	400	186.589	25.69	23.86	-7.123
0.0191	140.94	12020.4	0.148	406	190.083	28.358	23.953	-15.5318
0.0191	136.23	11855.2	0.167	403	196.619	27.051	24.819	-8.248
0.0191	130.5	11760.3	0.194	403	205.184	31.023	25.806	-16.8155
0.0191	125.05	11552.5	0.222	399	214.031	30.463	27.327	-10.294
0.0191	141.82	12034.6	0.144	406	188.913	28.507	23.584	-17.2684
0.0191	152.87	12208.4	0.105	406	175.294	25.103	19.675	-21.6223
0.0191	161.83	12251.7	0.085	403	165.583	19.11	17.228	-9.8521
0.0191	165.48	12243.4	0.079	401	161.919	22.682	16.642	-26.6282
0.0191	163.38	12091.5	0.086	397	164.005	17.48	17.561	0.4597
0.0191	167.07	12419	0.075	406	160.368	20.17	16.064	-20.3574
0.0191	195.86	3909.9	0.24	124	136.601	40.145	56.737	41.3319
0.0191	186.46	3967.4	0.317	127	143.57	47.737	69.657	45.9184
0.0191	178.17	4087.9	0.321	132	150.316	49.753	73.464	47.6584
0.0191	169.22	4047.7	0.389	132	158.318	59.388	83.32	40.299
0.0191	159.78	4003.2	0.466	132	167.704	71.096	89.185	25.4431
0.0191	150.96	3959.7	0.553	132	177.51	83.05	92.088	10.8838
0.0191	147.68	3943.1	0.58	132	181.439	90.575	93.958	3.7351
0.0191	140.51	3905.8	0.655	132	190.67	102.379	118.547	15.7923
0.0191	131.3	3768.8	0.787	129	203.943	129.727	132.694	2.2872
0.0191	195.86	4067.5	0.215	129	136.601	34.625	53.667	54.9934
0.0191	168.14	7809.7	0.128	255	159.34	15.483	34.895	125.3834
0.0191	163.38	7675.2	0.149	252	164.005	17.682	35.59	101.2798
0.0191	152.39	7212.4	0.181	240	175.846	21.022	32.945	56.719
0.0191	143.6	7428	0.204	250	186.589	21.679	33.657	55.2542
0.0191	137.5	7367.2	0.234	250	194.82	25.461	34.296	34.7017
0.0191	134.98	7224.1	0.263	246	198.431	28.948	36.141	24.845
0.0191	129.71	7170.6	0.298	246	206.43	32.025	36.756	14.7718
0.0191	119.51	7150.6	0.36	249	223.828	38.763	39.462	1.8035
0.0191	113.24	7082.9	0.394	249	236.032	43.443	41.731	-3.9408
0.0191	171.41	7777.2	0.108	253	156.287	13.559	32.234	137.7369
0.0191	159.28	9850.2	0.089	325	168.238	10.334	20.552	98.8744
0.0191	155.3	9892.9	0.103	328	172.554	11.81	22.293	88.7542
0.0191	149.55	9731.6	0.12	325	179.186	12.901	24.873	92.8047
0.0191	140.94	9355.8	0.154	316	190.083	15.347	27.948	82.1129
0.0191	134.57	9186.4	0.174	313	199.038	17.684	27.775	57.0625
0.0191	129.31	9468	0.183	325	207.056	17.688	26.559	50.1501
0.0191	125.05	9207.2	0.204	318	214.031	20.251	26.815	32.4175
0.0191	115.98	8912.1	0.263	312	230.548	25.977	27.084	4.2623
0.0191	109.28	8990.4	0.281	318	244.445	27.267	25.477	-6.564
0.0191	158.27	9717.1	0.096	321	169.309	11.656	21.995	88.6985
0.0191	148.15	11836.3	0.076	396	180.874	8.766	15.755	79.7428
0.0191	141.38	11731.3	0.092	396	189.497	9.709	16.805	73.0869
0.0191	134.15	11527.7	0.112	393	199.646	11.183	18.256	63.2455
0.0191	130.1	11637	0.117	399	205.807	11.443	18	57.2981
0.0191	125.05	11349.8	0.137	392	214.031	12.849	19.775	53.9013
0.0191	115.98	11368.7	0.165	398	230.548	14.855	20.497	37.9734
0.0191	106.41	10864.2	0.217	386	250.902	19.45	22.607	16.2267
0.0191	124.68	11603.9	0.131	401	214.673	12.29	18.712	52.246
0.0191	138.35	11653.7	0.099	395	193.627	9.754	17.229	76.6387
0.0191	152.87	11997.9	0.065	399	175.294	7.058	14.572	106.4546
0.0191	162.34	4015.4	0.446	132	165.055	65.145	89.101	36.773
0.0191	155.3	3981.3	0.5	132	172.554	71.771	87.154	21.4347
0.0191	152.39	3966.8	0.53	132	175.846	75.997	90.009	18.4379
0.0191	150.01	3775.1	0.575	126	178.626	87.038	92.231	5.9662
0.0191	144.04	3745.9	0.647	126	186.011	97.042	119.475	23.1163
0.0191	135.81	3880.8	0.703	132	197.222	103.209	124.799	20.9188
0.0191	132.52	3863	0.741	132	202.093	113.346	127.121	12.1532
0.0191	149.08	3950.2	0.538	132	179.747	77.752	89.229	14.7603
0.0191	162.86	4017.9	0.428	132	164.529	59.597	87.795	47.3145
0.0191	159.78	4003.2	0.451	132	167.704	62.869	89.396	42.1945
0.0191	137.92	7459.9	0.243	253	194.223	25.697	35.38	37.6809
0.0191	134.98	7429.7	0.259	253	198.431	25.987	35.353	36.041
0.0191	129.31	7166.6	0.298	246	207.056	31.485	36.594	16.227
0.0191	123.17	7189.6	0.331	249	217.26	35.132	37.302	6.1753
0.0191	121.69	7087.4	0.354	246	219.869	36.856	40.379	9.5606
0.0191	118.8	6970.8	0.374	243	225.16	39.464	43.066	9.126
0.0191	113.24	6826.9	0.428	240	236.032	45.468	50.005	9.9774
0.0191	100.94	6948.3	0.514	249	264.203	53.764	52.912	-1.5857
0.0191	110.91	7057.5	0.423	249	240.912	44.138	45	1.9545
0.0191	123.17	7276.2	0.324	252	217.26	34.299	35.789	4.3447
0.0191	131.3	9290.4	0.189	318	203.943	18.569	27.743	49.4024
0.0191	126.97	9058.7	0.214	312	210.838	20.153	28.246	40.16

D	DR	Re	X	Mass Flux	Pressure	$\phi^2_{LO,asp}$	$\phi^2_{LO,UT}$	Relative Error
m	--	--	--	Kg.m ⁻² .sec ⁻¹	KPa	--	--	%
0.0191	122.06	8993.8	0.236	312	219.214	22.704	28.046	23.5248
0.0191	115.29	9245.2	0.253	324	231.91	23.476	27.162	15.7022
0.0191	114.6	9207	0.262	323	233.278	24.271	27.244	12.2474
0.0191	112.24	9173.6	0.274	323	238.114	25.592	26.859	4.9515
0.0191	147.22	9553.2	0.299	320	182.006	29.299	40.257	37.4011
0.0191	104.86	8732	0.335	311	254.544	31.971	25.901	-18.9856
0.0191	99.19	8487.4	0.406	305	268.753	37.798	30.226	-20.032
0.0191	109.6	8712.1	0.31	308	243.735	30.202	25.907	-14.2196
0.0191	115.29	11214	0.168	393	231.91	14.009	20.677	47.6056
0.0191	110.91	11224	0.182	396	240.912	14.813	20.643	39.3589
0.0191	108.95	11190	0.192	396	245.156	15.627	20.9	33.7386
0.0191	106.1	11140.2	0.205	396	251.627	16.508	21.246	28.6995
0.0191	107.67	11083.1	0.2	393	248.016	17.088	21.217	24.167
0.0191	104.24	11164	0.213	398	256.013	17.802	21.493	20.7294
0.0191	99.48	10913.4	0.239	392	267.991	20.077	22.746	13.2896
0.0191	95.53	11011.4	0.258	398	278.815	20.556	23.047	12.1204
0.0191	101.53	11200.2	0.222	401	262.699	18.232	21.594	18.4427
0.0191	106.41	11399	0.193	405	250.902	15.749	20.208	28.3066
0.0191	178.75	3718.6	0.387	120	149.826	63.321	73.77	16.5012
0.0191	182.85	3548	0.364	114	146.432	62.653	65.823	5.0605
0.0191	190.15	3668.6	0.303	117	140.751	52.837	60.844	15.154
0.0191	181.67	3636.9	0.286	117	147.396	46.402	62.185	34.0131
0.0191	187.68	3565.7	0.256	114	142.626	42.95	56.309	31.1035
0.0191	193.93	3682.3	0.208	117	137.974	34.594	50.126	44.8985
0.0191	175.88	3707.1	0.35	120	152.286	52.337	70.437	34.5819
0.0191	171.41	3504.3	0.401	114	156.287	61.299	71.366	16.4227
0.0191	168.14	4042.7	0.34	132	159.34	49.177	79.367	61.3896
0.0191	164.95	4027.8	0.36	132	162.439	52.649	82.269	56.2598
0.0191	160.8	4008.1	0.429	132	166.641	63.523	88.087	38.6697
0.0191	157.27	3991	0.493	132	170.385	74.308	88.049	18.4926
0.0191	148.61	3588.9	0.629	120	180.31	106.434	112.475	5.6757
0.0191	188.91	4133.8	0.243	132	141.686	40.266	60.081	49.2124
0.0191	177.02	4454	0.298	144	151.298	44.434	68.257	53.6131
0.0191	159.78	3548.3	0.542	117	167.704	91.239	89.851	-1.5208
0.0191	139.21	3633.1	0.702	123	192.44	117.777	131.863	11.9604
0.0191	123.92	3728.8	0.868	129	215.964	142.889	118.059	-17.3773
0.0191	159.78	7369.5	0.17	243	167.704	20.634	34.5	67.1955
0.0191	156.28	7368.3	0.17	244	171.467	22.067	33.507	51.8452
0.0191	150.49	7674.7	0.191	256	178.067	22.045	35.929	62.9809
0.0191	143.15	7512.7	0.228	253	187.168	26.38	36.149	37.0339
0.0191	137.5	7367.2	0.262	250	194.82	29.183	36.823	26.1805
0.0191	164.95	7628.3	0.147	250	162.439	17.346	35.352	103.8018
0.0191	162.86	7792.3	0.149	256	164.529	18.699	36.44	94.8815
0.0191	157.77	7654	0.173	253	169.847	20.181	36.208	79.4197
0.0191	151.91	7508.4	0.201	250	176.399	23.345	36.75	57.4202
0.0191	141.82	7143.7	0.255	241	188.913	29.688	38.61	30.053
0.0191	139.21	7561.6	0.244	256	192.44	27.38	35.978	31.402
0.0191	135.81	7232.5	0.283	246	197.222	31.743	38.058	19.8931
0.0191	128.52	7333.1	0.303	252	208.311	33.563	35.68	6.3071
0.0191	135.81	7232.5	0.273	246	197.222	30.328	37.271	22.8953
0.0191	127.36	7320.7	0.296	252	210.204	34.878	34.639	-0.6838
0.0191	117.03	7123.8	0.387	249	228.516	43.704	42.218	-3.4005
0.0191	150.49	8184.4	0.172	273	178.067	19.436	35.257	81.4065
0.0191	157.77	7623.8	0.161	252	169.847	19.193	34.697	80.7771
0.0191	158.77	9662.5	0.107	319	168.773	12.002	23.811	98.3957
0.0191	150.96	10019.2	0.114	334	177.51	12.256	23.448	91.3104
0.0191	144.04	9483.8	0.145	319	186.011	15.212	27.579	81.2932
0.0191	134.15	9357.1	0.177	319	199.646	17.671	27.683	56.6552
0.0191	133.74	9087.8	0.188	310	200.256	19.173	28.655	49.4556
0.0191	130.1	9653.7	0.183	331	205.807	18.535	26.674	43.9094
0.0191	125.43	8777.8	0.226	303	213.389	24.588	28.466	15.772
0.0191	120.96	8720.1	0.251	303	221.183	25.425	28.277	11.2168
0.0191	137.08	9542.3	0.158	324	195.418	16.032	26.858	67.5222
0.0191	144.94	10030.8	0.122	337	184.86	13.423	23.454	74.7343
0.0191	162.86	9709.9	0.097	319	164.529	10.809	22.483	108.01
0.0191	149.55	9372.3	0.133	313	179.186	14.692	27.625	88.0231
0.0191	142.26	9550.3	0.147	322	188.33	15.902	27.24	71.2966
0.0191	136.65	9124.7	0.173	310	196.018	18.542	28.451	53.4382
0.0191	132.92	9604.5	0.171	328	201.479	17.502	26.609	52.0302
0.0191	129.31	9205.8	0.198	316	207.056	20.184	27.798	37.7267
0.0191	119.87	9137	0.228	318	223.165	22.149	26.813	21.0615
0.0191	114.94	8727	0.275	306	232.593	26.676	26.615	-0.2319
0.0191	146.76	12023.9	0.081	403	182.574	8.289	16.027	93.3404
0.0191	140.94	11931.6	0.092	403	190.083	9.631	16.539	71.7371
0.0191	134.57	11827.8	0.11	403	199.038	10.643	17.796	67.2009
0.0191	130.1	11782.8	0.12	404	205.807	11.565	18.258	57.8732
0.0191	128.52	11727.1	0.125	403	208.311	11.508	18.632	61.9134
0.0191	131.3	11335.5	0.127	388	203.943	11.971	19.827	65.6227
0.0191	126.97	11613.7	0.131	400	210.838	12.174	19.182	57.572
0.0191	122.43	11450.3	0.146	397	218.561	135.092	20.258	-85.0045
0.0191	116.68	11437.9	0.163	400	229.191	14.48	20.455	41.2587
0.0191	111.57	11178.7	0.188	394	239.51	16.486	21.262	28.9754
0.0191	151.91	12223.7	0.072	407	176.399	7.291	15.26	109.3121
0.0191	145.85	11771.2	0.086	395	183.714	8.499	16.775	97.3795
0.0191	137.92	11823.8	0.1	401	194.223	9.778	17.116	75.0391
0.0191	130.1	11578.7	0.123	397	205.807	11.734	18.831	60.4777
0.0191	123.17	11462.9	0.141	397	217.26	13.239	19.777	49.3825
0.0191	116.68	11352.1	0.163	397	229.191	14.469	20.523	41.8437
0.0191	108.31	11009.4	0.205	390	246.583	17.842	21.888	22.6785

D	DR	Re	X	Mass Flux	Pressure	$\Phi^2_{LO,asp}$	$\Phi^2_{LO,UT}$	Relative Error
m	--	--	--	Kg.m-2.sec-1	KPa	--	--	%
0.0191	130.9	11767	0.111	403	204.563	10.982	17.265	57.2102
0.0134	172.43	405014.7	0.04	4541	1000	14.012	13.09	-6.5739
0.0134	172.43	404568.7	0.04	4536	1000	13.919	13.093	-5.9337
0.0134	172.4	404836.3	0.067	4539	1010	22.603	17.936	-20.6491
0.0134	172.4	404301.1	0.067	4533	1010	23.254	17.94	-22.8513
0.0134	172.4	405995.8	0.098	4552	1010	32.777	21.246	-35.1806
0.0134	172.4	405282.2	0.099	4544	1010	33.031	21.359	-35.3373
0.0134	114.15	450225.8	0.022	4554	1500	6.118	6.707	9.6338
0.0134	114.15	447457.6	0.022	4526	1500	6.287	6.711	6.7393
0.0134	114.15	448742.8	0.042	4539	1500	10.14	11.899	17.3456
0.0134	114.15	448347.3	0.041	4535	1500	9.554	11.641	21.8438
0.0134	114.15	448742.8	0.069	4539	1500	15.659	16.891	7.8653
0.0134	114.15	447754.2	0.069	4529	1510	15.703	16.895	7.5906
0.0134	114.15	448545.1	0.099	4537	1510	20.984	21.496	2.4395
0.0134	114.15	449138.3	0.099	4543	1510	21.021	21.493	2.2468
0.0134	114.15	448940.5	0.129	4541	1510	24.4	23.958	-1.8092
0.0134	114.15	448248.5	0.127	4534	1510	24.551	23.802	-3.0494
0.0134	114.15	449039.4	0.159	4542	1500	27.303	26.023	-4.6877
0.0134	114.15	448545.1	0.159	4537	1500	27.253	26.025	-4.5048
0.0134	114.15	449138.3	0.174	4543	1510	27.159	26.675	-1.7817
0.0134	114.15	447556.4	0.176	4527	1510	27.208	26.77	-1.6082
0.0134	114.15	447556.4	0.191	4527	1500	28.894	27.423	-5.0897
0.0134	114.15	448446.2	0.19	4536	1500	28.811	27.375	-4.9824
0.0134	84.62	480954.8	0.019	4526	2000	4.06	4.589	13.0287
0.0134	84.62	480636	0.021	4523	2010	4.323	4.967	14.8841
0.0134	84.62	480954.8	0.041	4526	2010	7.118	8.744	22.8489
0.0134	84.62	480954.8	0.041	4526	2010	6.929	8.744	26.1951
0.0134	84.62	480317.2	0.07	4520	2000	11.719	13.111	11.8773
0.0134	84.62	480848.5	0.07	4525	2000	11.714	13.111	11.9247
0.0134	84.62	482655	0.097	4542	2000	14.888	16.707	12.2219
0.0134	84.62	481486.1	0.097	4531	2000	15.122	16.709	10.4939
0.0134	84.62	480954.8	0.131	4526	2010	17.231	19.094	10.8117
0.0134	84.62	480742.3	0.131	4524	2010	17.072	19.094	11.8412
0.0134	84.62	480954.8	0.157	4526	2010	17.618	20.486	16.2763
0.0134	84.62	481273.6	0.16	4529	2000	17.804	20.561	15.4825
0.0134	84.62	481061.1	0.178	4527	2010	17.943	21.015	17.1172
0.0134	84.62	480210.9	0.178	4519	2010	18.05	21.016	16.4309
0.0134	84.62	481061.1	0.204	4527	2010	19.115	21.583	12.9109
0.0134	84.62	480317.2	0.201	4520	2000	19.201	21.575	12.3619
0.0134	66.77	508427	0.022	4525	2500	3.283	4.08	24.2875
0.0134	66.77	507640.4	0.023	4518	2500	3.214	4.22	31.3023
0.0134	66.77	506966.3	0.042	4512	2510	5.643	6.88	21.928
0.0134	66.77	507528.1	0.042	4517	2500	5.889	6.88	16.8252
0.0134	66.77	508651.7	0.072	4527	2510	9.303	10.323	10.9667
0.0134	66.77	508202.3	0.072	4523	2500	9.18	10.323	12.4511
0.0134	66.77	508427	0.099	4525	2510	11.548	13.174	14.0834
0.0134	66.77	508089.9	0.099	4522	2510	11.578	13.175	13.7865
0.0134	66.77	508988.8	0.126	4530	2500	13.115	14.707	12.1325
0.0134	66.77	509550.6	0.126	4535	2500	13.294	14.706	10.618
0.0134	66.77	509438.2	0.161	4534	2510	13.469	16.251	20.6538
0.0134	66.77	510000	0.161	4539	2500	13.341	16.251	21.8091
0.0134	66.77	509325.8	0.178	4533	2500	13.497	16.602	23.002
0.0134	66.77	508427	0.181	4525	2500	13.437	16.665	24.0196
0.0134	66.77	509325.8	0.203	4533	2510	14.033	17.071	21.656
0.0134	66.77	507977.5	0.204	4521	2500	14.132	17.079	20.854
0.0134	172.43	538354.6	0.019	6036	1000	9.675	6.361	-34.2517
0.0134	172.43	539335.8	0.018	6047	1000	9.484	6.076	-35.9346
0.0134	172.43	539692.5	0.017	6051	1000	8.127	5.793	-28.719
0.0134	172.43	540049.3	0.018	6055	1010	8.041	6.074	-24.4566
0.0134	172.43	541476.3	0.038	6071	1000	13.933	11.704	-15.9995
0.0134	172.43	540584.4	0.035	6061	990	13.465	10.864	-19.3185
0.0134	114.15	597236.3	0.042	6041	1500	10.348	11.505	11.1835
0.0134	114.15	596148.8	0.043	6030	1500	9.925	11.758	18.4722
0.0134	114.15	597631.7	0.068	6045	1510	15.314	16.19	5.7205
0.0134	114.15	597532.8	0.07	6044	1510	15.61	16.489	5.6304
0.0134	114.15	597532.8	0.098	6044	1500	22.244	20.667	-7.0912
0.0134	114.15	597928.3	0.098	6048	1500	22.135	20.665	-6.6438
0.0134	84.62	639502	0.041	6018	2010	7.366	8.951	21.5082
0.0134	84.62	639076.9	0.039	6014	2010	7.235	8.56	18.3129
0.0134	84.62	642796.2	0.071	6049	2000	11.883	13.482	13.4559
0.0134	84.62	642052.3	0.071	6042	2010	11.648	13.475	15.6861
0.0134	84.62	644071.4	0.095	6061	2000	15.119	16.645	10.0914
0.0134	84.62	641202.3	0.098	6034	2010	15.333	17.013	10.962
0.0134	84.62	641627.3	0.128	6038	2010	18.506	19.108	3.2507
0.0134	84.62	641946.1	0.127	6041	2010	18.49	19.046	3.0039
0.0134	84.62	640883.4	0.14	6031	2000	19.585	19.885	1.5314
0.0134	84.62	642477.4	0.139	6046	2010	19.428	19.834	2.0881
0.0134	66.77	678202.3	0.044	6036	2510	5.792	7.544	30.2475
0.0134	66.77	677078.6	0.039	6026	2500	5.549	6.795	22.4539
0.0134	66.77	678988.8	0.069	6043	2500	8.918	10.446	17.1293
0.0134	66.77	677865.2	0.068	6033	2500	8.902	10.334	16.0823
0.0134	66.77	677977.5	0.099	6034	2500	11.351	13.605	19.8563
0.0134	66.77	678876.4	0.099	6042	2500	11.366	13.611	19.7545
0.0134	66.77	677303.4	0.128	6028	2510	13.641	15.263	11.8946
0.0134	66.77	678089.9	0.131	6035	2510	13.707	15.435	12.6085
0.003	740.75	1207.3	0.061	235.7	10.21	33.372	55.086	65.0685
0.003	712.85	2151.6	0.038	379.2	13.86	22.162	41.813	88.6682
0.003	683.61	3065.6	0.03	494.8	18	18.729	29.734	58.7571
0.003	659.59	3980.5	0.024	605.1	21.66	15.402	21.532	39.7991

D	DR	Re	X	Mass Flux	Pressure	$\phi^2_{LO,asp}$	$\phi^2_{LO,LUT}$	Relative Error
m	--	--	--	Kg.m ⁻² .sec ⁻¹	KPa	--	--	%
0.003	631.1	5076.2	0.02	723	26.41	13.635	17.525	28.5348
0.003	602.7	6354.2	0.017	852	31.79	11.365	14.087	23.9492
0.003	584.29	7580.5	0.015	981.6	35.66	10.238	10.919	6.6497
0.003	569.7	8500.8	0.014	1068.9	38.9	9.553	9.734	1.8947
0.003	553.05	9080	0.013	1111	42.83	9.132	9.027	-1.1466
0.003	531.84	9923.8	0.012	1169.8	48.17	9.235	8.094	-12.3572
0.003	669.77	1674.5	0.114	260.4	20.07	96.486	97.788	1.3489
0.003	635.01	3009.3	0.068	431.9	25.72	42.403	61.277	44.51
0.003	600.89	3759.2	0.059	502.4	32.16	36.395	49.745	36.6808
0.003	564.64	4839.1	0.049	603.6	40.07	30.005	41.895	39.6238
0.003	534.36	6235.6	0.04	737.8	47.52	24.626	33.441	35.7937
0.003	493.2	8001.3	0.033	885.7	58.97	20.522	24.632	20.0236
0.003	473.71	9503.7	0.029	1019.8	65.17	17.905	19.303	7.8049
0.003	478.98	10831	0.026	1128.4	71.24	16.255	16.322	0.408
0.003	458.09	11497.5	0.025	1163.1	78.97	15.762	15.668	-0.5999
0.003	440.04	12198.1	0.024	1201	86.21	15.175	14.952	-1.4735
0.003	569.7	2756.4	0.131	346.6	38.9	66.093	97.867	48.0739
0.003	541.9	3278.1	0.115	393.3	45.59	61.995	87.423	41.016
0.003	522.82	4342	0.086	504.8	50.55	46.296	67.613	46.0457
0.003	499.88	5228.9	0.075	585.1	56.97	40.144	58.781	46.4254
0.003	463.09	7632.1	0.055	804	68.76	29.353	41.25	40.5311
0.003	465.34	8344.1	0.051	853.1	76.21	26.97	37.15	37.7478
0.003	428.06	10412.8	0.043	1008.4	91.31	23.288	27.044	16.1286
0.003	416.24	11385.1	0.04	1083.4	96.62	21.186	24.81	17.1026
0.003	404.47	12146.7	0.038	1135.2	102.21	20.342	23.275	14.4165
0.003	399.19	12693.3	0.038	1178.4	104.83	20.086	22.987	14.4426
0.003	541.9	2454.6	0.201	294.5	45.59	106.722	117.003	9.6327
0.003	512.97	4010.2	0.128	458.9	53.24	68.235	90.995	33.3563
0.003	463.35	5019.3	0.11	529	68.67	57.664	76.53	32.7169
0.003	460.07	6139.5	0.093	622.9	78.21	48.81	64.832	32.8252
0.003	431.24	7906.1	0.076	769.1	89.93	38.242	51.661	35.0901
0.003	399.33	9347	0.067	867.9	104.76	34.04	40.368	18.5914
0.003	385.68	10916.1	0.059	995.2	111.86	29.93	33.67	12.4963
0.003	477.92	3068.7	0.219	331.6	63.79	122.731	117.448	-4.305
0.003	470.93	4291.2	0.165	442.2	74.14	85.042	101.703	19.5921
0.003	439.46	5380	0.138	529.3	86.45	68.929	84.047	21.9323
0.003	416.7	6794.4	0.113	647	96.41	55.523	69.286	24.7872
0.003	399.89	8355.6	0.094	776.4	104.48	45.978	57.289	24.6
0.003	367.11	10024.2	0.082	889.3	122.34	39.196	39.484	0.734
0.003	344.61	11177.5	0.076	957.6	136.69	36.513	36.176	-0.9215
0.003	425.86	4300	0.218	415.1	92.28	111.726	109.624	-1.8814
0.003	390.08	5218.9	0.189	478.7	109.52	93.68	93.958	0.2964
0.003	361.44	6239.8	0.164	549	125.79	80.851	80.773	-0.0975
0.003	340.38	7813.6	0.136	664.6	139.59	65.923	70.727	7.288
0.003	321.44	9515.5	0.115	789.3	152	55.341	47.227	-14.6616
0.003	309.29	11689.5	0.095	954	160.69	43.639	36.323	-16.7649
0.003	299.38	12444.7	0.09	1001.1	168.28	41.642	34.065	-18.1961
0.003	293.34	13627.5	0.083	1087.8	173.17	37.782	30.964	-18.0443
0.003	281.08	14796.1	0.079	1162	183.72	34.713	27.241	-21.5266
0.003	271.71	15615.9	0.075	1209.8	192.41	32.664	24.467	-25.0953
0.003	382.12	3812.1	0.292	345.8	113.79	147.671	112.576	-23.7657
0.003	358.78	5074.6	0.227	444.7	127.45	112.761	97.09	-13.8971
0.003	342.68	6254.5	0.189	534.1	138	89.005	82.949	-6.8049
0.003	330.16	7499.1	0.162	628.8	146.14	76.688	75.325	-1.7773
0.003	316.5	8710.5	0.141	717.9	155.45	64.651	60.824	-5.9189
0.003	297.22	9830.3	0.129	788.5	170	59.399	42.107	-29.1122
0.003	288.49	10749.3	0.12	852.7	177.24	54.999	36.853	-32.9926
0.003	367.68	3782	0.348	335.8	122	181.631	108.628	-40.1932
0.003	348.51	5538.8	0.25	477.6	134.07	118.736	93.165	-21.5354
0.003	318.86	6396.3	0.221	528.8	153.79	105.323	82.732	-21.4492
0.0525	28.13	295543.9	0.0204	930	800	4.681	3.956	-15.4692
0.0525	28.13	320565.6	0.0988	930	800	13.734	14.379	4.7015
0.0525	28.13	374785.3	0.14	930	800	18.951	18.825	-0.6684
0.0525	28.13	446165.3	0.177	930	800	22.141	23.349	5.4554
0.0525	28.13	560586.5	0.222	930	800	27.315	31.418	15.0198
0.0525	28.13	676374.6	0.259	930	800	32.584	33.751	3.5828
0.0525	28.13	822616.1	0.299	930	800	36.623	35.388	-3.3735
0.0525	28.13	985402	0.338	930	800	42.203	33.748	-20.0352
0.0525	28.13	291823.3	0.0394	930	800	7.366	6.688	-9.1999
0.0525	28.13	305480.1	0.0807	930	800	11.777	11.977	1.6955
0.0525	28.13	347753.1	0.122	930	800	15.691	16.767	6.8557
0.0525	28.13	408819.8	0.159	930	800	20.836	20.966	0.6205
0.0525	28.13	614525.8	0.24	930	800	31.101	34.175	9.884
0.0525	28.13	903658.3	0.319	930	800	42.642	34.707	-18.6087
0.0525	28.13	152852.7	0.0188	480	800	2.721	2.646	-2.783
0.0525	28.13	157013.3	0.0788	480	800	10.959	6.97	-36.4014
0.0525	28.13	194290	0.141	480	800	17.337	14.296	-17.5444
0.0525	28.13	233736.7	0.18	480	800	20.704	17.397	-15.9713
0.0525	28.13	317174.6	0.24	480	800	28.329	20.844	-26.4202
0.0525	28.13	426603.7	0.3	480	800	36.219	25.301	-30.1447
0.0525	28.13	508594.6	0.338	480	800	42.213	29.728	-29.5773
0.0525	28.13	662310.5	0.4	480	800	49.759	37.548	-24.5396
0.0525	28.13	842424.8	0.463	480	800	57.797	43.017	-25.5733
0.0525	28.13	962082.3	0.501	480	800	65.297	40.323	-38.2461
0.0525	28.13	151903.3	0.0579	480	800	8.151	5.67	-30.4382
0.0525	28.13	180191	0.123	480	800	14.178	11.564	-18.4356
0.0525	28.13	211003.7	0.159	480	800	17.202	16.149	-6.1219
0.0525	28.13	258553.1	0.2	480	800	22.247	18.711	-15.8937
0.0525	28.13	286388	0.22	480	800	24.967	19.71	-21.0536

D	DR	Re	X	Mass Flux	Pressure	$\phi^2_{LO,exp}$	$\phi^2_{LO,LUT}$	Relative Error
m	--	--	--	Kg.m-2.sec-1	KPa	--	--	%
0.0525	28.13	352606.1	0.261	480	800	27.96	22.036	-21.1852
0.0525	28.13	383569.6	0.278	480	800	30.284	22.964	-24.1694
0.0525	28.13	475089.5	0.323	480	800	38.996	27.834	-28.6236
0.0525	28.13	607553.1	0.379	480	800	44.893	35.559	-20.7912
0.0525	28.13	759496.9	0.435	480	800	55.515	41.857	-24.6019
0.0525	28.13	888693.9	0.478	480	800	58.575	41.771	-28.6879
0.0525	15.24	252126.9	0.0399	700	1400	4.82	5.6	16.1737
0.0525	15.24	263958	0.118	700	1400	10.978	12.806	16.6577
0.0525	15.24	338115.2	0.204	700	1400	16.491	17.198	4.288
0.0525	15.24	455143.7	0.279	700	1400	21.154	19.739	-6.6879
0.0525	15.24	537521.3	0.319	700	1400	23.567	21.618	-8.2735
0.0525	15.24	641575.7	0.362	700	1400	26.217	23.662	-9.7446
0.0525	15.24	746904.1	0.4	700	1400	28.329	26.176	-7.5992
0.0525	15.24	877925.7	0.442	700	1400	32.732	28.869	-11.8047
0.0525	15.24	251803.5	0.0812	700	1400	8.231	9.806	19.1339
0.0525	15.24	265465.9	0.121	700	1400	10.175	13.004	27.8032
0.0525	15.24	291316.2	0.159	700	1400	13.548	15.305	12.9706
0.0525	15.24	391310.1	0.242	700	1400	19.281	18.382	-4.6653
0.0525	15.24	551076.3	0.325	700	1400	25.409	21.926	-13.7078
0.0525	15.24	638973.4	0.361	700	1400	27.069	23.629	-12.7087
0.0525	15.24	881232.3	0.443	700	1400	34.287	28.924	-15.6422
0.0525	15.24	193548.9	0.00153	510	1400	1.064	1.174	10.4044
0.0525	15.24	183313	0.0429	510	1400	5.938	5.561	-6.3352
0.0525	15.24	182237.1	0.0597	510	1400	6.631	7.003	5.6132
0.0525	15.24	183265.6	0.0796	510	1400	8.554	8.568	0.1641
0.0525	15.24	194174.9	0.123	510	1400	11.162	12.527	12.2268
0.0525	15.24	213488.5	0.161	510	1400	13.973	15.298	9.4882
0.0525	15.24	225080.8	0.178	510	1400	14.541	15.933	9.571
0.0525	15.24	258572.8	0.217	510	1400	17.511	16.988	-2.9852
0.0525	15.24	306641.3	0.26	510	1400	19.486	17.806	-8.621
0.0525	15.24	332981.8	0.28	510	1400	20.904	18.293	-12.493
0.0525	15.24	357360.2	0.297	510	1400	21.678	18.821	-13.1797
0.0525	15.24	398181.2	0.323	510	1400	23.537	19.205	-18.4049
0.0525	15.24	508711.8	0.383	510	1400	26.619	21.025	-21.0141
0.0525	15.24	595063.5	0.423	510	1400	30.741	22.89	-25.537
0.0525	15.24	746269.6	0.484	510	1400	35.113	27.063	-22.9267
0.0525	15.24	893795.7	0.536	510	1400	39.614	29.768	-24.8541
0.0525	15.24	967670.7	0.56	510	1400	41.51	30.381	-26.8093
0.0525	15.24	192978.2	0.00306	510	1400	1.24	1.347	8.6958
0.0525	15.24	188099.3	0.0183	510	1400	3.512	3.011	-14.2665
0.0525	15.24	183254.2	0.0795	510	1400	8.385	8.56	2.0915
0.0525	15.24	193789.7	0.122	510	1400	11.353	12.424	9.4358
0.0525	15.24	213488.5	0.161	510	1400	13.796	15.298	10.8868
0.0525	15.24	258572.8	0.217	510	1400	17.722	16.988	-4.1419
0.0525	15.24	282830	0.24	510	1400	17.151	17.384	1.355
0.0525	15.24	398181.2	0.323	510	1400	23.537	19.205	-18.4049
0.0525	15.24	461764.8	0.359	510	1400	25.769	20.15	-21.8057
0.0525	15.24	639631.6	0.442	510	1400	31.996	23.846	-25.4717
0.0525	15.24	784301	0.498	510	1400	37.992	28.718	-24.4088
0.0525	15.24	899812.3	0.538	510	1400	42.205	29.814	-29.3589

VITA

Name: IHAB HISHAM ALSURAKJI

Place of Birth: Dammam-Saudi Arabia.

Nationality: Jordanian

Permanent Address: Nablus,
Hifa Street,
Palestine.

Telephone: +97-0599392180, +966-595722012

Email Address: ehab_sarkagy@yahoo.com

Educational Qualification:

M.S (Mechanical Engineering)

May2012

King Fahd University of Petroleum and Minerals

Dhahran, Saudi Arabia.

B. Sc (Mechanical Engineering)

June 2008

An-Najah National University.

Nablus, Palestine.